URANYL ION SENSITISED PHOTOOXIDATION OF ALKANES

A Thesis Submitted to the College of Graduate Studies and Research in partial Fulfilment of Requirements for the Degree of Doctor of Philosophy in the Department of Chemistry University of Saskatchewan Saskatoon

by

Xiangrong Xu

Winter 1997

PERMISSION TO USE

The author of this thesis agrees that the libraries of this University may make if freely available for inspection. I further agree that permission for copying of this thesis in any manner, in whole or in part, for scholarly purposes may be granted by the professor or professors who supervised my thesis work or, in their absence, by the Head of the Department or the Dean of the College in which my thesis work was done. It is understood that any copying or publication or use of this thesis or parts thereof for financial gain shall not be allowed without my written permission. It is also understood that due recognition shall be given to me and to the University of Saskatchewan in any scholarly use which may be made of any material in my thesis.

Requests for permission to copy or to make other use of material in this thesis in whole or part should be addressed to

Head of the Department Chemistry
University of Saskatchewan
Saskatoon, Saskatchewan S7N 0W0

ABSTRACT

The focus of this work is on the development of strategies to use a transition-metal complex as a photocatalytic agent in the conversion of low molecular weight alkanes into oxygen-containing substances, mainly alcohols and ketones. In this work, cyclic, branched and straight chain materials have been chosen as representative of the three major alkane subcategories, and all of the experiments have been carried out in aqueous solutions at ambient temperature and atmospheric pressure.

For these studies, uranyl ion was chosen to serve as the light antenna, or the "photo-catalyst". Results presented in this work show that at room temperature and atmospheric pressure along with visible light, the resulting excited uranyl ion $^{*}UO_2^{2+}$ is an effective species for oxygenation of all three alkane subcategories (cyclic, branched and straight chain hydrocarbons). Observed quantum yields of 0.022, 0.087 and 0.01 are found for the isobutane system, cyclopentane system and pentane system, respectively.

Peroxydisulfate has been shown to be an effective amplification agent for all these processes. In the presence of 1.0 mM peroxydisulfate, quantum yields increase 4 to 50 times for correspondingly different systems. In the isobutane system, the quantum yields higher than unity have

been achieved even though only 6% of the excited uranyl ions are quenched by isobutane.

Quantum yields increase with increased alkane and proton concentrations. In the absence of peroxydisulfate, uranyl ion concentration and light intensity have no significant influence on the quantum yield. However, in the presence of peroxydisulfate, increased light intensity leads to decreased quantum yield. Increased concentrations of peroxydisulfate favour higher quantum yields. In these uranyl-ion sensitised photooxidation processes, no net consumption of UO_2^{2+} can be detected in the presence of oxygen and/or of peroxydisulfate (pH < 1). When the pH is higher, a precipitate $UO_2(O_2)\cdot 2H_2O$ is formed. Extensive irradiation can lead to the occurrence of $UO_2(O_2)_2^{2-}$, $UO_2(O_2)_3^{4-}$ and some type of organic polymer. For the case of cyclopentane, Cu^{2+} is an effective agent to prevent the formation of these substances.

A mechanism of reversible reaction between excited hydrated uranyl ions has been proposed in the case of isobutane.

ACKNOWLEDGEMENTS

First of all, I wish to express my sincere gratitude to my supervisor, Dr. W. L. Waltz, who provided guidance and utmost support through all stages of this project. His love for research is a source of inspiration for me. I also wish to acknowledge my co-workers in the laboratory for insights and assistance: Drs. U. Dreger, P. Sedlák, and Savitri, and Messrs. Trevor Bergfeldt, Rod Nashiem and Hamid Golchoubian, as well as many others in our department who have given me a great deal of valuable help.

I also want to express my appreciation to the members of my research committee for their support and helpful suggestions: Drs: R. J. Woods, R. E. Verrall, R. M. Cassidy, D. B. Russell and D. Lee. The assistance of Mr. Ken Thoms with the GC and MS instrumentation is also greatly appreciated.

I would like to thank the University of Saskatchewan for financial support.

Finally, I wish to express my deepest gratitude to my wife Yanling, without her help and support this work might never have been completed.

TABLE OF CONTENTS

LIST OF TABLES

LIST OF FIGURES

1. INTRODUCTION

1.1 Statement of Purpose

Low molecular weight saturated hydrocarbons are important materials, and while they find use as energy sources, they are increasingly being used as chemical feedstocks in the chemical industry to produce oxygen-containing substances such as alcohols, ketones and carboxylic acids. Although the oxidation processes are, frequently, thermodynamically favorable, energy input is generally required to meet kinetic barriers. Most of the methods that have been studied or used employ high temperatures and pressures to overcome these barriers, and often toxic solvents and/or costly catalysts are employed as well. For example, butane requires 1000 psi and 200 °C to be oxidized to acetic acid by air.

Solar light has great potential to be used as the energy source in these oxidation processes, and in Section 1.3 several different approaches are discussed. As saturated hydrocarbons are transparent to wavelengths above 300 nm, a light receptor or light antenna is required to collect the light energy and then to transform the hydrocarbon to

oxygen-containing substances in the presence of sources of oxygen.

The focus of this work is on the development of strategies to use a transition-metal complex as a photocatalytic agent to transform low molecular weight alkanes into oxygen-containing substances, mainly alcohols and ketones. In this work, cyclic, branched and straight chain materials have been chosen as representative of the three major alkane subcategories, and all of the experiments have been carried out in aqueous solutions at room temperatures and ambient pressures. Although alkanes have limited solubilities in aqueous media, such solutions dissolve metal-complex ions and are also a potential source of "oxygen".

For these studies, uranyl ion was chosen to serve as the light antenna. Its advantageous properties and background information pertinent to its photochemical uses are presented in the next section.

1.2 Structure and Properties of Uranium Ions

1.2.1 Structure of UO_2^{2+}

Uranium is the heaviest element in nature. It is a f-transition metal with an electronic configuration $5f^3 6d^1 7s^2$. In UO_2^{2+}, the 6d-orbitals of uranium are thought to be

involved both in σ– and π–bonding with the 2p-orbitals of the oxygen atoms.[1,2,3,4] From the calculation of molecular orbital (MO) overlap integrals, the 5f-orbital of uranium is also suggested to be involved in the bonding.[1,2,5]

The geometry of the uranyl ion (UO_2^{2+}) is linear ($O=U=O^{2+}$).[6,7] The uranyl ion exhibits variable coordination numbers in its compounds, such as 4, 5 or 6 depending on ligands and conditions. A coordination number of six is the most frequently encountered and the ligands are usually coordinated in the plane perpendicular to the $O=U=O^{2+}$ axis. The $O=U=O^{2+}$ unit possesses three characteristic vibration frequencies. They are the symmetric stretching vibration (υ_1 or σ_γ^+), lying in the range 780-900 cm^{-1}; the asymmetric stretching vibration (υ_3 or $\sigma\mu^+$), lying in the range 800-1000 cm^{-1}.4 and the bending vibration (υ_2 or π_m), lying in the neighborhood of 200 cm^{-1}.

1.2.2 Hydrolysis and Complexation

In acid solution (pH < 3) uranyl ion exists in the form of UO_2^{2+}. As the pH is increased, hydrolysis occur. Baes[8] and Gustafson[9] measured the equilibrium constant for the following hydrolysis equilibrium:

$$UO_2^{2+} + H_2O \rightleftharpoons UO_2(OH)^+ + H^+ \qquad (1.2.2\text{-}1)$$

$$LogK_{11} = -5.7 \pm 0.3$$

The K_{11} is consistent with the upper limits based on the kinetic studies of Cole[10] and with that of Eliet.[11] When the pH is high, $UO_2(OH)_2$ is the main product of the hydrolysis. At low temperatures, the product is $UO_2(OH)_2 \cdot H_2O$.[12] In basic media, however, the hydrolysis product is a complex solution of uranates.[13] UO_2^{2+} has a strong tendency to form polynuclear species, such as $(UO_2)_2(OH)_2^{2+}$, $(UO_2)_3(OH)_5^+$, $(UO_2)_3(OH)_3^{3+}$, when uranyl ion concentrations are high. These forms are also affected significantly by anions.[8,14,15] The equilibrium constants in noncomplexing media are summarized below:[16]

$$2UO_2^{2+} + 2H_2O \rightleftharpoons (UO_2)_2(OH)_2^{2+} + 2H^+ \qquad (1.2.2\text{-}2)$$

$$LogK_{22} = -5.62$$

$$3UO_2^{2+} + 5H_2O \rightleftharpoons (UO_2)_3(OH)_5^+ + 5H^+ \qquad (1.2.2\text{-}3)$$

$$LogK_{35} = -15.63$$

The distribution of hydrolysis products are shown in **Figure** 1.2.2-1. The distribution curves shift to higher pH side with the decreasing uranyl concentration. When the

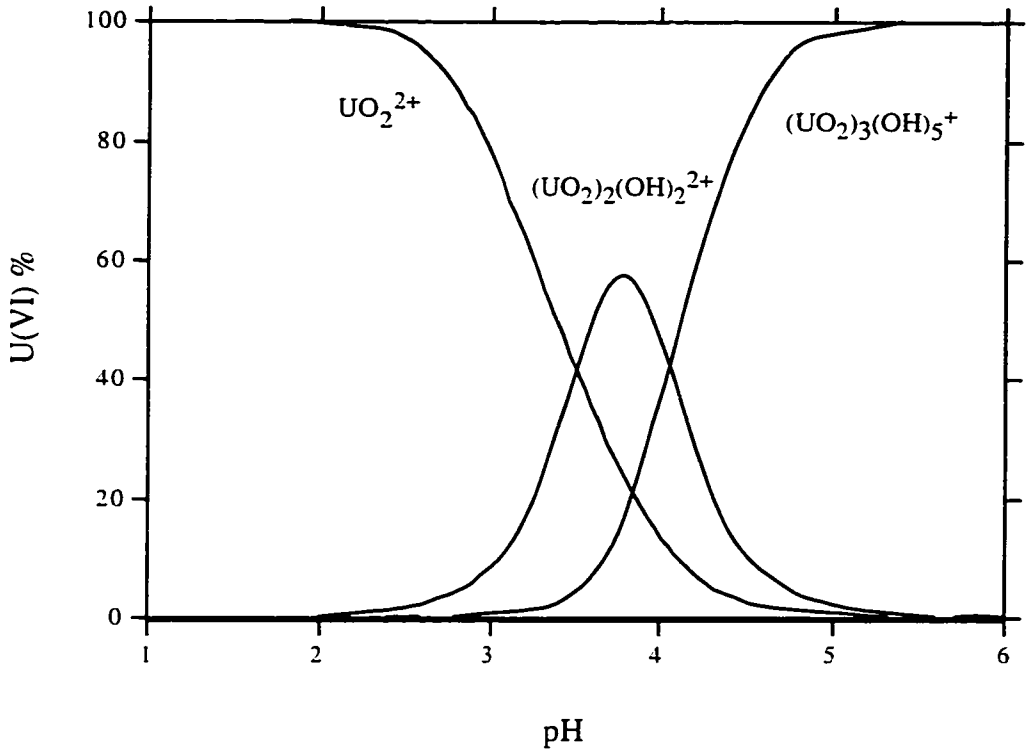

Figure 1.2.2-1. Distribution of hydrolysis products of UO_2^{2+}
I = 1 M; T = 25 °C. [U(VI)] = 0.1 M.
(after reference: Baes, Jr. C. F.; Mesmer, R. E. *The Hydrolysis of Cations* John Wiley: New Yerk, 1976; p178.)

concentration of uranyl decreases from 100 mM to 0.1 mM, these curves shift to the right by about 1 pH unit.[11]

The hydrolysis of $U^{4+}(aq)$ begins at high acidity and with less tendency towards polymerization. The equilibrium constants are listed below:[16]

$$U^{4+}(aq) + H_2O \rightleftharpoons UOH^{3+} + H^+ \qquad LogK_{11} = -0.65 \quad (1.2.2\text{-}4)$$

$$U^{4+}(aq) + 2H_2O \rightleftharpoons U(OH)_2^{2+} + 2H^+ \qquad LogK_{12} = -2.6 \quad (1.2.2\text{-}5)$$

$$U^{4+}(aq) + 3H_2O \rightleftharpoons U(OH)_3^{+} + 3H^+ \qquad LogK_{13} = -5.8 \quad (1.2.2\text{-}6)$$

$$U^{4+}(aq) + 4H_2O \rightleftharpoons U(OH)_4 + 4H^+ \qquad LogK_{14} = -10.3 \quad (1.2.2\text{-}7)$$

The hydrolysis Of UO_2^+ can not be properly investigated because of its ready disproportionation. Kraus and Nelson[17] did some work on this question and reported a pK of 8 for following equilibrum:

$$UO_2^+ + 2H_2O \rightleftharpoons UO_2OH + H_3O^+ \qquad LogK = -8 \quad (1.2.2\text{-}8)$$

All of the experiments reported here are carried out at pH < 3.1. Below this pH, U(VI) and U(V) are almost in their simple forms of UO_2^{2+} and UO_2^+. In this pH range, the reduction product U(IV) is hydrolyzed to different degrees. The extinction cofficient of U(IV) is thus affected more markedly by pH than U(VI) and U(V).

Uranyl ion can complex with a great number of ligands.[18,19] The stability order with inorganic anions is:[20]

$$ClO_4^- < I^- < Br^- < NO_3^- < Cl^- < SO_4^{2-} < F^- < OH^- < CO_3^{2-}, O_2^{2-}$$

Uranyl ion can also complex with many carboxylic acid ligands, such as acetic acid, oxalic acid, tartaric acid and citric acid, and with organic ligands which have multi coordinating atoms, such as EDTA, acetylacetone, N,N-dimethylacetoacetamide and thenoylacetone.[21] The formation of complexes strongly influences the life-time of the excited uranyl ion.[22] The absorption and emmision spectra shift when complexation occurs.[23] Uranyl ion has a strong tendency to form complexes with O_2^{2-} and $UO_2(O_2)$ is the simplest form. It is a light yellow solid and this process of forming $UO_2(O_2)$ has been suggested as one to be applied to the uranium mining industry.[24] The coordination number increases with increasing concentration of O_2^{2-}.[25] Under basic conditions, $[UO_2(O_2)_3]^{4-}$ is stable. The three O_2^{2-} ligands coordinate in the equatorial plane as shown in the following diagram:[26]

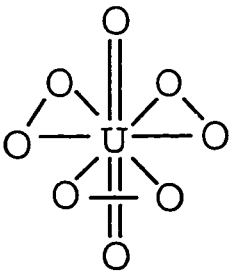

$U^{4+}(aq)$ also forms complexes with most inorganic anions and with similar stability order as for UO_2^{2+}:[27]

$$ClO_4^- < I^-,\ NO_3^- < Br^- < Cl^- < SCN^- < SO_4^{2-} < F^-$$

These complexes are usually more stable than the corresponding complexes of UO_2^{2+}. U(IV) complexes with small organic ligands are generally less stable than those of UO_2^{2+}. However, $U^{4+}(aq)$ can form very stable complexes with some hexadentate ligands, such as EDTA and DCTA (Log(K) > 25).[21] Complexation of $U^{4+}(aq)$ with F^-, PO_4^{3-} and IO_3^- will result in precipitates.

There are very few reports on the complexes of UO_2^+. It is considered to form a very weak complex with SO_4^{2-} and it is reported to form a complex with sulfosalicylic acid with a pK of 5.14.[28,29] The weakest complexing agent, $HClO_4$ was used in the present experiments.

1.2.3 Redox Reactions

UO_2^{2+} is a weak oxidant in its ground state but in its lowest electronically excited state($*UO_2^{2+}$), uranyl ion is a very strong oxidant with E^0 = 2.6 V.[30] Excited uranyl ion is able to oxidize many organic substances and this will be dicussed in Section 1.3. In the photooxidation process, $*UO_2^{2+}$ is reduced to UO_2^+ and $U^{4+}(aq)$. To employ $*UO_2^{2+}$ as a

"catalyst", the reoxidation of $UO_2^{\cdot}$ and $U^{4+}(aq)$ by oxygen or other oxidants is essential. Other redox reactions of UO_2^{2+}, $UO_2^{\cdot}$ and $U^{4+}(aq)$ with organic "intermediates", such as free radicals, ions, are also important in the photooxidation process.

In aqueous solution, uranium ions can exist in a number of redox states, such as $U^{3+}(aq)$, $U^{4+}(aq)$, $UO_2^{\cdot}$ and UO_2^{2+} with UO_2^{2+} being the most stable form. In the absence of oxidants, $U^{4+}(aq)$ is also stable. $U^{3+}(aq)$ is a strong reducing agent and it has even been reported to reduce water to hydrogen.[31] $UO_2^{\cdot}$ is stable at pH = 2 - 4 in the absence of oxidants, but when the pH is lower than 2, disproportionation occurs:

$$2UO_2^{\cdot} + 4H^{+} \rightleftharpoons U^{4+}(aq) + UO_2^{2+} + 2H_2O \qquad (1.2.3\text{-}1)$$

As shown in the above equation, acid strongly affects the equilibrium position. Nelson and co-workers[32] used polarographic and potentiometric techniques to obtain a value of $K = (1.7 \pm 0.3) \times 10^7$. Bell[33] employed a spectophotometric method to study this process and the K was determined to be 7×10^4 at zero ionic strength. When the ionic strength equals 0.48 M, K is 8.5×10^6. Under our experimental conditions, the equilibrum (1.2.3-1) strongly shifts towards the right side at pH = 1, but when the pH is 3, the shift is to the left.

The rate equation for this disproportionation is found experimentally to be:

$$-d[UO_2^+]/dt = k_d[UO_2^+]^2[H^+] \qquad (1.2.3\text{-}2)$$

Gordon and Taube measured the k_d value as 435 $M^{-2}s^{-1}$ at an ionic strength of I = 1.58 M and 600 $M^{-2}s^{-1}$ at I = 3.8 M.[34] These values are close to that measured by Newton and Baker[35] using a different method. Ekstrom[36] studied the mechanism of the disproportionation and from his kinetic data at $[UO_2^{2+}]$ = 1.0 M and I = 2.5 M, k_d is calculated to be 747 $M^{-2}s^{-1}$. Ekstrom also found that the rate of the disproportionation was retarded by UO_2^{2+}. In contrast to the effect of UO_2^{2+}, F^- was reported to increase the disproportionation rate remarkably, and in the presence of F^-, the rate was so high that direct measurement of it was impossible.[37] Ekstrom investigated the mechanism of the disproportioation of UO_2^+ and reported the complexation of U(VI) and U(V). It was found that the presence of U(VI) stablized U(V).

In our experimental conditions, the disproportionation of UO_2^+ at pH = 1 is too fast to be measured by any common method.

The standard potential of UO_2^{2+}/UO_2^+ and $UO_2^+/U^{4+}(aq)$ couples are 0.16 V and 0.53 V, respectively.[38,39] Molecular oxygen can oxidize UO_2^+ to UO_2^{2+}, and the kinetic rate law can be expressed as:[40]

$$-d[UO_2^+]/dt = k_{U(V)}[UO_2^+][O_2] \qquad k_{U(V)} = 62.7\ M^{-1}s^{-1} \qquad (1.2.3\text{-}3)$$

When oxygen is bubbled in our system ($[O_2] \approx 2$ mM), the half-life of the reaction is calculated to be 5.5 seconds (considering $[O_2]$ is constant). Cu^{2+} can greatly increase the UO_2^{+} oxidation rate and this effect is shown in the following expressions:[40]

$$-d[UO_2^{+}]/dt = k_{obs}[UO_2^{+}]; \quad k_{obs} = k_U[O_2] + k_{cat}[Cu^{2+}] \qquad (1.2.3\text{-}4)$$

$$k_U = 31.4 \pm 1.0\ M^{-1}s^{-1}; \qquad k_{cat} = 930\ M^{-1}s^{-1}$$

Although UO_2^{2+} is a weak oxidant, it can readily oxidize α-hydroxyl organic radicals.[41,42] For example, UO_2^{2+} can oxidaize 2-propanol radical:

$$(CH_3)_2(OH)C\cdot + UO_2^{2+} \longrightarrow (CH_3)_2CO + UO_2^{+} + H^{+} \qquad (1.2.3\text{-}5)$$

the k value for reaction (1.2.3-5) is equal to 1.10(± 0.22) x 10^8 $M^{-1}s^{-1}$.[43] UO_2^{+} is considered to be a good reducing agent for alkylperoxide free radicals such as the cyclopentane peroxyradical:[44]

$$c\text{-}C_5H_9O_2\cdot + UO_2^{+} \longrightarrow c\text{-}C_5H_9OOUO_2^{+} \qquad (1.2.3\text{-}6)$$

$$c\text{-}C_5H_9OOUO_2^{+} + H^{+} \longrightarrow c\text{-}C_5H_8O + UO_2^{2+} + H_2O \qquad (1.2.3\text{-}7)$$

$U^{4+}(aq)$ can be also oxidized by molecular oxgyen, however acid hinders this oxidation:

$$-d[U^{4+}(aq)]/dt = k_{U(IV)}[U^{4+}][O_2]/[H^+] \qquad (1.2.3\text{-}8)$$

At 25 °C, $k_{U(IV)}$ has been calculated to be 3.6×10^{-2} s^{-1}.[45] Cu^{2+} can increase this rate.[46] Other inorganic free radicals, such as SO_4^- can also readily oxidize $U^{4+}(aq)$.[47]

1.2.4 Isotopic Exchange

Oxygen-exchange in UO_2^{2+} is a useful tool for investigating mechanistic features. Uranyl oxygen exchange in acid solution proceeds very slowly ($t_{1/2} \approx 10^4$ h), but light and reducing agents can strongly accelerate this process. In the presence of reducing agents such as Eu^{2+} and Cr^{2+}, which are capable of transforming uranyl ion to uranoyl (UO_2^+), the oxygen-exchange rate was found to be greatly increased.[34,48] Gaziev and coworkers[49,50,51] investigated the influence of other substances in the presence of light, and found that the ions that can reduce electronically excited $*UO_2^{2+}$ (Fe^{2+}, Ce^{3+}, Mn^{2+}) increase the oxygen-exchange quantum yield and that the ions that can oxidize UO_2^+ (Fe^{3+}, Ag^+) decrease the oxygen-exchange quantum yield. Those cations that can not change the valence state of UO_2^{2+} or UO_2^+, such as Mg^{2+}, La^{3+}, and Th^{4+}, only slightly reduce the oxygen-exchange quantum yields.[52] Oxidizing anions ($S_2O_8^{2-}$) greatly decrease the quantum yield of oxygen-exchange. In contrast to cations that reduce $*UO_2^{2+}$, anions capable of reducing $*UO_2^{2+}$

(Cl^-, Br^-) decrease the exchange quantum yield which has been attributed to the quenching of $*UO_2^{2+}$ by the reversible process of electron transfer.[50]

Irradiation can accelerate the oxygen-exchange between UO_2^{2+} and water molecule. Uranyl oxygen-exchange occurs over almost all of the absorption range of UO_2^{2+} (305-470 nm) and the oxygen-exchange increases with increasing wavelength, reaching a maximum at 440 nm, and then decreases and vanished at 470 nm.[53] In the presence of ethanol, which can be oxidized by $*UO_2^{2+}$, the exchange quantum yield increases as the wavelength changes from 305 to 366 nm, and then remains unchanged up to 470 nm. From this point, the author suggested that the lowest component of the first triplet state is 488 nm, and the $*UO_2^{2+}$ in this state can oxidize alcohol but not the water.[54] F^- is reported to be an effective catalyst for the disproportionation of UO_2^+.[37] In the presence of F^- no oxygen-exchange is found.[55]

Based on the above observations, it has been proposed that UO_2^+ is the intermediate for the oxygen-exchange.[52,56]

1.3 Photophysical and Photochemical Features of Uranyl Ion

1.3.1 Absorption and Emission Properties

The absorption spectrum of UO_2^{2+} is shown in **Figure** 1.3.1-1. It is a highly structured spectrum in the visible range with the band maximum occuring at 415 nm.[57,58] This spectrum can be resolved mathematically into 24 Gaussium bands in 7 groups. The first 13 bands are assigned to the three components of the triplet state ($^3\Pi_\mu$), corresponding to 468, 414 and 360 nm. The vibronic fine structure is superimposed on these absorptions (see the bands under the envelope line in **Figure** 1.3.1-1).[59] The absorption and emission processes of U(VI) can be described using the energy level diagram of **Figure** 1.3.1-2.[60] The ground electronic state of UO_2^{2+} is considered to be a singlet state ($^1\Sigma_g^+$) with the electronic configuration $(1\sigma_\mu^+)^2(1\sigma_g^+)^2(1\pi_\mu)^4(1\pi_g)^4$, and the lowest excited electronic state to be a triplet state ($^3\Pi_\mu$) with the electronic configuration $(1\sigma_\mu^+)^2(1\sigma_g^+)^2(1\pi_\mu)^4(1\pi_g)^3(\delta\mu)^1$. The absorption spectrum in the visible range is considered to be a singlet-triplet transition ($^1\Sigma_g^+ \rightarrow {}^3\Pi_\mu$).[7] This transition is symmetry-forbidden with a small extinction coeffcient. The energy difference between $^3\Pi_\mu$ and $^3\Delta_\mu$ is not great and is

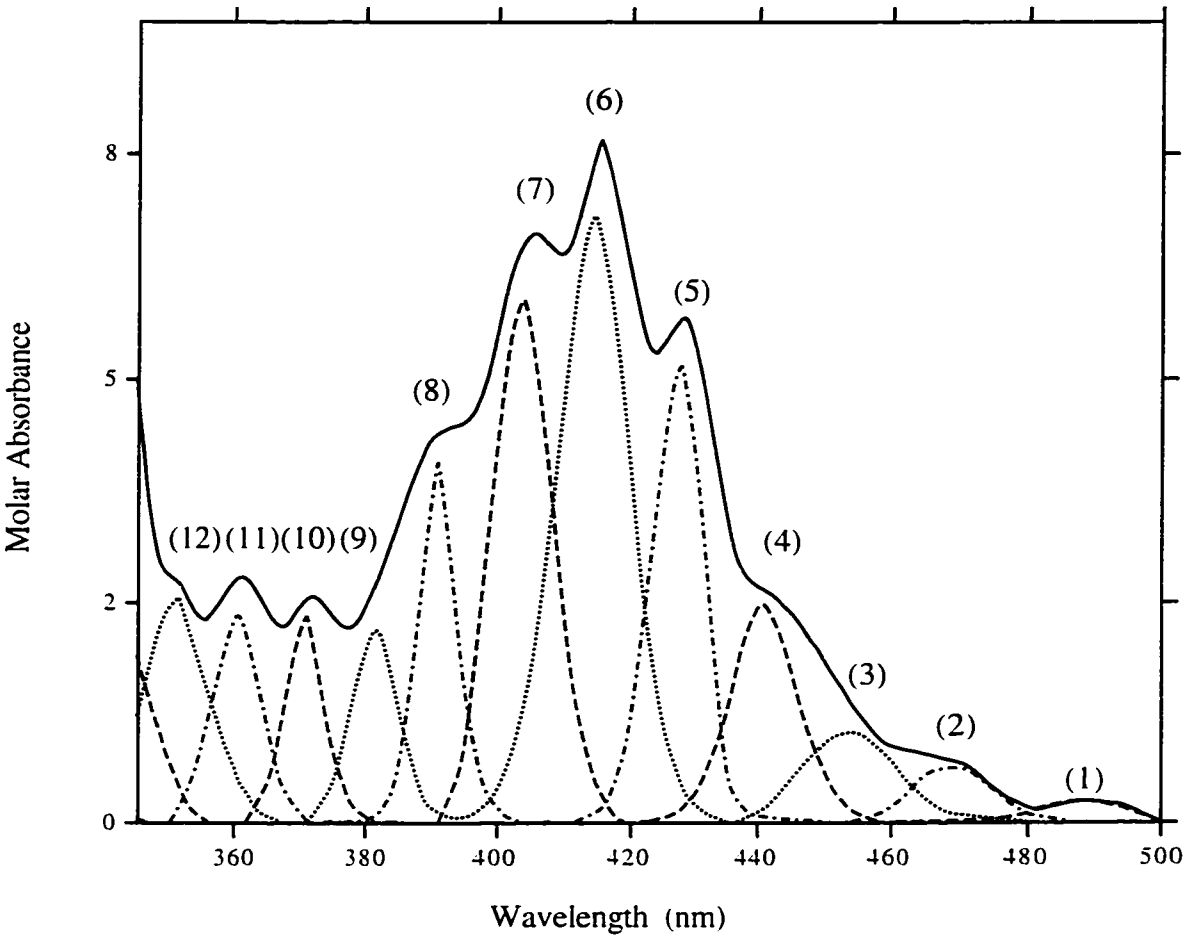

Figure 1.3.1-1. Absorption spectrum of uranyl ion in $HClO_4$ solution $[UO_2^{2+}] = 9.15$ m M; $[HClO_4] = 1.4$ mM.
(after reference: Burrows, H. D. *J. Chem. Soc. Review* **1974**, *3*, 139.)

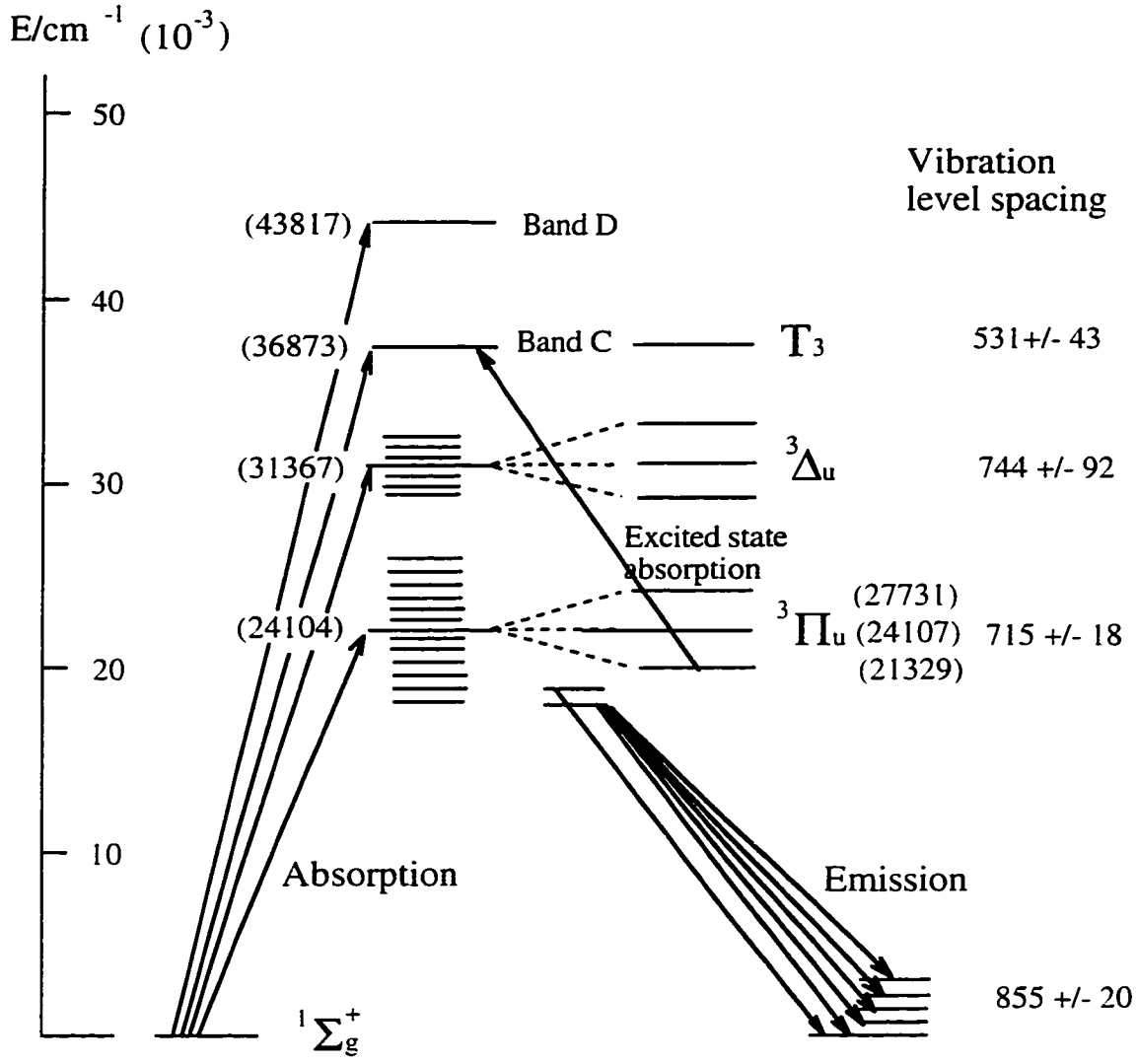

Figure 1.3.1-2. Energy level diagram of uranyl ion.
(after reference: Burrows, H. D. *J. Chem. Soc. Review* **1973**, *3*, 139.)

strongly dependent on the electrostatic field. In some cases, $^3\Delta_\mu$ is possibly the lowest excited state and the transition then becomes $^1\Sigma_g^+ \rightarrow$ $^3\Delta_\mu((1\sigma_\mu^+)^2(1\sigma_g^+)^2(1\pi_\mu)^4(1\pi_g)^3(\phi\mu)^1)$.[61] $\delta\mu$ and $\phi\mu$ are the non-bonding orbitals on uranium and π_g is the bonding orbital mainly featuring the p-orbital of oxygen atom. From a molecular orbital view, the transition means that an electron is transferred from the highest filled p-orbital to a non-bonding orbital on the uranium. So the photochemical reduction of $*UO_2^{2+}$ is actually the filling of the vacancy (hole) in the non-bonding orbital of uranium.

Excited species usually deactivate via three pathways. The first one is emission (fluorescence and phosphorescence); the second is radiationless transitions (vibrational relaxation); and the third is quenching by other molecules. The emission rate depends on the properties of the excited species or their Einstein probability of spontaneous emission (A_{nm}).[62] The other two processes are strongly affected by the environment.[63] Excited uranyl ion exhibits strong emission. **Figure** 1.3.1-3 shows the emission spectrum of UO_2^{2+} after being excited with irradiation of $\lambda_{irr.}$ = 415 nm. The spectrum is influenced by pH. A pH increase is associated with a red shift and longer lifetimes. This is considered as the hydrolysis of UO_2^{2+}, since the hydrolyzed species have longer lifetimes in aqueous solution.[11,64] The

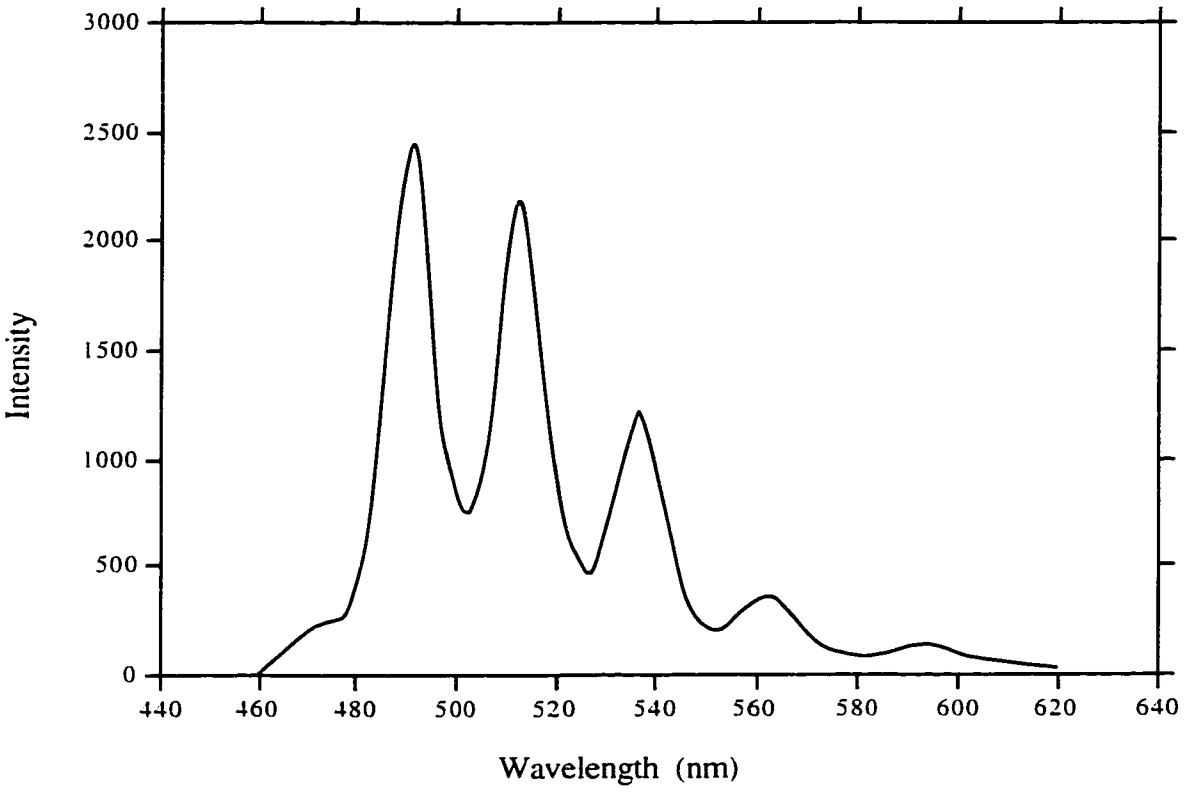

Figure 1.3.1-3. Emission spectrum of uranyl ion.
$[UO_2^{2+}] = 0.1$ M; $[HClO_4] = 1$ M; $\lambda_{exc.} = 308$ nm.
(after reference: Eliet, V.; Bigoglio, G.; Omenetto, N.; Parm, L.; Grenthe, I. *J. Chem. Soc. Faraday Trans.* **1995**, *91(15)*, 2275.)

concentration of UO_2^{2+} and other ions in the solution also affect the emission. These effects are called quenching and will be discussed in the following section.

1.3.2 Quenching

Energy can be transfered from the excited $*UO_2^{2+}$ to other species through interaction. This process is called quenching. When the energy acceptor is involved in a chemical reaction, the process is called chemical quenching. If no chemical reaction occurs, it is referred to as physical quenching. The photosensitized reaction involves chemical quenching processes.

In the quenching processes, if the concentration of the quenching substance remains constant and the quencher only interacts with the active excited state, the kinetic equation for the quenching process can be expressed as:[63]

$$\phi^0/\phi = 1 + k_q\tau[Q] \qquad (1.3.2\text{-}1)$$

This equation is known as the Stern-Volmer equation, where $K_{SV} = k_q\tau$ is the Stern-Volmer constant, [Q] is the concentration of quencher Q, ϕ^0 and ϕ are the emission quantum yields without and with quencher Q, respectively,

and k_q is the quenching rate constant and τ is the lifetime in the absence of Q.

Metal ions, such as Ti^+, Ag^+, Hg_2^{2+} and Fe^{2+} can quench $*UO_2^{2+}$ very efficiently. Most other metal ions have relatively smaller quenching constants. **Table** 1.3.2-1 shows the quenching rate constants for $*UO_2^{2+}$ by some metal ions.

Quenching by metal ions is shown to be a dynamic process, and the correlation of the logarithm of the quenching rate with the metal ion ionization potential suggests that intermolecular electron transfer is the predominant mechanism.[65] The medium is important to the quenching; different media and temperatures can strongly affect the quenching.[66,67,68,69,70,71]

Quenching by anions, such as CN^-, F^-, Cl^-, Br^-, I^- and SCN^-, is also considered to proceed via an electron transfer mechanism.[72] Some quenching constants for $*UO_2^{2+}$ by anions are shown **Table** 1.3.2-2.

Quenching by organic substances can involve physical and/or chemical mechanisms.[73] Physical quenching by aromatic species occurs very efficiently.[74,75] In this case, there is no kinetic isotopic effect, i.e., $k_q(C_6H_6)/k_q(C_6D_6) = 1.0/1.0$, and it is suggested to be an electron donor-acceptor interaction.[76,77] Recently, Bakac and coworkers reported the occurrence of chemical quenching by aromatic species. They found that benzaldehyde was formed from the photooxidation of toluene and that an isotopic effect of 1.2/1.0 was

Table 1.3.2-1.[78] Quenching constants for UO_2^{2+} by some cations.

Quencher[a]	$k_q(M^{-1}s^{-1})$	Ionization Potential(V)
Ag^+	3.48×10^9	21.5
Ba^{2+}	$< 4 \times 10^3$	35.5
Ce^{3+}	3.05×10^5	33.3
Co^{2+}	9.70×10^6	33.5
Cu^{2+}	2.69×10^6	30.6
Fe^{2+}	6.68×10^8	30.6
Fe^{3+}	$\leq 5.40 \times 10^7$	56.8
Hg_2^{2+}	1.00×10^9	26
Mn^{2+}	3.41×10^6	33.7
Ni^{2+}	5.53×10^6	35.16
Pb^{2+}	3.20×10^7	31.9
Ti^+	$5x10^9$	20.4

a) pH = 2.0-2.5 (HNO_3).

Table 1.3.2-2.[79] Quenching constants for UO_2^{2+} by some anions.[a]

Quencher	$k_q(M^{-1}s^{-1})$	Oxidation Potential(eV)
CN^-	4.7	
F^-	9.3	2.87
Cl^-	7.4×10^3	1.36
Br^-	1.6×10^5	1.07
SCN^-	2.8×10^5	0.77
I^-	2.8×10^5	0.54

a) In 0.67 M H_3PO_4.

observed.[80] In the presence of H_2O_2 and UO_2^{2+}, benzene can also be oxidized to phenol with a quantum yield of 0.70.[44]

Alcohol systems are well-known quenchers of $*UO_2^{2+}$. There are kinetic isotopic effects for alcohols as exemplified by the data in **Table** 1.3.2-3.[43,81]

In alcohol systems, the α-hydrogen atom abstraction mechanism is generally accepted.[82,83] It is notable that 2-methyl-2-propanol or t-butanol, which has no α-hydrogen, exhibit a low value of k_q compared to other alcohols. This feature was a factor in our choice of studying isobutane in detail because the expected alcohol is t-butanol, which is the dominant product and does not continuously react. Ketone and alkene systems were also widely studied. **Table** 1.3.2-4 and **Table** 1.3.2-5 list kinetic data of some ketones and alkenes.

It is found that the quenching constants are strongly affected by solvent. The quenching constants of alkenes in H_2O are about 1.7 times those found in H_2O/CH_3CN solution. Alkanes usually have smaller quenching constants. **Table** 1.3.2.-6 lists these data for some alkanes.

The quenching constant is usually obtained by measuring the emmision decrease after the addition of quencher. It reflects the total effect of physical and chemical quenching. Different substances have different ratios for these two quenching processes. Chemical quenching is usually obtained by the measurement of the quantum yield of the

Table 1.3.2-3.[84] Quenching constants for UO_2^{2+} by some alcohols.[a]

Quencher	K_{SV}(in H_2O) (M^{-1})	$k_q x10^6$ ($M^{-1}s^{-1}$)[b]
CH_3CH_2OH	45.1	18.8
$(CH_3)_2CHOH$	95.7	39.9
$(CD_3)_2CDOD$	42.4	17.7
$(CH_3)_3COH$	2.06	0.86
cyclo-C_4H_7OH	139	57.9
cyclo-C_5H_9OH	147	61.5
cyclo-$C_6H_{11}OH$	201	83.7
$C_6H_5CH_2OH$	3587	1494.8
$(C_6H_5)_2CHOH$	2859	1191.5

a) $[UO_2^{2+}]$= 0.05 M; pH = 3 ($HClO_4$).

b) Calculated from $K_{SV} = k_q\tau$; τ = 2.4 μs.

Table 1.3.2-4.[73] Stern-Volmer constants for quenching of UO_2^{2+} by some ketones and alkenes.[a]

Quencher	$K_{SV}(M^{-1})$
Cyclopent-2-enone	13.3
$(CH_3)_2C=CHCOCH_3$	416
3,4,4,-trimethlcyclohex-2-enone	210
3,5-Dimethylcyclohex-2-enone	232
$CH_3CH=C(CH_3)CH$	800
Cycloheptatriene	2320
Cyclopentene	240
Cyclohexene	1320

a) Aqueous acetone solution (48% acetone v/v).

Table 1.3.2-5.[44] Quenching constants for UO_2^{2+} by some alkenes.[a]

Quencher	$k_q x10^{-5} (M^{-1}s^{-1})^a$
3,3-dimethyl-1-butene	26.9
1-hexene	32.8
trans-3-hexene	77.5
c-hexene	176
2,3-dimethyl-2-butene	410

a) 1:1 H_2O/CH_3CN solution.

Table 1.3.2-6.[44] Quenching constants for UO_2^{2+} by some alkanes.[a]

Quencher	$k_q x 10^{-6} (M^{-1}s^{-1})$
methane	<0.1
ethane	1.4
butane	2.6
cyclopentane	2.4

a) 0.6 M H_3PO_4 aqueous solution.

chemical product. Alcohols usually have a higher ratio of chemical to physical quenching.

In addition to the quenching properties of the excited uranyl ion by other substances, the properties of excited uranyl ion itself were also widely studied. Acid concentration strongly affects $*UO_2^{2+}$ emission intensity, the emission intensity decreasing with increasing pH. Under some conditions, a biexponential decay has been found.[85,86] For example, when the pH increases to about 3, or in the presence of some ligands, such as $H_2PO_4^-$, biexponental decay occurs.[87] Some ligands, such as F^- and $H_2PO_4^-$, can strongly increase the $*UO_2^{2+}$ emission intensity and its lifetime rather than decrease it. This was explained in terms of their substitution for coordinated water molecules, which are considered stronger quenchers.[22] Molecular oxygen has no obvious effect on the lifetime of $*UO_2^{2+}$,[22,23] and this makes it possible to employ UO_2^{2+} as a "photo-catalyst" with oxygen as the real oxidant.

Based on the emission properties of the excited uranyl ion, two major mechanisms were suggested by two research groups. Formosinho's group proposed that the first step reaction of excited uranyl ion involves a fast equilibrum of $*UO_2^{2+}$ with H_2O, and the emission comes from $*UO_2^{2+}$ and the equilibrated species. Equilibrum constants for $*UO_2^{2+}$ with H_2O have been estimated from their experimental data by Formosinho and co-workers and these data are shown below:[88,89,90,91]

$$*UO_2^{2+} + H_2O \rightleftharpoons *UO_2OH^+ + H^+ \qquad K_1 = 1x10^{-2} \qquad (1.3.2\text{-}2)$$

$$*UO_2OH^+ + H_2O \rightleftharpoons *UO_2(OH)_2 + H^+ \qquad K_2 = 4x10^{-3} \qquad (1.3.2\text{-}3)$$

$$*UO_2(OH)_2 + H_2O \rightleftharpoons *UO_2(OH)_3^- + H^+ \qquad K_3 = 1x10^{-3} \qquad (1.3.2\text{-}4)$$

Figure 1.3.2-1 shows the distribution of hydrolysis products of $*UO_2^{2+}$. From this data, $*UO_2^{2+}$ seems to exhibit a higher degree of hydrolysis than UO_2^{2+}, but at pH = 1, $*UO_2^{2+}$ is the dominant excited species.

Marcantonatos proposed that the first step reaction of excited uranyl is also a fast equilibrum of $*UO_2^{2+}$ with H_2O, but it is not a hydrolysis process. The author suggested that it is a hydrogen abstraction process:[92,93,94]

$$*UO_2^{2+} + H_2O \rightleftharpoons *UO_2H^{2+} + \cdot OH \qquad (1.3.2\text{-}5)$$

and then $*UO_2H^{2+}$ releases its proton:

$$*UO_2H^{2+} + H_2O \rightleftharpoons *UO_2^+ + H_3O^+ \qquad (1.3.2\text{-}6)$$

The mechanism of the decay (or quenching) of excited uranyl ion is important to understand with respect to its photochemical and photophysical processes, and it is still

an open question. From the experiments reported here, a great deal of information about the chemical quenching

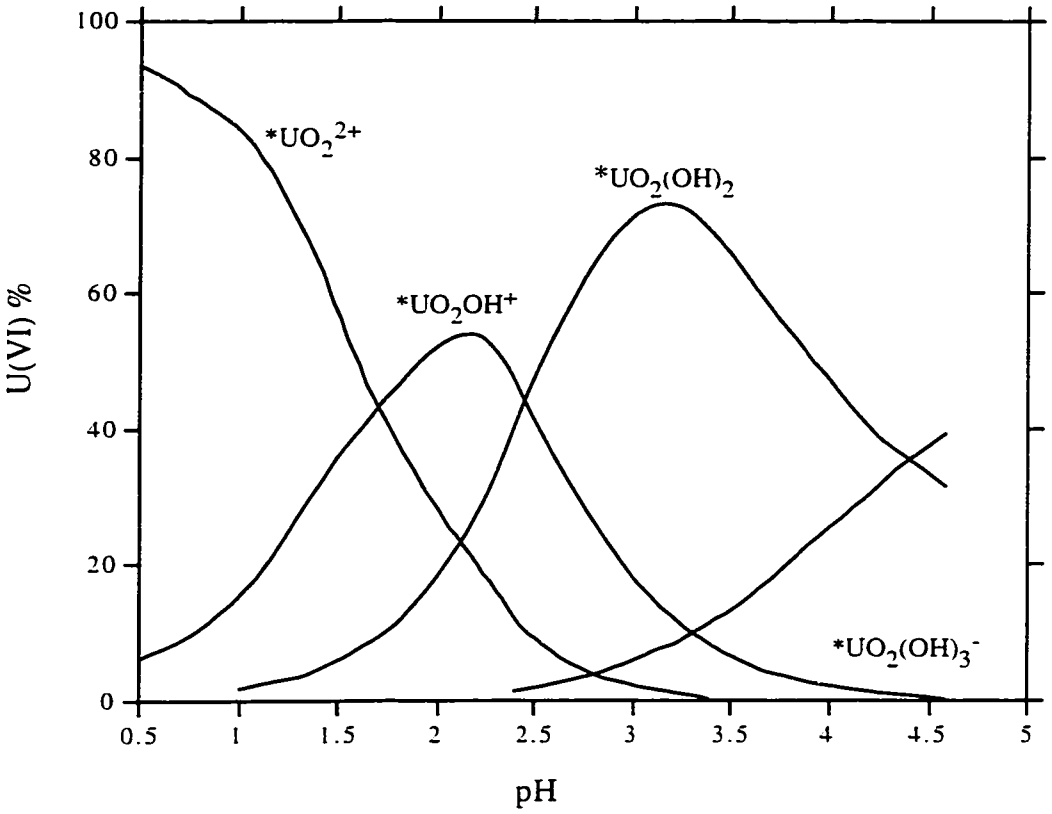

Figure 1.3.2-1. Distribution of hydrolysis products of $*UO_2^{2+}$.
$[UO_2^{2+}] = 0.1$ M.
(after reference: Miguel, M. G. Formosinho, S. J.; Cardoso, A. C. *J. Chem. Soc. Faraday Trans. 1* **1984**, *80*, 1537.)

process was obtained. Based on this information and the information regarding emission, oxygen-exchange and γ-radiation, the mechanism will be discussed in more detail in Chapter 3.

1.3.3 Photooxidation of Some Organic Substances

A photocatalytic system using solar energy and molecular oxygen would be ideal because both oxygen and sunlight are readily available. For this purpose, excited uranyl ion has many advantages such as a long lifetime, a high standard reduction potential, good absorption of visible light by its ground state and is not quenched by oxygen. For these reasons it has been widely investigated for use in the oxidation of many organic substances, such as alcohols, ketones, acids, alkenes and so on.

In photochemistry, the quantum yield(ϕ) is a very important parameter both in theoretical and applied studies. The quantum yield is a measure of the efficiency of use of absorbed photons. It is the ratio of the number of moles of the product formed to the number of moles of photons absorbed at a given wavelengh. In the absence of chain reactions, the value of ϕ value can range from zero to one.

Alcohols with α-hydrogens can be readily oxidized by $*UO_2^{2+}$, giving as final products a ketone or a carboxylic

acid, with $U^{4+}(aq)$ also being formed.[84] When CH_3OH is used, CO_2 is the final product. In the presence of O_2, $U^{4+}(aq)$ will be reoxidized back to its original state of UO_2^{2+}.[95,96,97] **Table** 1.3.3-1 shows the quantum yields of the oxidation of some alcohols by $*UO_2^{2+}$.

From the isotopic effects on the quantum yields, an α-hydrogen abstraction mechanism is proposed:

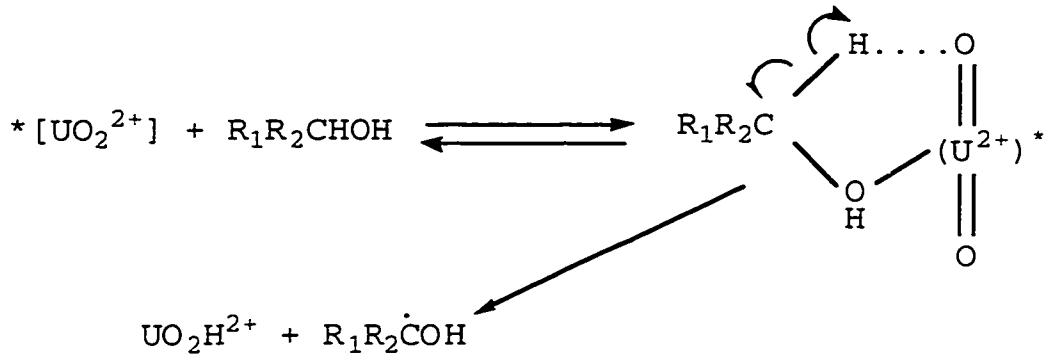

(1.3.3-1)

UO_2H^{2+} then decomposes to UO_2^{+}, and the UO_2^{+} further disproportionates to UO_2^{2+} and $U^{4+}(aq)$. The quantum yield for $U^{4+}(aq)$ is about 0.5-0.6.[98] The free radical $R_1R_2OH\,C\cdot$ will be contineously oxidized by UO_2^{2+} or disproportionate to the corresponding ketone and alcohol.[84] In the case of a primary alcohol, it is first oxidized to an aldehyde and then to a carboxylic acid.[67] The α-hydrogen abstraction mechanism is also supported by e.s.r. studies.[99]

Table 1.3.3-2 shows the ionization potential and C-H bond energy of some alcohols.

Table 1.3.3-1.[77] Quantum yields in photooxidation of alcohols by $*UO_2^{2+}$.[a]

Alcohol	ϕ[b]
C_2H_5OH	0.31
C_2H_5OD	0.30
C_2D_5OD	0.14
$(CH_3)_2CHOH$	0.34
$(CD_3)_2CDOD$	0.18
n-butyl alcohol	0.36
isobutyl alcohol	0.36
sec-butyl alcohol	0.36
tert-butyl alcohol	0.02

a) $[UO_2^{2+}]$ = 0.02M; [alcohol] = 0.06 M; irradiation by 405 nm.

b) Quantum yields obtained by the loss of alcohols.

Table 1.3.3-2.[92] Ionization potentials and bond energies of some alcohols.

Alcohol	Ionization potential(eV)	C-H bond Energy(kJ mol^{-1})
Methanol	10.85 (250)[a]	393 (94.3)[a]
Ethanol	10.50 (242)	386 (92.1)
Isopropanol	10.1 (233)	379 (90.4)
t-Butanol	9.7 (224)	416 (99.3)

a) kcal/mol.

It is found that a plot of $\log(k_q)$ versus bond energy is linear but a plot of $\log(k_q)$ versus ionization potential is not. These results support an α-hydrogen abstraction mechanism rather than an electron transfer process. In the quenching of $*UO_2^{2+}$ by alcohols, chemical quenching accounts for about 20%, but this percentage is different for different substances. In the case of benzene, it is close to zero. **Table** 1.3.3-3 shows the physical and chemical quenching constants of some alcohols.

Photooxidations of formaldehyde and arylaldehydes have been reported.[100,101] The quantum yields for arylaldehydes are about 0.16 and increase when there is a deactivating substituent group, such as the -NO2 group, on the aryl ring. The following mechanism is suggested:

$$*[UO_2^{2+}] + ArCHO \longrightarrow UO_2^{+} + Ar\dot{C}O + H^{+} \qquad (1.3.3\text{-}2)$$

$$2Ar\dot{C}O \longrightarrow ArCOCOAr \qquad (1.3.3\text{-}3)$$

$$ArCOCOAr + H_2O \longrightarrow ArCHO + ArCOOH \qquad (1.3.3\text{-}4)$$

The oxidation of carboxylic acids leads to the release of CO_2.[102,103,104] In this case, the quantum yields are about 0.5, and the following mechanism has been suggested:[105]

Table 1.3.3-3.[106] Physical and chemical quenching constants of some alcohols.[a]

Alcohol	Physical quenching $k_q \times 10^{-7} (M^{-1}s^{-1})$	Chemical quenching $k_q \times 10^{-7} (M^{-1}s^{-1})$
Methanol	57.4	14.0
Ethanol	112.0	28.4
Isopropanol	176.0	55.0
t-Butanol	8.19	<0.007

a) In 1M H_3PO_4.

$$*[UO_2^{2+} \cdot (HCOO^-)_2] \longrightarrow UO_2^+ + \cdot COO^- + HCOO^- + H^+ \quad (1.3.3\text{-}5)$$

$$\cdot COO^- + H^+ \longrightarrow \cdot COOH \quad (1.3.3\text{-}6)$$

$$2 \cdot COOH \longrightarrow HCOOH + CO_2 \quad (1.3.3\text{-}7)$$

Most of the above photooxidation processes have been investigated as a means to obtain $U^{4+}(aq)$, and some of them have been suggested for use in the reprocessing of spent nuclear fuel.[96,105,107]

The studies of the photooxidation of hydrocarbons using uranyl ion began relatively late. Early studies in this area have been done by Balzani and coworkers,[30] However the oxidation of olefins by the $*UO_2^{2+}$ was not observed. Sato and co-workers first reported the photooxidation of an olefin sensitized by $*UO_2^{2+}$.[108] They investigated the oxidation of trimethylethylene in pyridine solution with uranyl acetate as the catalyst and proposed a mechanism involving free radicals as shown below:

$$UO_2^{2+} \xrightarrow{h\upsilon} *UO_2^{2+} \xrightarrow{H_2O} UO_2H^{2+} + \cdot OH \quad (1.3.3\text{-}8)$$

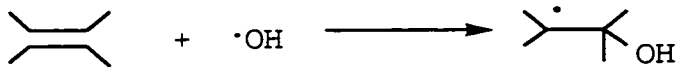

(1.3.3-9)

(1.3.3-10)

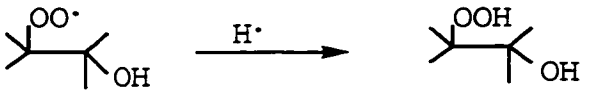

(1.3.3-11)

Subsequently, Sato and co-workers studied this system further and found some phenomena that were contradictory to the above proposed mechanism. For example, the reaction was not affected by free radical scavengers (such as tri-t-butylphenol).[109] Thus the following mechanism, called long-range electron-transfer, was proposed:

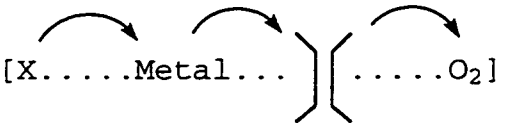

(1.3.3-12)

where X = ligand. It was suggested that this transfer takes place within the coordination sphere of the metal ion. The product is the corresponding alkane with the substitution group X. In the case of uranyl ion, they proposed that the reaction was carried out through the following intermediate:

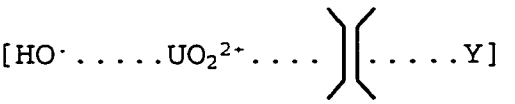

(1.3.3-13)

where Y is the substitution group. Mooney and co-workers studied another alkene system using uranyl-polymolybdate(IV) as the catalyst.[110,111] They irradiated a very dilute aqueous solution of cyclohexene (about 1-2 mM) with light from a mercury-xenon lamp. Their proposed mechanism involved a carbonium radical:

(1.3.3-14)

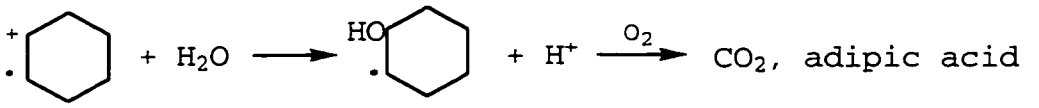

(1.3.3-15)

where $Mo^{VI} = Mo_mO_y^{p-}$. Park and Tomiyasu studied this catalyst in greater detail.[112] They observed a high quantum yield. When [$HClO_4$] = 0.92 M, [1,4-cyclohexadiene] = 0.256 M, the quantum yield for U^{4+}(aq) was 0.273. They proposed the mechanism shown in **Figure** 1.3.3-1. An electron-transfer process was proposed to take place within the exciplex:

$$[^{*}UO_2^{2+}\cdots Q] \underset{k_{-2}}{\overset{k_2}{\rightleftharpoons}} [UO_2^{+}\cdots Q^{+}] \qquad (1.3.3\text{-}16)$$

They also studied the relationship of the Gibbs-energy of

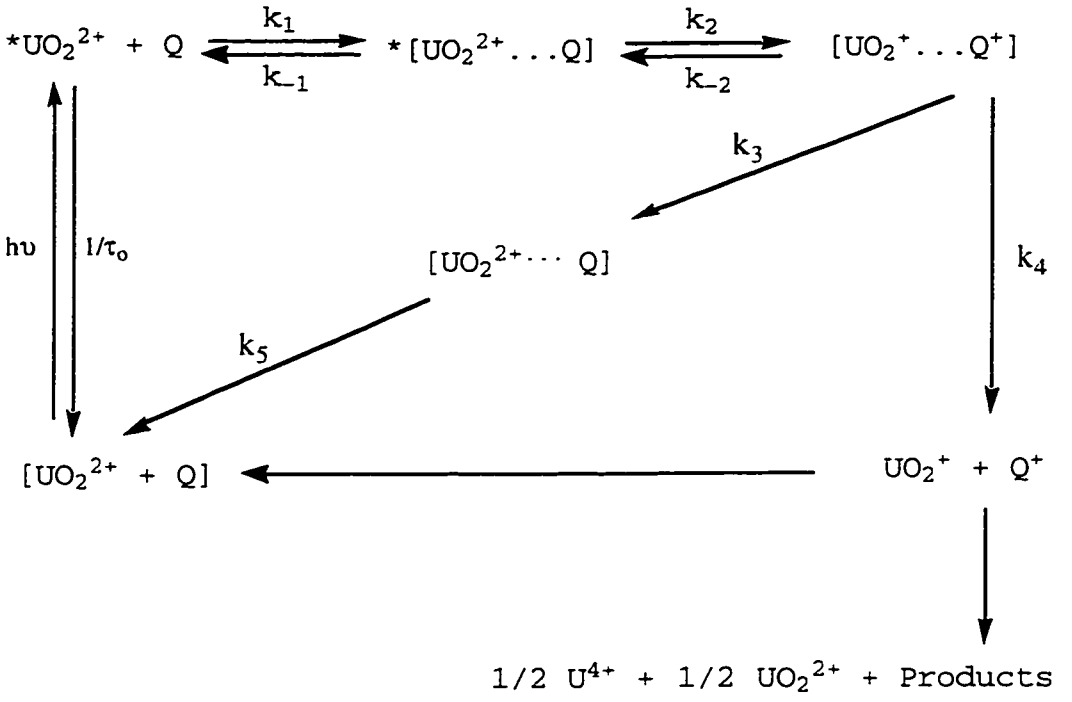

Figure 1.3.3-1. Proposed mechanism for the photooxidation of cyclohexene.

electron transfer (ΔG) with the $\log(k_q)$. It is found that the slope of $\log(k_q)$ versus ΔG was usually smaller than that expected from the Rehm-Weller correlation.[113,114] This feature has also been found by other researchers. Rehm and Weller predicted that for an exergonic complete electron transfer, the plot of $\log(k_q)$ versus ΔG should show a slope of $(-3/2)RT$ (about 16.9/eV). That the observed slope is usually smaller in the quenching process of $^*UO_2^{2+}$ by an olefin than is predicted suggests that the electron-transfer from olefin to $^*UO_2^{2+}$ is not a likely rate-determining step. Hydrogen abstraction still seems to be important with the alkenes.

Shul'pin and Nizova[115] first reported research work on an alkane system. In their paper, cyclohexane, toluene and ethylbenzene were irradiated separately using a high-pressure mercury lamp, and UO_2Cl_2 served as the catalyst in the presence of oxygen in a solution of CH_3COOH. Cyclohexanone, cyclohexanol, benzaldehyde and acetophenone were produced, respectively. They also reported work on photolysis of methane saturated in a UO_2Cl_2-CH_3CN solution. This acetonitrile solution was irradiated with a 1000 watt high-pressure mercury lamp for 3.5 h resulting in the production of 3.5×10^{-5} M formaldehyde.

Colmenarers reported, [116] in a patent, that C_1-C_8 hydrocarbons were found when a mixture of CO, C_2H_4 and C_2H_6 was irradiated using a mercury-xenon lamp in the presence of a light-transparent SiO_2 aerogel doped with UO_2^{2+}.

During the courses of the studies for this thesis, Bakac and coworkers reported that $*UO_2^{2+}$ emmision was quenched by methane, ethane, butane, 2,2,3,3-tetramethybutane, n-pentane, n-hexane, cyclopentane and cyclohexane in aqueous phosphoric acid media and/or 1:1 H_2O/CH_3CN solutions.[44] They also measured the products for the photooxidation of cyclopentane in aqueous H_3PO_4 system and observed cyclopentanone as the only product. No quantum yields were given and so the efficiencies of these processes remain unknown.

In the photocatalyzed oxidation of alkanes, other compounds such as a rhodium system,[117,118] titanium,[119] and $(SiW_{12}O_{40})^{4-}$ loaded titanium[120] have been also investigated by some researchers.[121] As these systems usually have low efficiencies, or have very complicated catalyst recycling processes, and/or they are not "real" recycling processes, progress in these areas was limited.

Although a great deal of work has been done in the photochemistry and photophysics for the uranyl ion, the studies on uranyl ion sensitized photooxidation of alkanes has just started. The quantum yields of many alkanes, the effects of the conditions, other solvents and other ions, and the mechanisms are still unknown. Our work has focussed on several alkanes in order to identify the photo-products in detail, to measure the quantum yield for 414 nm radiation, and to elucidate the effects of various parameters on their yields. These alkanes are drawn from the cotegories of branched, cyclic and straight chain.

[1] Belford, R. L. *J. Chem. Phys.* **1960**, *34*, 318.

[2] Belford, R. L.; Belford, G. *J. Chem. Phys.* **1961**, *3*, 1330.

[3] Newman, J. B. *J. Chem. Phys.* **1965**, *43*, 1691.

[4] McGlynn, S. P.; Smith, J. K.; Neely, W. C. *J. Chem. Phys.* **1961**, *35*, 105.

[5] Belford, R. L. *J. Chem. Phys* **1960**, *34*, 1691.

[6] Fleming, J. E.; Lynton, H. *Chem. and Ind.* **1960**, 1415.

[7] McGlynn, S. P.; Smith, J. K. *J. Mol. Spec.* **1961**, *6*, 164.

[8] Baes, C. F.; Meyer, N. *Inorg. Chem.* **1962**, *1*, 780.

[9] Gusta, R. L.; Richard, C.; Martell, A. E. *J. Am. Chem. Soc.* **1960**, *82*, 1526.

[10] Cole, G. L.; Eyring, E. M.; Rampton, D. T.; Silzars, A.; Jensen, R. P. *J. Phys. Chem.* **1967**, *71*, 2771.

[11] Eliet, V; Bidoglio, G; Omenetto, N.; Parma, L.; Grenthe, I. *J. Chem. Soc., Faraday Trans.* **1995**, *91*, 2275.

[12] Gayer, K. H.; Leider, H. *J. Am. Chem. Soc.* **1955**, *77*, 1448.

[13] Ricci, J. E.; Loprest, F. J. *J. Am. Chem. Soc.* **1955**, *77*, 2119.

[14] Rush, R. M.; Johnson, J. S.; Kraus, R. M. ORNL-3278, (1963).

[15] Rush, R. M.; Johnson, J. S.; Kraus, R. M. *Inorg. Chem.* **1962**, *1*, 378.

[16] Baes, J. C. F.; Mesmer, R. E. *The Hydrolysis of Cations* ; Wiley: New York, 1976; p 178.

[17] Kraus, K. A.; Nelson, F. *J. Am. Chem. Soc.* **1949**, *72*, 2517.

[18] Hodge, H. C. *Uranium Plutonium Transplutonic Elements* ; Wiley: New York, 1973; Chapter 2.

[19] Bagnall, K. in *Comprehensive Coordination Chemistry*; Wilkinson, G.; Gillard, R. D.; Mccleverty, J, A., Eds.; Pergamon: Oxford, 1987; Chapter 40.

[20] Chernyaev, I. I. *Compounds of Uranium*; Daiel Davey: New York, 1966.

[21] Sillén, L. G.; Martell, A. E. In *Stability Constants of Metal-Ion Complexes*; The Chemical Society: London, 1964.

[22] Moriyasu, M.; Yokoyama, Y.; Ikeda, S. *Inorg. Chem.* **1977**, *39*, 2199.

[23] Billing, R.; Zakharova, G. V.; Atabekyan, L. S.; Hennig, H. *J. Photochem. Photobiol. A* : Chem., **1991**, *59*, 163.

[24] Hardwick, T. J. U.S. Patent 4 428 911, 1984.

[25] Abramovilch, S.; Rabani, J. *J. Phys. Chem.* **1976**, *80*, 1562.

[26] Alcock, N. W. *J. Chem. Soc. (A)* **1968**, 1588.

[27] Petit, N. *Properties de l'uranium(III) et de l'uranium(IV)* (Nucleaires de Fountenay-aux- Roses) CEA-BIB-141 (1969).

[28] Elving, P. J.; Krivis, A. F. *J. Inorg. Nucl. Chem.* **1959**, *11*, 234.

[29] Collect, C. *J. Chem. Soc., Chem. Commun.* **1964**, *29*, 905.

[30] Balzani, V.; Bolletta, F.; Gandolfi, M. T.; Maestri, M. *Top. Curr. Chem.* **1978**, *75*, 1.

[31] Sato, A. *Bull. Chem. Soc. Jpn.* **1967**, *40*, 2107.

[32] Nelson, F; Kraus, K. A. *J. Am. Chem. Soc.* **1951**, *73*, 2157.

[33] Bell, J. T.; Friedman, H. A.; Billings, M. R. *J. Inorg. Nucl. Chem.* **1974**, *36*, 2563.

[34] Gordon, G.; Taube, H. *Inorg. Chem.* **1961**, *16*, 272.

[35] Newton, T. W.; Baker, F. B. *Inorg. Chem.* **1965**, *4*, 1166.

[36] Ekstrom, A. *Inorg. Chem.* **1974**, *13*, 2237.

[37] McEwen, D. J.; Vries, T. D. *Can. J. Chem.* **1957**, *35*, 1225.

[38] Neta, P.; Huie, R. E.; Ross, A. B. *J. Phys. Chem. Ref. Data* **1988**, *17*, 1027.

[39] Hensler, E.; Leronz, W. J. In *Standard Potentials in Aqueous Solution*; Bard, A. J.; Parsons, R.; Jordan, J., Eds.; Marcel Dekker: New York, 1985; Chap 21.

[40] Bakac, A.; Espenson, J. H. *Inorg. Chem.* **1995**, *34*, 1730.

[41] Kemp, T. J.; Martins, L. J. A. In *Techniques and Applications of Fast Reactions in Solution* ; Gettins, W. J.; Wyn-Jones, E. D., Eds.; Reidel Dordrecht: Holland 1979; p 549.

[42] Guha, S. N.; Moorthy, P. N.; Rao, K. N. *Radiat. Phys. Chem.* **1987**, *29*, 425.

[43] Azenha, M. E. D. G.; Burrows, H. D.; Formosinho, S. J.; Miguel, M. G. M. *J. Chem. Soc., Faraday Trans. 1* **1989**, *85*, 2625.

[44] Wang, W.; Bakac, A.; Espenson, J. H. *Inorg. Chem.* **1995**, *34*, 6034.

[45] Halpern, J.; Smith, J. G. *Can. J. Chem.* **1956**, *34*, 1419.

[46] Hassan, R. M. *J. Coord. Chem.* **1992**, *27*, 255.

[47] Gogolev, A. V.; Makarow, I. E.; Fedoseer, H. A.; Pikae, A. K. *High Energy Chem.* **1986**, *20*, 229.

[48] Gordon, G.; Taube, H. *J. Inorg. Nucl. Chem.* **1961**, *19*, 189.

[49] Gaziev, S. A.; Gorshkov, N. G.; Mashriov, L. G.; Suglobov, D. N. *Radiokhimiya* **1986**, *28(6)*, 755.

[50] Gaziev, S. A.; Gorshkov, N. G.; Mashriov, L. G.; Suglobov, D. N. *Radiokhimiya* **1986**, *28(6)*, 764.

[51] Gaziev, S. A.; Gorshkov, N. G.; Mashriov, L. G.; Suglobov, D. N. *Radiokhimiya* **1986**, *28(6)*, 770.

[52] Gaziev, S. A.; Gorshkov, N. G.; Mashriov, L. G.; Suglobov, D. N. *Inorg. Chem. Acta* **1987**, *139*, 345.

[53] Okuyama, K.; Yshikawa, Y.; Kato, Y.; Fukutomi, H. *Bull. Res. Lab. Nucl. React. Jpn.* **1978**, *3*, 39.

[54] Gaziev, S. A.; Mashriov, L. G.; Suglobov, D. N. *Radiokhimiya* **1989**, *31(2)*, 48.

[55] Rofer-Depoorter, C. K.; Depoorter, G. L. *J. Inorg. Nucl. Chem.* **1978**, *40*, 2049.

[56] Gorshkov, N. G.; Zabelinskaya, N. K. *Radiokhimiya* **1992**, *34(3)*, 78.

[57] Bell, J. T.; Biggers, R. E. *J. Mol. Spec.* **1965**, *17*, 247.

[58] Bell, J. T.; Biggers, R. E. *J. Mol. Spec.* **1967**, *22*, 262.

[59] Bell, J. T.; Biggers, R. E. *J. Mol. Spec.* **1968**, *25*, 312.

[60] Rabinowitch, E.; Belfort, R. L. *Spectroscopy and Photochemistry of Uranyl Compounds;* Pergamon: Oxford, 1964.

[61] Jatkar, S. K. K.; Khedekar, A. V.; Mukhedkar, A. J. *J. of Univ. of Poona* **1968**, *34*, 66.

[62] Calvert, J. G.; Pitts, J. N. *Photochemistry*; Wiley: New York, 1966; p 173.

[63] Barltrop, J. A.; Coyle, J. D. *Principles of Photochemistry;* Wiley: Chichester, England, 1978; Chapter 4.

[64] Moulin, C.; Decambox, P. *Anal. Chem.* **1995**, *67*, 348.

[65] Burrows, H. D.; Formosinho, S. J.; Miguel, M. G. M; Coelho, F. P. *J. Chem. Soc., Faraday Trans.1* **1976**, *72(1)*, 49.

[66] Matsushima, R.; Fuijmori, H.; Sakuraba, S. *J. Chem. Soc., Faraday Trans. 1* **1974**, *70*, 1702.

[67] Katsumura, Y.; Abe, H.; Yotsuyanagi, T.; Ishigure, K. *J. Photochem. Photobiol. A.: Chem.*, **1989**, *50*, 183.

[68] Sandhu, S. S.; Brar, A. S.; Sarpal, A. S. *Indian J. Chem. Sect. A* **1978**, *16*, 587.

[69] Sandhu, S. S.; Brar, A. S.; Sarpal, A. S. *Indian J. Chem. Sect. A*,**1979**, *18*, 19.

[70] Sandhu, S. S.; Brar, A. S.; Sarpal, A. S. *Indian J. Chem. Sect. A* **1980**, *19*, 413.

[71] Sandhu, S. S.; Brar, A. S.; Sarpal, A. S. *Indian J. Chem. Sect. A* **1980**, *19*, 902.

[72] Yokoyama, Y.; Moriyosu, M; Ikeda, S. *Inorg. Chem.* **1976**, *38*, 1329.

[73] Ahmad, M.; Cox, A.; Kemp, T. J.; Sultana, O. *J. Chem. Soc., Perkin 2* **1975**, 1867.

[74] Miguel, M. G. M.; Formosinho, S. J.; Leitão, M. L. P. *J. Photochem.* **1986**, *33*, 209.

[75] Sidhu, M. S.; Bhatia, P. V. K.; Anju; Singh, R. J. *Proc. Nat. Acac. Sic. India.* **1994**, *64(A)*, 453.

[76] Matsushima, R.; Sakuraba, S. *J. Am. Chem. Soc.* **1971**, 7143.

[77] Matsushima, R. *J. Am. Chem. Soc.* **1972**, 6010.

[78] Burrows, H.D.; Formosinho, S. J.; Miguel, M. G. M; Coelho, F. P. *J. Chem. Soc., Faraday Trans.1* **1976**, *72*, 163.

[79] Matsushima, R.; Fuijmori, H.; Sakuraba, S. *J. Chem. Soc., Faraday Trans. 1* **1974**, *70*, 1702.

[80] Mao, Y.; Bakac, A. *J. Phys.. Chem.* **1996**, *100*, 4219.

[81] Hill, R. J.; Kemp, T. J.; Allen, D. M.; Cox, A. *J. Chem. Soc., Faraday Trans. 1* **1974**, *70*, 847.

[82] Burrows, H. D.; Formosinho, S. J. *J. Chem. Educ.* **1978**, 125.

[83] Sergeeva, G. I. *Khimiya Vysokikh Energii* **1974**, *8(1)*, 38.

[84] Cunningham, J.; Sirjaranai, S. *J. Photochem. Photobiol. A: Chem.*, **1990**, *55*, 219.

[85] Marcantonatos, M. D. *Inorg. Chim. Acta* **1978**, *26*, 41.

[86] Marcantonatos, M. D. *Inorg. Chim. Acta* **1977**, *25*, L101.

[87] Zhou, P.; Wang, Z. L.; Xu, Y. Z.; Zhang, L.; Wang, Y. B. *J. Radioanal. Nucl. Chem., Letters* **1993**, *175(2)*, 81.

[88] Formosinho, S. J.; Miguel, M. G. M. *J. Chem. Soc., Faraday Trans. 1* **1984**, *80*, 1717 (part 1).

[89] Miguel, M. G. M.; Formosinho, S. J.; Cardoso, A. C. *J. Chem. Soc., Faraday Trans. 1* **1984**, *80*, 1735 (part 2).

[90] Miguel, M. G.; Formosinho, S. J.; Cardoso, A. C. *J. Chem. Soc., Faraday Trans. 1* **1984**, *80*, 1745 (part 3).

[91] Burrows, H. D.; Cardoso, A. C.; Formosinho, S. J.; Miguel, M. G. M. *J. Chem. Soc., Faraday Trans. 1* **1985**, *81*, 49 (part 4).

[92] Marcantonatos, M., *J. Chem. Soc., Faraday Trans. 1* **1979**, *75*, 2273.

[93] Marcantonatos, M., *J. Chem. Soc., Faraday Trans. 1* **1980**, *76*, 1093.

[94] Marcantonatos, M., *J. Chem. Soc., Faraday Trans. 1* **1989**, *85*, 2481.

[95] Nagaishi, R.; Katsumura, Y.; Ishigure, K.; Aoyagi, H.; Yoshida, Z.; Kimura, T. *J. Photochem. Photobiol. A: Chem.*, **1996**, *96*, 45.

[96] Lu, Z.; Chen, X; Yuan, S.; Li, S.; Zhang, C. *He Huaxue Yu Fangshe Huaxue* **1982**, *4*, 161.

[97] Xu, H.; Hu, J.; Zhang, X; Duan, Y.; Zhang, R. *He Huaxue Yu Fangshe Huaxue* **1983**, *5*, 266.

[98] Bell, J.; Buxton, S. R. *Inorg. Chem.* **1974**, *36*, 1575.

[99] Greatorex, D.; Hill, R. J.; Kemp, T. J.; Stone, T. J. *J. Am. Chem. Soc.* **1972**, *68*, 2059.

[100] Wang, T.; Qiu, L.; Zhang, S. *J. Nucl. Radiochem.* **1985**, *7*, 17.

[101] Matsushima, R.; Mori, K.; Suzuki, M. *Bull. Chem. Soc. Jpn.* **1976**, *49*, 38.

[102] Heckler. G. E.; Taylor, A. E.; Jensen, C.; Percival, D.; Jensen, R.; Fung, P. *J. Phys. Chem.* **1963**, *67*, 1.

[103] Balzani, V; Carassiti, V. *Photochemistry of Coordination Compounds*; Academic: London, 1970; p 289

[104] Norton, B. M. *Ohio J. Sci.* **1966**, *66*, 42.

[105] Zhang, X.; Hu, J.; Zhou, Z.; Duan, Y.; Xu, H; Zhang, R. *He Huaxue Yu Fangshe Huaxue* **1985**, *7(3)*, 142.

[106] Sergeeva, G.; Ghibisov, A.; Levshin, L.; Karyakin, A. *J. Chem. Soc., Commun.* **1974**, 159.

[107] Depoorter, G. L. *J. Inorg. Nucl. Chem.* **1978**, *40*, 1895.

[108] Murayama, E; Sato, T. *Bull. Chem. Soc. Jpn.* **1978**, *51*, 3022.

[109] Murayama, E.; Kokda, A.; Sato, T. *J. Chem. Soc., Perkin Trans. 1* **1980**, 947.

[110] Mooney, W.; Chauveau, F.; Tran-Thi, T.; Folcher, G. *J. Chem. Soc., Perkin Trans. 2* **1988**, 1479.

[111] Mooney W.; Folcher, G.; Tran-Thi, T.; Folcher, G. *Inorg. Chim. Acta* **1985**, *110*, 119.

[112] Park, Y. Y.; Tomiyasu, G. *J. Photochem. Photobiol. A: Chem.* **1992**, *64*, 25.

[113] Rehm, D.; Weller, A. *Ber Bunsenges. Phys.* **1969**, *73*, 834.

[114] Rehm, D.; Weller, A. *Isr. J. Chem.* **1970**, *8*, 259.

[115] Nizova, G. V.; Shul'pin, G. B. *J. General Chem.* **1991**, *60*, 1895.

[116] Colmenares, C.; Calif, A. U. S. Patent 5 030 607, 1991.

[117] Sakakura, T.; Tanaka, M. J.; *J. Chem. Soc., Commun.* **1987**, *111*, 758.

[118] Maguire, J. A.; Boese, W. T.; Goldman, A. S. *J. Am. Chem. Soc.*, **1989**, *111*, 7088.

[119] Matthews, R. W. *Pure & Appl. Chem.* **1992**, *64(9)*, 1285.

[120] Gratzel, M.; Thampi, K. R.; Kiwi, J. *J. Phys. Chem.* **1989**, *93*, 4128.

[121] Bergman, R. G. *Science* **1984**, *223*, 902.

2. EXPERIMENTAL

2.1 Solvents and Chemical Reagents

In most of the experiments, Millipore water has been used for the preparation of solutions. It is obtained by further purifying distilled water with a Millipore Super-Q system, as follow. Distilled water from a Barnstead still was circulated through a carbon cartridge (CDFC 02203) to remove organic contaminants, through two mixed strong acid/strong base ion-exchange resin cartridges (CDMB 022 02) to remove inorganic ions, and through a 0.45 μm porosity Durapore Hydrophilic Cartridge filter (CVHL 02T P3) to remove fine particulate matter. The resistivity of the water was checked with a Meg-Ω-Meter resistivity monitor mounted directly onto the system; the resistivity of the water produced was approximately 17 MΩ/cm.

Methanol, acetone (BDH, glass-distilled Omnisolv grade), tetrahydrofuran (THF, BDH AnalaR grade; there is 0.1% quinol in THF to prevent autooxidation by the air) were used as received. ACS grade perchloric acid $HClO_4$ was usually used.

In some cases, to check the effects of impurities, higher grades of perchloric acid, such as BDH Aristar or Alfa ultrapure, were utilized. Hydrogen peroxide, copper sulfate, nitric acid, hydrochloric acid (BDH ACS grade) were used as received. For $K_2S_2O_8$, Fisher Scientific grade, three times recystalized, and SIGMA photographic grade were employed. Aqueous solutions of $K_2S_2O_8$ are not stable and they were kept in a refrigerator to slow down the decomposition since higher temperature accelerates the decomposition of $K_2S_2O_8$. In neutral solution and at room temperature, its half-life is about 170 days.[122]

In the experiments, various sources of uranyl ion have been used. Stock solutions were made from UO_3, which comes from Cameco (see section 2.3). For the calibration, identification and other purposes, the followings were used: $UO_2(ClO_4)_2 \cdot 2H_2O$ (ROC/RIC), $UO_2(NO_3)_2 \cdot 6H_2O$ (May & Baker LTD, Dagenham, England; >99%), $UO_2(SO_4)_2 \cdot 3.5H_2O$ (BDH) and $UO_2(CH_3COO)_2 \cdot 2H_2O$ (Fisher Scientific).

Other chemicals that are not listed here will be discussed in the corresponding sections.

2.2 Photolysis Devices

2.2.1 Photolysis Apparatus

The irradiation system used to investigate the uranyl ion sensitized photooxidation of alkanes is schematically shown

in **Figure** 2.2.1-1. The lamp used for irradiation was a 1000 Watt Hg(Xe) arc lamp (Oriel 6293) located in a fan-cooled universal housing (Oriel 66021) with a condensing lens for beam collimation. The power source was an Oriel 68820 universal 400-1000 W power supply. To filter out infrared and UV light, an 11 cm water cell and a 9.6 cm cell containing an aqueous solution of 0.1 M $CuSO_4$ (cut off at 310 and 640 nm) were placed in front of the beam. In some cases, to further reduce the UV, a colored filter (Schott Glass Technologies INC, GG400) was employed. An interference filter (Edmond Scientific Co., CWL415, λ_{max} = 415 nm and FWHM = 12 nm) was utilized to isolate the 415 nm mercury emission band for the measurement of quantum yields. The absorption spectra of $CuSO_4$ solution, the interference filter CWL415 and filter GG400 are shown in **Figure** 2.2.1-2, **Figure** 2.2.1-3 and **Figure** 2.2.1-4, respectively. To change the light intensity, a set of neutral density filters were used (attenuation coefficients are 50%, 25%, 15% and 5%).

The irradiation cell, which was housed in a darkened box, was a variable volume water-jacketed cell with quartz window. A small (15 x 1.5 mm) magnetic stirring bar was placed inside the cell and a Corning magnetic stirrer (PC-353) was situated under the cell as shown in **Figure** 2.2.1-5. This cell was designed in our laboratory to solve the

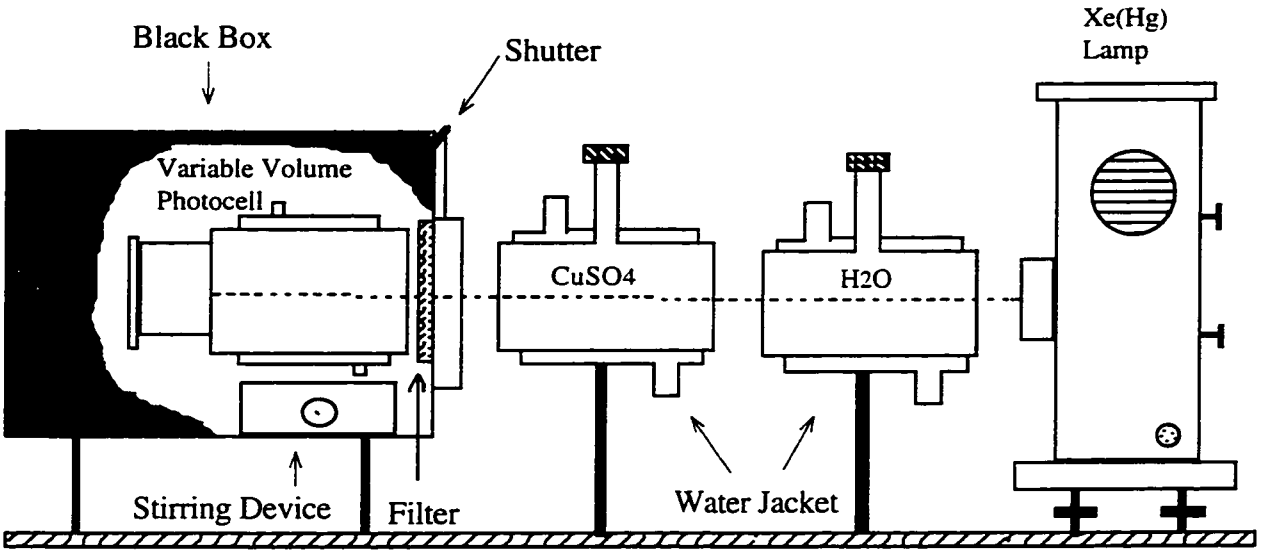

Figure 2.2.1-1 Photolysis apparatus.

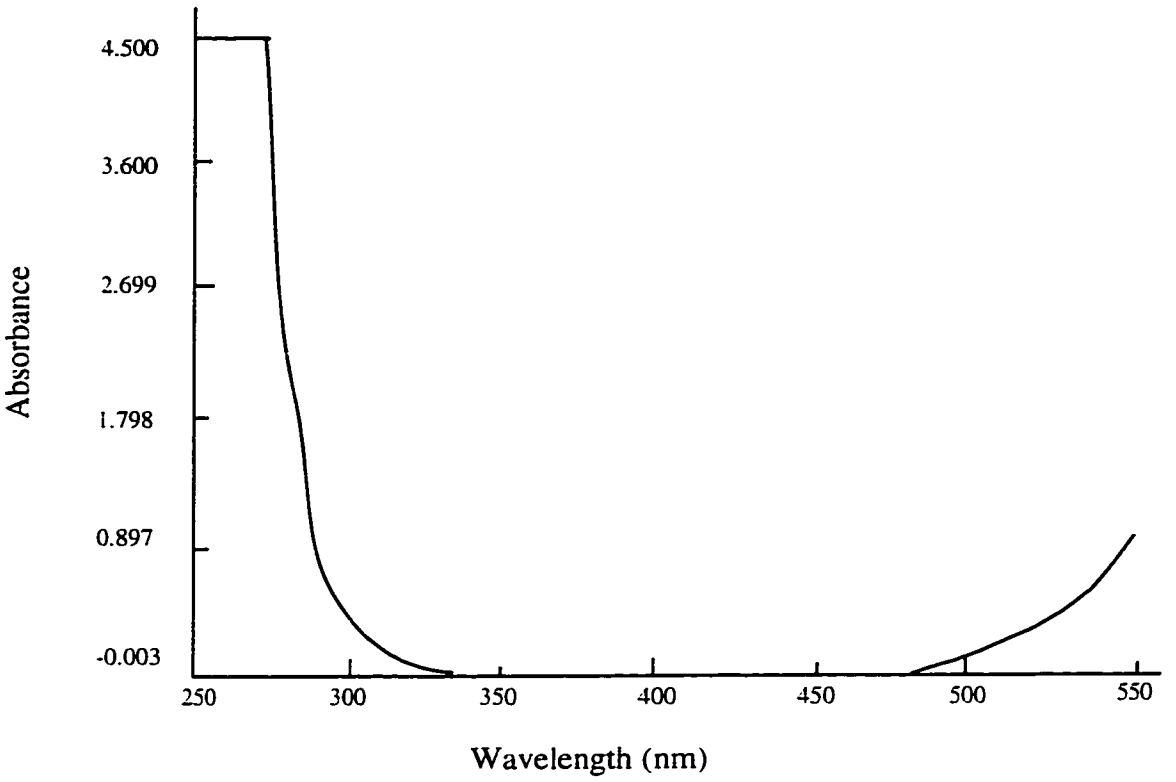

Figure 2.2.1-2. Absorption spectrum of $CuSO_4$ solution.
$[Cu^{2+}] = 0.1$ M; 0.5 cm length cell.

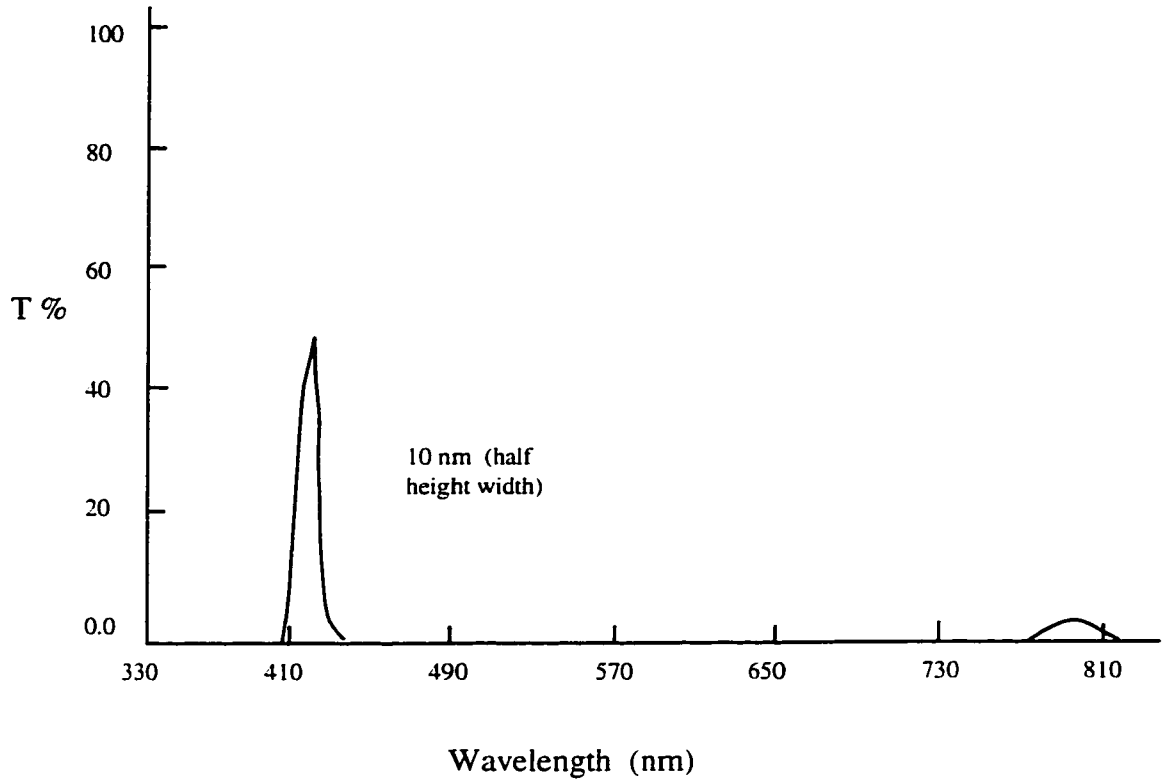

Figure 2.2.1-3. Transmission spectrum of CWL415 interference filter.

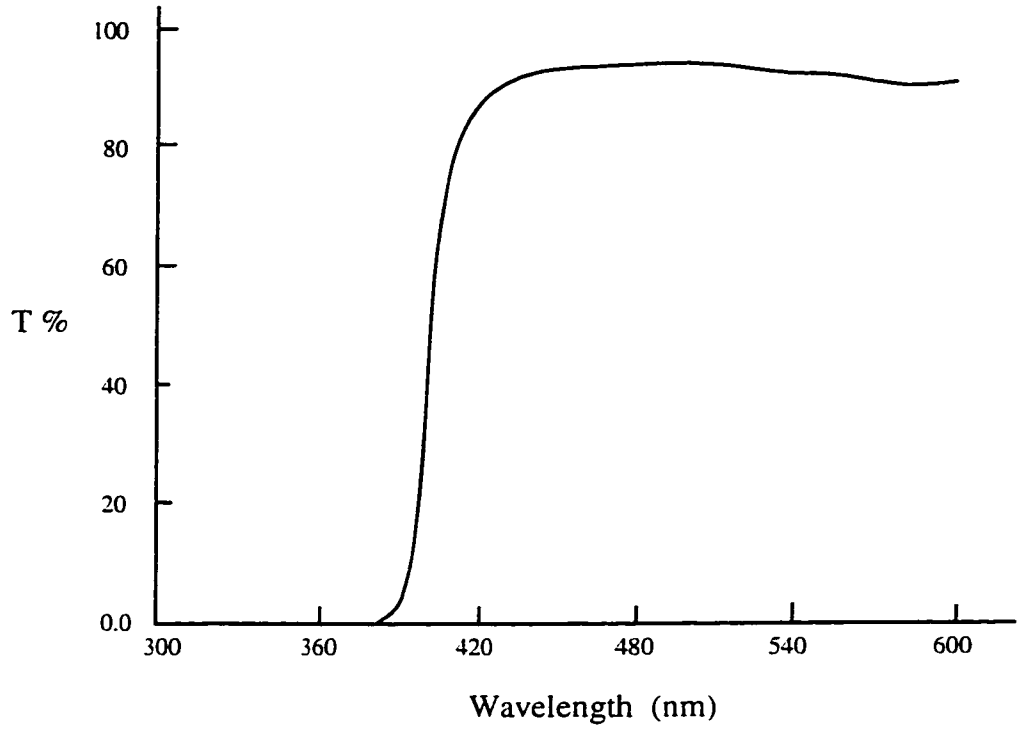

Figure 2.2.1-4. Transmission spectrum of GG400 filter.

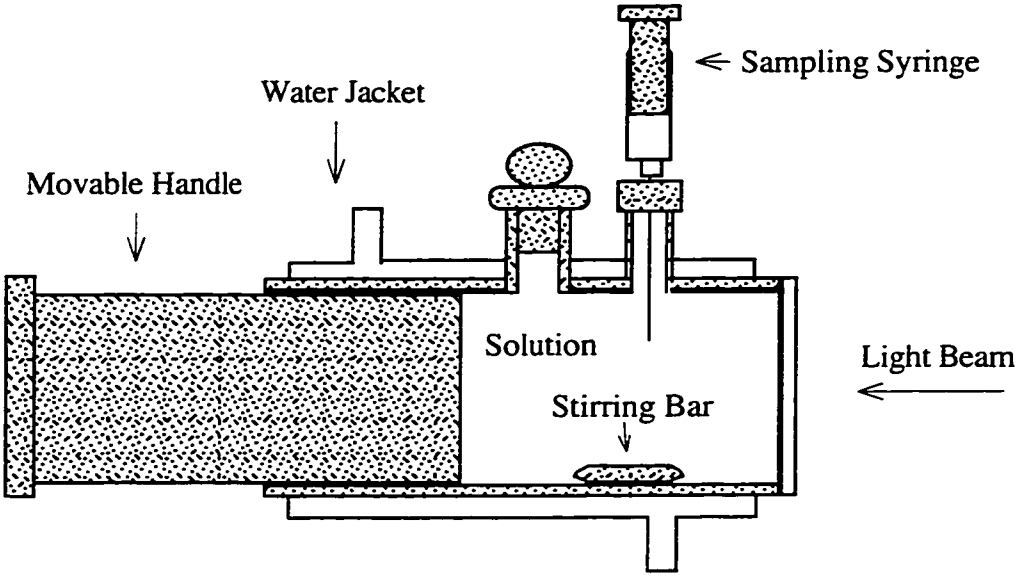

Figure 2.2.1-5. Variable volume photolysis cell.

problem of loss of volatile solutes from the liquid to the gas phase. It has a movable piston which makes it possible to take samples from the liquid phase without creating a gas phase. This feature is important for the studies of gaseous or volatile solutes. Since the distribution coefficients between the liquid and gas phases of these substances make it very complicated to trace their total amounts. When using this cell, one must limit the sample volume below a certain value to ensure that the liquid solution remaining in the cell has a path length sufficient to absorb more than 99% of the light. The cell was checked for leaks before each experiment. **Figure** 2.2.1-6 shows one of such test.

The saturation of hydrocarbons in uranyl solution was achieved by using oxygen or nitrogen as the carrier gases to introduce liquid phase hydrocarbon into the uranyl solution. In some cases, a separatory funnel was used for the saturation. Isobutane is a gas and was directly bubbled (at 10-60 mL/min) through the uranyl solution. When concentrations other than saturation concentration were needed, isobutane was bubbled together with nitrogen. In studies of the effect of oxygen, oxygen was bubbled together with isobutane. The systems used to bubble alkanes to the uranyl solution are shown in **Figure** 2.2.1-7.

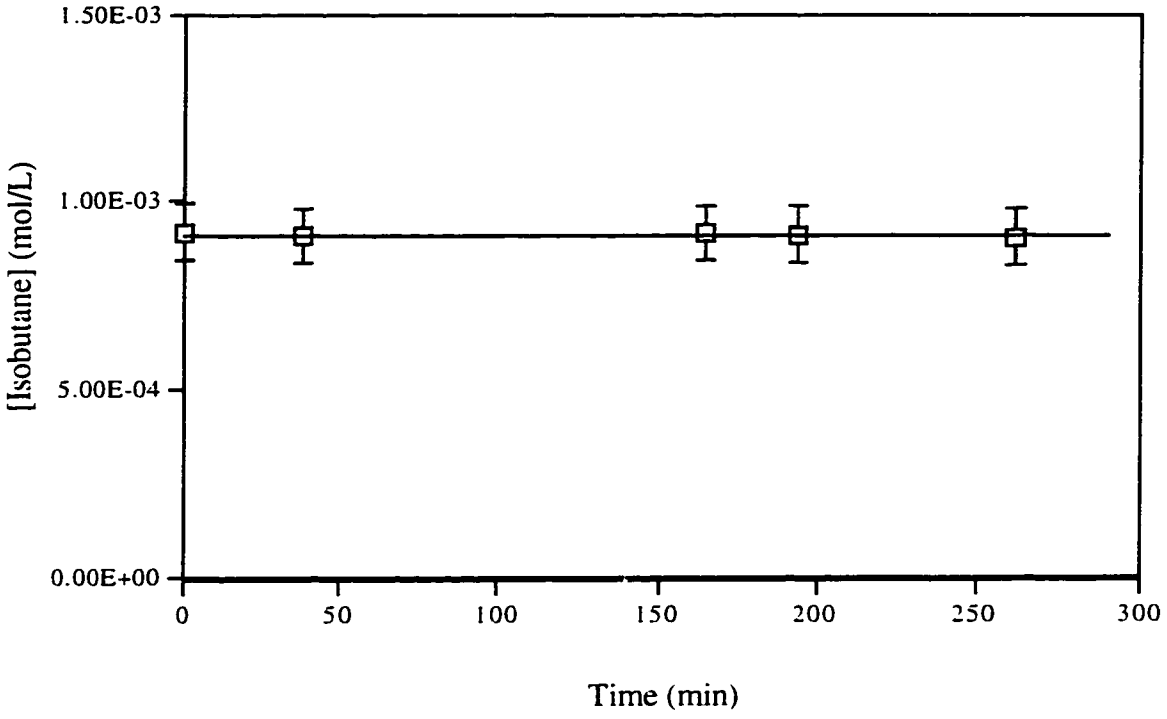

Figure 2.2.1-6. Isobutane leak test in the variable volume photolysis cell.
The cell was filled with uranyl solution (36.5 mM; pH = 0.95) and isobutane was bubbled for 1 hour at a flow rate of 45 mL/min (25 °C; stirred). Gas was removed and the photocell was closed for equilibrum for 20 min to a equilibrum. Samples (1 μL) were taken and injected directly into the GC.

1. System to Bubble Liquid Hydrocarbons

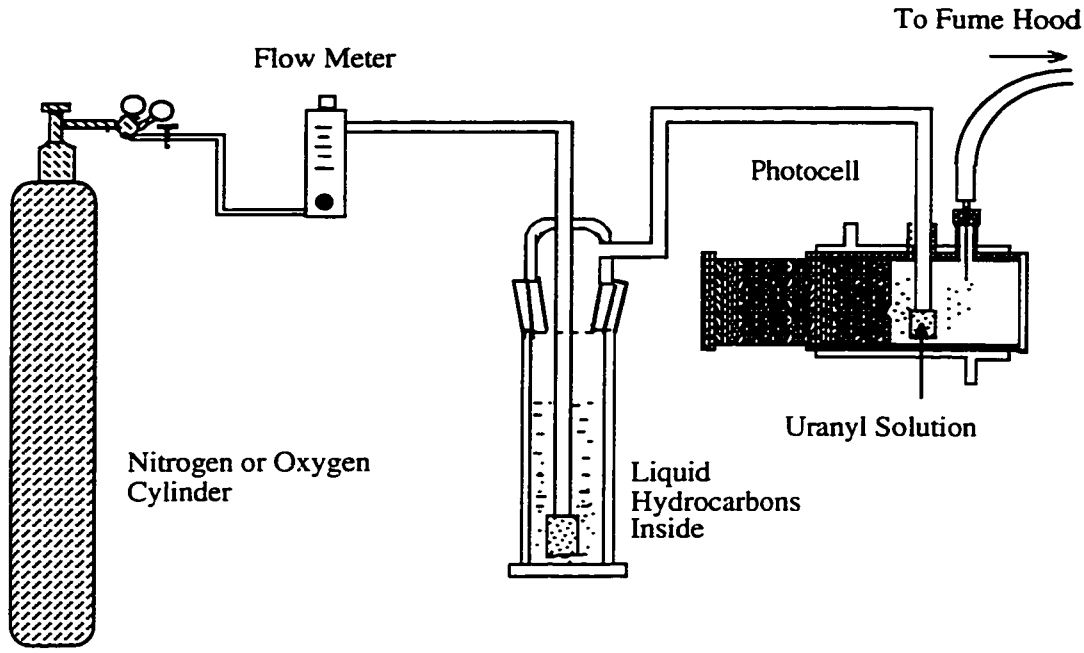

2. System to Bubble Gaseous Hydrocarbons

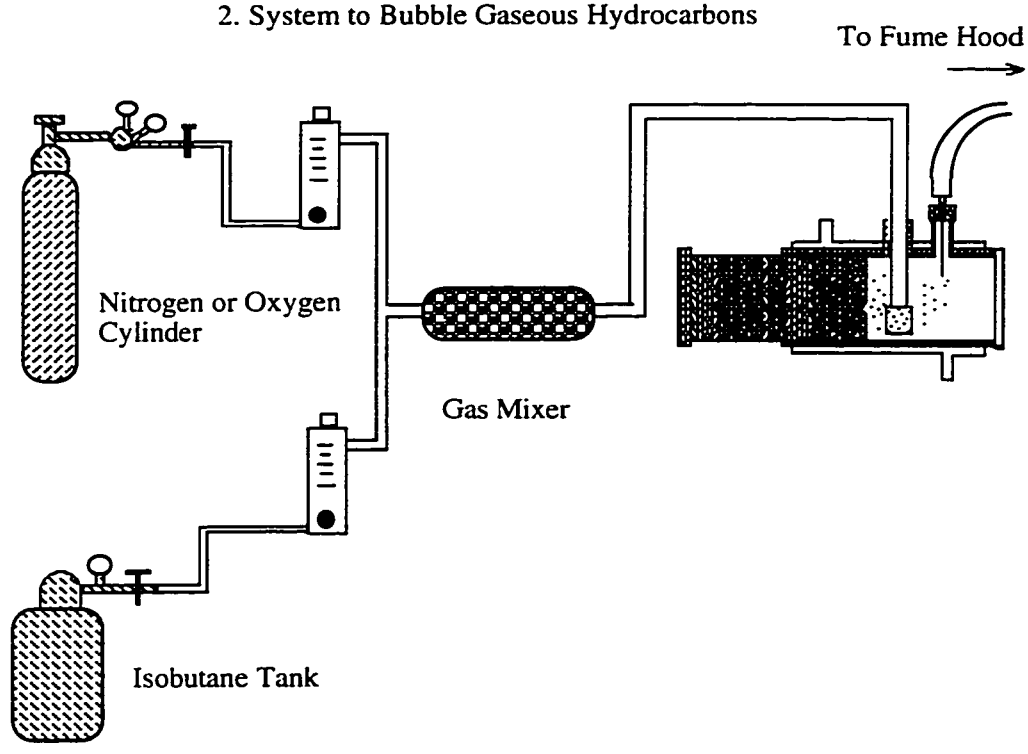

Figure 2.2.1-7. Systems to Bubble Hydrocarbons

2.2.2 Actinometry

The potassium ferrioxalate system developed by Parker Hatchard[123,124] was used for the measurement of the light intensity. It is very sensitive over a wide range of wavelengths, and is simple to use. When sulfuric acid solutions of $K_3Fe(C_2O_4)_3$ are irradiated in the range from 250 to 577 nm, simultaneous reduction of iron to the ferrous state and oxidation of oxalate ion occur. The quantum yields of Fe^{2+} formation have been accurately determined, and light absorption by the reactant is good for the range 468-253.7 nm (see **Table** 2.2.2-1). The ferrous ion product and its oxalate complex do not absorb incident radiation measurably during the photolysis, but after irradiation, the ferrous ion is made to be highly absorbing and easily analyzable by formation of the red-colored 1,10-phenanthroline Fe^{2+} complex.

Table 2.2.2-1. Quantum yields of Fe^{2+} in the $K_3Fe(C_2O_4)_3$ chemical actinometer.[a]

Wavelength nm	$K_3Fe(C_2O_4)_3$ mol/L	Fraction of Light absorbed (l = 15 mm)	$\phi(Fe^{2+})$
579	0.15	0.118	0.013
468	0.15	0.850	0.93
436	0.15	0.997	1.01
	0.006	0.615	1.11
405	0.006	0.962	1.14
366	0.006	1.00	1.21
	0.15	1.00	1.15
334	0.006	1.00	1.23
253.7	0.006	1.00	1 25

a) T = 22 °C.

The quantum yields increase only slowly with decrease in wavelength, as seen in **Table** 2.2.2-1. Also, the quantum yield has a very small dependence, over a considerable range, on reactant and product concentrations, intensity of the incident light, and temperature. The pure solid reactant was prepared by recrystallizing $K_3Fe(C_2O_4)_3 \cdot 3H_2O$, from warm water and then drying in an oven at 45 °C (this process must be carried out in the dark). The resulting solid can be stored in the dark for long periods of time without change.

In the experiments, a 3.87 mM solution of $K_3Fe(C_2O_4)_3$ was used. In a 8.7 cm path length, it absorbs more than 99.9 % of the light at 415 nm (the molar extinction coefficient $\varepsilon_{415nm}(Fe^{3+})$ is 115 $M^{-1}cm^{-1}$). The 3.87 mM solution of $K_3Fe(C_2O_4)_3$ was prepared by dissolving 0.676 grams of $K_3Fe(C_2O_4)_3$ in 360 mL of H_2O, to which 40 mL 1.0 N H_2SO_4 was added. For all quantitative work the preparation and the manipulation of the ferrioxalate solutions must be carried out in a dark room, using a red photographic safelight.

The actinometry consisted of irradiating a $K_3Fe(C_2O_4)_3$ solution (3.87 mM, 95.8 mL) for an accurate measured period of time (e.g. 10.0, 20.0, 30.0 minutes) at 22°C. After a measured period, 1 mL aliquots of the irradiated solutions were taken, using a calibrated pipette, and placed into a 50 mL volumetric flask. Then 5 mL 0.1% (by weight) 1,10-phenanthroline aqueous solution and 5 mL buffer solution (prepared from 600 mL of 1 M NaO_2CCH_3 and 360 mL 0.05 M H_2SO_4 diluted to 1 liter) were added to the flask and diluted

with water to the mark. After storing the solutions for 20 minutes, the absorbance of 1,10-phenanthroline-Fe^{2+} complex solutions was measured at 510 nm in the spectrophotometer using an 1 cm cell. The molar extinction coefficient ε of the complex is reported to be 1.11 x 10^4 M^{-1} cm^{-1} at 510 nm.[123,124] From these data, the moles of Fe^{2+} formed during the photolysis can be calculated by:

$$moles(Fe^{2+}) = \frac{V_1 V_3 A}{\varepsilon l V_2} \qquad (2.2.2\text{-}1)$$

where

moles(Fe^{2+}) = moles of Fe^{2+} photoproduced (mol/L),

V_1 = the volume of actinometer solution irradiated (L),

V_2 = the volume of aliquot taken for analysis (L),

V_3 = the final volume to which the aliquot V_2 is diluted (L),

A = the measured absorbance of the solution at 510 nm,

l = the path length of the spectrophotometer cell used (cm),

ε is the experimental value of the molar extinction coefficient of the Fe^{2+} (ε = 1.11 x 10^4 M^{-1} cm^{-1}).

The light intensity can be calculated by:

$$I = \frac{moles(Fe^{2+})}{\Phi(Fe^{2+})t} \qquad (2.2.2\text{-}2)$$

where

I = light intensity (Einstein min^{-1}),

$\phi(Fe^{2+})$ = quantum yield of Fe^{2+} from the irradiation of $K_3Fe(C_2O_4)_3$ solution at 415 nm (it is 1.11),

t = irradiation time (minute).

The experimental values were substituted into the above two equations (For a typical case of V_1 = 95.8 mL; V_2 = 1 mL; V_3 = 50 mL; l = 1 cm; $\varepsilon = 1.11 \times 10^4$ M^{-1} cm^{-1} and $\Phi(Fe^{2+})$ = 1.11), the light intensity was:

$$I = 3.89 \times 10^{-4} \times A/t \text{ (Einstein/min)} \qquad (2.2.2\text{-}3)$$

2.3 Preparation of Compounds

2.3.1 Preparation of Uranyl Solution

In the experiments, all uranyl solutions, except indicated otherwise, have been made from UO_3. UO_3 was a gift from Cameco and it has natural abundance. The photochemical behavior of the solutions made from UO_3 and from $UO_2(ClO_4)_2$ were compared and no significant differences were observed.

Table 2.3.1-1 shows the analytical data for UO_3 provided by Cameco personnel.

The general procedure for preparing acidified $UO_2(ClO_4)_2$ solution was as follows: An amount of UO_3 was weighed into a beaker and an equivalent number of moles of perchloric acid was added. The mixture was then heated to about 80 ^{0}C with stirring until all of the solid dissolved. The solution was filtered and left for a day before using it. This solution was the stock solution (concentration usually about 1.2 mol/L). The solution to be irradiated was made by dilution of the above stock solution, as described below:

Example:

1) Weigh 178.5 g of UO_3.
2) Put it in a 500 mL beaker, add 102.5 mL of 70% $HClO_4$ and about 150 mL of Millipore water.
3) Heat it to about 80 ^{0}C and stir it until all solids are dissolved.
4) Filter (202 reeve angel filter paper WHATMAN INC) the solution and leave it for one day.
5) Dilute solution to 500 mL with Millipore water. This stock solution has a pH close to 1 and a [UO_2^{2+}] about 1.2 mol/L).
6) Take 30 mL of the stock solution into a 1 L volumetric flask and add 8.5 mL of 70% $HClO_4$, then dilute it to 1 L with Millipore water.

Table 2.3.1-1. Analysis of UO_3 composite sample.

Sample Provided by Cameco

Listed below are the analytical results for a composite sample made up from eight UO_3 lots from Blind River. The results are a combination of analysis done in Port Hope as well as results reported by Blind River.

Analyte	Result (ppm U Basis)	Analyte	Result (ppm U Basis)
Ag	<0.2	Al	<5
B	<0.1	Be	<0.4
C	35	Ca	<5
Cd	<0.2	Cl	25
Co	<5	Cr	7
Cu	<1	Dy	<0.05
Eu	<0.10	F	<5
Fe	30	Gd	<0.02
K	<10	Mg	<1
Mn	<1	Mo	0.8
Na	<5	Nb	<0.1
Ni	<5	NO_3	0.5
P	20	Pb	<1
Sb	<1	Si	<10
Sm	<0.10	Sn	<1
Th	<5	Ti	<0.1
V	<0.5	W	<1
Zn	<5	Zr	2
U	82.75%		

Thus was obtained the solution having pH ≈ 1 and $[UO_2^{2+}]$ ≈ 37 mM.

2.3.2 Preparation of U^{4+} Solution

U(IV) was prepared by a photochemical method.[99] In this procedure, formic acid or ethanol was added to $UO_2(ClO_4)_2$ solution. Before irradiation, nitrogen was bubbled through the solution to expel all of the dissolved oxygen. A 1 kW Hg(Xe) lamp was used as the irradiation source and a $CuSO_4$ solution was employed as the light filter to cut off the UV components.

In a typical preparation of a U^{4+} solution, 95.8 mL of 34 mM (pH = 1, $HClO_4$) uranyl solution was introduced into the photolysis cell, and 0.1 mL of formic acid and 0.4 mL 70% $HClO_4$ were added. Nitrogen was bubbled through this solution for 30 min at the flow rate of 30 mL/min with the Hg(Xe) lamp adjusted to 880 W. After 100 min irradiation, almost all of the formic acid was consumed. The solution was left under nitrogen atmosphere for 20 min before using. The overall reaction is shown below:

$$UO_2^{2+} + HCOOH + 2H^+ \xrightarrow{h\nu} U^{4+} + CO_2 + 2H_2O \qquad (2.3.2\text{-}1)$$

2.3.3 Preparation of $[UO_2(O_2)]\cdot 2H_2O$

Uranyl peroxide $[UO_2(O_2)]\cdot 2H_2O$ is a light yellow solid substance.[125] It dissolves in strongly acidic solutions to give UO_2^{2+}. It can be prepared by precipitation of uranyl ion using hydrogen peroxide:[126]

$$UO_2^{2+} + H_2O_2 + 2H_2O \longrightarrow [UO_2(O_2)]\cdot 2H_2O(s) + 2H^+ \qquad (2.3.3\text{-}1)$$

In the preparation, 4 g of $UO_2(NO_3)_2\cdot 6H_2O$ was dissolved in 100 mL water, and 0.2 mL of concentrated HNO_3 was added. The solution was heated to about 70 ^{0}C and 8 mL of 34% H_2O_2 was introduced into the solution with stirring. A light-pale yellow precipitate appeared. After digestion for 30 min at 70 ^{0}C, the precipitate was washed with water several times by decantation and then filtered under suction. The precipitate was thoroughly washed with water and transferred to a glass dish. The precipitate then was put in an oven and dried at 70 ^{0}C for 12 hr and kept in a desiccator. When the temperature is higher than 90 ^{0}C, the product $[UO_2(O_2)]\cdot 2H_2O$ will convert to U_2O_7.[127] The analytical results are listed in **Table** 2.3.3-1. The IR spectrum of the product is presented in Chapter 3 and it is consistent with the reported spectrum.

Table 2.3.3-1. Analysis of photoproduced precipitate and comparison with calculated values for $[UO_2(O_2)]\cdot 2H_2O$.

	Uranium%	Peroxide%	Hydrogen%
Photoproduced	69.6	9.57±0.2	1.11
Calculated	70.4	9.47	1.18

2.3.4 Preparation of $K_4[UO_2(O_2)_3]$

Potassium triperoxyuranate $K_4[UO_2(O)_3]$ is a dark yellow solid substance. It dissolves in water to yield $UO_2(O_2)_3^{4-}$. It can be prepared by complexation of $[UO_2(O_2)]\cdot 2H_2O$ with hydrogen peroxide under strongly basic conditions:[26]

$$[UO_2(O_2)]\cdot 2H_2O + 2H_2O_2 + 4OH^- \longrightarrow UO_2(O_2)_3^{4-} + 6H_2O \quad (2.3.4\text{-}1)$$

In the preparation, 0.55 g KOH was added to 10 mL water, and after dissolution, 1 mL of 34% H_2O_2 was added. One gram of $[UO_2(O_2)]\cdot 2H_2O$ was introduced with stirring into the solution. The color of the solution immediately turned dark red. The solution was then cooled in an ice water bath to about 5 ^{0}C, and 3 mL ethanol was added. A dark yellow crystalline precipitate appeared. This precipitate was filtered and washed with ethanol. The precipitate was dried in an oven at 60 ^{0}C for 2 hr, and then kept in a desiccator.

The molar ratio of O_2^{2-}/U in the prepared sample was found to be 2.6. Considering the uncertainty of the analytical technique, this value is consistent with the formula of $UO_2(O_2)_3^{4-}$. The IR spectrum of the product agrees well with the literature result and it will be discussed in Chapter 3.

2.4 Products Analysis

2.4.1 Organic Substances

The measurement of organic substance was carried out using a Hewlett Packard 5890 Gas-Chromatograph (GC). The data were processed using a PC286 computer employing the program Baseline 810. In the measurement of gaseous hydrocarbon products with carbon number less than 5, a GSQ column (30 m x 0.546 mm, J&W Scientific) was used, while a DB-210 column (30 m x 0.53 mm, J&W Scientific) was utilized for the measurement of alcohol and ketone products.

In each experiment, either 145 mL or 95.8 mL, for the variable volume photolysis cell, of UO_2^{2+} aqueous solution were irradiated using the Xe(Hg) lamp with a GG400 or CWL415 filter placed in front of the photolysis cell. In addition, there were always water and $CuSO_4$ solution filters placed before the lamp to absorb the heat and the UV components of irradiation light. At different intervals of time, a sample was withdrawn with a 5 mL syringe and passed through a Sep-pak cartridge. In this operation, the following conditions were used:

Syringe Pump: Model 341B (Orion Research Incorporated USA).
Syringe: 5 mL (plastic) (W.Graf GmbH & Co.Western Germany).

Sep-Pak: tC18 plus (Millipore Corporation USA).

Conditions of sample preparation :

Sample Volume: 5 mL.

Pump Flow Rate: 1 mL/min

Temperature: room temperature (about 22°C).

The organic substance that was retained on the Sep-pak cartridge was then eluted with 1.17 mL of an internal standard solution (a full 1 mL syringe) followed by 1.5 mL solvent (THF or methanol depending on the systems being analyzed). The eluate (2.67 mL) was collected in a vial and 1 μL of this solution was injected into the gas chromatograph for analysis. For analysis of gaseous samples, 5 to 100 μL gas-tight microsyringes were used to directly draw the sample from inside the photolysis cell.

Cyclopentane, cyclohexane and pentane were introduced into the uranyl solution using oxygen or nitrogen as the carrier gases. In some cases, when mass balance experiments were carried out, the solution was saturated with these compounds in the photolysis cell or in a separatory funnel and was then transferred to the photolysis cell. Isobutane was directly bubbled through the solution at a flow rates of 20-50 mL/min or was bubbled together with oxygen or nitrogen (using two flow regulators and a Y type tube, see **Figure** 2.2.1-6).

The definition of the quantum yield is expressed by the following equation:

$$\text{Quantum Yield} = \frac{\text{moles of products photoproduced}}{\text{moles of photons absorbed at a specific wavelength}}$$

(2.4.1-1)

If the concentration of product multiplied by (volume/light intensity) (C·V/I) is used as the Y-axis and irradiation time as the X-axis, then the quantum yield ϕ can be obtained as the slope of a plot of C·V/I versus time:

$$C \cdot V/I = \phi \times t \qquad (2.4.1\text{-}2)$$

The standard solutions for the calibrations of liquid organic substances were prepared by weighting. Isobutane is a gaseous product and its calibration was made by the following method.

For uranyl solutions, the absolute peak area of the chromatogram was used to obtain the standard curve.

In this method, isopropanol was selected as the solvent for isobutane. The advantages of using it as the solvent are:

1. Isobutane is highly soluble in it (about 1.2 M);
2. Isopropanol has a smaller vapor pressure (compared to THF, methanol, acetone and ether).
3. Isopropanol has a smaller thermal expansion coefficient.

4.Isopropanol is well separated from isobutane in the GC. First, isopropanol was added to a weighed Erlenmeyer flask (including the rubber cap and the stirring bar). The flask was sealed and a needle was used to release the air pressure inside. The flask and contents were weighed again to obtain the weight of the isopropanol. The isobutane tank then was connected to the flask by a tube with a needle as shown in **Figure** 2.4.1-1. Then the isopropanol was stirred and the pressure of the isobutane regulated to 7 psi. After about two minutes, the regulator was closed. The needle was disconnected and the flask and contents were weighed (usually about 0.25 g isobutane dissolved in the isopropanol). From the weight of the isobutane and the weight of the solvent, the mass percentage of isobutane was obtained (this is the concentrated solution of isobutane). This solution then was diluted to a suitable level for direct injection. In the dilution process, a known volume of isopropanol (about 52 mL) was added into another flask (50 mL flask with screw cap) and was weighed. Then about 0.3 mL of the above concentrated solution was transferred to this flask and the flask was weighted again. Since the exact mass of isobutane that was transferred and the exact volume of the solvent (with less than 0.2% error) is known, one can calculate the molarity of the isobutane in this flask. It was found to be about 0.5 mM using the above procedure. This solution was directly injected into the GC and the absolute-

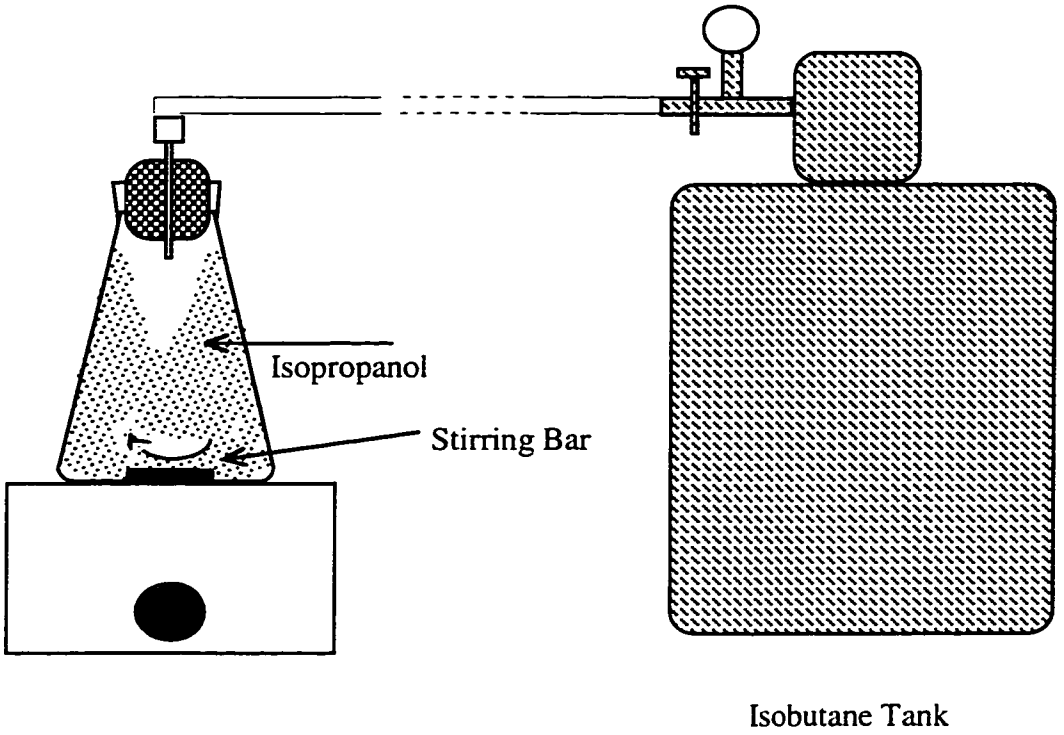

Figure 2.4.1-1. Set up for the preparation of standard isobutane solution.

peak area of isobutane was obtained. An isobutane saturated uranyl solution was also directly injected. A guard column was installed before the analysis column to prevent contamination by uranium. The isobutane areas were compared and the solubility of isobutane in uranyl solution was obtained. The solubility of isobutane in 34 mM aqueous uranyl solution at 22 °C and 0.95 atmosphere pressure is 0.914 ± 0.017 mM. The reported value in water at 25 °C and 1 atmosphere pressure is 0.94 mM.[128]

The calibrations of other small molecular-weight hydrocarbons were carried out in a GSQ column. A gas-tight syringe was employed. A standard gas mixture (Matheson-Gas Product Canada) was obtained from Dr. N. Bakshi of the Chemical Engineering Department, U. of S. The concentrations are listed in **Table** 2.4.1-1.

The detailed gas chromatography (GC) analysis procedures employed are described below:

In the measurement of the **photoproducts of cyclopentane and cyclohexane**, methyl-n-butyl ketone was used as an internal standard and THF as the elution solvent and the following conditions were typically used:

Column: DB-210,

Helium flow rate: 1.9 mL/min,

Air flow rate: 275 mL/min,

Hydrogen flow rate: 25 mL/min,

Sample injection volume: 1 μL

Injection temperature: 200 °C,

Table 2.4.1-1. Analysis of C_1-C_4 hydrocarbon standard gas mixture.[a]

Substances	Concentration (mol%)
Methane	2.15 ± 0.2
Ethene	0.707 ± 0.014
Ethane	0.850 ± 0.018
Propene	0.779 ± 0.016
Propane	0.540 ± 0.011
Isobutane	0.533 ± 0.010
1-butene	0.202 ± 0.004
n-butane	0.205 ± 0.004
trans-2-butene	0.188 ± 0.004
cis-2-butene	0.198 ± 0.004

a) The main component is nitrogen.

Detector temperature: 250 ^{0}C,

Peak processing parameters:

Derivation threshold 1 (coarse): 78,

Derivation threshold 1 (fine): 130,

Baseline point: 10,

Filter width: 13,

Skim ratio: 3,

Temperature program was:

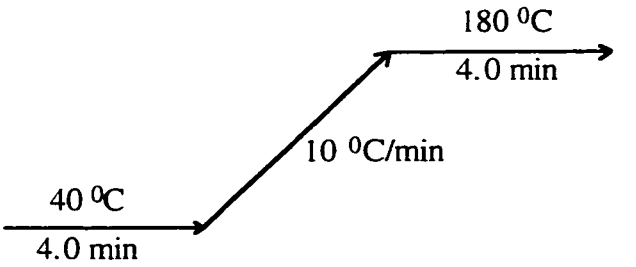

In the measurement of **photoproducts of isobutane**, methyl-n-butyl ketone was used as an internal standard and methanol as the elution solvent with the following conditions:

Column: DB-210,

Helium flow rate: 2.4 mL/min,

Air flow rate: 275 mL/min,

Hydrogen flow rate: 25 mL/min,

Sample injection volume: 1 μL

Injection temperature: 200 ^{0}C,

Detector temperature: 250 ^{0}C,

Peak processing parameters:

Derivation threshold 1 (coarse): 95,

Derivation threshold 1 (fine): 500,

Baseline point: 10,

Filter width: 13,

Skim ratio: 2,

Temperature program was:

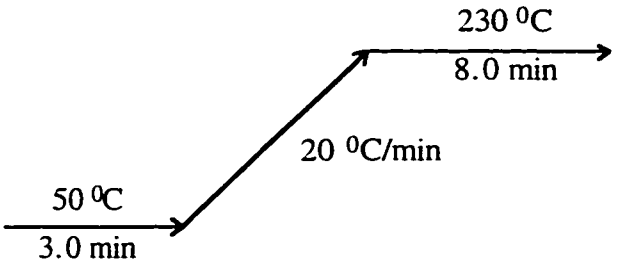

In the measurement of the **gaseous hydrocarbon photoproducts of isobutane**, direct injection was employed and the following conditions were used:

Column: GSQ,

Helium flow rate: 12 mL/min,

Air flow rate: 300 mL/min,

Hydrogen flow rate: 44 mL/min,

Sample injection volume: 1 µL

Injection temperature: 200 °C,

Detector temperature: 250 °C,

Peak processing parameters:

Derivation threshold 1 (coarse): 80,

Derivation threshold 1 (fine): 70,

Baseline point: 10,

Filter width: 13,

Skim ratio: 4,

Temperature program was:

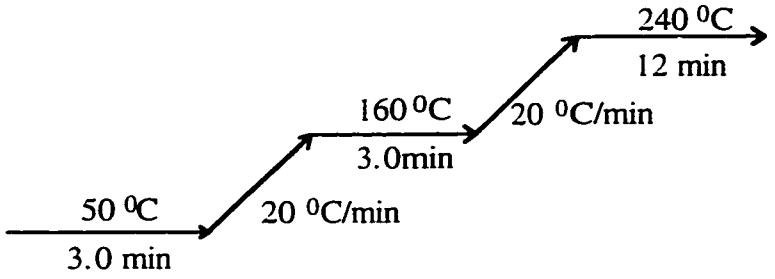

2.4.2 Uranium Species

The uranium content in $UO_2(O_2)\cdot 2H_2O$ was measured spectrophotometrically using a Cary 2315 W visible spectrophotometer. A $UO_2(O_2)\cdot 2H_2O$ sample was dissolved in 1 M $HClO_4$ solution and then its absorbance was measured at 414 nm at room temperature (about 22 °C).

After dissolving, $UO_2(O_2)\cdot 2H_2O$ forms UO_2^{2+}. So the measurement of uranium content in $UO_2(O_2)\cdot 2H_2O$ is actually the measurement of UO_2^{2+} (U(VI)). $UO_2(O_2)\cdot 2H_2O$ can be easily dissolved in concentrated $HClO_4$ solution. It can be also dissolved in diluted $HClO_4$ solution but at a much low rate, for instance, at pH = 1, it takes about 10 hr. The absorption spectrum of UO_2^{2+} in $HClO_4$ solution is shown in **Figure** 2.4.2-1. It has a maximum absorbance at 414 nm. A calibration curve was made using U_3O_8. $UO_2(CH_3COO)_2\cdot 2H_2O$ (Fisher Scientific) was used for the preparation of U_3O_8. About 20 g of $UO_2(CH_3COO)_2\cdot 2H_2O$ was put in a crucible and

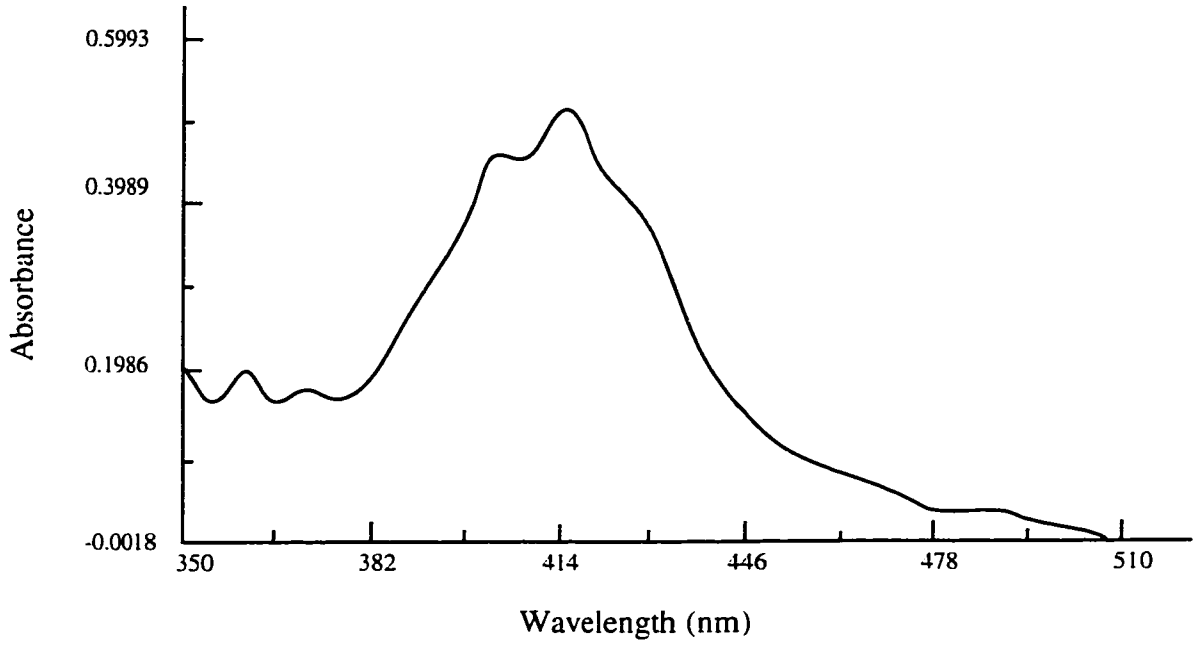

Figure 2.4.2-1. Absorption spectrum of UO_2^{2+}.
$[UO_2^{2+}]$ = 63.6 mM; pH = 1.1 ($HClO_4$); 1.0 cm cell.

heated in a muffle furnace for 4 hr at a temperature of 800 ^{0}C. In this process, the yellow $UO_2(CH_3COO)_2$ first changed its color to red yellow then to deep black green. After cooling, it was kept in a desiccator. It was then used to make uranyl perchloric acid solution for the measurement of molar extinction coefficients of UO_2^{2+} at different concentrations of $HClO_4$. The values are listed in **Table** 2.4.2-1.

Some samples were also reanalyzed by SRC (Saskatchewan Research Council) using a delayed neutron counting method (after correction for the U^{235} content) and/or laser phosphorescence method. The results obtained for the uranium content (U of S) were consistent well and within 2% with that of SRC (see Chapter 3). The measurement of the concentration of U(IV) (U^{4+}) was also performed using a spectrophotometric method.[98] U(IV) has five major absorption peak ranging from 400 to 700 nm and the maximum absorbance is located at 652 nm. The absorption spectrum of U(IV) is shown in **Figure** 2.4.2-2.

The calibration of the U(IV) concentration was carried out by a volumetric method. U(IV) was prepared by the photoreduction method described previously.

The absorbance of U(IV) samples were measured and their concentrations were determined by redox-titration using $K_2Cr_2O_7$.[108, 129] A 0.1000 N $K_2Cr_2O_7$ solution was prepared by

Table 2.4.2-1. The molar extinction coefficients of UO_2^{2+} at different concentrations of $HClO_4$.[a]

Concentration of $HClO_4$	Extinction Coefficient at 414 nm ($M^{-1}cm^{-1}$)
pH = 3	8.28 ± 0.17
pH = 2	8.01 ± 0.15
pH = 1.1	7.88 ± 0.15

a) T = 22 °C

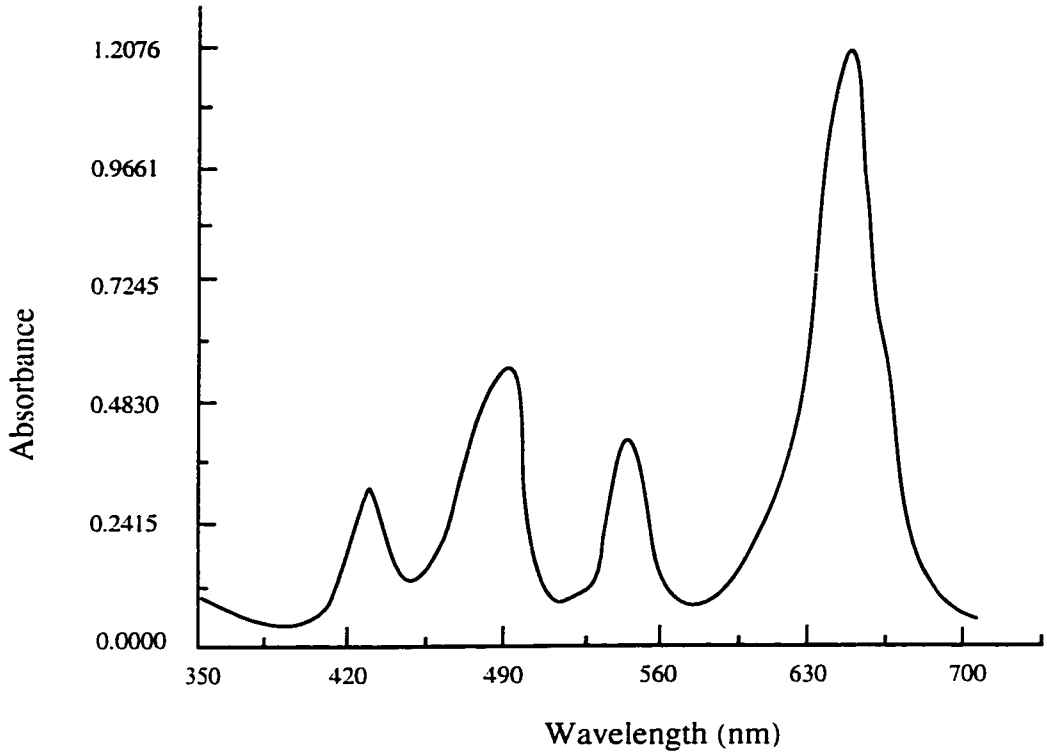

Figure 2.4.2-2. Absorption spectrum of U(IV). [U(IV)] = 28.6 mM; pH = 1.1 ($HClO_4$); 1.0 cm cell.

dissolving 4.903 g of $K_2Cr_2O_7$ in 1 L of Millipore water. The titration was carried out in an atmosphere of nitrogen. Two or three drops of 0.1 M Fe^{3+} solution was used as a catalyst and two drops of 0.05% sodium diphenylamine-4-sulfonate aqueous solution as indicator. The titrations were performed at 40 °C and at a rate of 1 drop/3 seconds.

The molar extinction coefficients of U^{4+} at different concentrations of $HClO_4$ are listed in **Table** 2.4.2-2. These values are consistent with reported values.[130]

U(V) was detected at 740 nm by using a HP 8451A Diode Array spectrophotometer. U(V) forms a complex with UO_2^{2+} and has an extinction coefficient of 24.3 $M^{-1}cm^{-1}$ at 740 nm.[33, 36]

2.4.3 Peroxides

Depending on the concentration and purpose, peroxides, O_2^{2-}, were measured by using two methods. For solid samples and higher peroxide concentrations, an oxidation titration method[131] was employed while for lower peroxide concentrations, a peroxide-test strip was used. In the titration, $KMnO_4$ was used as the oxidant.[132,133] In the preparation of 0.100 M $KMnO_4$ solution, 4.35 g of $KMnO_4$ was

Table 2.4.2-2. Molar extinction coefficients of $U^{4+}(aq)$ at different concentrations of $HClO_4$.[a]

Concentration of $HClO_4$	Extinction Coefficient at 652 nm ($M^{-1}cm^{-1}$)
pH = 0.97	43.5 ± 0.65
pH = 1.06	41.4 ± 0.62
pH = 1.16	40.3 ± 0.60
pH = 1.64	32.0 ± 1.6

a) T = 22 °C

weighed and dissolved in Millipore water. Then the solution was boiled for one hour and filtered. $K_2C_2O_4$ was used for the calibration of $KMnO_4$ solution. $KMnO_4$ solutions are not stable. Beyond one or two days, it must be calibrated again. In the titration of peroxides, 10 drops of 0.1 M $MnSO_4$ solution were utilized as the catalyst. For the titration of solid samples, the solid was added to a certain amount of 5 M H_2SO_4 solution and titrated with $KMnO_4$ solution with constant stirring (solid does not need to be dissolved before the titration starts). In the detection of low peroxide concentrations, Merckoquant 10011 Peroxid(e)-Test (Merck, Darmstadt Germany) strip is a sensitive method. This method is able to detect peroxide concentrations down to 1 x 10^{-5} mol/L. In the measurement, a strip is immersed in the solution, pulled out and its color compared with that of the standard paper.

2.4.4 Other Substances

Mass spectral analysis were used to further identify our organic products. A VG Analytical VS70E instrument with Vax 4000-60 digital Data Station was employed. The analysis conditions used are described below:

EC/CI Source

Source Temperature: 200 °C

EI mode; 70 eV.

Trap Current: 100 μA.

GC: Fisons 8060

Scan rate: 1 sec/dec

Mass range: 20-500 amv.

CHN elemental analysis were carried out by using an auto-CHN analyzer (PERKIN-ELMER 2400 CHN) with AD-4 auto balance.

2.5 Spectroscopic Measurements

2.5.1 Infrared Spectra

All infrared spectra were obtained on a single-beam Bio-Rad FTS-40 FTIR equipped with a TGS (triglycine sulfate) detector and interfaced to an SPC 3240 data station. For powder measurements, a Bio-Rad diffuse reflectance assembly was used. A small amount of the sample of interest was mixed with spectrograde KBr (BDH Spectrosol) and finely ground in an agate mortar. The sample mixture and pure ground KBr were added to separate sample cups. These were carefully leveled and placed into the sample holder, which was inserted into the instrument. The spectra were taken at a resolution of 4.0 cm^{-1}. For liquid solutions, a Buck Scientific attenuated reflectance (ATR) assembly with a ZnSe crystal was employed. Solutions were introduced into the cavity in the middle of the cell until the ZnSe crystal was covered (a volume of

approximately 3 mL). Single-beam spectra were referenced to a background single beam spectrum of the empty cell. A total of 300-1000 scans were used to obtain the background spectrum of the cell itself.

2.5.2 Emission Spectra

A Spex Fluorolog-2 Spectrofluorometer with 450 W Xe arc lamp (1909 Lamp Housing), a R928 red-sensitive photomultiplier detector, and a cooling system (1914F) were used to measure emission spectra. The 1608B spectramate was utilized for both the excitation and emission spectra grating, and a single-beam sampling module(1691) was mounted between them.

A Spex computer (PC 486) with DM3000 software was interfaced to the above instrument for collection, storage and processing of data.

The voltage on the PMT was maintained at 950 V and the instrument was operated in the photon-counting mode, with emission signals from the sample ratioed to a reference signal monitored by a Rhodamine B quantum counter utilizing a PMT at 400 V. The excitation wavelength was 415 nm. Both the excitation and emission band widths for most experiments were 0.9 nm (slit width = 2 mm; step length = 0.1 mm; integration time = 0.1 s) and spectra were typically scanned in the region 450-650 nm for the emission spectrum of excited uranyl ion.

A micro-stirring bar was used during the measurements and both the sample and reference solution were placed in a Spex 1 cm water-jacketed cell holder. Right-angle(RA) and single/reference(S/R) modes were selected. An automatic repeating scan and averaging program was usually used to obtain intensity data.

2.5.3 UV-visible Absorption Spectra

For UV-visible absorption spectra, a Cary 2315 spectrophotometer with a DS-15 data station was used. Typically, spectra were run in auto-gain mode with a spectral bandwidth of 1.0 nm, response time of 0.50 sec and scan rates of 1.0 nm/sec. The step length is 5.0 nm and the gain is 17.4. The resulting spectra were plotted on a chart recorder or stored on computer disk using the DS-15. Solutions were placed in 0.5, 1.0, 5.0 cm Suprasil quartz cells (Hellma) and kept at room temperature. When absorbance at a fixed wavelength was measured, the spectrophotometer was set to this wavelength and two blanks were put into the holders and the autozero function was used to zero the absorbance before the measurements.

[122] Brndyopadhyay, M.; Konar, R. S. *J. Indian Chem. Soc.* **1974**, *Vol. LI*. 722.

[123] Parker, C. A. *Proc. Roy. Soc. (London),* **1953**, A220, 104.

[124] Hatchard, C. G; Parker, C. A. *Proc. Roy. Soc. (London)* **1956**, A235, 518.

[125] Katz, J. J; Rabinowitch, E. *The Chemistry of Uranium*; New York, 1951; p 292.

[126] Chakravort, M. C. *Inorg. Synth.* **1987**, *25*, 144.

[127] Boggs, J. E; Chehabi, M. E. *J. Am. Chem. Soc.* **1957**, *79*, 4258.

[128] Wetaufr, D. B. *J. Am. Chem. Soc.* **1964,** *86*, 508.

[129] Zhao, Z. F.; Liu, D. A. *Analytical Chemistry*; Bejing, 1978; p 295.

[130] Betts, R. H.; *Can. J. Chem.* **1955**, *33*, 1775.

[131] Connor, J. A.; Ebsworth, A. V. *Adv. Inorg. Chem. Radiochem.* **1964**, *6*, 345.

[132] Suhumb, W. C.; Satterfield, C. N.; Wentworth, R. L.; *Hydrogen Peroxide*; Reinhold: New York, 1995.

[133] Klassen, W. V.; Marchingtion, D.; McGowan, H. C. E. *Anal. Chem*. **1994**, *66*, 2921.

3. RESULTS

In this study, three types of alkanes (cyclic, branched and straight chain hydrocarbons) were selected. The isobutane system was used for the mechanitic investigation because this system is simple as there is only one predominant product (tertiary butyl alcohol or 2-methyl-2-propanol) and this product does not undergo further oxidation reaction under the conditions applied. In this system, the influence of peroxydisulfate on the quantum yield was investigated. A quantum yield of 0.022 was obtained, and under some conditions, it increased to 1.1.

In the cyclopentane system, the main products obtained were cyclopentanol and cyclopentanone, whichcan be further oxidized. A total quantum yield of 0.087 was obtained. A photoproduced precipitate and some peroxide products were investigated in this system.

n-Pentane was also investigated. Even though the n-pentane concentration is 10^{-4} M level, a total quantum yield of about 0.01 was obtained.

Cyclohexane was also investigated and it can also be photooxidized.

3.1 Photolysis of Isobutane in the Absence of $K_2(S_2O_8)$

3.1.1 Photolysis

Isobutane is a gaseous substance at room temperature and pressure (bp = -11.7 °C). It has nine primary hydrogen atoms and one tertiary hydrogen atom. The tertiary hydrogen atom has the lowest bonding energy, so it is expected to have a relatively higher quantum yield and to give rise to one dominant product, 2-methyl-2-propanol. In uranyl ion sensitized oxidation of alcohols, aldehyde and other oxygen-containing hydrocarbons, the α-hydrogen atom abstraction is usually the first step of the oxidation process, as proposed in Chapter 1. Since 2-methyl-2-propanol has no α-hydrogen atom, it is not expected to be further oxidized. Consequently isobutane is most suitable for the basic studies of uranyl ion sensitized photooxidation. The following are some basic properties of isobutane:

$$BH \longrightarrow B\cdot + H\cdot \qquad 91 \text{ kcal/mol} \qquad (3.1.1\text{-}1)$$

$$BH \rightleftharpoons B\cdot + H^+ + e^- \qquad E^\circ = -1.89 \text{ V} \qquad (3.1.1\text{-}2)^{134}$$

$$BH + H_2O \rightleftharpoons BOH + 2H^+ + 2e^- \qquad E^\circ = -0.31 \text{ V} \qquad (3.1.1\text{-}3)^{134}$$

Its solubility in water at 25 °C is 0.94 mM and the measured value in our system is 0.914 mM (see Section 2.4).

The devices described in Section 2.2 were used in the photolysis. In the first irradiation experiment, a GG400 filter (cut off wavelength < 400 nm light) was used. Uranyl solution was introduced into the photolysis cell and isobutane was bubbled through the solution for 30 min. Before irradiation, several samples were analyzed and no thermal reaction products were found. The analysis of products showed that 2-methyl-2-propanol was the major product (**Figure** 3.1.1-1) (in figures, we use t-butanol to represent 2-methyl-2-propanol). Isobutene (or isobutylene) was also found in ca 2% amount of that of isobutane, but its value fluctuated. It was determined that some of the isobutene comes from the thermal dehydration of 2-methyl-2-propanol in the GC injection chamber. The production of 2-methyl-2-propanol increases with irradiation time. When the irradiation was stopped, the 2-methyl-2-propanol concentration did not increase further. This means that there was no post-irradiation reactions for 2-methyl-2-propanol, as expected.

For the determination of the quantum yield, a CWL415 filter (415 nm band-pass filter) was used to narrow the wavelength irradiation (see Section 2.4.1). The results are shown in **Figure** 3.1.1-2. The initial quantum yield of 0.032 ± 0.0014 was obtained from the slope of a plot of $C \cdot V/I$ versus time (**Figure** 3.1.1-3) (see equation 2.4.1-2).

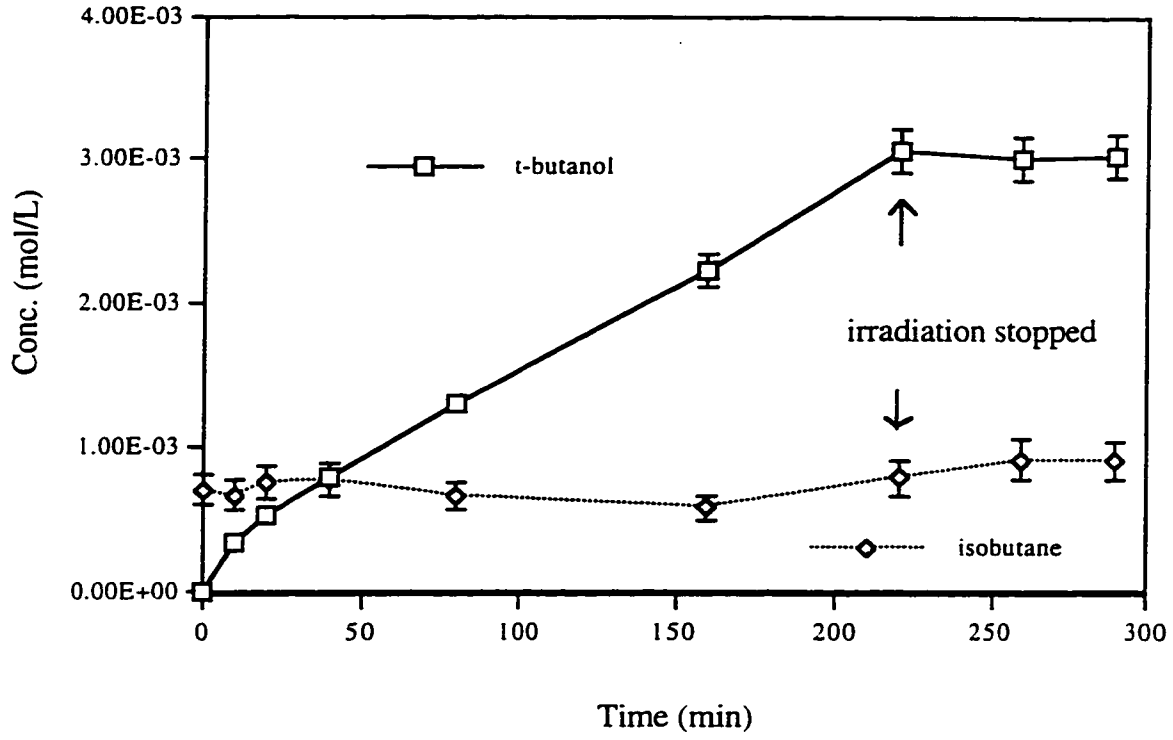

Figure 3.1.1-1. Photo-production of t-butanol from isobutane with GG400 filter.

$[UO_2^{2+}]$ = 34.8 mM; pH = 1.1 ($HClO_4$); V_{irrad} = 145 mL; T = 25 °C. Isobutane is bubbled for 30 min before irradiation and continuously bubbled during irradiation.

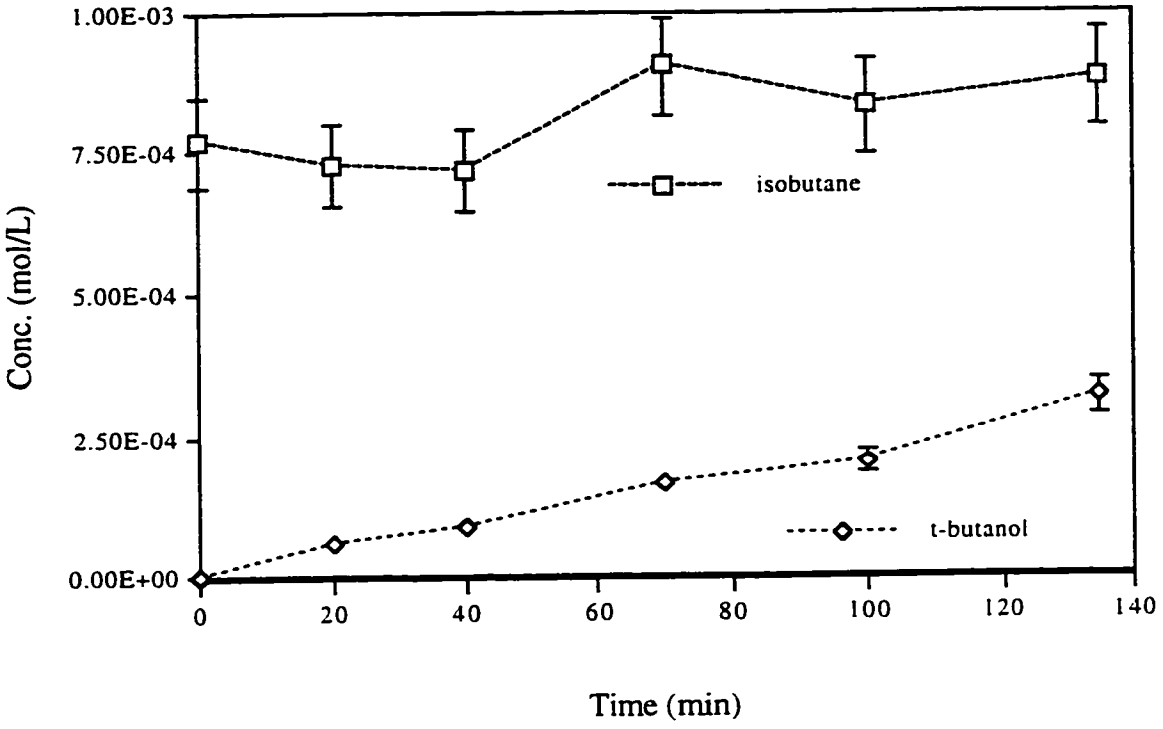

Figure 3.1.1-2. Photoproduction of t-butanol from isobutane with CWL415 filter.
$[UO_2^{2+}]$ = 34.8 mM; pH = 1.1 ($HClO_4$); V_{irrad} = 145 mL; T = 25 °C; I = 9.08 x 10^{-6} Einstein/min; λ_{irr} = 415 nm. Isobutane is bubbled for 30 min before irradiation and continuously bubbled during irradiation.

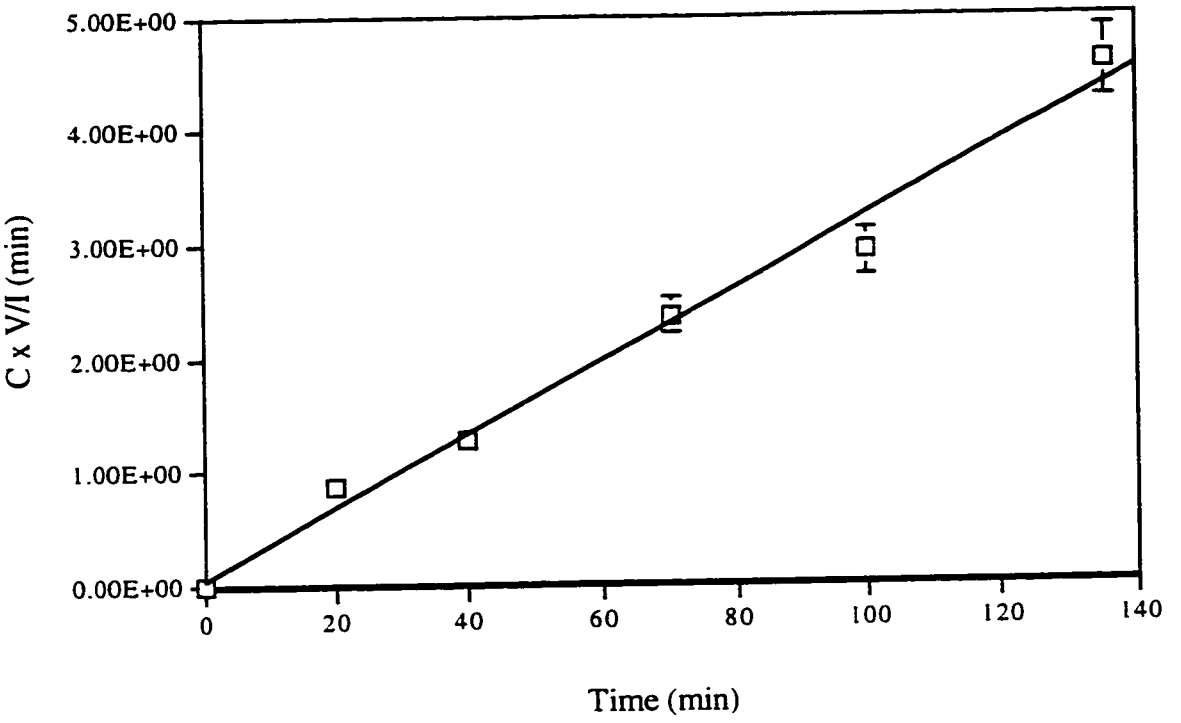

Figure 3.1.1-3. Relationship of [t-butanol]xVolume/(Light Intensity) with irradiation time.
$[UO_2^{2+}]$ = 34.8 mM; pH = 1.1 ($HClO_4$); V_{irrad} = 145 mL; T = 25 °C; I = 9.08 x 10^{-6} Einstein/min; λ_{irr} = 415 nm. Isobutane is bubbled for 30 min before irradiation and continuously bubbled during irradiation.

Curve fitting equation: $y = 3.20E\text{-}02x + 5.07E\text{-}02$ $r^2 = 9.85E\text{-}01$

(Note: unless specified otherwise the quantum yield refers to 2-methyl-2-propanol; BH refers to isobutane and BOH refers to 2-methyl-2-propanol.)

3.1.2 Mass Balance

Mass balance experiments were carried out in order to determine the distribution of the products and the efficiency of the conversion in the photooxidation process. In these experiments, a variable volume photolysis cell (see Chapter 2) was employed, so that no gas-phase develops even with the continuous sampling. This design eliminates any complications arising from mass distributions between the gas and the liquid phases. As mentioned before, the maximum amount of solution taken from this photolysis cell was kept below a certain level to ensure that the remaining solution had a sufficient path length to absorb more than 99% of the incident light. Two parallel experiments (with Millipore water) were carried out and the results are shown in **Tables** 3.1.2-1 and 3.1.2-2.

Table 3.1.2-1. Mass balance in the photolysis of isobutane (I).[a]

Irrad.Time (min)	-Δ[BH] [M]x10^4	Δ[BOH] [M]x10^4	Δ[Isobutene] [M]x10^4	P[b] (%)
30	0.890	0.620	0.0223	72
60	1.34	1.38	0.0724	100
180	3.08	2.58	0.148	90
235	3.71	3.12	0.162	88
270	4.28	3.45	0.176	85
420	5.66	4.75	0.271	89

a) Millipore water was used. I = (7.14 ± 0.05) x 10^{-6} Einstein/min; $[BH]_0$ = 8.64 x 10^{-4} M; $[UO_2^{2+}]$ = 34.8 mM; pH = 1.1 ($HClO_4$); V_{irrad} = 95.8 mL; T = (25 ± 0.15) °C; λ_{irr} = 415 nm.

b) P = (Δ[t-butanol] + Δ[isobutene])/(-Δ[isobutane]) x 100%.

Table 3.1.2-2. Mass balance in the photolysis of isobutane (II).[a]

Irrad.Time (min)	-Δ[BH] [M]x10^4	Δ[BOH] [M]x10^4	Δ[Isobutene] [M]x10^4	P[b] (%)
30	1.34	0.779	0.0303	61
67	1.78	1.34	0.0417	78
146	2.58	1.98	0.0821	81
173	2.68	2.07	0.106	82
245	3.99	2.98	0.134	79
480	5.70	4.77	0.231	89

a) Millipore water was used. I = (7.14 ± 0.05) x 10^{-6} Einstein/min; $[BH]_0$ = 8.55 x 10^{-4} M; $[UO_2^{2+}]$ = 34.8 mM; pH = 1.1 ($HClO_4$); V_{irrad} = 95.8 mL; T = (25 ± 0.15) °C; λ_{irr} = 415 nm.

b) P = (Δ[t-butanol]+ Δ[isobutene])/(-Δ[isobutane]) x 100%.

From these results, it can be seen that during the beginning of the photolysis, the transformation rate is low, and then it increases to a stable level around 84%. Triply distilled water was also used to perform this experiment to check for the possible influence of impurities in water. The results are shown in **Table** 3.1.2-3. It appears that there are no significant differences between these results and those obtained using Millipore water, so the latter has been generally used.

The initial quantum yields for these mass balance experiments are summarized in **Table** 3.1.2-4.

Since the loss of isobutane exceeds the amount of 2-methyl-2-propanol, we also serached for other potential products were.

3.1.3 Hydrolysis of Isobutene

The photolysis of isobutane also produced some isobutene. Isobutene is not stable in aqueous solution. Its subsquent hydrolysis gives rise to 2-methyl-2-propanol. In order to determine if the 2-methyl-2-propanol found in our system is a primary product of photolysis or comes from the hydrolysis of isobutene, or from both of them, the hydrolysis kinetics of isobutene was investigated. **Figure** 3.1.3-1 shows the relationship between the logarithm of isobutene

Table 3.1.2-3. Mass balance in the photolysis of isobutane(III).[a]

Irrad.Time (min)	-Δ[BH] [M]x10^4	Δ[BOH] [M]x10^4	Δ[Isobutene] [M]x10^4	P (%)
32	1.04	0.690	0.0040	64
67	1.51	1.36	0.0310	92
100	2.12	1.39	0.0621	68
140	2.82	1.86	0.0867	69
181	3.28	2.31	0.116	74
430	5.52	4.36	0.249	83

a) Triply distilled Water was used. I = (7.14 ± 0.05) x 10^{-6} Einstein/min; $[BH]_0$ = 8.39 x 10^{-4} M; $[UO_2^{2+}]$ = 36.4 mM; pH = 0.95 ($HClO_4$); V_{irrad} = 95.8 mL; T = (25 ± 0.15) °C; λ_{irr} = 415 nm.

b) P = (Δ[t-butanol] + Δ[isobutene])/(-Δ[isobutane]) x 100%.

Table 3.1.2-4. Quantum yields in mass balance experiment.[a]

Solvent	Quantum yield for loss of BH	Quantum Yield for formation of BOH
Millipore water (Table 3.1.2-1)	0.033	0.020
Millipore water (Table 3.1.2-2)	0.035	0.019
Triply distilled water (Table 3.1.2-3)	0.035	0.021

a) pH = 1.1; [BH] = 0.7 mM.

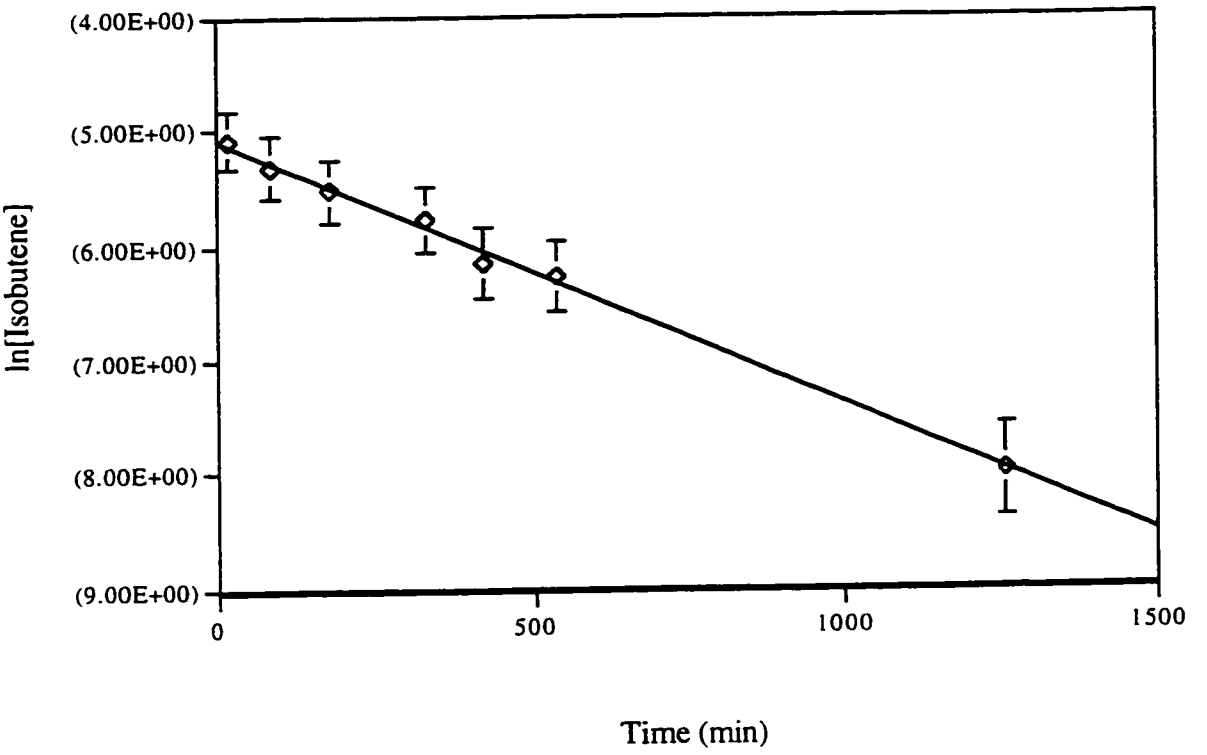

Fig.3.1.3-1. Relationship of ln[Isobutene] with time in the hydrolysis of isobutene.
$[UO_2^{2+}]$ = 36.8 mM; pH = 0.95 ($HClO_4$); V = 95.8 mL; T = 25 °C.
Isobutene was bubbled for 20 min at a rate of 16 mL/min then the photolysis cell was closed. (note: nnumber in bracket is negative)

Curve fitting equation: y = -2.31E-03x - 5.08E+00 r^2 = 9.96E-01

As $\ln[\text{Isobutene}] = \ln[\text{Isobutene}]_o - kt$; slope = -k,
so k = 2.31 x 10^{-3} min^{-1} or k = 3.85 x 10^{-5} s^{-1}

concentration and time. As expected, the ln[Isobutene] is a good linear function of time, and from the slope, the first order reaction rate constant of 2.31×10^{-3} min^{-1} or 3.85×10^{-5} s^{-1} is obtained. So the halflife of isobutene is calculated to be about 5.0 hours at pH = 1. The calculated value of k in pure water, at 35 °C, from the data of Balig and Whalley is 1.23×10^{-5} s^{-1}.[135] Considering these data, the 2-methyl-2-propanol formed in our experiments can not be attributed to the hydrolysis of isobutene.

3.1.4 Other Products

GSQ is a non-polar gas-chromatographic column. It is suitable for the separation of relatively low molecular weight hydrocarbons. However, as the Sep-pak cartridge used is not adequate for retaining the small non-polar hydrocarbons for the detection of these molecules, direct injection of gas phase samples was employed. In the analysis of the latter, small amounts of methane, propane, propene and ethane were found in the irradiation of isobutane-saturated uranyl solution. Some radical-coupling products such as 2,5-dimethylhexane, 2,5-dimethyl-1-hexene and 2,2,3,3-tetramethylbutane were also found. The concentrations are estimated to be of the order of 10^{-6} mol/L or less. Besides these substances, 2,4-dimethylpentane, 2,4-dimethyl-1-pentene and 2,5-dimethyl-1,5-hexadiene were also found but in even smaller amounts. These results are listed

in **Table** 3.1.4-1. It was also found that in the presence of oxygen, the production of methane decreased to 15% and propane decreased to 45% of that produced in the absence of oxygen, but the concentration of propene slightly increased. This is due to the reaction of oxygen with the free radicals. This result will be discussed in Chapter 4.

The C_7, C_8 products are shown in reaction (3.1.4-1).

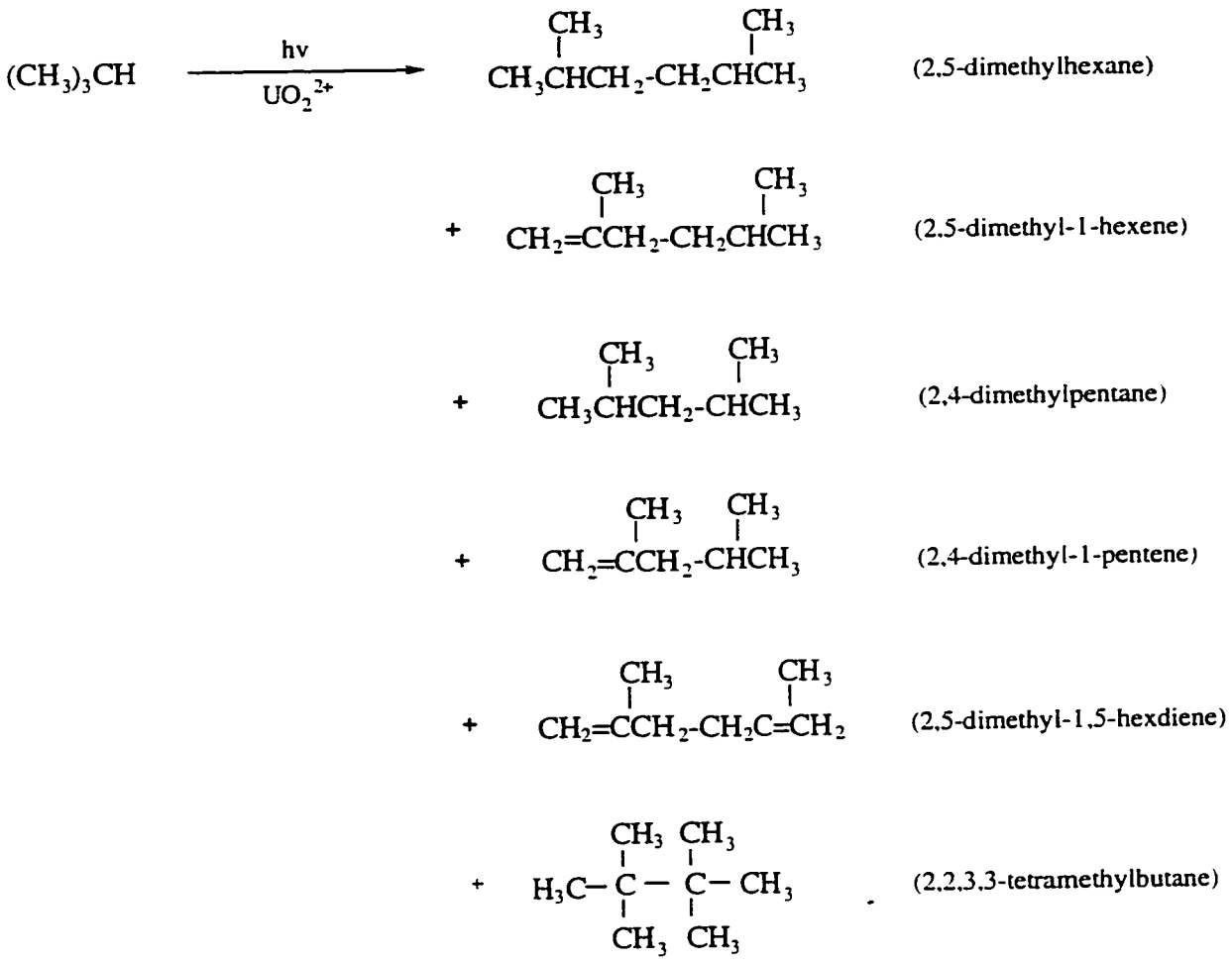

(3.1.4-1)

These products can be envisioned as arising from the reactions of the following four radicals:

Table 3.1.4-1. Photolysis products of isobutane.[a]

Products	Concentration (10^{-6} M)
t-butanol	660
methane	0.73[b]
Propane	80%[c]
Propene	30%[c]
Ethane	30%[c]
2,5-dimethylhexane	1.1[d]
2,5-dimethyl-1-hexene	80%[e]
2,2,3,3-tetramethylbutane	70%[e]
2,4-dimethylpentane	20%[e]
2,4-dimethyl-1-pentene	20%[e]
2,5-dimethyl-1,5-hexadiene	10%[e]
2,2,4-trimethyl pentane	3%[c]

a) Light intensity I = 9.32 x 10^{-6} Einstein/min; V_{irrad} = 145 mL. 30 min irradiation with GG400 filter for methane, ethane, propane and propene. 150 min irradiation with GG400 filter for other hydrocarbons.

b) Assuming all the methane was dissolved in the solution, the Henry's constant of 39166 /atm was used for the calculation.

c) Relative to methane

d) concentration in gas-phase, V_{gas} = 15 mL.

e) The concentration in gas-phase relative to 2,5-dimethylhexane.

(a) $\cdot CH_2CH(CH_3)$ (b) $\cdot CH(CH_3)$ (c) $\cdot CH_2\text{-}C(CH_3)=CH_2$ (d) $\cdot C(CH_3)_3$

The possible production paths of these free radicals will be discussed in Chapter 4.

3.1.5 Production of U(IV) and U(V) Species

In the irradiation of isobutane-saturated uranyl solution, the oxidation of isobutane is expected to be accompanied by the reduction of UO_2^{2+}. Among the reduced forms of UO_2^{2+}, $U^{4+}(aq)$ is the most stable one in the pH range investigated and so it should exist if oxygen or other oxidants are not present in this system. The results are shown in **Table** 3.1.5-1.

If the oxidation products of isobutane were strictly 2-methyl-2-propanol, its concentration should be equal to the amount of $U^{4+}(aq)$. It can be seen that the concentration of $U^{4+}(aq)$ produced is higher than that of 2-methyl-2-propanol. It is closer to but still consistently higher than the loss of isobutane. This indicates that other products could be produced, such as carboxylic acid. Oxidation of isobutane to carboxylic acid requires more electrons than oxidation to alcohol, thus more of the of $U^{4+}(aq)$ could be formed. Carboxylic acid could not be detected with the column used in the mass

Table 3.1.5-1. Production of U^{4+}(aq) and t-butanol.[a]

Expt#	1	2	3
[t-butanol]x10^4 mol/L	4.55	4.77	4.36
[U(IV)]x10^4 mol/L	5.75	6.16	5.93
-[isobutane]x10^4 mol/L	5.62	5.70	5.51

a) I = 7.14 x 10^{-6} Einstein/min; $[UO_2^{2+}]$ = 34.8 mM; pH = 1.1 ($HClO_4$); T = 25 °C; V_{irrad} = 95.8 mL; λ_{Irr} = 415 nm.

balance experiments.

When oxygen was bubbled through the solution during the irradiation, very low concentrations of $U^{4+}(aq)$ (less than 7 x 10^{-5} mol/L) were detected and no change in concentration of UO_2^{2+} was found. This means that in the presence of oxygen, photoproduced $U^{4+}(aq)$ can be reoxidized to its original state (UO_2^{2+}).

In the absence of oxidants in the solution and with the pH adjusted to 3.1, U(V) was detected after a short period of irradiation. **Figure** 3.1.5-1 is the absorbance difference spectrum (original uranyl solution as the reference). The peak at 740 nm belongs to the complex of U(V) with UO_2^{2+} or $U_2O_4^{3+}$ with ε = 24.3 $M^{-1}cm^{-1}$. This complex has another shoulder from 400 nm to 640 nm.[36] This shoulder is also visible in **Figure** 3.1.5-1 but part of this peak overlaps the negative peak of U(VI); The negative peak arises because the original UO_2^{2+} solution was used as the reference. In this spectrum, the small peak at 652 nm is attributed to $U^{4+}(aq)$. The production of U(V) is shown in **Figure** 3.1.5-2. The concentration of U(V) is almost directly proportional to the irradiation time. The U(V) concentration increases after irradiation is stopped, while U(IV) decreases (**Table** 3.1.5-2). This indicates that under this condition, the equilibrium between U(V) and U(IV) shifts to U(V).

When this solution was continuously irradiated for several hours, a fresh pink precipitate was formed. This precipitate disappeared readily when oxygen was bubble

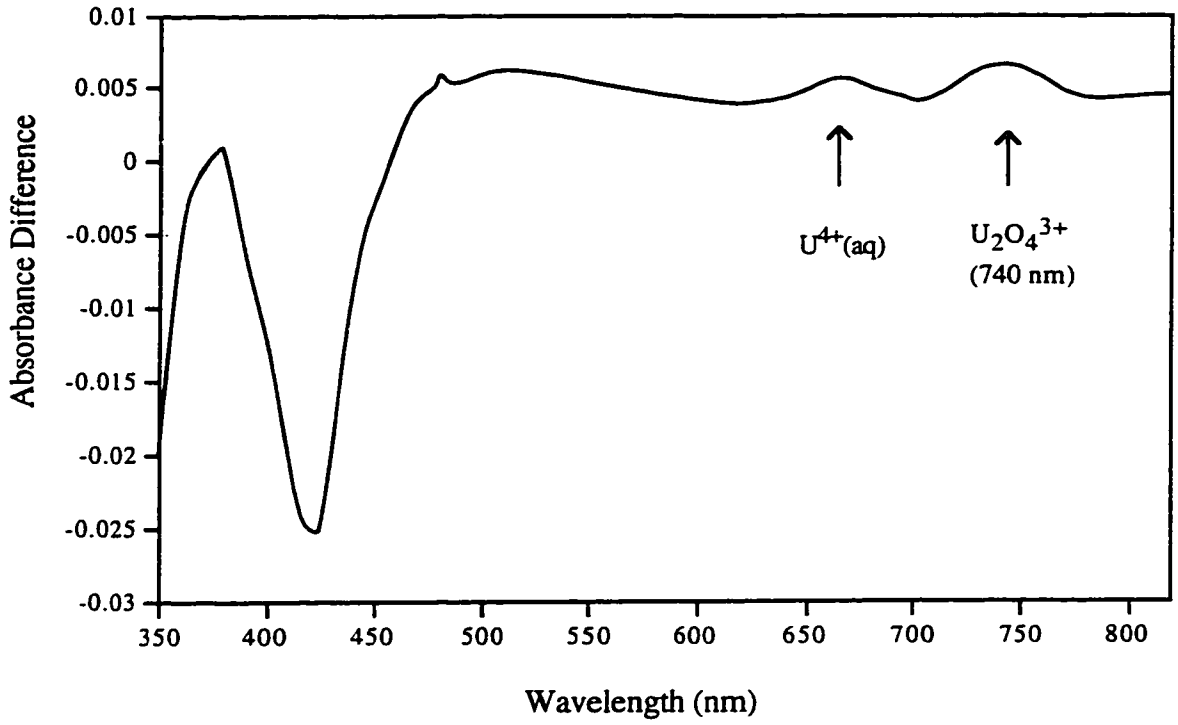

Figure 3.1.5-1. Absorption spectrum of $U_2O_4^{3+}$ with the original unirradiated UO_2^{2+} as the reference.

$[UO_2^{2+}]$ = 34.5 mM; pH = 3.1 ($HClO_4$); V_{irrad} = 110 mL; T = 25 °C; GG400 filter. Irradiated 80 min. An unirradiated solution is used as the reference.

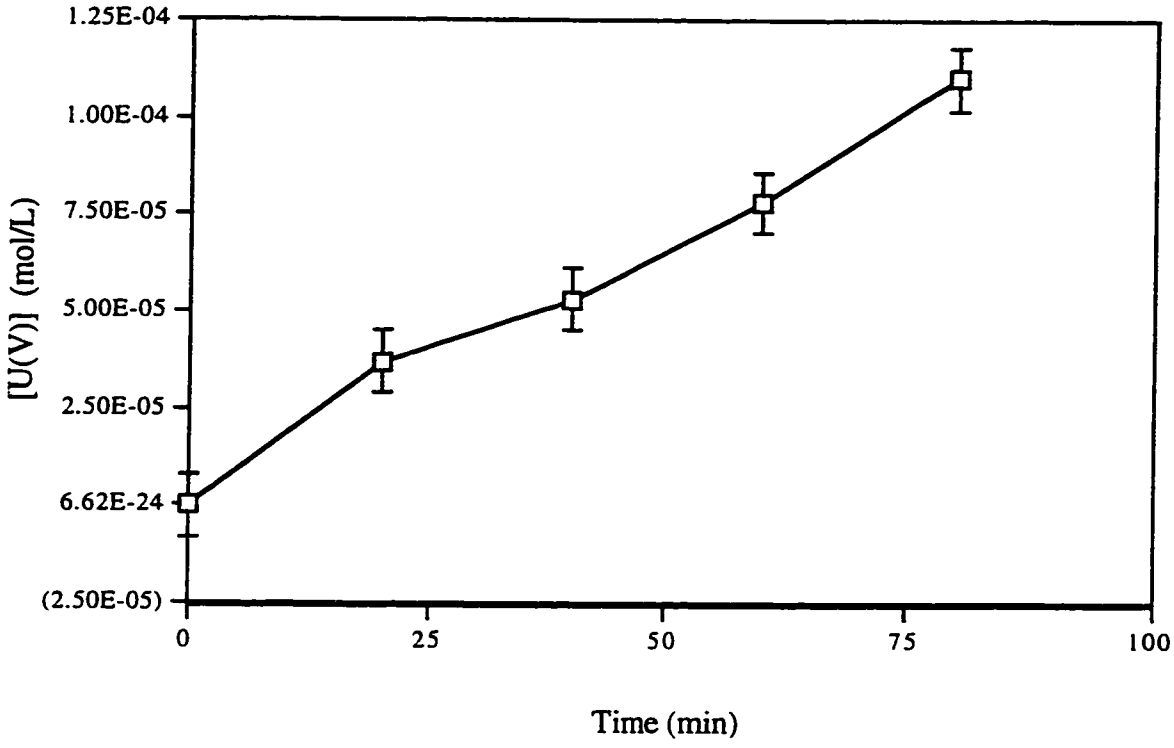

Figure 3.1.5-2. Photoproduction of U(V) in the irradiation of isobutane.
$[UO_2^{2+}]$ = 34.5 mM; pH = 3.1 ($HClO_4$); V_{irrad} = 110 mL; T = 25 °C; GG400 filter. Isobutane is bubbled for 60 min before irradiation and continuously bubbled during irradiation.

Table 3.1.5-2 The change Concentrations of U(VI), U(V) and U(IV) after stopping irradiation.[a]

Time	[U(VI)] mM	[U(V)] mM	[U(IV)] mM
t = 4 min	2.2	0.12	0.01
t = 14 min	1.8	0.13	0.009
t = 4 min	2.8	0.18	0.02
t = 14 min	2.5	0.19	0.012
t = 4 min	3.4	0.26	0.02
t = 14 min	3.1	0.26	0.012

a) $[UO_2^{2+}]$ = 34.8 mM; pH = 3.1 ($HClO_4$); T = 25 °C; V_{irrad} = 110 mL; λ_{Irr} = 415 nm.

through the solution. This precipitate has nct been identified. It could be a compound of U(V).

It is known that low pH favors the disproportionation of U(V) (see Section 1.2), and thus U(V) was not expected to be found at pH = 1.1. This conclusion is consistent with experiment. In our experiments, no U(V) is found at pH = 1.1.

3.1.6 Production of Peroxides

In the presence of oxygen and at pH = 3.0, a yellow precipitate was produced on irradiation of isobutane-saturated uranyl solution, and at the same time peroxide species were also detected in the solution. This yellow precipitate has been identified as $UO_2(O_2)\cdot 2H_2O$ (see Section 3.3). When the pH was decreased to 1 or when $Cu^{2+}(aq)$ was added, no precipitate was found and no peroxide species were detected. This uranyl peroxide compound will be discussed in detail in Section 3.3.

3.1.7 Quenching of Excited Uranyl Ion ($*UO_2^{2+}$) by Isobutane

Uranyl ion has strong luminescence and its spectrum ranges from 450 nm to 650 nm as shown in **Figure** 3.1.7-1. Isobutane can quench the excited uranyl ion and diminish its luminescence. The quenching constant was obtained from quenching experiments in the absence and presence of

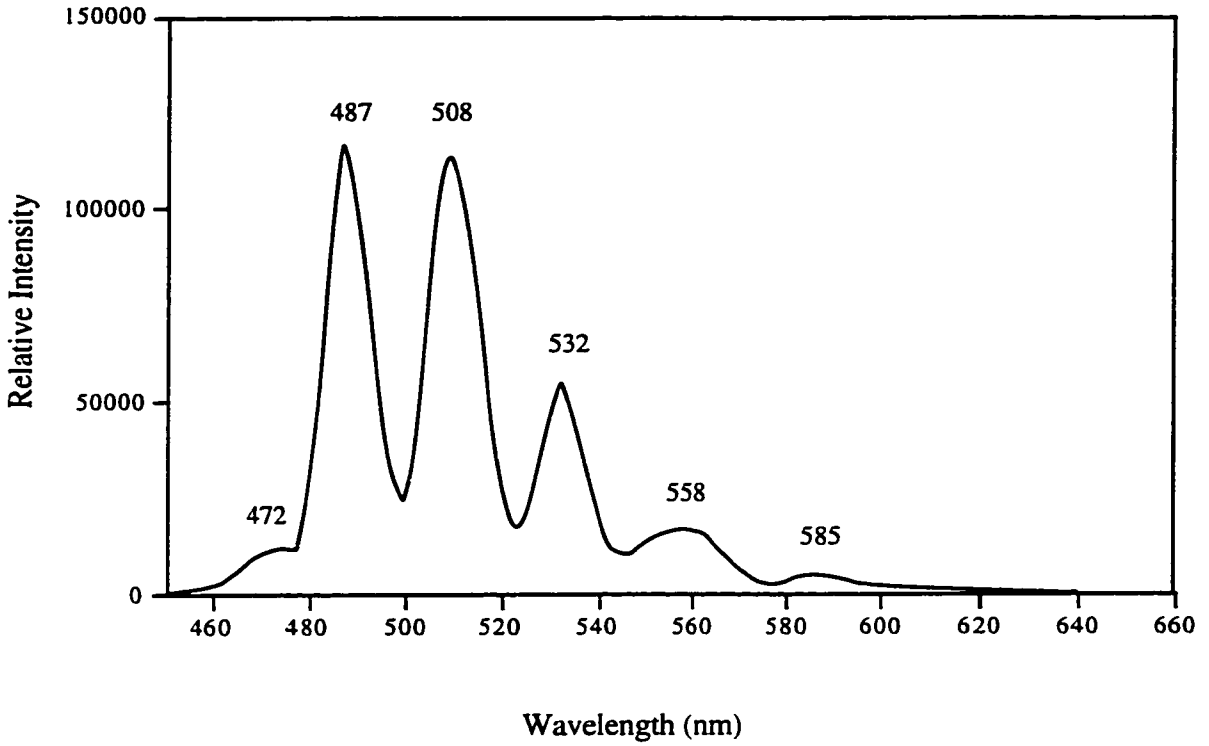

Figure 3.1.7-1. Emission spectrum of uranyl ion. $[UO_2^{2+}]$ = 12.3 mM; pH = 1.0 ($HClO_4$); T = 25 °C; Excitation wavelength is 415 nm.

isobutane, the results are shown in **Table** 3.1.7-1.

Because the solubility of isobutane is limited and it is difficult to measure accurately at low concentrations, just two emission values were estimated, one in the absence and one in the presence of isobutane. Each value is the average of ten measurements and each measurement was automatically scanned 5 times and averaged. The differences between these average values is less than 1.5%.

The Stern-Volmer equation is used to calculated the quenching constant. It has the following form:

$$I_0/I = 1 + K_{sv}[Q] \quad \text{or} \quad I_0/I = 1 + k_q\tau[Q]$$

where I_0 is the intensity in the absence of quenching substance Q; I is the intensity in the presence of Q; K_{sv} is the Stern-Volmer constant, k_q the quenching constant; τ is the lifetime in the absence of Q (i.e. it is the lifetime of the hydrated exited uranyl ion); and [Q] is the concentration of quencher. From the Stern-Volmer equation, the quenching constant of excited uranyl ion by isobutane is calculated to be $(3.5 \pm 0.56) \times 10^7\ M^{-1}s^{-1}$. Using this measured value, $\tau = 2.1\ \mu s$.

Table 3.1.7-1. Emission intensity of uranyl ion in the presence and absence of isobutane.[a]

Condition	Average Integrated Emission Intensity
Absence of isobutane	1.21×10^5
	5.01×10^5 [b]
Presence of isobutane (0.91 mM)	1.13×10^5
	4.56×10^5 [b]

a) $[UO_2^{2+}]$ = 12.3 mM; pH = 0.95 ($HClO_4$); T = 25 °C; Excitation wavelength is 415 nm.

b) These were measured using a different spectrofluorometer (Spex Fluorolog222) and using different instrument parameters.

3.1.8 Effect of Concentration of Isobutane

In these experiments, a differential method was used to overcome the difficulty of controlling the isobutane concentrations. Irradiation and the bubbling of isobutane into the solution were started at the same time. Thus the concentration of isobutane increased continuously (**Figure** 3.1.8-1) and the production rate of 2-methyl-2-propanol (the slope of the curve of [t-butanol] versus time) increased continuously. From this figure, some isobutane concentrations were selected and the corresponding slopes of production of 2-methyl-2-propanol at these points were also determined. Since these slopes have a direct relation with the quantum yield, one can obtain the quantum yields for different isobutane concentrations. The results are shown in **Figure** 3.1.8-2. The quantum yield increases with increasing isobutane concentration.

3.1.9 Effect of Concentration of Acid

The effect of perchloric acid concentration on the quantum yield is shown in **Figure** 3.1.9-1. The quantum yield increases with increasing concentration of perchloric acid, but the slope of the curve of the quantum yield decreases with increase in the perchloric acid concentration. When the

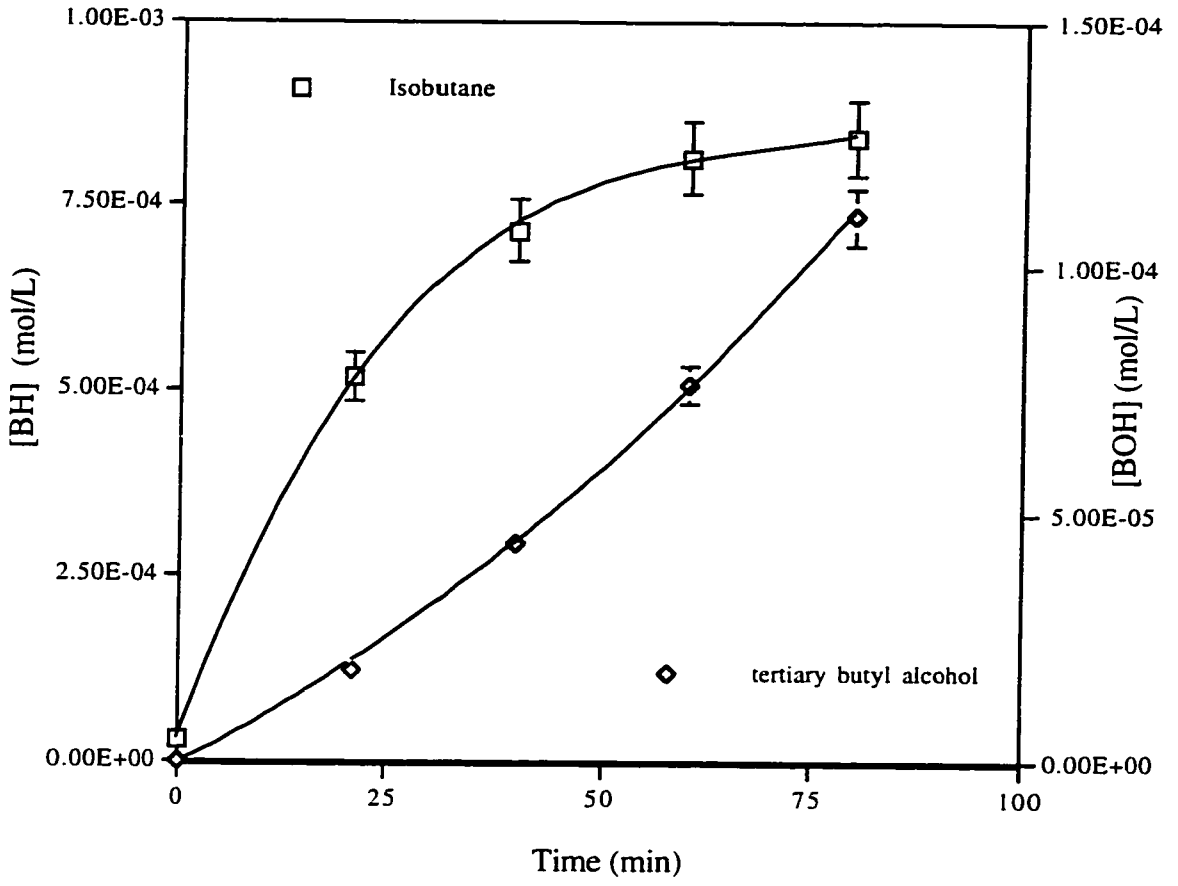

Figure 3.1.8-1. The Relationship of concentrations of photoproduced t-butanol and isobutane with time.

$[UO_2^{2+}]$ = 34.8 mM; pH = 1.1 ($HClO_4$); V_{irrad} = 145 mL; T = 25 °C; I = 9.32 x 10^{-6} Einstein/min; λ_{irr} = 415 nm. Before irradiation nitrogen was bubbled for 20 min and then isobutane was bubbled for 5 min. During irradiation, isobutane was continuously bubbled at the rate of 10 mL/min. (note:

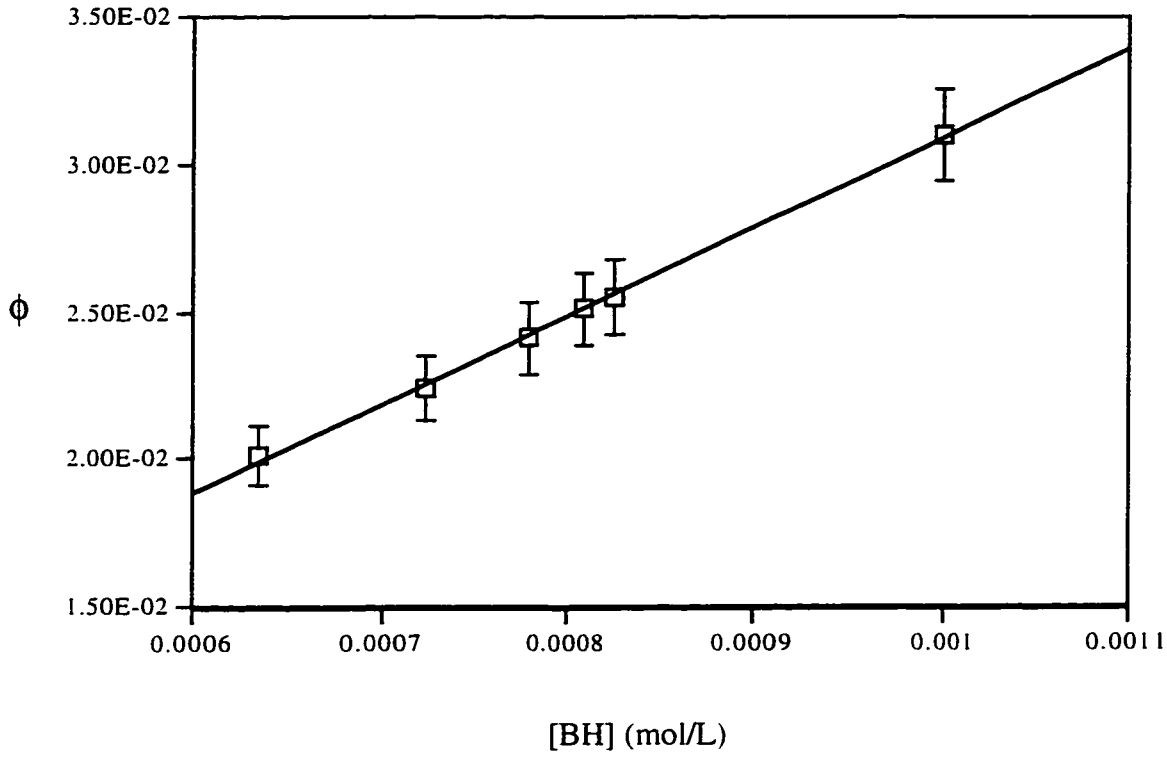

Figure 3.1.8-2. Dependence of quantum yield of t-butanol on the concentration of isobutane.
$[UO_2^{2+}]$ = 34.8 mM; pH = 1.1 ($HClO_4$); V_{irrad} = 145 mL; T = 25 °C; I = 9.32 x 10^{-6} Einstein/min; λ_{irr} = 415 nm. Before irradiation nitrogen was bubbled for 20 min and then isobutane was bubbled for 5 min. During irradiation, isobutane was continuously bubbled at the rate of 10 mL/min (note: values of [BH] come from the isobutane curve in Figure 3.1.8-1, and values of ϕ come from the coressponding slopes of tertiary butyl alcohol curve in Figure 3.1.8-1).

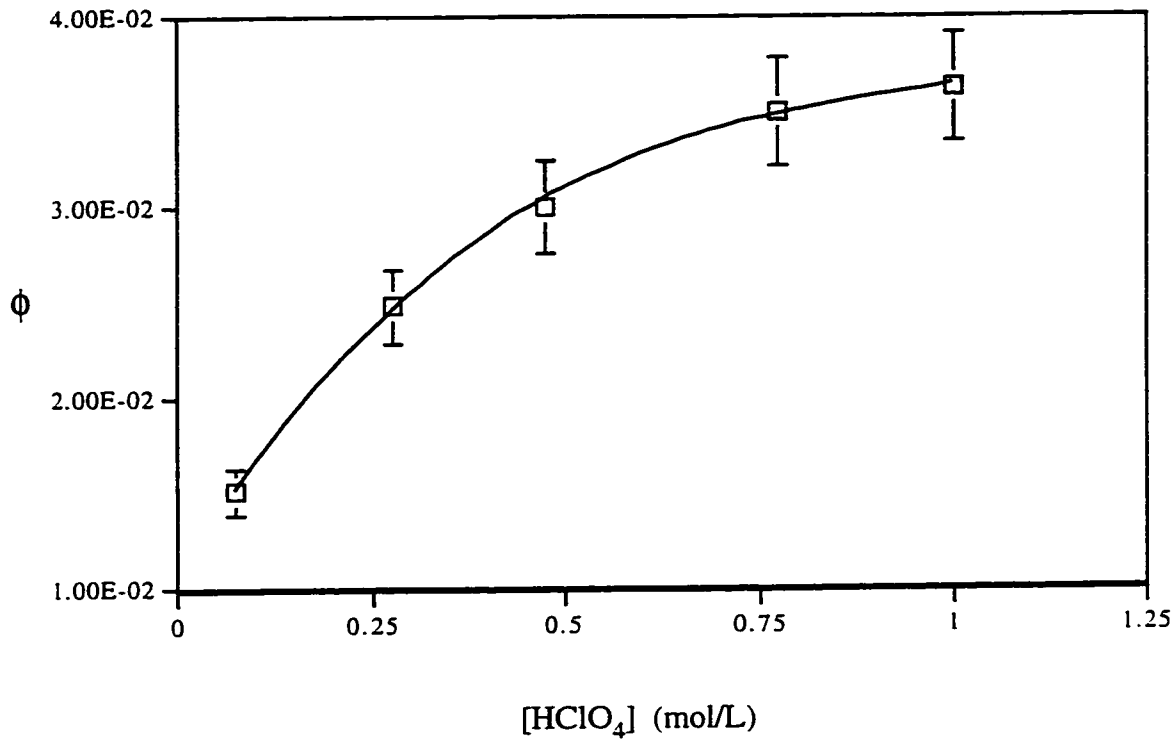

Figure 3.1.9-1. Dependence of quantum yield on the concentration of $HClO_4$.

$[UO_2^{2+}]$ = 34.8 mM; $[BH]_{average}$= 0.60 mM; V_{irrad} = 150 mL; T = 25 °C; I = 6.98 x 10^{-6} Einstein/min; λ_{irr} = 415 nm. Isobutane was bubbled for 30 min before irradiation and continuously bubbled during irradiation.

perchloric acid concentration was very low, for example lower than 0.01 mol/L, the quantum yield remained almost the same value (**Figure** 3.1.9-2). This shows that the effect of acid is based on a complicated kinetic process.

3.1.10 Effect of Light Intensity

The light intensity does not affect the quantum yield. The results are shown in **Figure** 3.1.10-1. This is expected as discussed in Chapter 4.

3.1.11 Effect of Concentration of Uranyl Ion

Table 3.1.11-1 shows the results of the effect of uranyl concentration on quantum yield. The concentration of uranyl ion does not have a significant effect on the quantum yield in the experimental range studied.

3.1.12 Effects of Other Substances

In the presence of oxygen, no $U^{4+}(aq)$ was found as described previously, but acetone is formed. **Figure** 3.1.12-1 shows the results. One can see that as isobutane concentration decreases, 2-methyl-2-propanol concentration increases with time. If oxygen is bubbled into the solution, acetone is produced immediately, and at the same time, the

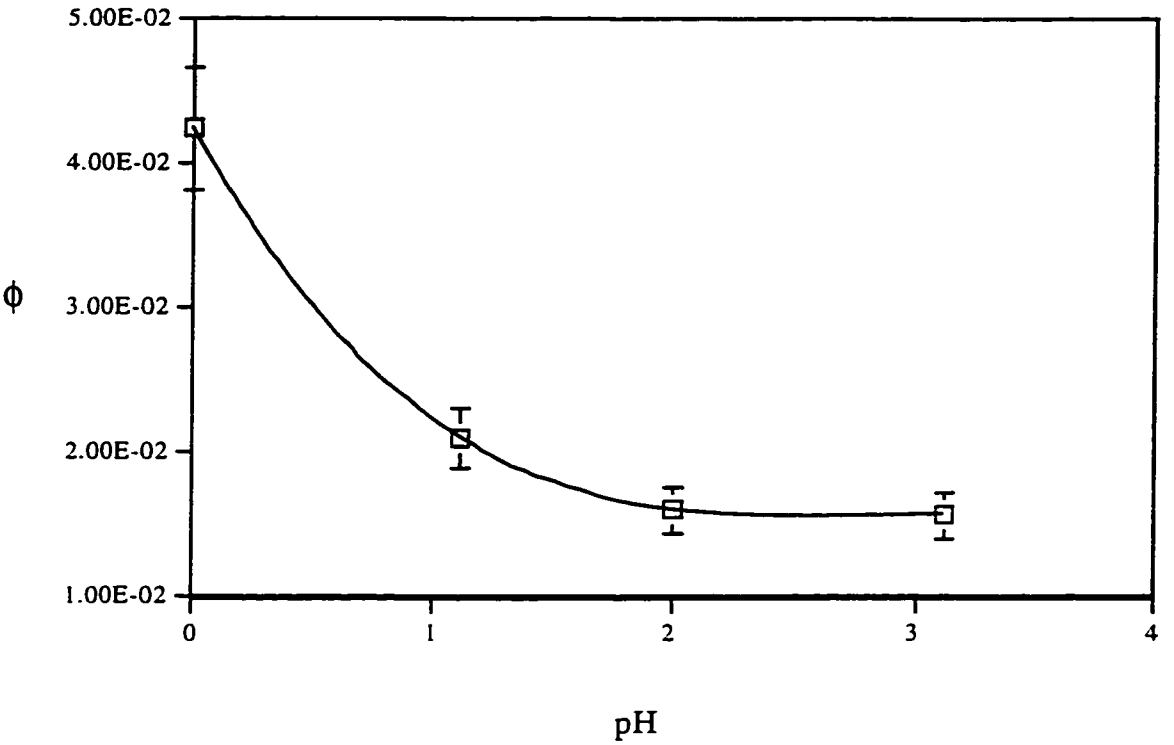

Figure 3.1.9-2. Dependence of quantum yield on pH. $[UO_2^{2+}]$ = 34.8 mM; $[BH]_{average}$= 0.70 mM. V_{irrad} = 145 mL; T = 25 °C; I = 9.32 x 10^{-6} Einstein/min; λ_{irr}= 415 nm. Isobutane was bubbled for 30 min before irradiation and continuously bubbled during irradiation.

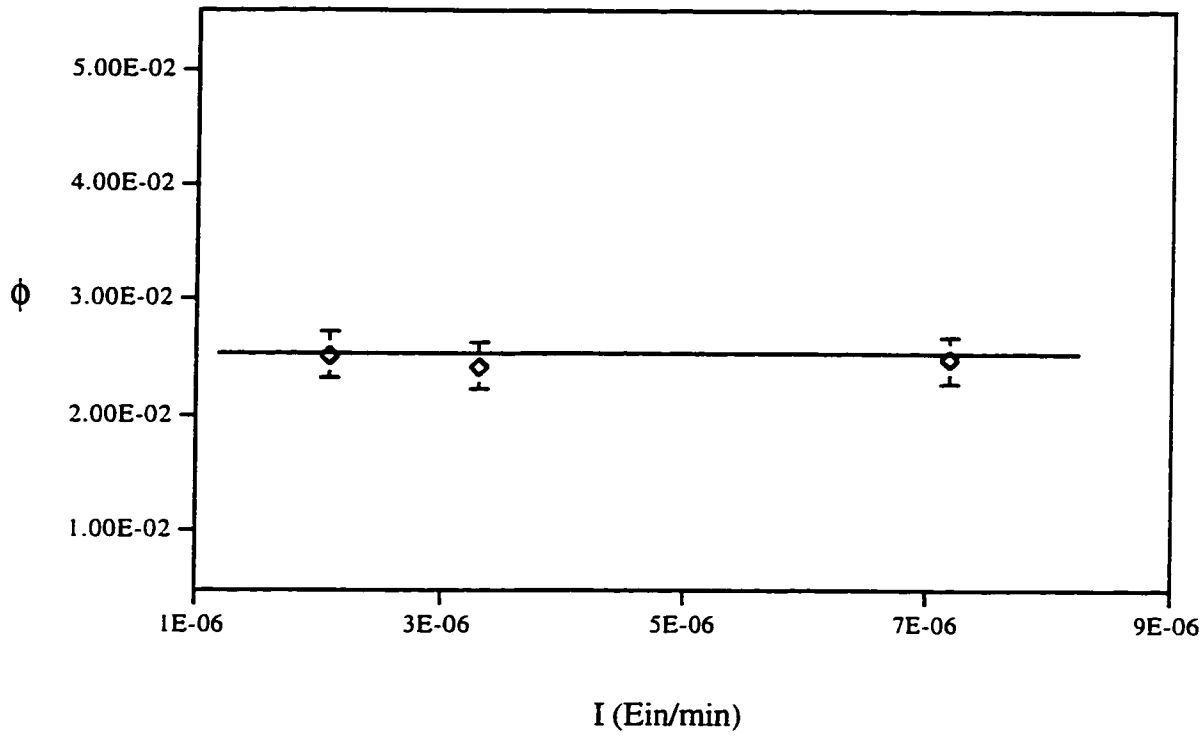

Figure 3.1.10-1. Dependence of quantum yield on light intensity . $[UO_2^{2+}]$ = 36.5mM; [BH] = 0.80 mM; pH = 1.0 ($HClO_4$); V_{irrad} = 95.8 mL; T = 25 °C; λ_{irr} = 415 nm. Isobutane was bubbled for 50 min before irradiation and continuously bubbled during irradiation .

Table 3.1.11-1. Effect of uranyl ion concentration on the quantum yield.[a]

$[UO_2^{2+}]$/mM	ϕ
24.6	0.023
36.9	0.023
110.7	0.020
147.6	0.022

a) I = (6.59 ± 0.05) x 10^{-6} Einstein/min; $[BH]_0$ = 8.1 x 10^{-4} M; pH = 0.95 ($HClO_4$).

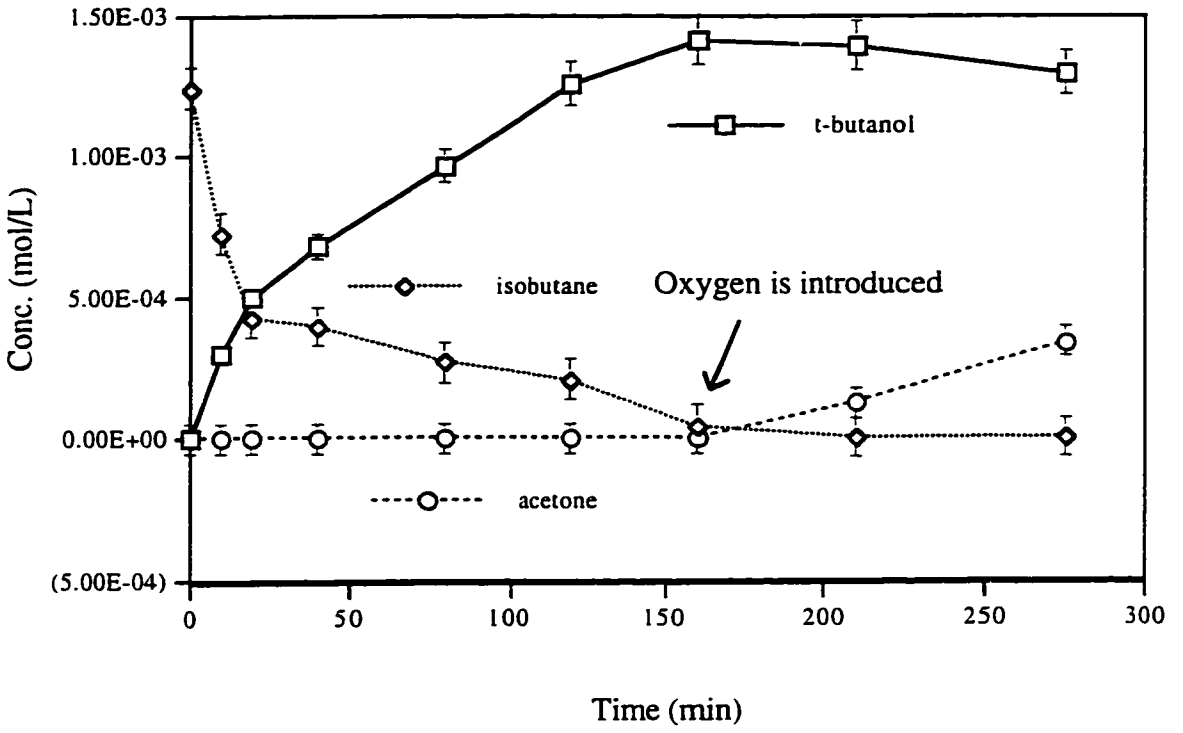

Figure 3.1.12-1. Photoproduction of t-butanol and acetone. $[UO_2^{2+}]$ = 34.8 mM; pH = 1.1 ($HClO_4$]; V_{irrad} = 145 mL; T = 25 °C; GG400 filter. Isobutane was bubbled for 30 min before irradiation.

2-methyl-2-propanol concentration decreases. The production of acetone is due to the reaction of tertiary butyl radical with oxygen (see Section 4.1.1). The slight decrease in concentration of 2-methyl-2-propanol may be due to further oxidation of it.

The photooxidation of 2-methyl-2-propanol was investigated using 2-methyl-2-propanol as the starting substance. In the absence of oxygen, it was found that the concentration of 2-methyl-2-propanol did not change during the irradiation (**Figure** 3.1.12-2). But when oxygen is present, 2-methyl-2-propanol was quickly oxidized to acetone (**Figure** 3.1.12-3). This demonstrates that in the presence of oxygen, 2-methyl-2-propanol, at least, is one of the sources producing acetone. From the comparison of their slopes, one can see that the decrease in the rate of 2-methyl-2-propanol production is greater than the increase in the rate of acetone. It seems that either acetone is not the only product of 2-methyl-2-propanol or that acetone could be further oxidized.

The effects of cations were investigated to see how they affect the quantum yield and if they could increase the quantum yield for 2-methyl-2-propanol. When Ag^{+} was added to the isobutane-saturated uranyl solution and irradiated, after 20 minutes a black precipitate was formed but not identified. It probably is due to the reduction of Ag^{+} to Ag by butyl radical or other intermediates. Addition of Cr^{3+} as $CrK(SO_4)_2 \cdot 12H_2O$ slightly decreased the production rate of

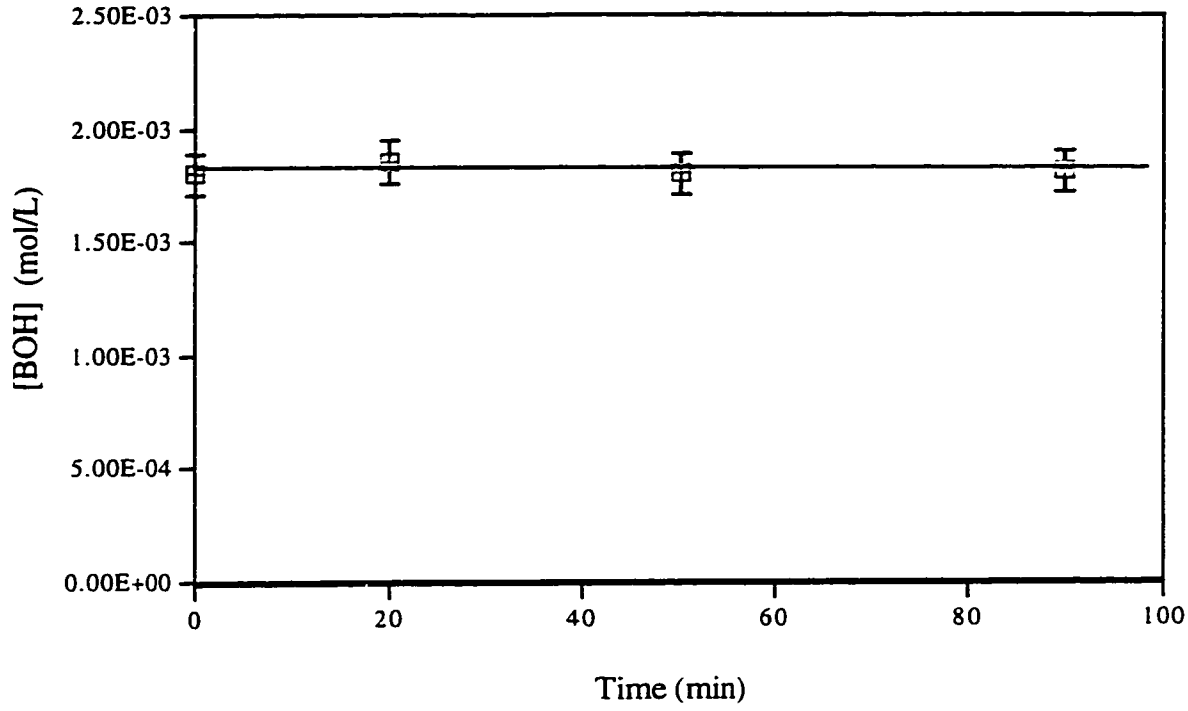

Figure 3.1.12-2. Irradiation of t-butanol in the absence of oxygen. $[UO_2^{2+}]$ = 34.8 mM; pH = 1.1 ($HClO_4$); V_{irrad} = 145 mL; T = 25 °C; GG400 filter.

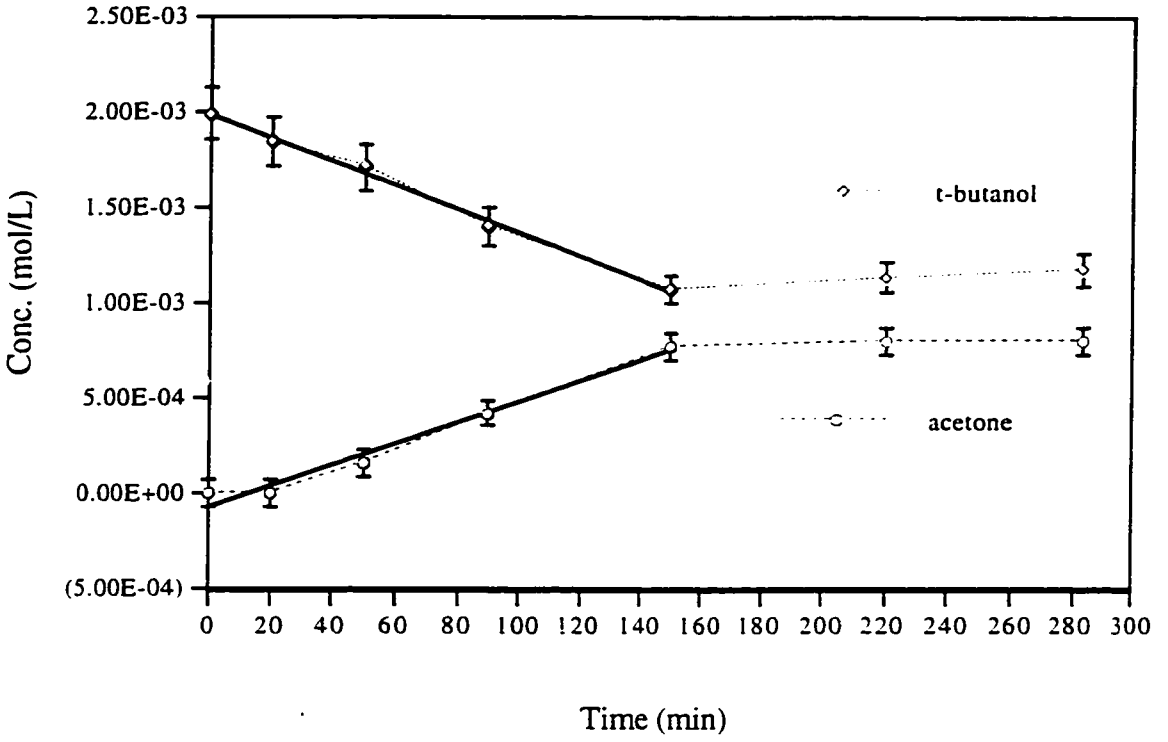

Figure 3.1.12-3. Irradiation of t-butanol in the presence of oxygen. $[UO_2^{2+}]$ = 34.8 mM; pH = 1.1 ($HClO_4$); V_{irrad} = 145 mL; T = 25 °C; GG400 filter.

Curve fitting equation for the first five points of t-butanol:

$$y = -6.15E\text{-}06x + 1.98E\text{-}03 \quad r^2 = 9.95E\text{-}01$$

Curve fitting equation for the first five points of acetone:

$$y = 5.46E\text{-}06x - 6.92E\text{-}05 \quad r^2 = 9.78E\text{-}01$$

2-methyl-2-propanol.

Some anions have a strong effect on the lifetime of excited uranyl ion. It was reported that in the presence of F^- or $H_2PO_4^-$ and HPO_4^{2-}, the excited uranyl ion has a much longer lifetime than in $HClO_4$ solution; the lifetime increased from 2.2 μs (in $HClO_4$) to about 150 μs (in 0.2 M NaF) and 170 μs (in 1 M H_3PO_4).[22] A longer lifetime is usually expected to enhance the quantum yield. In the present experiments, it was found that in 0.66 mol/L H_3PO_4 solution (pH = 0.92), the quantum yield of 2-methyl-2-propanol is about the same as that in the aqueous $HClO_4$ system while in 0.2 mol/L NaF solution (pH = 6.5), the quantum yield is close to zero (<0.0005). In both systems, a slight red shift of 6 nm in F^- system and 7 nm in the H_3PO_4 system, compared to the UO_2^{2+} absorption spectra in aqueous $HClO_4$, was found, but the structure of the spectrum remained the same. This means that the ground state of the structure of uranyl ion does not change significantly. These results also indicate that the quantum yield is not directly related to the lifetime of excited species. After the addition of NaF, the pH of the solution changed from 1 to 6.5. The different uranyl-floride complexes are shown in **Table** 3.1.12-1.[136] These results show that all uranyl ions are complexed by fluoride ions, and most of them are in forms of UO_2F_2 and $UO_2F_3^-$. This means that F^- strongly affects the properties of excited uranyl ion. As it will be

Table 3.1.12-1. Distribution of uranyl-floride complex in 0.2 M NaF.

Species	Percentage(%)
UO_2^{2+}	0
UO_2F^+	10
UO_2F_2	44
$UO_2F_3^{3-}$	40
$UO_2F_4^{4-}$	6

discussed in Chapter 4, the oxidation potential of excited uranyl ion decreases from 2.8 V to 2.4 V after coordination by F^-.

3.2 Photolysis of Isobutane in the Presence of $K_2(S_2O_8)$

3.2.1 Photolysis

Addition of peroxydisulfate significantly increases the quantum yield for 2-methyl-2-propanol. For example in the presence of 1.0 mM of peroxydisulfate, the quantum yield of 2-methyl-2-propanol increased almost ten times (**Figure** 3.2.1-1). In the dark or for irradiation in the absence of uranyl ion, no products were found. Since the peroxydisulfate anion neither absorbs visible light nor quenches the excited uranyl ion, it seems that it must react with some photogenerated intermediate(s).

3.2.2 Mass Balance

In the presence of peroxydisulfate, besides the increased quantum yield, the formation of 2-methyl-2-propanol and a small amount of isobutene can account for the loss of isobutane i.e. there is a mass balance. **Tables** 3.2.2-1 and 3.2.2-2.

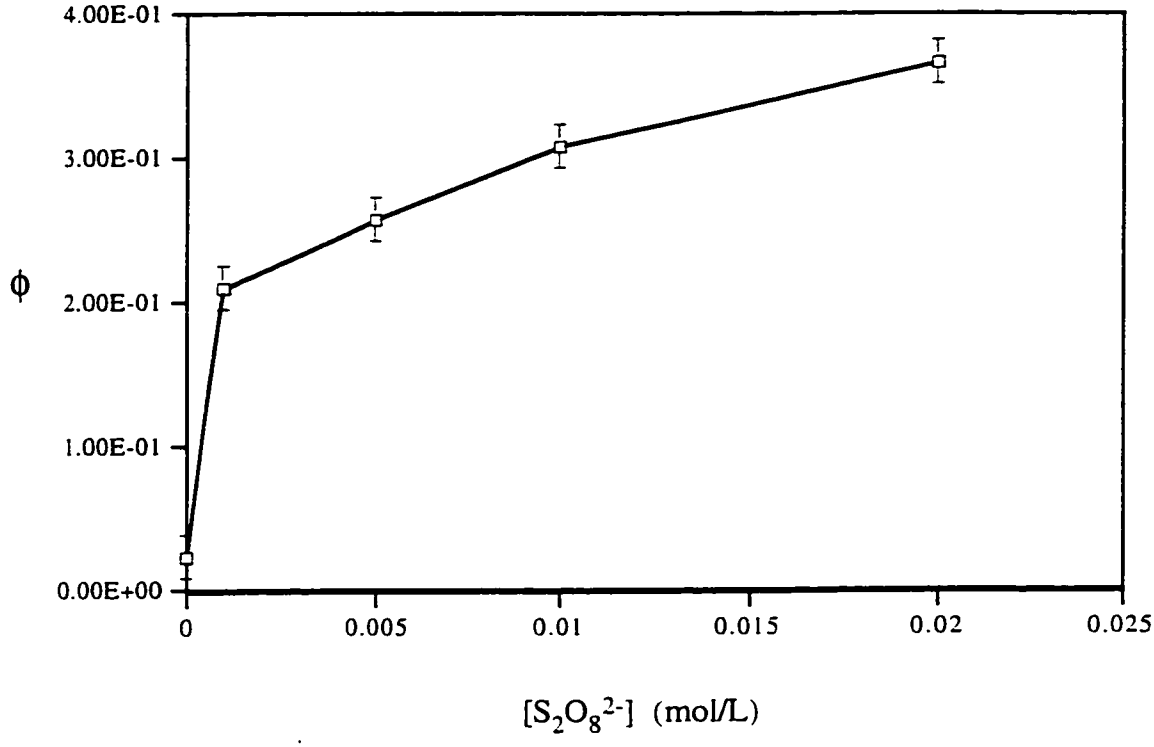

Figure 3.2.1-1. Relationship of quantum yield with the concentration of $S_2O_8^{2-}$.
$[UO_2^{2+}]$ = 34.8 mM; [BH] = 0.70 mM; pH = 1.1 ($HClO_4$); V_{irrad} = 145 mL; T = 25 °C; I = 9.08 x 10^{-6} Einstein/min; λ_{irr} = 415nm. Isobutane was bubbled for 30 min before irradiation and continuously bubbled during irradiation.

Table 3.2.2-1. Mass balance arising from the photolysis of isobutane in the presence of peroxydisulfate with Millipore Water.[a]

Irrad.Time (min)	-Δ[Isobutane] [M]x10^4	Δ[t-butanol] [M]x10^4	Δ[Isobutene] [M]x10^4	P[b] (%)
10	2.23	1.63	0.0020	73
24	3.87	3.92	0.0487	103
40	5.43	5.19	0.325	102
60	6.25	5.21	0.969	99
78	7.17	5.14	0.145	74

a) $I=(7.14 \pm 0.05) \times 10^{-6}$ Ein/min; $[BH]_0=8.11 \times 10^{-4}$ M; $[K_2S_2O_8]$ = 2.07 mM; $[UO_2^{2+}]$ = 34.8 mM; pH = 1.1 ($HClO_4$); V_{irrad} = 95.8 mL; T = (25 ± 0.15) °C; λ_{irr} = 415 nm.

b) P = {Δ[t-butanol] + Δ[isobutene]}/(-Δ[isobutane]) x 100%.

Table 3.2.2-2. Mass balance arising from the photolysis of isobutane in the presence of peroxydisulfate with Triply Distilled Water.[a]

Irrad.Time (min)	-Δ[Isobutane] [M]x10^4	Δ[t-butanol] [M]x10^4	Δ[Isobutene] [M]x10^4	P[b] (%)
14	2.26	1.45	0.0042	66
29	3.33	3.25	0.0061	99
43	4.22	3.95	0.098	96
57	5.04	4.86	0.158	100
78	6.65	4.93	0.094	76

a) $I = (7.14 \pm 0.05) \times 10^{-6}$ Ein/min; $[BH]_0 = 7.05 \times 10^{-4}$ M; $[K_2S_2O_8] = 2.07$ mM; $[UO_2^{2+}] = 36.4$ mM; pH = 0.95 ($HClO_4$); $V_{irrad} = 95.8$ mL; T = (25 ± 0.15) °C; $\lambda_{irr} = 415$ nm.

b) P = {Δ[t-butanol] + Δ[isobutene]}/(-Δ[isobutane]) x 100%.

show the results obtained with Millipore water and triply distilled water, respectively. As the results are essentially the same, Millipore water was used in other experiments.

In the presence of peroxydisulfate, $U^{4+}(aq)$ was not detected. Peroxydisulfate can affect the quenching rate of $*UO_2^{2+}$ by isobutane. In its presence, the quenching constant decreases from $3.5 \times 10^7\ M^{-1}s^{-1}$ to $2.60 \times 10^7\ M^{-1}s^{-1}$. This decrease means that the interaction of isobutane with excited uranyl ion decreases. Thus the increased quantum yield in the presence of peroxydisulfate can not be attributed to the direct interaction of isobutane with the excited uranyl ion.

3.2.3 Effect of Concentration of $K_2(S_2O_8)$

In these experiments, the light intensity was kept at a low level in order to keep the rate of consumption of the isobutane at a low level so that it can be replenished by bubbling, i.e. approximately the same concentration level of isobutane is maintained from one experiment to the next one.

The quantum yield increases with increasing concentration of peroxydisulfate (**Figure** 3.2.3-1). It can be seen that at the lower concentrations of peroxydisulfate, the quantum

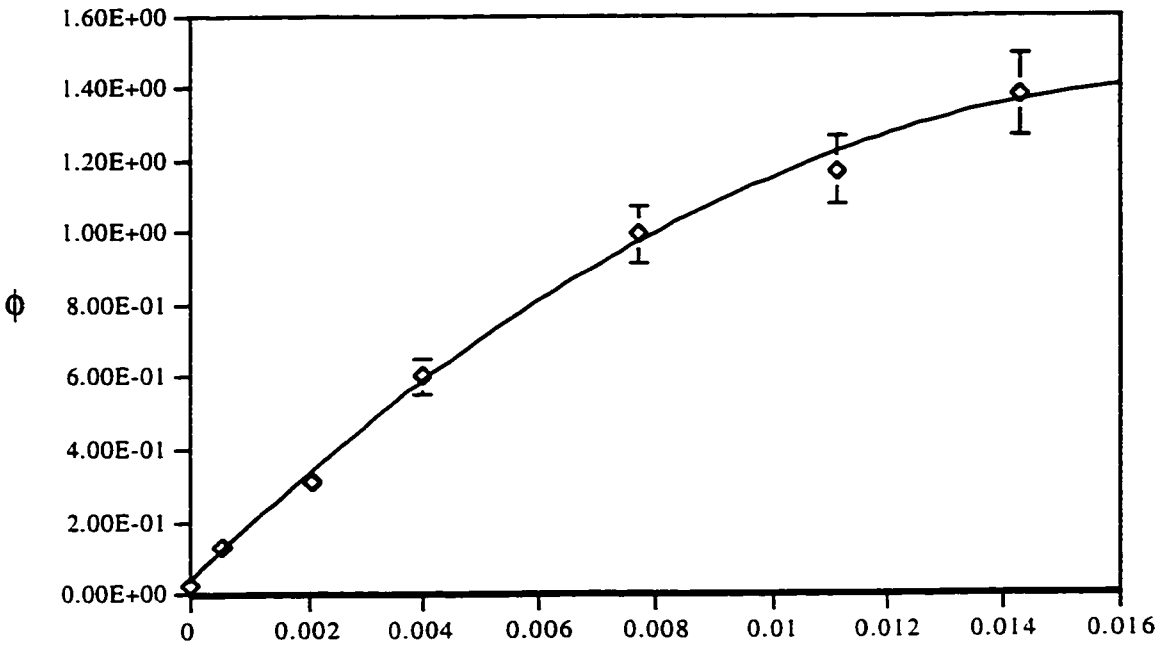

Figure 3.2.3-1. Dependence of quantum yield on the concentration of $S_2O_8^{2-}$.
$[UO_2^{2+}]$ = 34.8 mM; pH = 0.95 ($HClO_4$); $[BH]_{average}$= 0.80 mM; T = 25 °C; I = 2.11 x 10^{-7} Einstein/L·s; λ_{irr}= 415 nm.

$[S_2O_8^{2-}]$ M	ϕ
0.00E+00	0.024
5.20E-04	0.13
2.07E-03	0.35
4.00E-03	0.60
7.71E-03	0.99
1.11E-02	1.17
1.43E-02	1.38

yield is almost a linear function of peroxydisulfate concentration but when the concentration of peroxydisulfate is higher, the curve bends downwards.

3.2.4 Effect of Concentration of Isobutane

Figure 3.2.4-1 shows the dependence of the quantum yield on the concentration of isobutane in the presence of peroxydisulfate. The dependence of quantum yield with isobutane concentration is close to a straight line.

In the absence of peroxydisulfate, the quantum yield also increases with the increase of isobutane concentration, but the rate is about 20 times less.

3.2.5 Effect of Concentration of Acid

In the studies on the effect of perchloric acid on quantum yield, a lower light intensity was also used for the same reason as given earlier. The results are shown in **Figure** 3.2.5-1. The quantum yield increases with increasing concentration of perchloric acid, but not linearly.

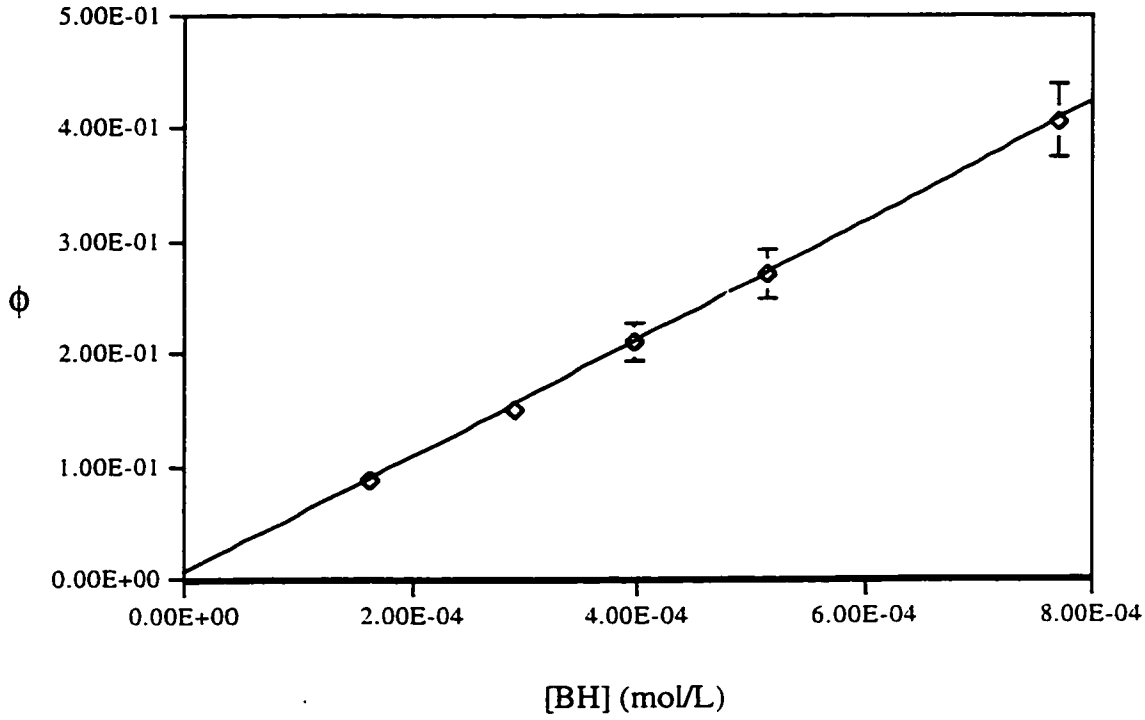

Figure 3.2.4-1. Dependence of quantum yield on the concentration of isobutane in the presence of $S_2O_8^{2-}$.
$[UO_2^{2+}]$ = 33.8 mM; pH = 0.95 ($HClO_4$); $[K_2S_2O_8]$ = 14.3 mM; V_{irrad} = 95.8 mL; T = 25 °C; I = 1.28 x 10^{-6} Einstein/L·s; λ_{irr} = 415 nm.

[BH] M	ϕ
1.60E-04	0.087
2.89E-04	0.15
3.97E-04	0.21
5.14E-04	0.27
7.71E-04	0.41

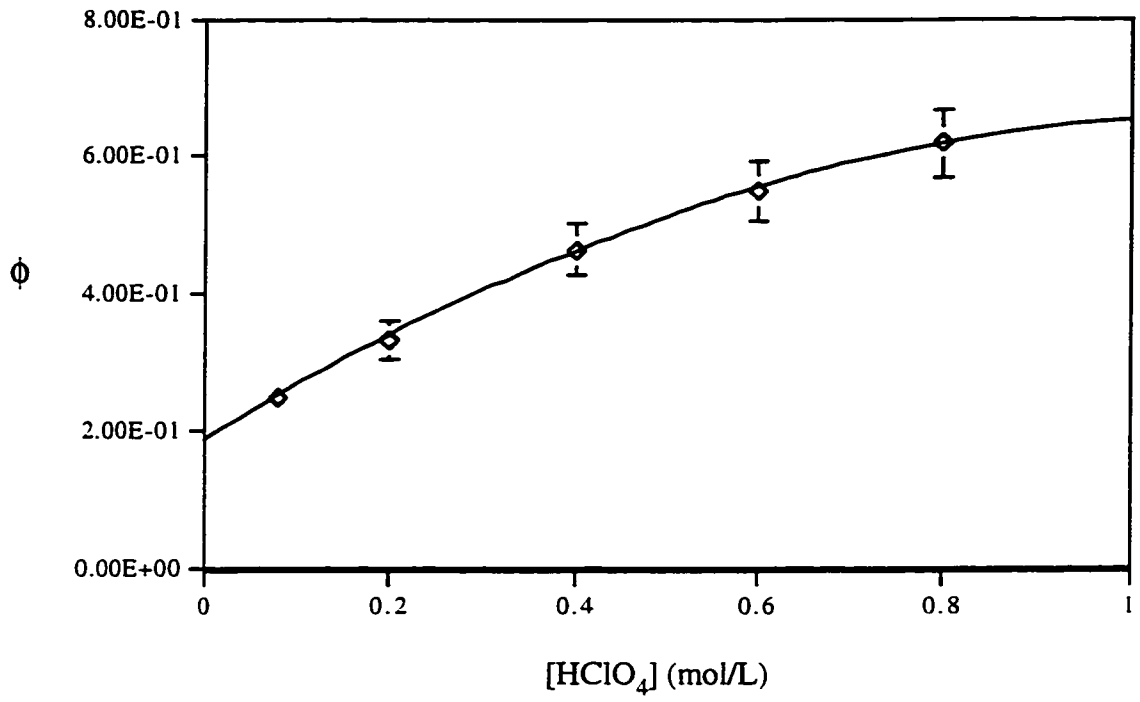

Figure 3.2.5-1. Dependence of quantum yield on the concentration of $HClO_4$.

$[UO_2^{2+}]$ = 34.6 mM; $[BH]_{average}$ = 0.70 mM; $[K_2S_2O_8]$ = 5 mM; V_{irrad} = 103 mL; λ_{irr} = 415 nm; T = 25 °C; I = 1.21×10^{-6} Einstein/L·s. Isobutane was bubbled for 40 min before irradiation and continuously bubbled during irradiation.

$[HClO_4]$ M	ϕ
0.079	0.25
0.200	0.33
0.400	0.47
0.600	0.55
0.800	0.62

The amplification factor of peroxydisulfate at different acid concentrations was investigated, and the results are shown in **Table** 3.2.5-1. It is seen that the amplification factor does not change when the acid concentration varies from 0.001 to 0.1 M. but it increases slightly when acid concentration further increases.

3.2.6 Effect of Light intensity

The effect of light intensity on the quantum yield was investigated and the results are shown in **Figures** 3.2.6-1 to 3.2.6-4. The slope of each plot gives the quantum yield for that particular condition. These four quantum yield points at different light intensities are plotted in **Figure** 3.2.6-5. The quantum yield decreases nonlinearly with increasing light intensities. This dependence of quantum yield on light intensity is reflected in the reaction mechanism and it will be discussed in Chapter 4.

Table 3.2.5-1. Amplification factor of peroxydisulfate at different acid concentrations.[a]

$[HClO_4]$ M	ϕ	ϕ' (no $S_2O_8^{2-}$)	ϕ/ϕ'
0.001	0.15	0.016	9
0.01	0.13	0.016	8
0.1	0.18	0.021	9
1	0.71	0.042	17

a) [BH] = 0.4 mM; $[S_2O_8^{2-}]$ = 10 mM; T = 25 °C; I = 7.50×10^{-6} Einstein/min.

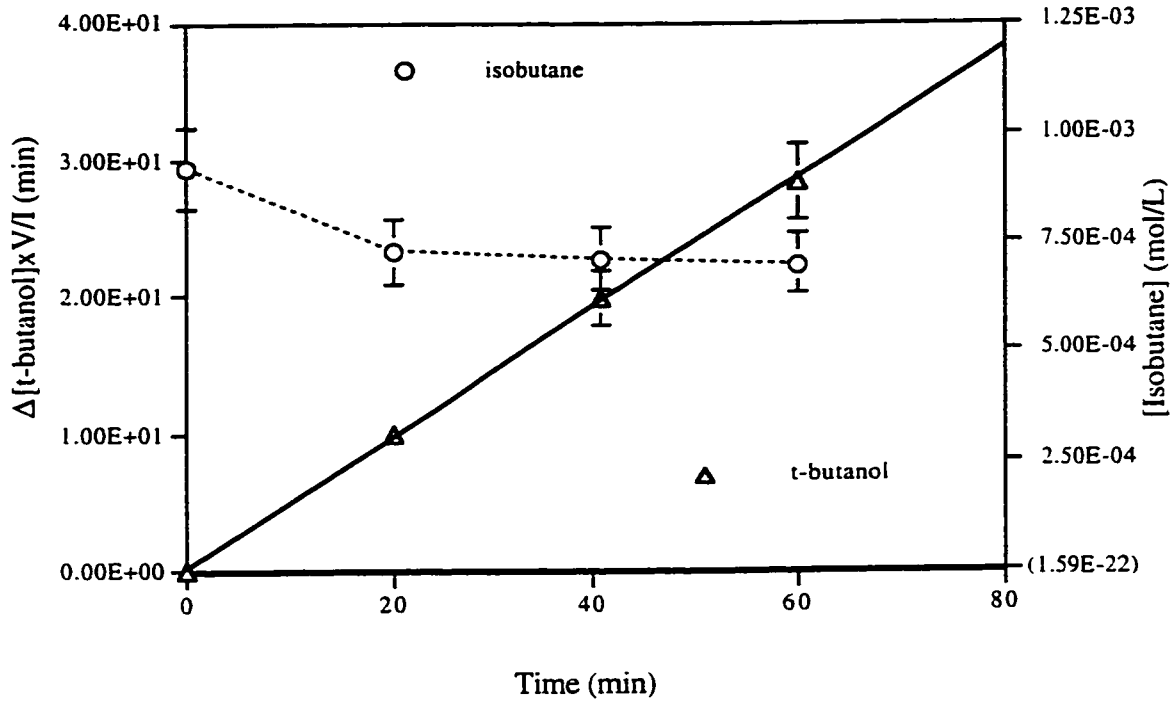

Figure 3.2.6-1. Relationship of [t-Butanol]xVolume/(Light Intensity) with irradiation time in the photoproduction of t-butanol from isobutane with the light intensity $I = 7.38 \times 10^{-6}$ Einstein/min.
$[UO_2^{2+}] = 36.9$ mM; pH = 0.95 ($HClO_4$); $[K_2S_2O_8] = 14.3$ mM;
$V_{irrad} = 103.2$ mL; $T = 25 \pm 0.15$ °C; $\lambda_{irr} = 415$ nm; Millipore water.
Isobutane was bubbled for 30 min before irradiation and continuously bubbled during irradiation.

Curve fitting equation: $y = 4.75E\text{-}01x + 2.23E\text{-}01$

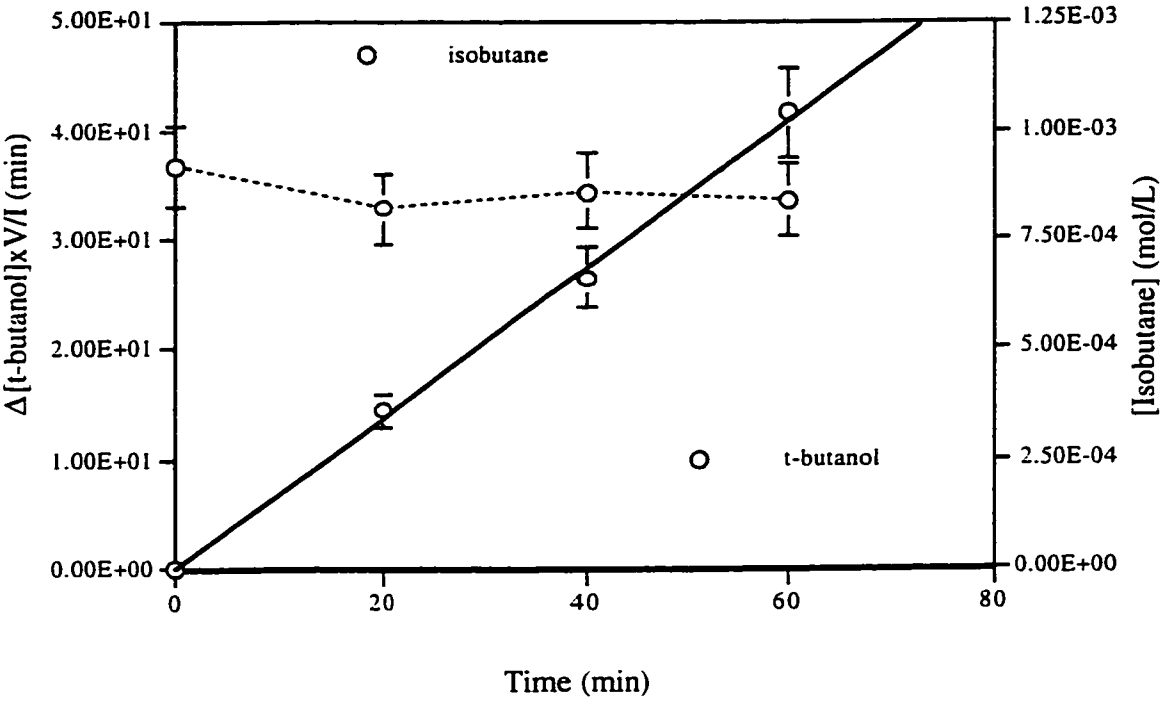

Figure 3.2.6-2. Relationship of [t-Butanol]xVolume/(Light Intensity) with irradiation time in the photoproduction of t-butanol from isobutane with the light intensity $I = 3.24 \times 10^{-6}$ Einstein/min.
$[UO_2^{2+}] = 36.9$ mM; pH = 0.95 ($HClO_4$); $[K_2S_2O_8] = 14.3$ mM;
$V_{irrad} = 103.2$ mL; T = 25 ± 0.15 °C; $\lambda_{irr} = 415$ nm; Millipore water. Isobutane was bubbled for 30 min before irradiation and continuously bubbled during irradiation.

Curve fitting equation: y = 6.84E-01x + 1.40E-01

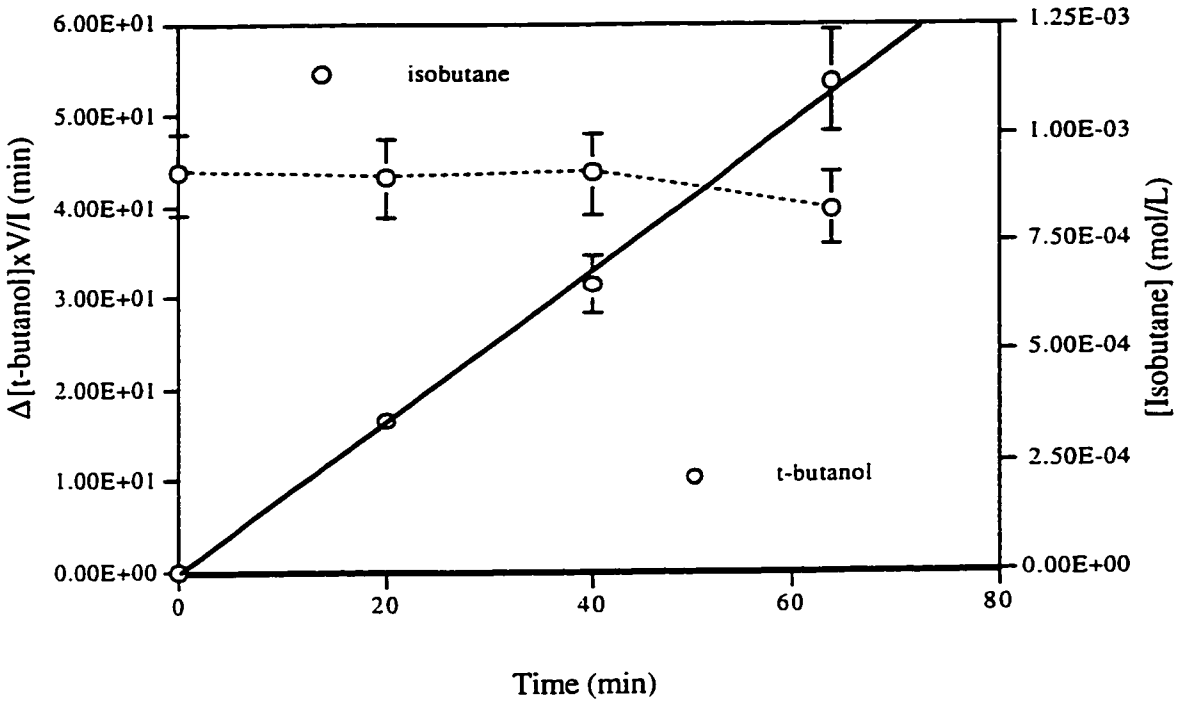

Figure 3.2.6-3. Relationship of [t-Butanol]xVolume/(Light Intensity) with irradiation time in the photoproduction of t-butanol from isobutane with the light intensity I = 2.13×10^{-6} Einstein/min.
$[UO_2^{2+}]$ = 36.9 mM; pH = 0.95 ($HClO_4$); $[K_2S_2O_8]$ = 14.3 mM;
V_{irrad} = 103.2 mL; T = 25 ± 0.15 °C; λ_{irr} = 415 nm; Millipore water.
Isobutane was bubbled for 30 min before irradiation and continuously bubbled during irradiation.

Curve fitting equation: y = 8.32E-01x - 2.73E-01

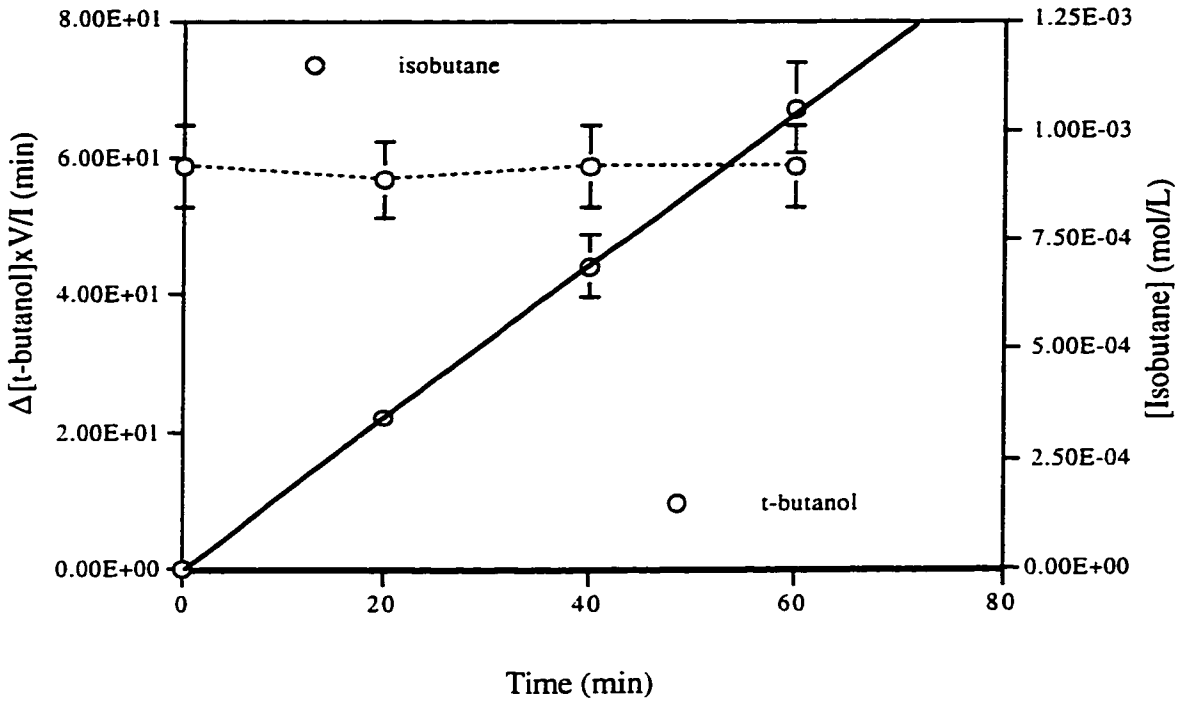

Figure 3.2.6-4. Relationship of [t-Butanol]xVolume/(Light Intensity) with irradiation time in the photoproduction of t-butanol from isobutane with the light intensity I = 1.25×10^{-6} Einstein/min.
$[UO_2^{2+}]$ = 36.9 mM; pH = 0.95 ($HClO_4$); $[K_2S_2O_8]$ = 14.3 mM;
V_{irrad} = 103.2 mL; T = 25 ± 0.15 °C; λ_{irr} = 415 nm; Millipore water.
Isobutane was bubbled for 30 min before irradiation and continuously bubbled during irradiation.

Curve fitting equation: y = 1.12E+00x - 1.20E-01

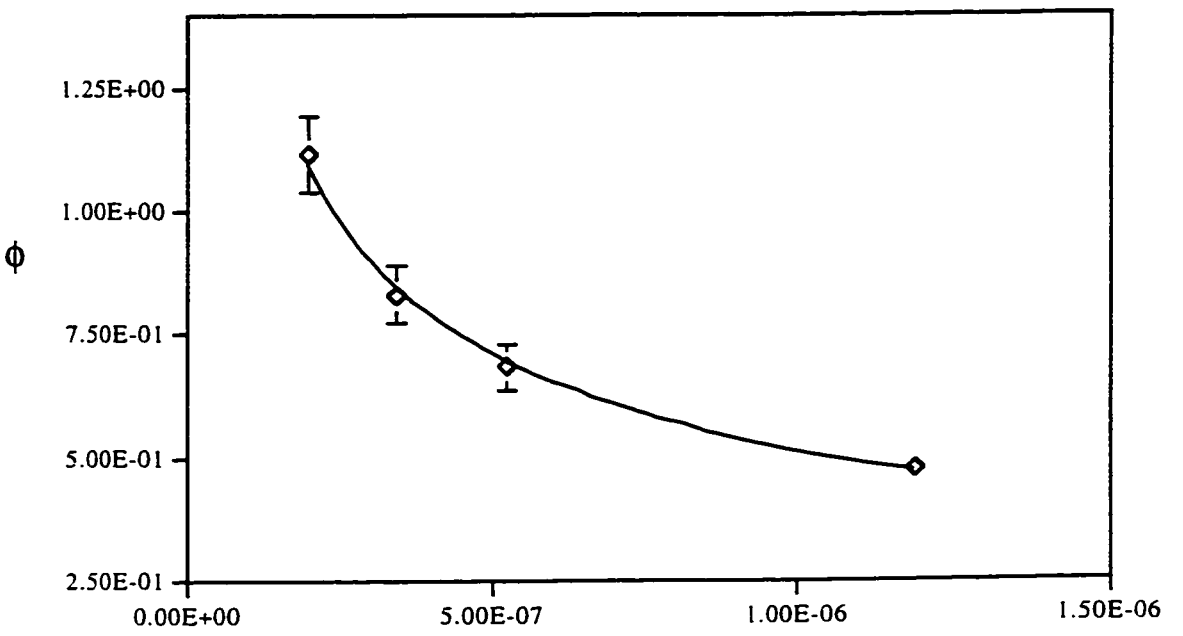

Figure 3.2.6-5. Dependence of quantum yield on light intensity in the presence of 14.3 mM $S_2O_8^{2-}$.

$[K_2S_2O_8]$ = 14.3 mM; $[UO_2^{2+}]$ = 36.9 mM; $[BH]_{average}$ = 0.84 mM; pH = 0.95 ($HClO_4$); V_{irrad} = 103.2 mL; T = 25 ± 0.15 °C; λ_{irr} = 415 nm; Millipore water. Isobutane was bubbled for 30 min before irradiation and continuously bubbled during irradiation.

I (Ein/L.s)	ϕ
2.02E-07	1.12
3.44E-07	0.83
5.23E-07	0.68
1.19E-06	0.48

3.3 Photolysis of Cyclopentane

3.3.1 Photolysis

Cyclopentane (C_5H_{10}) is a liquid at room temperature and pressure. All its hydrogen atoms are secondary ones. Its solubility in water is reported as 2.23 mM.[137] In this work a value of 1.74 mM was obtained in 34.8 mM uranyl solution(see Chapter 2). For brevity, we use CpH_2, CpHOH, CpO, CpHOHene and CpOene to represent cyclopentane, cyclopentanol, cyclopentanone, 2-cyclopenten-1-ol and 2-cyclopenten-1-one, respectively.

In the photolysis studies, cyclopentane was introduced into the uranyl solution by bubbling oxygen through pure liquid cyclopentane and then into the uranyl solution that was in the photolysis cell. No thermal reaction of cyclopentane with the uranyl solution was found in a test experiments conducted for four hours. When this solution is irradiated, cyclopentanol and cyclopentanone are produced (**Figure** 3.3.1-1). The cyclopentanol concentration remains approximately constant after the initial induction period is passed. In contrast, cyclopentanone concentration increases rapidly at the beginning and thereafter it increases at a nearly constant rate. In **Figure** 3.3.1-2, a band-pass filter CWL415 was employed to obtain the quantum yield at 415 nm. The initial production rates of cyclopentanol and cyclopentanone are about the same, but at longer times, the

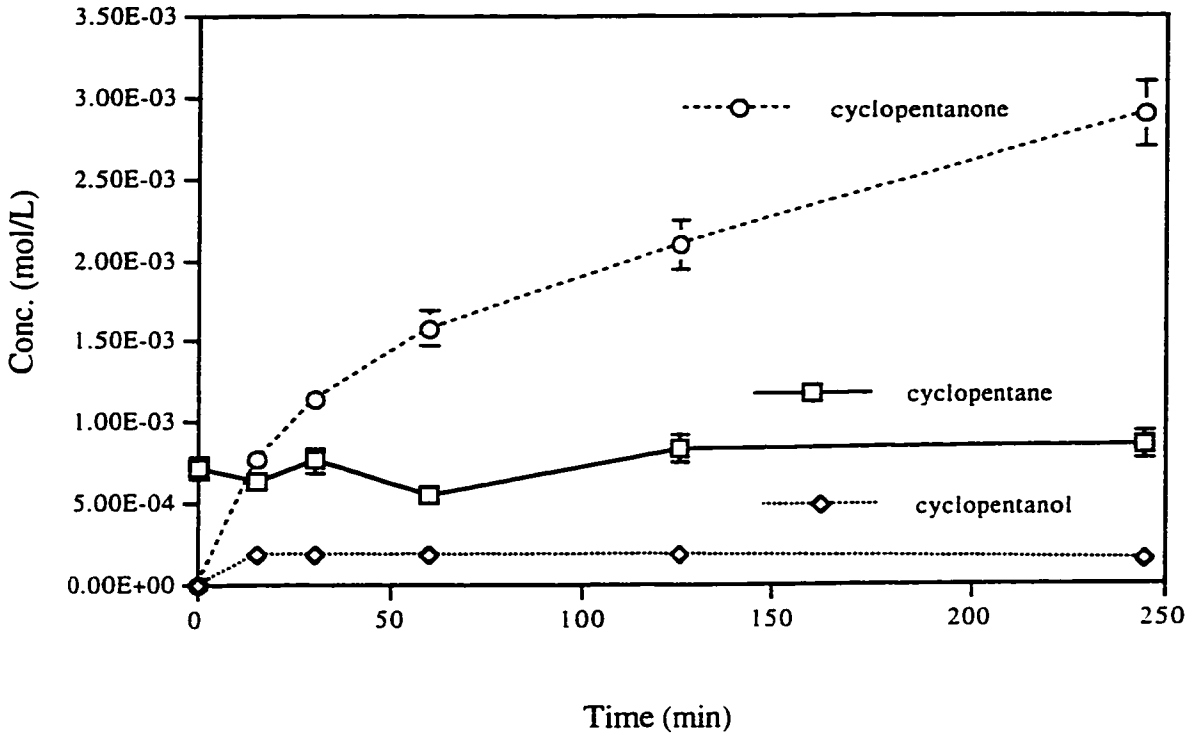

Figure 3.3.1-1. Photoproduction of cyclopentanol and cyclopentanone from cyclopentane.
$[UO_2^{2+}]$ = 34.8 mM; pH = 1.1 ($HClO_4$); V_{irrad} = 145 mL; T = 25 °C.
No filter. Bubbling cyclopentane and oxygen during irradiation.
(bubbling cyclopentane and oxygen for 30 min before irradiation)

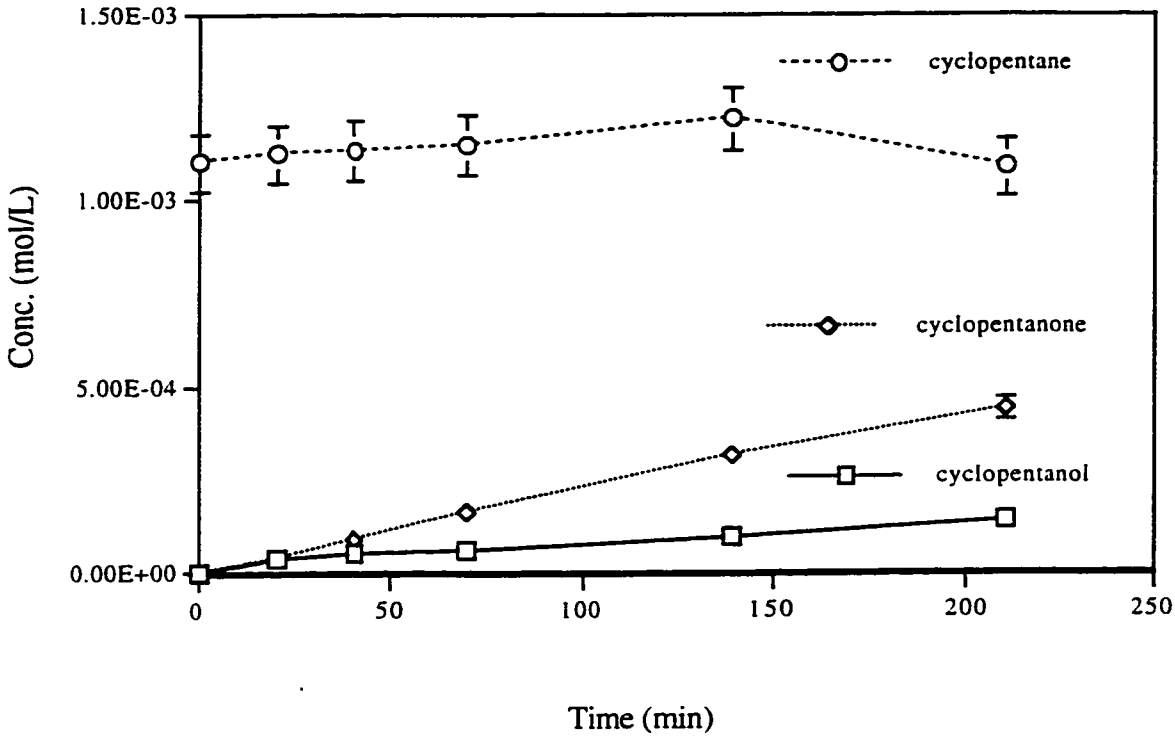

Figure 3.3.1-2. Photoproduction of cyclopentanol and cyclopentanone with CWL415 filter.
$[UO_2^{2+}]$ = 34.8 mM; pH = 1.1 ($HClO_4$); V_{irrad} = 145 mL; T = 25 °C; $I_{(415\ nm)}$ = 8.27 x 10^{-6} Einstein/min; λ_{irr} = 415 nm. Oxygen carrying cyclopentane was bubbled for 20 min before irradiation and continuously bubbled at the rate of 100 mL/min during irradiation.

rate of production of the cyclopentanol decreases. In **Figure** 3.3.1-3, the quotient (Concentration x Volume)/(Light Intensity) is plotted versus time and the initial quantum yield can be obtained from the initial slopes (see Chapter 2). An initial quantum yield of 0.046 is obtained for both cyclopentanol and cyclopentanone. However, the quantum yield for cyclopentanol then decreases at longer times. The photoproduction of cyclopentanol and cyclopentanone using the band-pass filter CWL415 but at a lower bubbling rate was also studied. A result similar to that of **Figure** 3.3.1-2 was obtained, however, the initial quantum yields for cyclopentanol and cyclopentanone are smaller, they are 0.030 and 0.035, respectively.

To determine if cyclopentanol is itself reactive, aqueous cyclopentanol was used as starting material. Irradiation of the cyclopentanol yields cyclopentanone, as shown in **Figure** 3.3.1-4 (with band-pass filter CWL415) and in **Figure** 3.3.1-5 (without band-pass filter CWL415). **Figure** 3.3.1-6 shows that the rate of loss of cyclopentanol is larger than the rate of formation of cyclopentanone. Furthermore the results after 30 min in **Figure** 3.3.1-5 suggest that cyclopentanone can be photooxidized too. The average quantum yield for production of cyclopentanone from cyclopentanol is 0.145 and the average quantum efficiency (or quantum yield

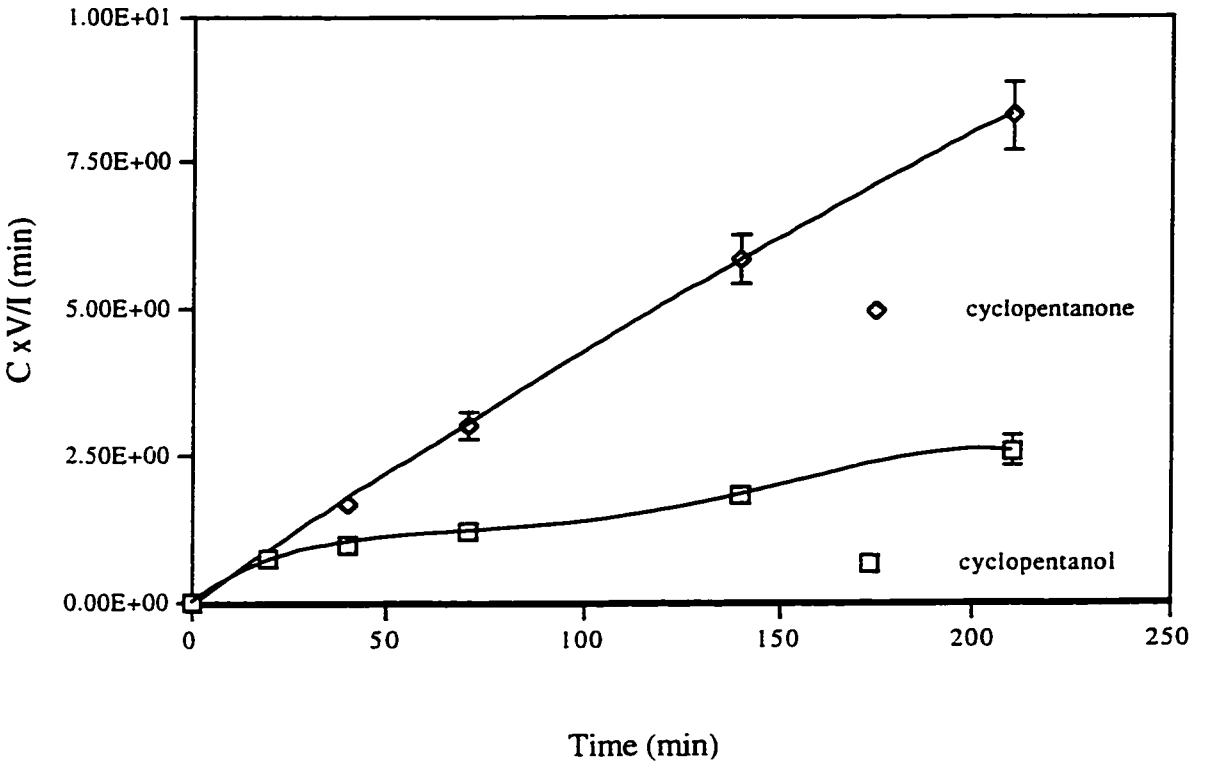

Figure 3.3.1-3. Relationship of [Cyclopentane] x Volume/(Light Intensity) with irradiation time.
$[UO_2^{2+}]$ = 34.8 mM; pH = 1.1 ($HClO_4$); V_{irrad} = 145 mL; T = 25 °C; I = 8.27 x 10^{-6} Einstein/min; λ_{irr} = 415 nm. Oxygen carrying cyclopentane was bubbled for 20 min before irradiation and continuously bubbled at the rate of 100 mL/min during irradiation.

Curve fitting equations:

Cyclopentanone: $y = -2.84E\text{-}05x^2 + 4.60E\text{-}02x - 8.72E\text{-}02$ $r^2 = 1.00E+00$

Cyclopentanol: $y = -1.04E\text{-}08x^4 + 4.70E\text{-}06x^3 - 6.90E\text{-}04x^2 + 4.58E\text{-}02x + 9.42E\text{-}03$ $r^2 = 9.99E\text{-}01$

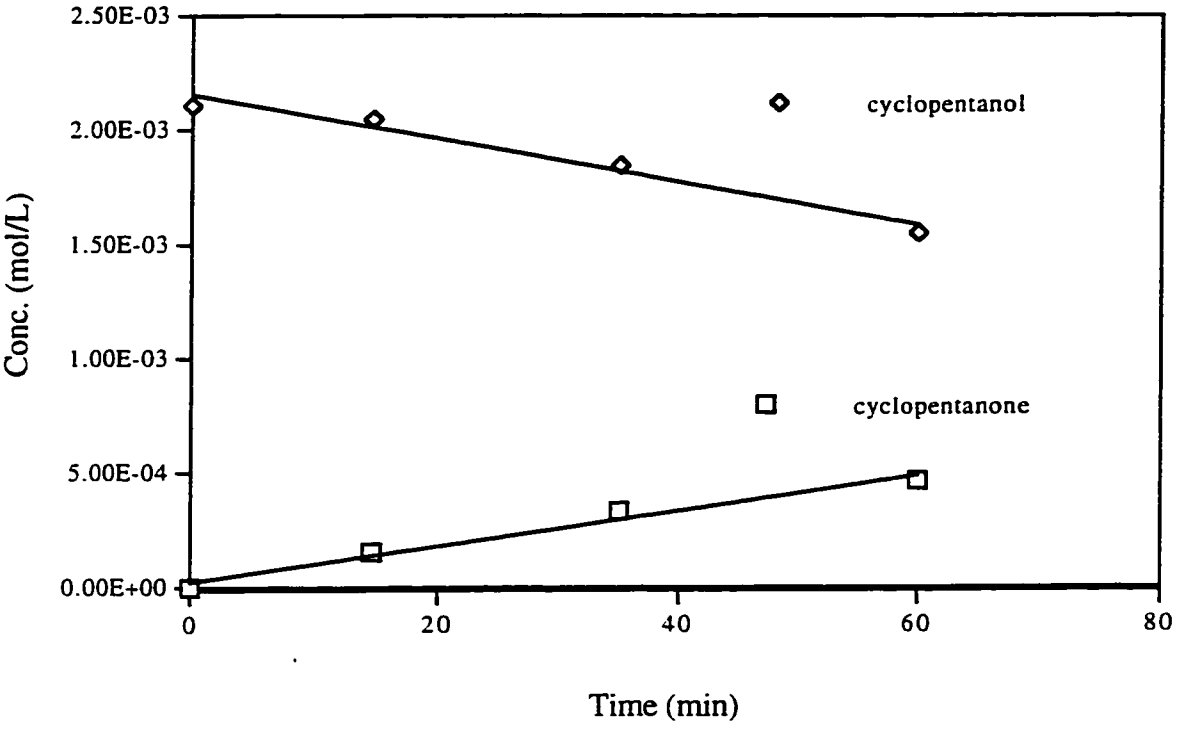

Figure 3.3.1-4. Photoproduction of cyclopentanone by the photolysis of cyclopentanol with CWL415 filter.
$[UO_2^{2+}]$ = 34.8 mM; pH = 1.1 ($HClO_4$); V_{irrad} = 145 mL; T = 25 °C; I = 8.27 x 10^{-6} Einstein/min; λ_{irr} = 415 nm (with oxygen over the solution).

Curve fitting equations:

Cyclopentanol : y = -9.580E-06x + 2.153E-03 r^2 = 9.721E-01

Cyclopentanone: y = 7.78E-06x + 2.65E-05 r^2 = 9.78E-01

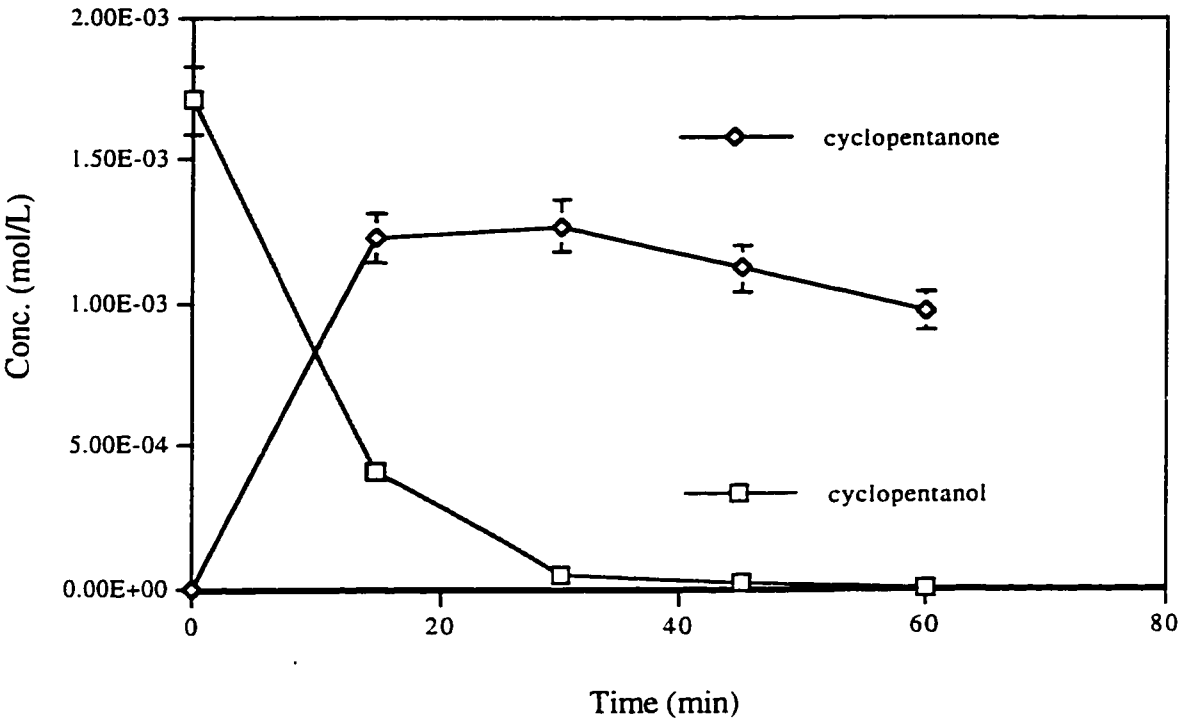

Figure 3.3.1-5. Photoproduction of cyclopentanone by the photolysis of cyclopentanol.
$[UO_2^{2+}]$ = 34.8 mM; pH = 1.1 ($HClO_4$); V_{irrad} = 145 mL; T = 25 °C.
No filter. (with oxygen over the solution).

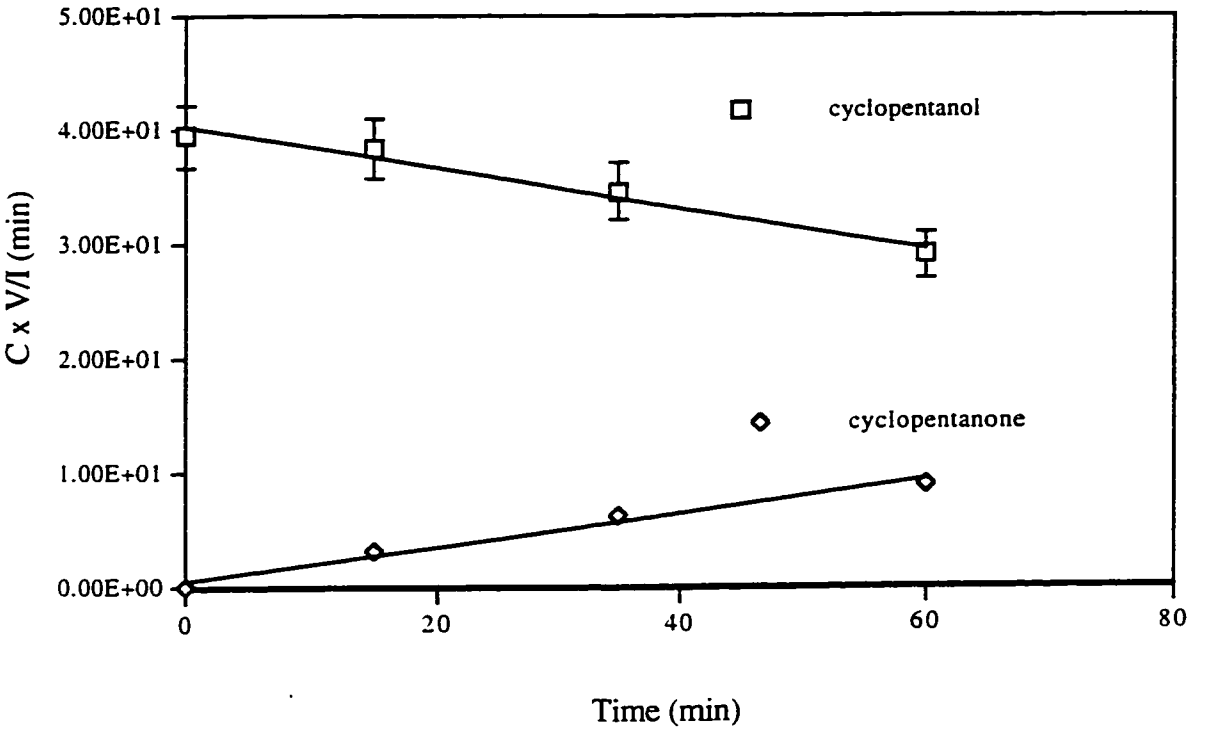

Figure 3.3.1-6. Relationship of [Cyclopentanone] x V/I in the photolysis of cyclopentanol with CWL415 filter.
$[UO_2^{2+}]$ = 34.8 mM; pH = 1.1 ($HClO_4$); V_{irrad} = 145 mL; T = 25 °C; I = 8.27 x 10^{-6} Einstein/min; λ_{irr} = 415 nm (with oxygen over the solution).

Curve fitting equations:

Cyclopentanol: y = -1.79E-01x + 4.02E+01 r^2 = 9.72E-01

Cyclopentanone: y = 1.45E-01x + 4.95E-01 r^2 = 9.78E-01

loss) for cyclopentanol is 0.179. Both of these values are notably higher than that for the photolysis of cyclopentane. In the irradiation of cyclopentane, the product is more active than the reactant, and as shown in **Figure** 3.3.1-1, the cyclopentanol concentration remains low. This make it difficult to obtain accurate mass balance analysis.

3.3.2 Effects of Added Metal Ions on Irradiation Products

In the presence of oxygen at high light intensity or high pH (for example pH = 3), a pale yellow precipitate was formed after a short period of irradiation. Its identification will be discussed in the following section. In order to prevent the formation of the precipitate, effects of Ag^{+}, Fe^{3+} and Cu^{2+} were investigated. Ag^{+}, Fe^{3+} and Cu^{2+} can oxidize UO_2^{+}; Fe^{3+} and Cu^{2+} can catalyze the decomposition of H_2O_2; and as well, Cu^{2+} has a very high rate of reaction with free alkyl radicals. In the experiments, Ag^{+} and Fe^{3+} ions were found to be ineffective in preventing the formation of the precipitate, while copper ion (Cu^{2+}) was effective.

In the presence of copper ion, no precipitate is formed but a new substance has been found, and identified by GC-MS to be "2-cyclopenten-1-one". In this case, a much lower concentration of cyclopentanone is obtained relative to that in the absence of copper ion. **Figure** 3.3.2-1 shows the

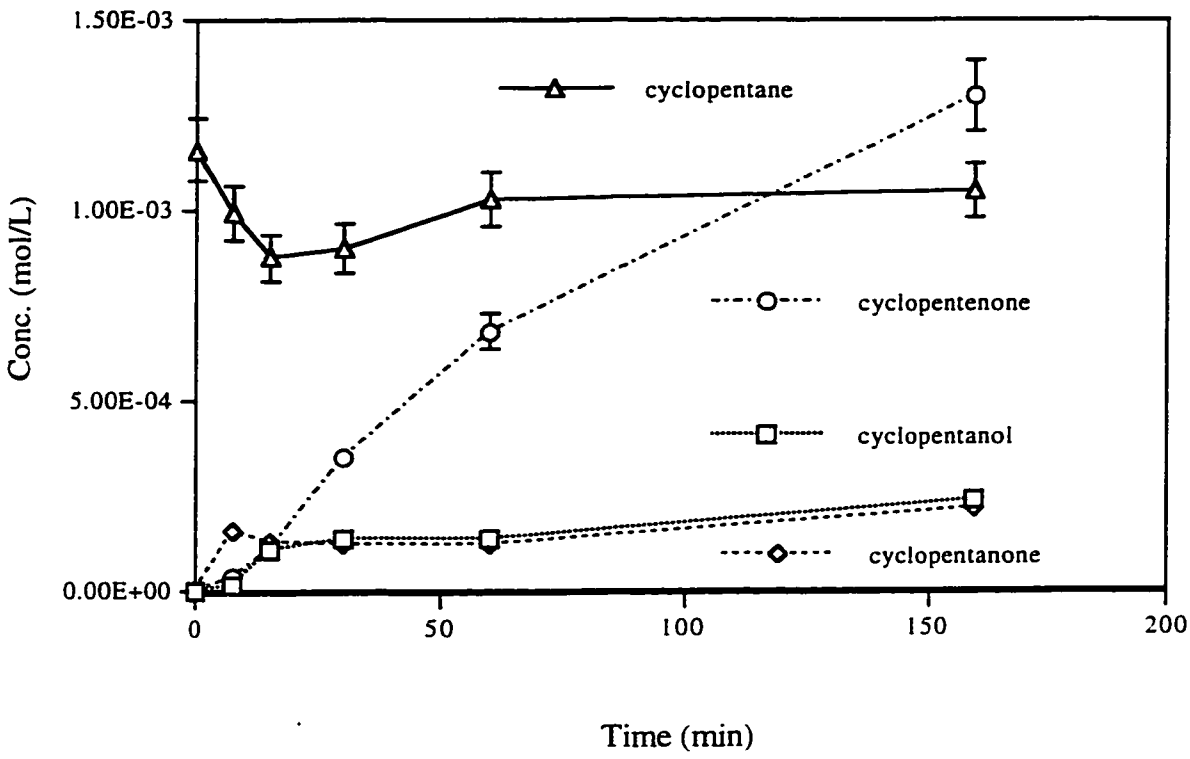

Figure 3.3.2-1. Photolysis of cyclopentane in the presence of 3.0 mM copper ion.
$[UO_2^{2+}]$ = 34.8 mM; pH = 1.1 ($HClO_4$); V_{irrad} = 145 mL; T = 25 °C; I = 8.27 x 10^{-6} Einstein/min; λ_{irr} = 415 nm. Oxygen carrying cyclopentane was bubbled for 20 min at the rate of 30 mL/min before irradiation and continuously bubbled during irradiation.

results in the presence of copper ion. Both cyclopentanol and cyclopentanone are found to be low in concentrations, only the 2-cyclopenten-1-one concentration steadily increases. A lower concentration of copper ion without bubbling of cyclopentane during the irradiation was also investigated, and the results are shown in **Figure** 3.3.2-2. When the concentration of copper ion is decreased, little change, if any, of 2-cyclopenten-1-one and cyclopentanol from those shown in **Figure** 3.3.2-1 was observed, but the concentration of cyclopentanone reached a higher level. These results indicate that UO_2^{2+}, Cu^{2+} and light are essential for the production of 2-cyclopenten-1-one and that its production rate depends slightly on the concentration of copper ion.

In the presence of copper ion, if cyclopentanol or cyclopentanone are used as the starting substances, 2-cyclopenten-1-one is also obtained. These results are shown in **Figures** 3.3.2-3 and 3.3.2-4. It is seen that in the presence of copper ion, both cyclopentanone and cyclopentanol can be photooxidized to 2-cyclopenten-1-one. **Figure** 3.3.2-5 presents the results of altering various parameters during the irradiation. In the absence of oxygen, cyclopentanol is the original product and then cyclopentanone is produced. When copper ion is added, 2-cyclopenten-1-ol is produced immediately and the

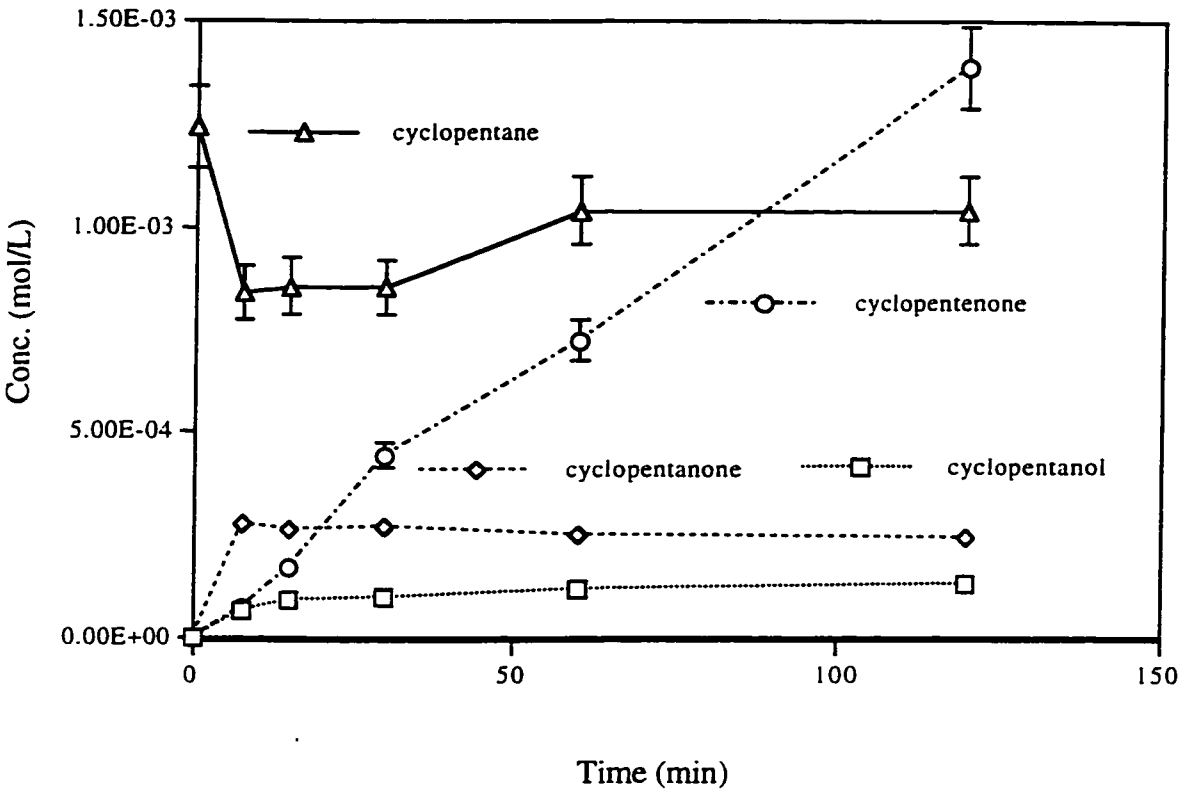

Figure 3.3.2-2. Photolysis of cyclopentane in the presence of 0.5 mM copper ion.
$[UO_2^{2+}]$ = 34.8 mM; $[Cu^{2+}]$ = 0.5 mM; pH = 1.1 ($HClO_4$); V_{irrad} = 145 mL; T = 25 °C; I = 8.27 x 10^{-6} Einstein/min; λ_{irr} = 415 nm. Oxygen carrying cyclopentane was bubbled for 20 min at the rate of 30 mL/min before irradiation and continuously bubbled during irradiation.

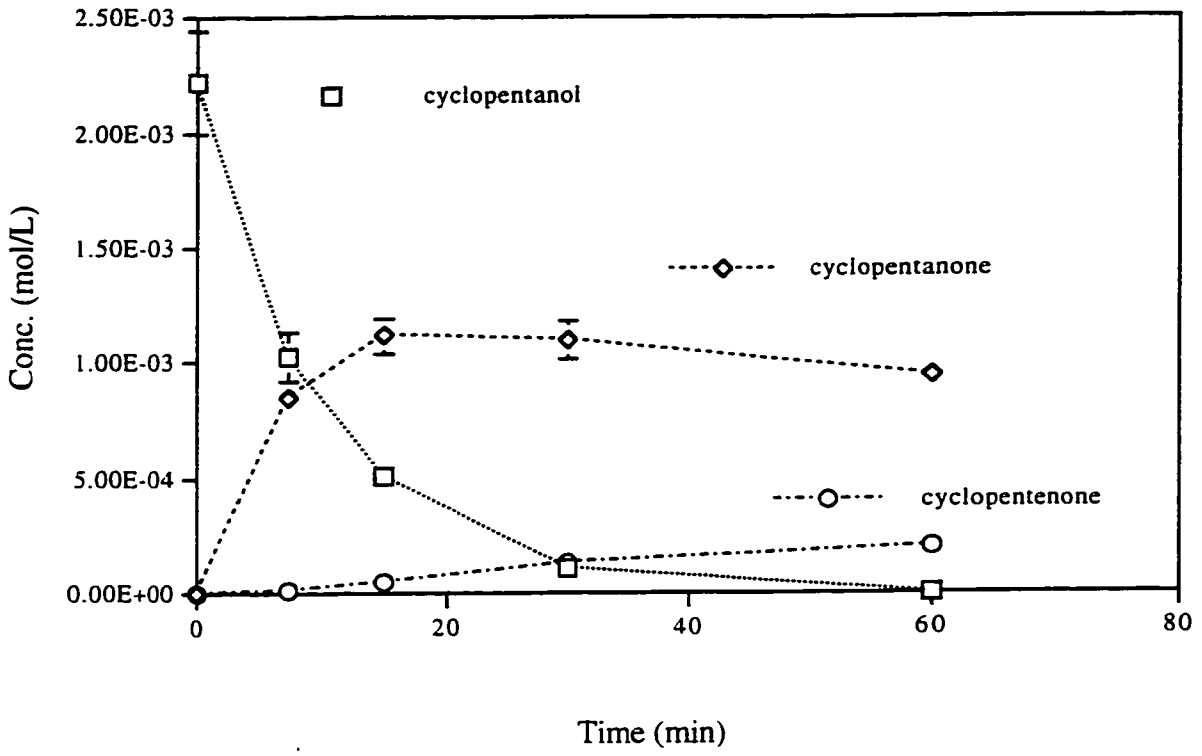

Figure 3.3.2-3. Photolysis of cyclopentanol in the presence of 0.5 mM copper ion.
$[UO_2^{2+}]$ = 34.8 mM; $[Cu^{2+}]$ = 0.5 mM; pH = 1.1 ($HClO_4$); V_{irrad} = 145 mL; T = 25 °C; No filter.

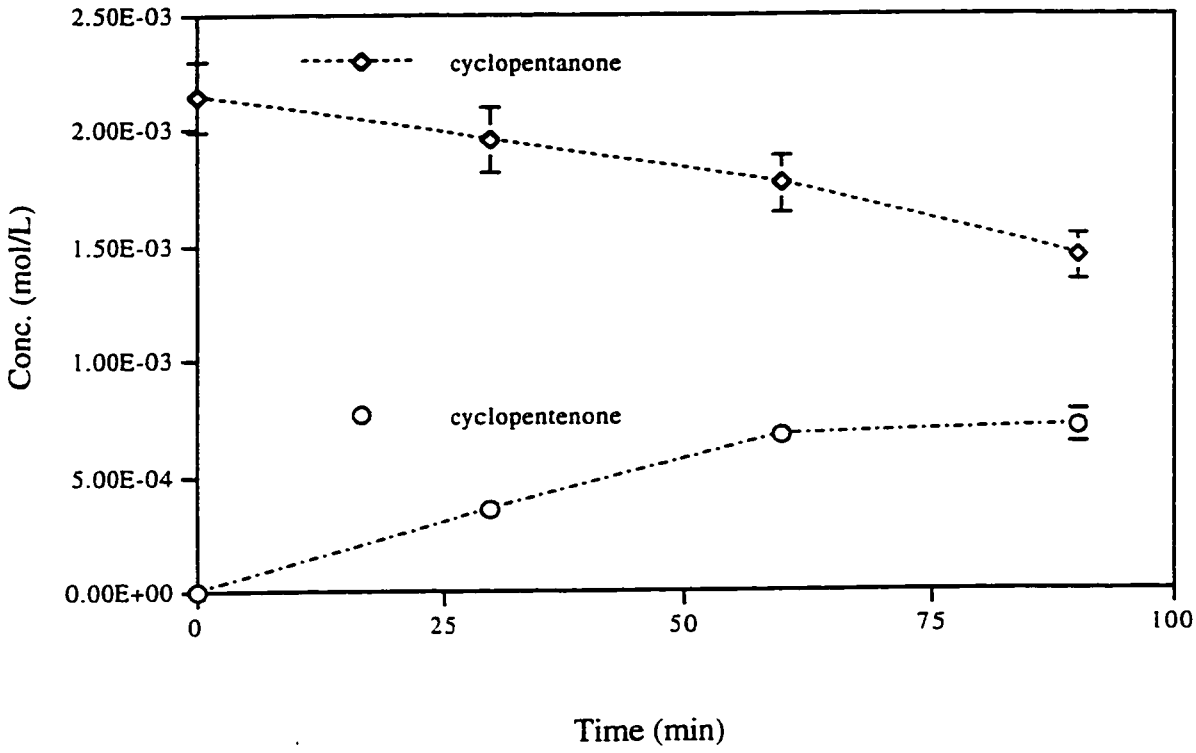

Figure 3.3.2-4. Photolysis of cyclopentanone in the presence of 0.5 mM copper ion.
$[UO_2^{2+}]$ = 34.8 mM; $[Cu^{2+}]$ = 0.5 mM; pH = 1.1 ($HClO_4$); V_{irrad} = 145 mL; T = 25 °C; No filter.

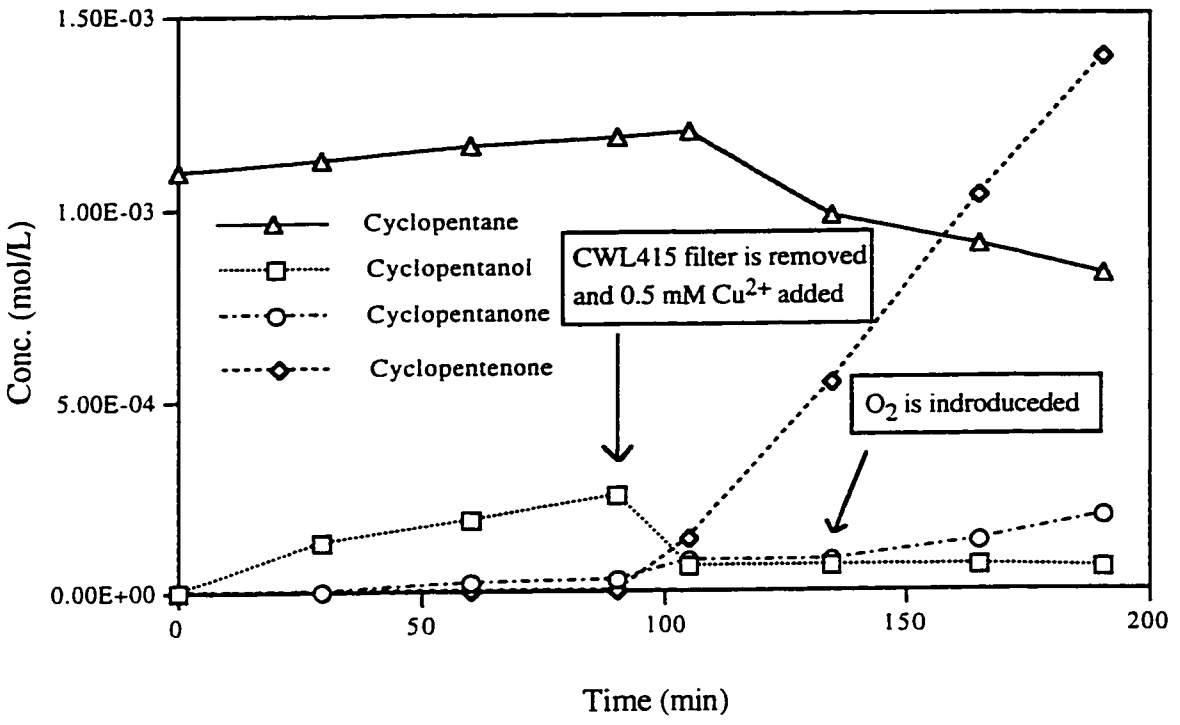

Figure 3.3.2-5. Photoproduction of cyclopentanol, cyclopentanone and 2-cyclopenten-1-one.
$[UO_2^{2+}]$ = 34.8 mM; pH = 1.1 ($HClO_4$); V_{irrad} = 145 mL; T = 25 °C; No filter. Bubbling rate is 30 mL/min. Nitrogen carrying cyclopentane is bubbled for 20 min before irradiation.

cyclopentanol concentration decreases quickly. When oxygen is introduced, cyclopentanone production is faster.

In the photolysis of cyclopentane with copper ion in solution, besides 2-cyclopenten-1-one, small amounts of cyclopentene and of 2-cyclopenten-1-ol have also been detected.

3.3.3 Production of $[UO_2(O_2)]\cdot 2H_2O$

As mentioned previously, a pale yellow precipitate was produced during the photooxidation of some organic substances by excited uranyl ion. In the presence of oxygen, at pH = 1 and using the band-pass filter CWL415, irradiation (3 h) of a uranyl solution saturated with cyclopentane, yielded no precipitate. However when the light intensity was increased (no filter), a precipitate was found after 10 min of irradiation. In this case, the precipitate is more readily produced than in the isobutane system. When the lamp power was decreased from 880 W to 300 W or the irradiation hole from 12 cm^2 to 4 cm^2 (this decreases the light intensity but still keeps a wide range of light wavelength), after 3 hours irradiation no precipitate was found. When the band-pass filter CWL415 (low light intensity, 415 nm) was used but the pH was changed from 1.1 to 3.0, a precipitate appeared. These results indicate that a high light intensity and a high pH favor the production of a precipitate. Light wavelength looks having no significant influence on the

production of the precipitate. This means that the mechanism of producing the precipitate is related to the excited uranyl ion concentration, photoproduced intermediates and other proton-involving reactions.

A number of organic reagents were studied, such as pentane, octane, pentanol, pentanone, cyclopentane, cyclopentanol and pentanoic acid, and they all produced the same colored precipitate. Different acids, such as $HClO_4$, H_2SO_4 and HNO_3, were also investigated and a precipitate was produced in each case. The precipitates produced from different organic substances or different acids have the same color. They are not soluble in common organic solvents such as methanol, acetone and chloroform. It was found that using an alcohol or ketone as a starting material, instead of alkanes, give a higher production rate of precipitate.

When there is $S_2O_8^{2-}$ in the solution (about 9 mM), irradiation of cyclopentane still produced a precipitate. However, when cyclopentanol was used as the original substance, no precipitate is observed. **Table** 3.3.3-1 summarizes these results.

Table 3.3.3-1. Production of precipitate under different conditions.[a]

System	no $S_2O_8^{2-}$	with $S_2O_8^{2-}$
$O_2 + UO_2^{2+}$	no ppt	--
$O_2 + UO_2^{2+} + C_5H_{10}$	ppt (yellow)	ppt (yellow)
$N_2 + UO_2^{2+} + C_5H_{10}$	ppt (black)	ppt (black)
$O_2 + UO_2^{2+} + C_5H_9OH$	ppt (yellow)	no ppt

a) $CuSO_4$ filter; $[S_2O_8^{2-}]$ = 9 mM; Irradiation time = 2 hours.

Whenever precipitate appears, there is always a positive test for peroxide. In the absence of oxygen, peroxydisulfate and other oxidants, $U^{4+}(aq)$ has also been found.

3.3.4 Analysis of $[UO_2(O_2)]\cdot 2H_2O$

The photoproduction of a precipitate in uranyl solution saturated with organic substances has not been reported previously. To understand this process, the precipitate must be identified. Spectrophotometric method and delayed neutron counting methods were used to determine the uranium content. Analysis results of uranium content of the precipitates produced from different organic systems along with an authentic $UO_2(O_2)\cdot 2H_2O$ sample are listed in **Table** 3.3.4-1. It can be seen that all these experimental values are close to the calculated value of 69.6% for the formula: $UO_2(O_2)\cdot 2H_2O$.

The results of the C,H,N-elemental analysis are shown in **Table** 3.3.4-2. It can be seen that the hydrogen content of synthesized $UO_2(O_2)\cdot 2H_2O$ is very close to that of photoproduced precipitate. The calculated value for $UO_2(O_2)\cdot 2H_2O$ is 1.18% and the average value for the precipitate is 1.10%. Another fact is that almost no carbon was found in this precipitate. This means that the precipitate is not an organic substance. This is also consistent with the fact that it does not dissolve in common organic solvents.

A titration method was used for the analysis of the peroxide content. The results are listed in **Table** 3.3.4-3. The infrared spectra of the precipitates produced by different methods are very similar to each other, and to that of the synthesized $UO_2(O_2)\cdot 2H_2O$. **Figure** 3.3.4-1 shows the spectrum of one of the precipitates and that of an authentic $UO_2(O_2)\cdot 2H_2O$ sample. There are several peaks that will be discussed in Chapter 4. All these analysis results indicate that the precipitates have the same formula $UO_2(O_2)\cdot 2H_2O$.

3.3.5 Production of $[UO_2(O_2)_n]^{m-}$

As mentioned in section 3.3.2, irradiation of cyclopentane produces a precipitate of $UO_2(O_2)\cdot 2H_2O$. It has been also found that when this solution is continuously irradiated (about 6 hours of intense irradiation with only the use of copper ion solution as filter), the precipitate decreases and then disappears, and the solution turns to a deep yellow color. After the uranyl ions are precipitated with KOH solution and the solid removed by filtration, the deep yellow color remains. When acid was added to the solution, this color disappears and it returns again upon addition of sufficient base. It is found that pH = 3 is the color turning point. This yellow colored substance could not be extracted with organic solvents such as alcohol, ketone, chloroform or benzene and is not precipitated by many metal

Table 3.3.4-1. Uranium content analysis.[a]

Organic reagent	acid	U%[b]	U%[c]
Cyclopentanone	HNO_3	68.8	68.9
Cyclopentanol	HNO_3	69.4	69.3
Cyclopentanol	$HClO_4$	67.7	69.6
t-butanol	$HClO_4$	68.7	70.0
Octanol	$HClO_4$	68.7	69.0
Cyclopentane	$HClO_4$	66.6	-
Cyclopentane	HNO_3	67.8	
Pentanonic acid	$HClO_4$	70.4	-
Pentanol	$HClO_4$	69.1	-
Butanol	$HClO_4$	65.6	-
$UO_2(O_2)\cdot 2H_2O$[d]	HNO_3	69.6	68.9
$UO_2SO_4\cdot 3.5H_2O$	H_2O	58.2	

a) The organic reagent is dissolved in uranyl solution with acid in it and irradiated. The produced precipitate is then separated and dried for above analysis.

b) Measured by Delayed Neutron Counting Method (by Saskatchewan Research Council).

c) Measured by Spectrophotometric Method.

d) synthized (not by photolysis).

Table 3.3.4-2. Analysis of carbon, hydrogen, and nitrogen.

Expt#	C%	H%	N%
1[a]	0.23	1.10	0.02
1[a]	0.13	1.06	0.03
2[b]	0.05	1.19	0.01
2[b]	0.12	1.03	0.03

a) The precipitate is produced by irradiation of cyclopentanol-uranyl nitrate solution.

b) Synthesized $UO_2(O_2) \cdot 2H_2O$.

Table 3.3.4-3. Analysis of peroxide content.

Species	O_2^{2-}%
$UO_2(O_2)\cdot 2H_2O$	9.47% (calculated by formula)
$UO_2(O_2)\cdot 2H_2O$ (synthesized)	9.57%
Photoproduced Precipitate	9.30%

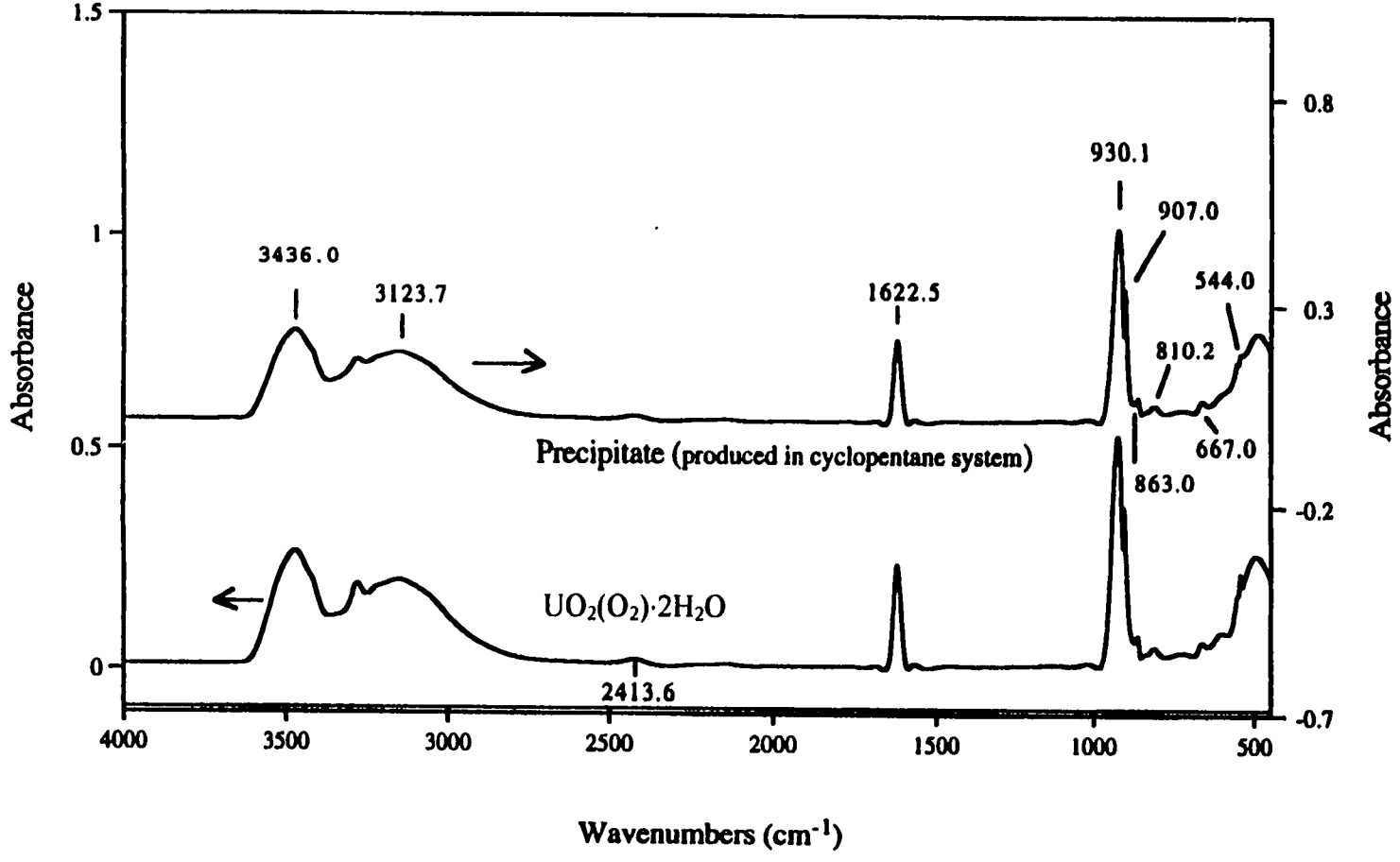

Figure 3.3.4-1. Infrared spectrum of $UO_2(O_2)\cdot 2H_2O$ and the photoproduced precipitate. (KBr is used as the mixture powder)

ions (Fe^{2+}, Cu^{2+}, Co^{2+}, Ba^{2+}, Mn^{2+}, Hg^{2+}, Ni^{2+}, Cd^{2+}, Ag^{+}, Ce^{3+}, Cr^{3+}).

3.3.6 Analysis of $[UO_2(O_2)_n]^{m-}$

This deep yellow solution is found to contain uranium and peroxides. On the base of all of the above information, this deep yellow substance is presumed to be a uranium peroxide compound with the formula of $[UO_2(O_2)_n]^{m-}$. To prove this, $K_4[UO_2(O_2)_3]$ was synthesized according to the method described in Section 2.1. This synthesized material also shows a deep yellow color when dissolved in water, and also has the same color-change properties at different acidities with the color occurring at the same pH. **Figures** 3.3.6-1 and 3.3.6-2 are the IR spectra of prepared $K_4UO_2(O_2)_3$ and $Na_4[UO_2(O_2)_3]$, respectively. The absorption bands are consistent with that reported for $K_4[UO_2(O_2)_3]$.[138] Since KBr is the inactive reagent in the IR spectrum, to decrease the interference for detecting the IR spectrum of the deep yellow substance, HBr was chosen to adjust the acidity. **Figures** 3.3.6-3 and 3.3.6-4 are the IR spectra of the photoproduced deep yellow precipitate and $KClO_4$ respectively. The precipitate was obtained using the same procedure as used in the preparation of $K_4[UO_2(O_2)_3]$. The main interference substance is $KClO_4$ (its solubility in water is small but a certain amount still remains in solution). From the comparison of these spectra, it can be concluded that $UO_2(O_2)_3^{4-}$ (or $[UO_2(O_2)_n]^{m-}$ n = 2,3)

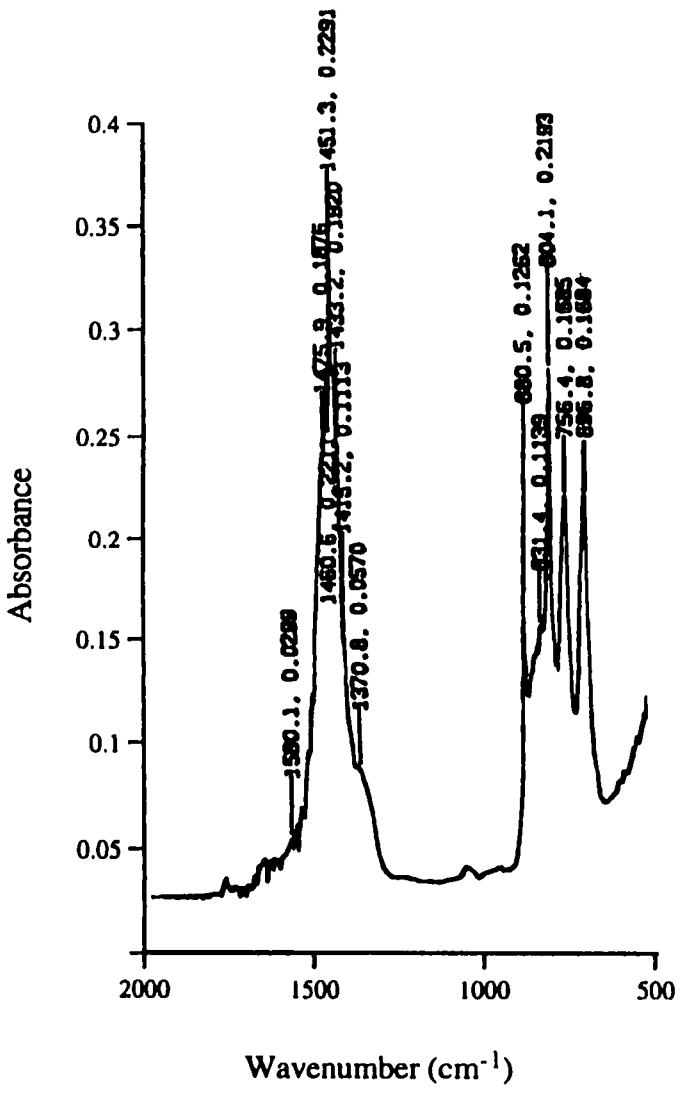

Figure 3.3.6-1. Infrared spectrum of $K_4[UO_2(O_2)_3]$. (KBr is used as the mixture powder)

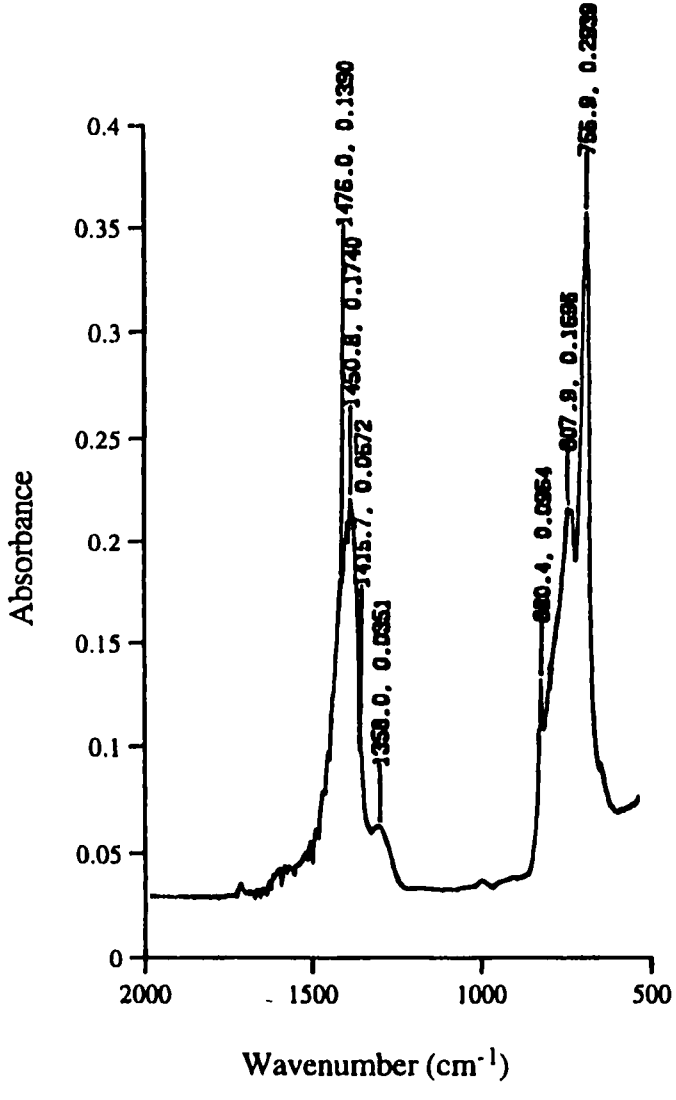

Figure 3.3.6-2. Infrared spectrum of $Na_4[UO_2(O_2)_3]$. (KBr is used as the mixture powder)

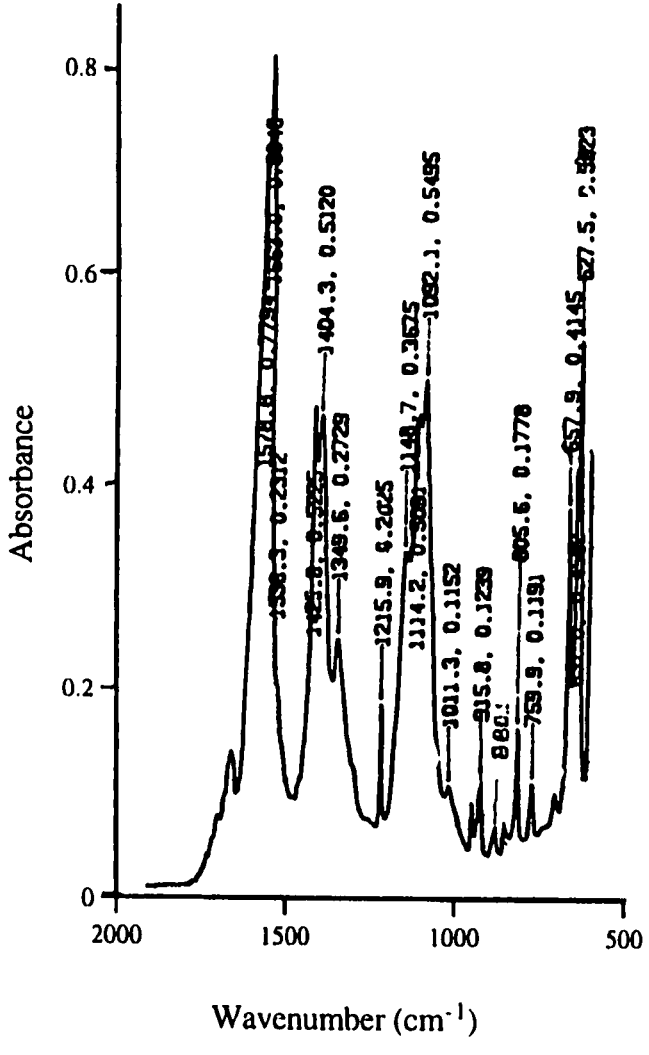

Figure 3.3.6-3. Infrared spectrum of photoproduced $K_4[UO_2(O_2)_3]$. (KBr is used as the mixture powder)

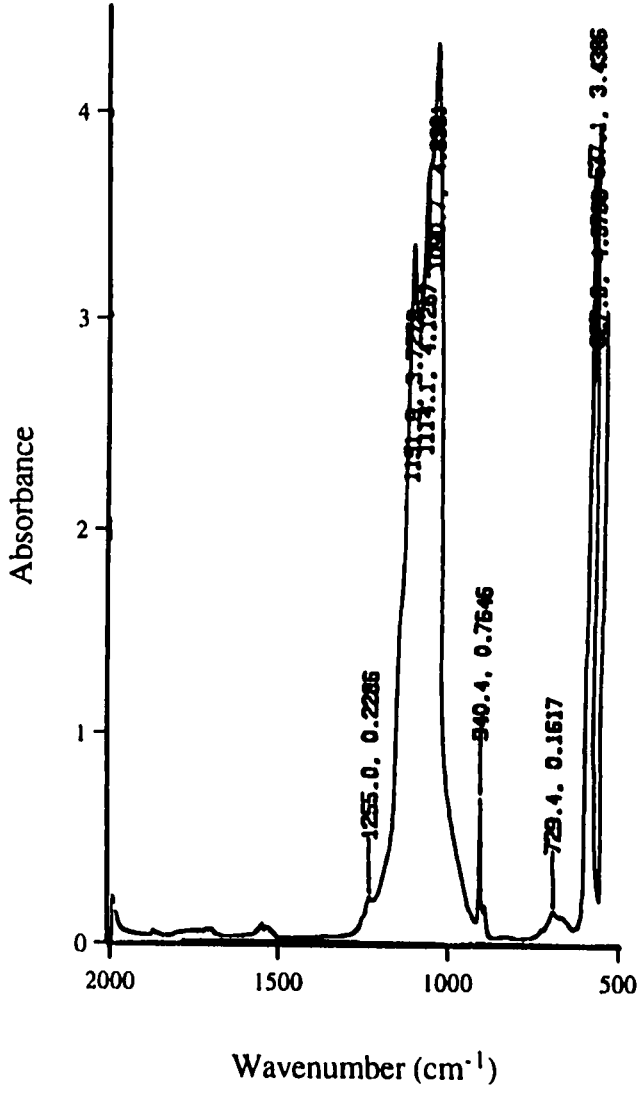

Figure 3.3.6-4. Infrared spectrum of $KClO_4$. (KBr is used as the mixture powder)

is the substance which is photoproduced. The assignments of the absorption bands shown in these figures will be discussed in Chapter 4.

To check for the photooxidation ability of $UO_2(O_2)_3^{4-}$, a solution of $Na_4[UO_2(O_2)_3]$ (0.002 mole/l; pH = 7) was prepared, and its absorption spectrum measured. The absorption spectrum of $Na_4[UO_2(O_2)_3]$ is quite different from that of UO_2^{2+}. The molar extinction coefficient of $Na_4[UO_2(O_2)_3]$ is 180 M^{-1} cm^{-1} at 414 nm. This value is much higher than the value of 7.8 $M^{-1}s^{-1}$ for uranyl ion. This compound is soluble in water. A $Na_4[UO_2(O_2)_3]$ solution was saturated with cyclopentane and irradiated in the presence of a CWL415 band-pass filter and a copper ion solution filter (high light intensity) ,respectively. In both cases, no cyclopentanol or cyclopentanone has been found. So it appear $UO_2(O_2)_3^{4-}$ is not particularly photochemically active. However, when this solution was irradiated for about 8 hours, cyclopentanol and cyclopentanone were detected. In this case, $UO_2(O_2)\cdot 2H_2O$ was also observed. This probably reflects the equilibrium between $UO_2(O_2)_3^{4-}$, $UO_2(O_2)$, UO_2^{2+}, with the production of cyclopentanol and cyclopentanone being due to UO_2^{2+}. When the deep yellow solution is irradiated continuously (for about 8 hours), a precipitate is formed again, but this precipitate is different from $UO_2(O_2)\cdot 2H_2O$. It has a range of color from light yellow to brown. The viscosityies are different between these precipitates. The brown precipitate is a solid and is

soluble in methanol and acetone. No uranium was found in this precipitate. The analysis of C, H, N contents of this precipitate are 62.97%, 6.99% and 0.42%, respectively (N is an impurity). The mass ratio of H/C for this precipitate is 0.111/1. This value is between the mass ratio of 7H/5C (0.117) and the mass ratio of 6H/5C (0.101). These results suggest an organic polymer with the following repeating units:

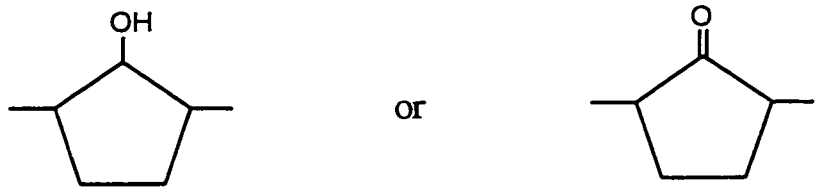

7H/5C 6H/5C

3.3.7 Photolysis of Cyclopentane and Hydrogen Peroxide System

Hydrogen peroxide absorbs in the range 190 - 350 nm. It is reported that the photoreaction in this range is:[139]

$$H_2O_2 \longrightarrow 2HO\cdot \qquad (3.3.7\text{-}1)$$

If aqueous cyclopentane and H_2O_2 is irradiated with only a copper ion solution filter (absorbing below 300 nm), one

expects cyclopentane to be oxidized. To compare with our uranyl system, some photolysis experiments of aqueous H_2O_2 and cyclopentane were carried out. The results are summarized in the following equations:

$$CpH_2 + H_2O_2 \xrightarrow{Thermal,\ 25^0C} \text{no oxidation products} \quad (3.3.7\text{-}2)$$

$$CpH_2 + H_2O_2 \xrightarrow{h\nu} CpHOH\ (35\%) + CpO\ (65\%) \quad (3.3.7\text{-}3)$$

$$CpH_2 + H_2O_2 \xrightarrow{h\nu,\ Cu^{2+}} CpHOH\ (35\%) + CpO\ (65\%) \quad (3.3.7\text{-}4)$$

(no CpOene)

where pH = 1.08; $[S_2O_8^{2-}]$ = 30 mM; $[Cu^{2+}]$ = 0.5 mM.

The same ratio of CpHOH to CpO was obtained as that in the irradiation of the $CpH_2 + UO_2^{2+}$ system, but no CpOene was found even though there was copper ion in the solution. It is seen that in this system, the products ratio is the same as in the uranyl system, but the effect of copper ion is quite different.

3.4 Photolysis of Cyclohexane

The solubility of cyclohexane in water is reported as 0.69 mM,[138] and the value measured in this work is 0.613 ± 0.018. When cyclohexane-saturated uranyl solutions kept

under nitrogen were irradiated, very little alcohol was found. A quantum yield of 0.0025 was obtained (**Figure** 3.4-1) In the presence of oxygen, the initial quantum yields of alcohol and ketone were 0.028 ± 0.003 and 0.027 ± 0.003, respectively (**Figure** 3.4-2). When the light intensity was decreased to 45%, about the same initial quantum yields (0.025 ± 0.002, 0.025 ± 0.002) were obtained. In the presence of 1 mM peroxydisulfate, the quantum yields were 0.069 ± 0.0035 for the cyclohexanone and 0.046 ± 0.0038 for the cyclohexanol (**Figure** 3.4-3). It was also noticed that different sources of cyclohexane gave different results. An older source gave higher quantum yield. This could be due to the exposure of the cyclohexane to air.

3.5 Photolysis of Pentane

The solubility of pentane in water is 0.58 mM.[138] In n-pentane, there are both primary and secondary hydrogen atoms and it is expected to form several products depending upon where hydrogen abstraction occurs. In the irradiation of pentane-saturated uranyl solution, higher light intensity (GG400 filter) was used in order to form detectable amounts of products. The following products were found by GC-MS analysis.

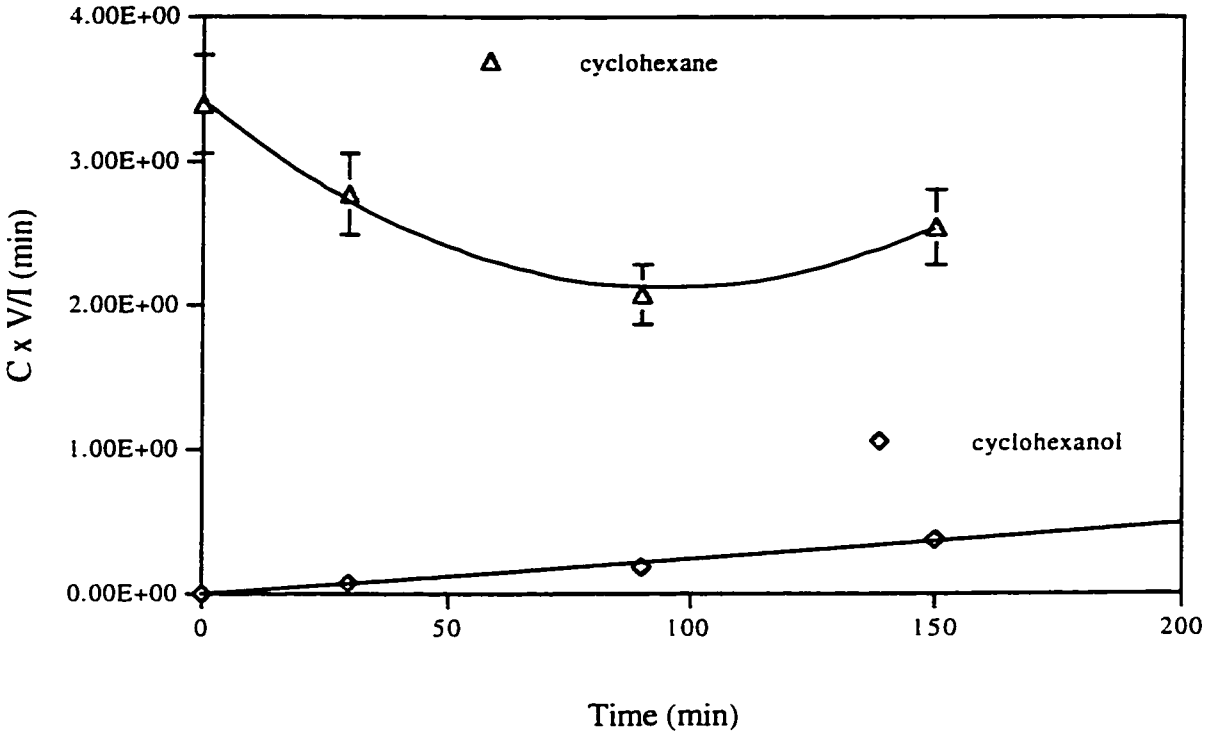

Figure 3.4-1. Relationship of [Products] x Volume/(Light intensity) with irradiation time in the photolysis of cyclohexane in the presence of nitrogen.
$[UO_2^{2+}]$ = 34.8 mM; pH = 1.1 ($HClO_4$); V_{irrad} = 145 mL; T = 25 °C; I = 8.27 x 10^{-6} Einstein/min; λ_{irr} = 415 nm. Saturated with cyclohexane.

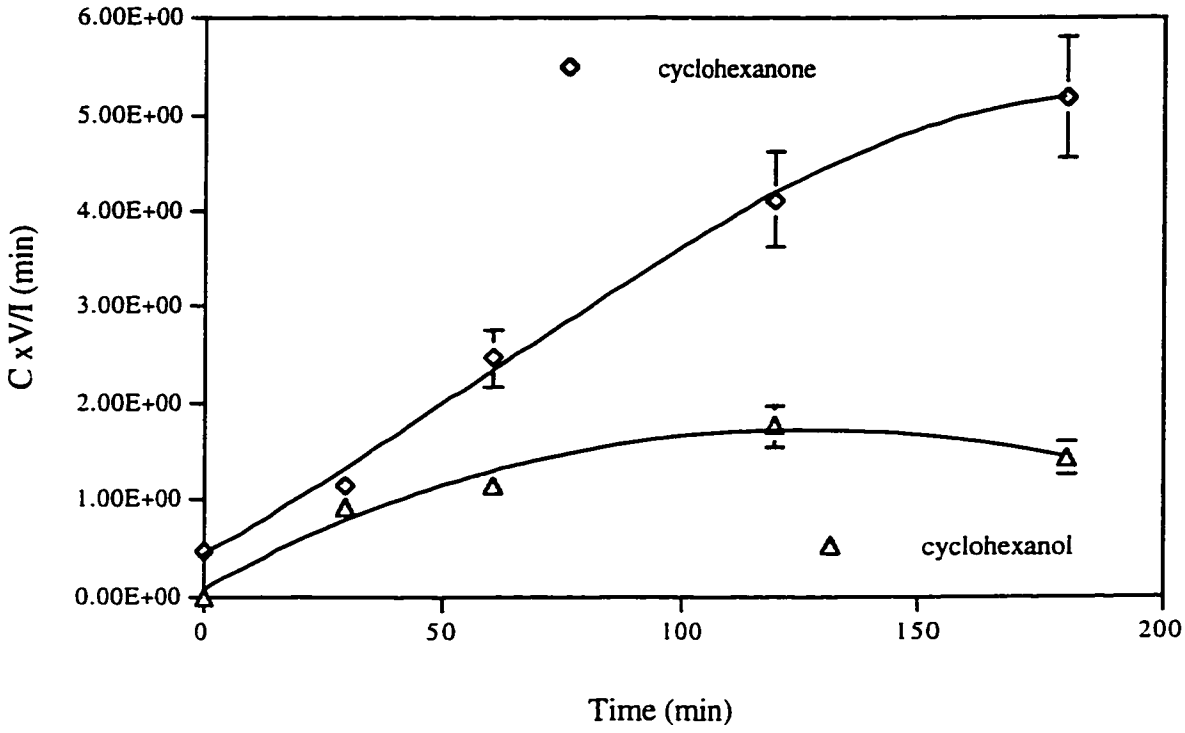

Figure 3.4-2. Relationship of [Products] x Volume/(Light intensity) with irradiation time in the photolysis of cyclohexane in the presence of oxygen.
$[UO_2^{2+}] = 34.8$ mM; pH = 1.1 ($HClO_4$); $V_{irrad} = 175$ mL; T = 25 °C; $I = 8.27 \times 10^{-6}$ Einstein/min; $\lambda_{irr} = 415$ nm. Saturated with cyclohexane.

Curve fitting equations:

Cyclohexanone:
$y = -6.34E\text{-}07x^3 + 1.09E\text{-}04x^2 + 2.74E\text{-}02x + 4.07E\text{-}01 \quad r^2 = 9.96E\text{-}01$

Cyclohexanol:
$y = 5.36E\text{-}08x^3 - 1.20E\text{-}04x^2 + 2.75E\text{-}02x + 4.55E\text{-}02 \quad r^2 = 9.75E\text{-}01$

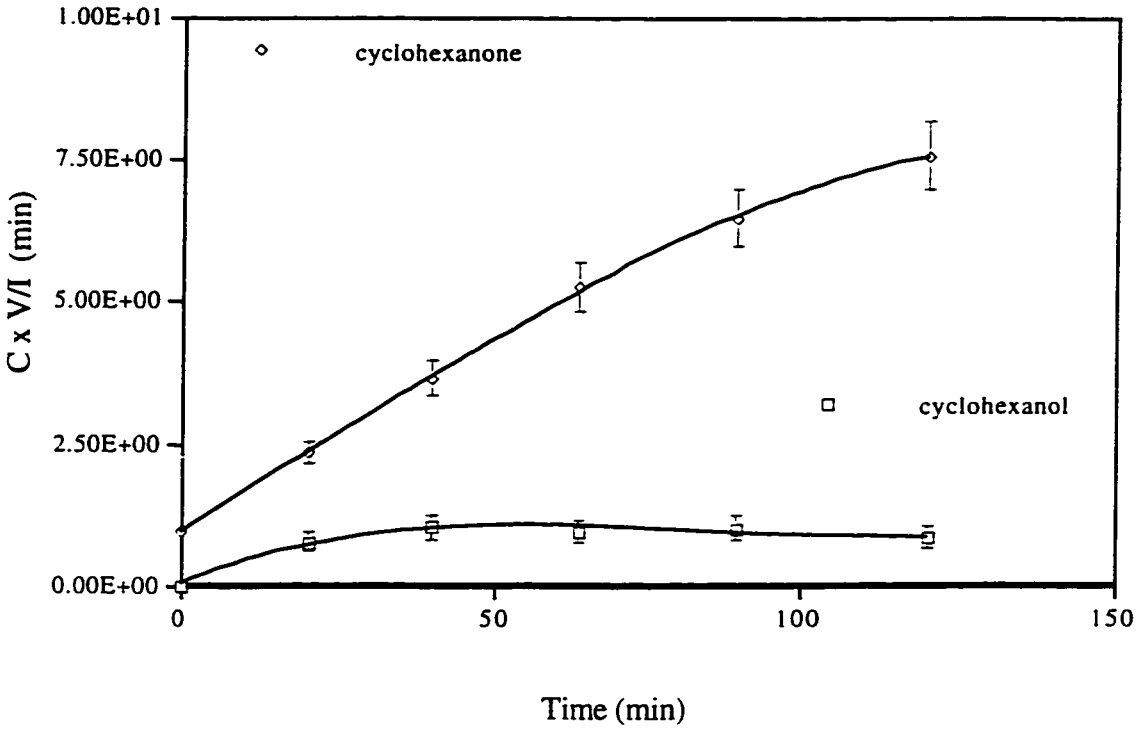

Figure 3.4-3. Relationship of [Products] x Volume/(Light Intensity) with irradiation time in the presence of 1 mM $S_2O_8^{2-}$.

$[UO_2^{2+}]$ = 34.8 mM; pH = 1.1 ($HClO_4$); V_{irrad}=175 mL; T = 25 °C; I = 8.27 x 10^{-6} Einstein/min; λ_{irr} = 415 nm. Oxygen carrying cyclohexane was bubbled for 30 min before irradiation and continuously bubbled during irradiation.

Curve fitting equations:

Cyclohexanone: $y = -1.20E\text{-}06x^3 + 2.79E\text{-}05x^2 + 6.90E\text{-}02x + 9.65E\text{-}01$
$r^2 = 1.00E+00$

Cyclohexanol: $y = 2.53E\text{-}06x^3 - 6.30E\text{-}04x^2 + 4.62E\text{-}02x + 2.86E\text{-}02$
$r^2 = 9.70E\text{-}01$

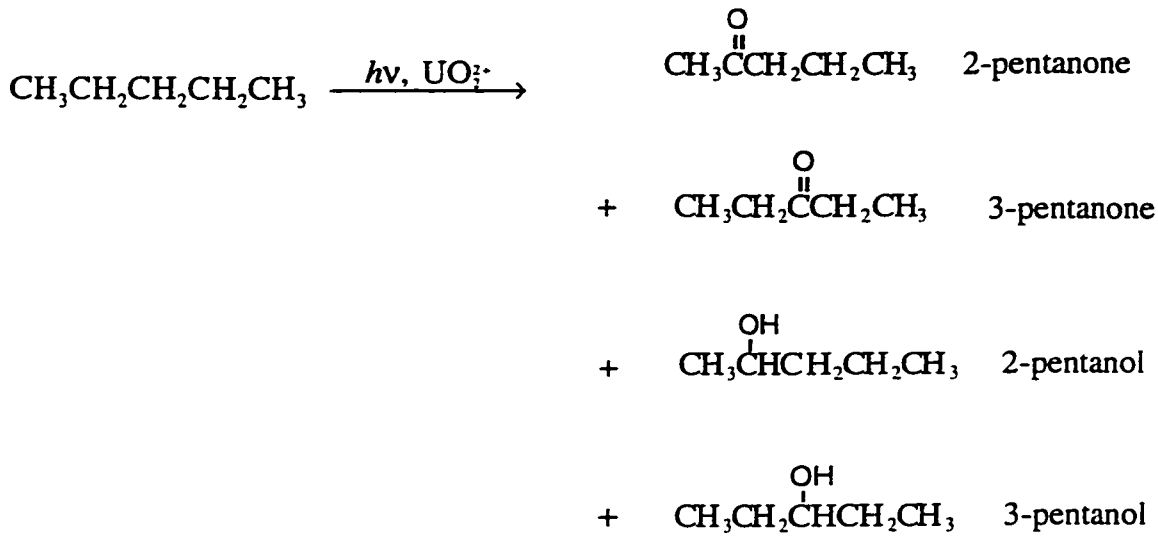

(3.5-1)

The initial production rates for ketones and alcohols in solution bubbled with nitrogen are about the same (**Figure** 3.5-1). These results are different from the cases of isobutane, cyclopentane and cyclohexane, where, in the presence of nitrogen, only alcohol (in isobutane) was found or ketone is formed very slowly (in cyclopentane and cyclohexane). The total quantum yields of alcohol and ketone are estimated to be 0.008. In the presence of oxygen and 1 mM peroxydisulfate, the initial quantum yields of 3-pentanol, 2-pentanol, 3-pentanone and 2-pentanone are 0.0026, 0.0030, 0.0130 ± 0.0007, 0.015 ± 0.0008, respectively (**Figure** 3.5-2).

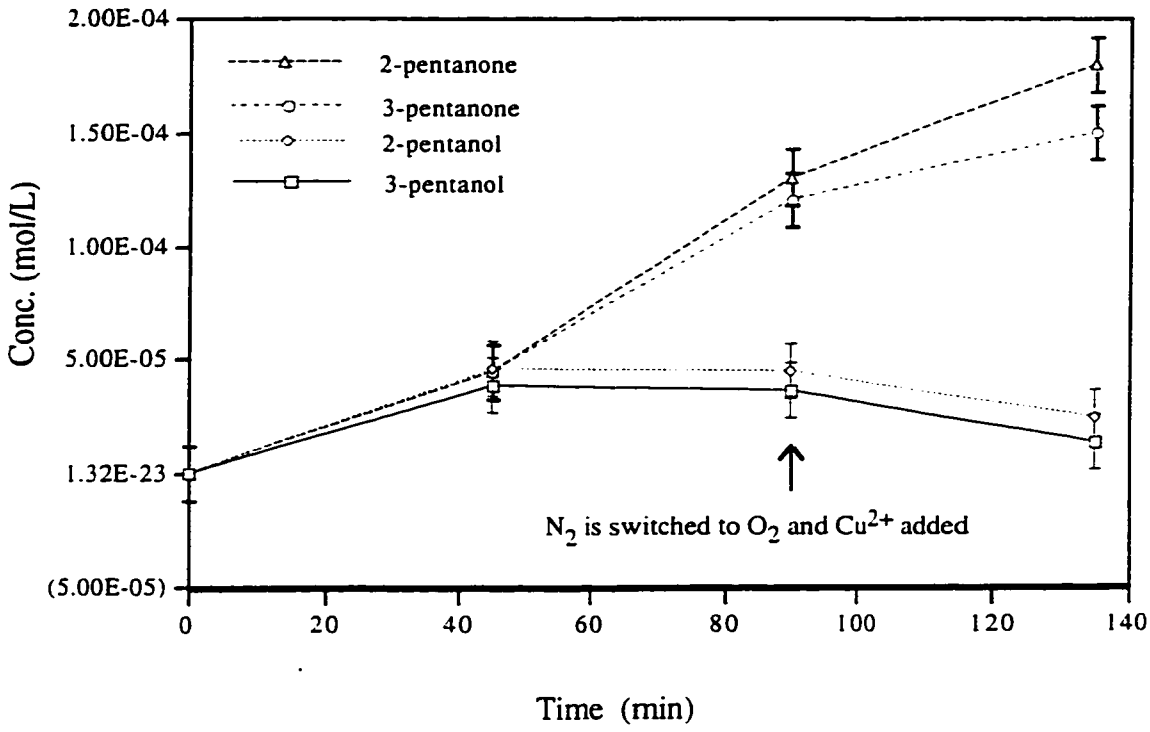

Figure 3.5-1 Photolysis of n-pentane with nitrogen and then with oxygen.
$[UO_2^{2+}]$ = 34.8 mM; pH = 1.1 ($HClO_4$); V_{irrad} = 175 mL; T = 25 °C; GG400 filter. (bubbling n-pentane with nitrogen for 30 min before irradiation).

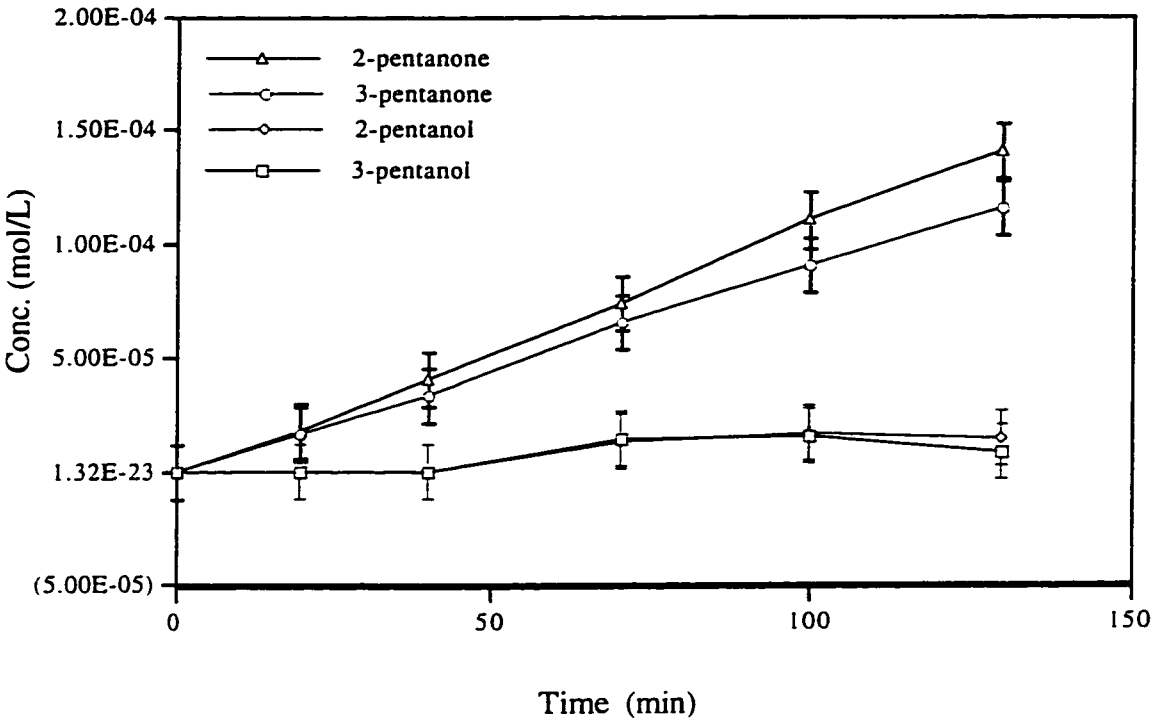

Figure 3.5-2. Effect of $S_2O_8^{2-}$ on the photolysis of n-pentane. $[UO_2^{2+}]$ = 34.8 mM; $[K_2S_2O_8]$ = 1mM; pH = 1.1 ($HClO_4$); V_{irrad}=175 mL; T = 25 °C; I = 8.27 x 10^{-6} Einstein/min; λ_{irr} = 415 nm; Oxygen carrying pentane was bubbled for 30 min before irradiation and continuously bubbled at the rate of 40 mL/min during irradiation.

[134] Sen, A. *Platinum Metals Rev.* **1991**, *35(3)*, 126.

[135] Baliga, B. T.; Whalley, E. *Can. J. Chem.* **1964**, *42*, 1019.

[136] Moriyasu, M.; Yokoyama, Y.; Ikeda, S. *Inorg. Chem.* **1977**, *39*, 2199.

[137] Price, L. C. *AM. Assico. Petrol. Geol. Bull.* **1976**, *60*, 230.

[138] Nelson, H. Q. *Rec. Trav. Chim.* **1968**, *87*, 528.

[139] Hideo, O. *Photochemstry of Small Molecules* ; Wiley: New York, 1978; Chapter 7.

4. DISCUSSION

4.1 Isobutane System in the Absence of $K_2S_2O_8$

4.1.1 Discussion of Results

As mentioned in the introduction, excited uranyl ion is a very powerful oxidant. In the oxidation of organic substances with functional groups, such as alcohol, aldehyde, hydrazine and some carboxylic acids, the quantum yields for the organic substances are relatively high (0.4-0.7). In some cases, a quantum yield as high as 0.7 has been attained for $U^{4+}(aq)$.[140] In the oxidation of isobutane, the observed value of the quantum yield for tertiary-butyl alcohol formation is about 0.03. However, the solubility is limited at room pressure. At ca. one atmosphere pressure of isobutane, only about 7% of the electronically excited uranyl ion is quenched by isobutane. If the pressure were increased so that percent quenching approached to 100%, then the limiting quantum yield would be about 0.5. In the oxidation of methanol, it is generally accepted that the first step is the abstraction of the α-hydrogen atom (see

Chapter 1). The strength of this α-hydrogen carbon bond ($HOCH_2$-H) is known to be 93 kcal/mol, which is about the same as that of the tertiary hydrogen carbon bond in isobutane ($(CH_3)_3C$-H, 93.6 ± 0.5 kcal/mol).[141] By contrast, the strong primary C-H bond does not appear to undergo abstraction as only trace amounts of the anticipated products are found. The major product is tertiary butyl alcohol, the percentage being greater than 90% of the loss of isobutane.

The large amount of tertiary butyl alcohol and the small amount of isobutene can be attributed to C-H bond cleavage, however there are traces of products that can also be attributed to C-C bond cleavage (Table 3.1.4-1). In the absence of oxygen and pH = 1, $U^{4+}(aq)$ was found. When the pH was changed to pH = 3, UO_2^+ was also detected. Based on these facts, the following mechanism is proposed, where BH, B· and BOH designate isobutane, tertiary butyl radical and tertiary butyl alcohol, respectively.

The first step is the formation of the excited uranyl ion (for convenience, only one coordinated water molecule of uranyl ion is indicated):

$$H_2OUO_2^{2+} \xrightarrow{h\nu} *[H_2OUO_2^{2+}] \qquad (4.1.1\text{-}1)$$

The excited uranyl ion reacts with isobutane as follows:

$$*[H_2OUO_2^{2+}] + BH \xrightarrow{k_q} *[H_2OUO_2 \cdot BH^{2+}] \qquad (4.1.1\text{-}2)$$

The $*[H_2OUO_2 \cdot BH^{2+}]$ immediately decomposes according to:

$$*[H_2OUO_2 \cdot BH^{2+}] \xrightarrow{k_a} UO_2^{+} + B\cdot + H^{+} \qquad (4.1.1\text{-}3)$$

The production of UO_2^{+} and B· is analogous to the photooxidation of functionalized organic substances by $*UO_2^{2+}$.[67,100,105,142,143] The production of free radical B· is then oxidized by UO_2^{2+}.

$$UO_2^{2+} + B\cdot \longrightarrow UO_2^{+} + B^{+} \qquad (4.1.1\text{-}4)$$

From B^{+}, the following products are produced (bold face is used for the products that have been found in this work):

$$B^{+} + H_2O \longrightarrow \mathbf{BOH} + H^{+} \quad \text{(major)} \qquad (4.1.1\text{-}5)$$

$$B^{+} \longrightarrow \mathbf{isobutene} + H^{+} \quad \text{(minor)} \qquad (4.1.1\text{-}6)$$

Since other products containing different amounts of C are found, C-C bond cleavage may occur:

$$*[H_2OUO_2 \cdot BH^{2+}] \longrightarrow H_2OUO_2^{2+} + \cdot CH(CH_3)_2 + \cdot CH_3 \qquad (4.1.1\text{-}7)$$

In alcohol systems, C-C bond cleavage was also reported.[144,145] Free-radical transfer reactions may subsequently occur:

$$\cdot CH(CH_3)_2 + BH \longrightarrow \mathbf{CH_3CH_2CH_3}\ \text{(propane)} + B\cdot \qquad (4.1.1\text{-}8)$$

Analogous to B·, the isopropyl radical can be oxidized by UO_2^{2+}:

$$\cdot CH(CH_3)_2 + UO_2^{2+} \longrightarrow UO_2^{+} + {}^{+}CH(CH_3)_2 \qquad (4.1.1\text{-}9)$$

$${}^{+}CH(CH_3)_2 \longrightarrow \mathbf{CH_2{=}CHCH_3}\ \text{(propene)} + H^{+} \qquad (4.1.1\text{-}10)$$

$${}^{+}CH(CH_3)_2 + H_2O \longrightarrow \mathbf{(CH_3)_2CHOH} + H^{+} \qquad (4.1.1\text{-}11)$$

Analogous reactions for $\cdot CH_3$ are:

$$\cdot CH_3 + BH \longrightarrow \mathbf{CH_4} + B\cdot \qquad (4.1.1\text{-}12)$$

$$\cdot CH_3 + \cdot CH_3 \longrightarrow \mathbf{CH_3CH_3} \qquad (4.1.1\text{-}13)$$

$$\cdot CH_3 + UO_2^{2+} + H_2O \longrightarrow \mathbf{CH_3OH} + UO_2^{+} + H^{+} \qquad (4.1.1\text{-}14)$$

Some of the alkyl radicals may possibly be oxidized by UO_2^{+} or $^{*}UO_2^{2+}$ as well, in analogy to 4.1.1-4 and 4.1.1-9. UO_2^{+} produced in the above reactions can disproportionate:[32]

$$2UO_2^{+} + 4H^{+} \longrightarrow UO_2^{2+} + U^{4+} + 2H_2O \qquad (4.1.1\text{-}15)$$

From bond-energy considerations, the methyl radical should have a strong ability to abstract a hydrogen from other hydrocarbons. The possible radicals produced along with primary species are shown below:

(a) $\cdot C(CH_3)_3$ (b) $\cdot CHCH_3$ (c) $\cdot CH_3$

(d) $\cdot CH_2CHCH_3$ (e) $\cdot CH_2\text{-}C{=}CH_2$ (f) $\cdot CH{=}CCH_3$

(g) $\cdot CH_2CH_3$ (h) $\cdot CH_2CH_2CH_3$ (i) $\cdot CH{=}CHCH_3$

Products reflecting the existence of the above radicals have been found in our experiments. Their subsequent bimolecular processes can lead to the observed C_7 and C_8 species:

$$2 \cdot CH_2CHCH_3 \longrightarrow CH_3CHCH_2\text{-}CH_2CHCH_3 \quad \text{(2,5-dimethylhexane)} \qquad (4.1.1\text{-}16)$$

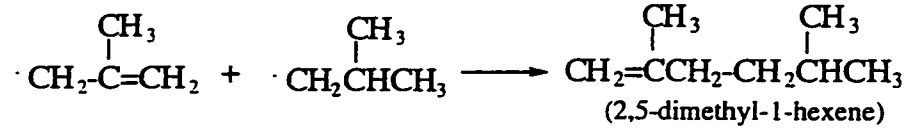

(2,5-dimethyl-1-hexene)

(4.1.1-17)

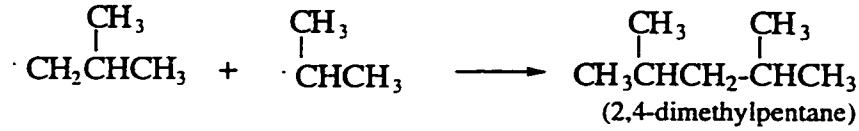

(2,4-dimethylpentane)

(4.1.1-18)

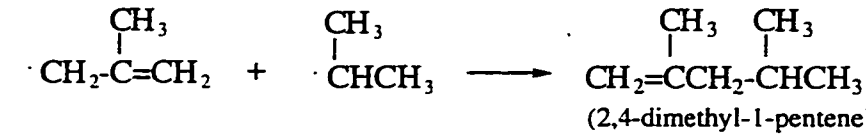

(2,4-dimethyl-1-pentene)

(4.1.1-19)

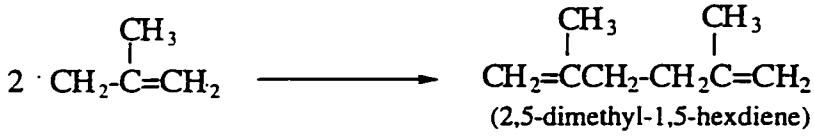

(2,5-dimethyl-1,5-hexdiene)

(4.1.1-20)

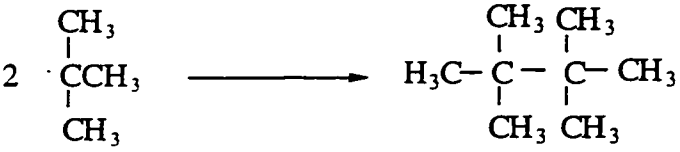

(2,2,3,3-tetramethylbutane)

(4.1.1-21)

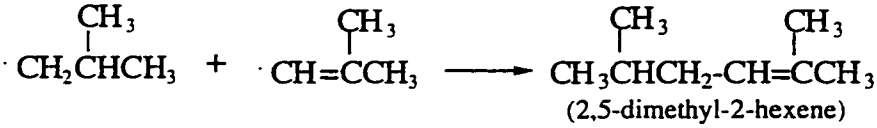

(2,5-dimethyl-2-hexene)

(4.1.1-22)

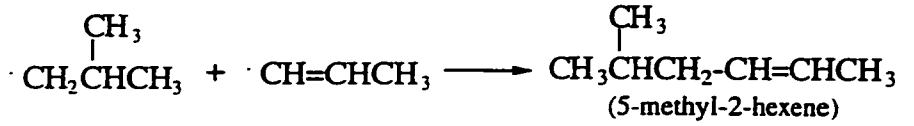

(4.1.1-23)

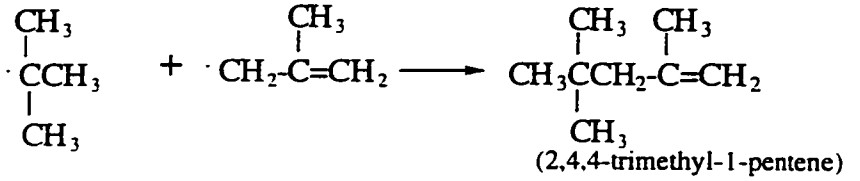

(4.1.1-24)

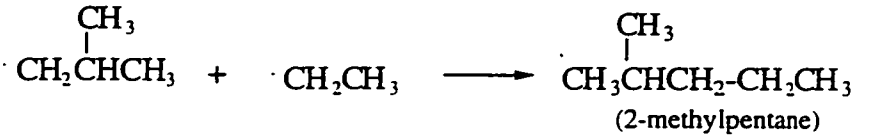

(4.1.1-25)

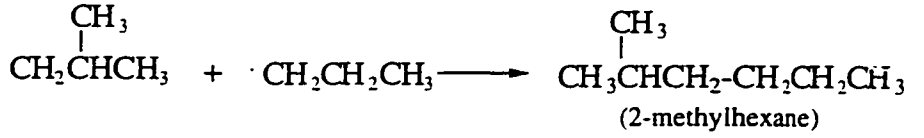

(4.1.1-26)

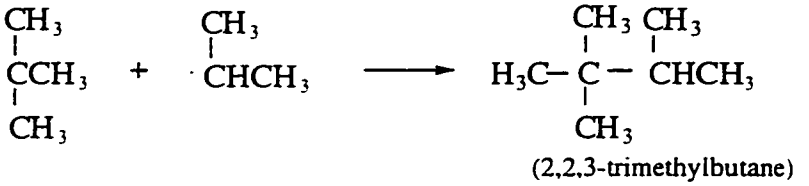

(4.1.1-27)

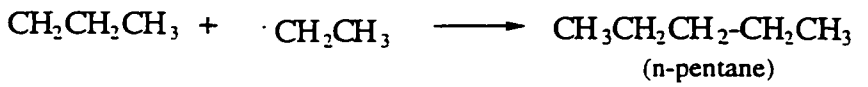

(4.1.1-28)

The product of the combination of two t-butyl radicals (reaction 4.1.1-21) might be expected to have a relatively high concentration, but this was not found to be the case in

this work. In gas-phase at 25 °C, the rate of disproportionation is about ten times that of the recombination reaction.[146] Disproportionation may occur under our conditions; however it seems likely that the tertiary butyl radical may be consumed, at least in part due to the reaction with UO_2^{2+}. Other products listed in **Table** 3.1.4-1, acetone, methanol, 2-propanol and carbon dioxide, were also detected. **Figure** 4.1.1-1 shows possible reactions that could have produced these minor products. However, the total amount of these degradation products is less than 1% of that of t-butyl alcohol.

From the mass balance experiments (**Tables** 3.1.2-1,3.1.2-2,3.1.2-3) and the results of the measurement of minor products, it is seen that the total amount of isobutane, isobutene, and the minor products is about 88% of the total loss of isobutane. This suggests that minor amounts of other products remine unidentified. Electron balance can be performed through the measurement of the reduction product U^{4+}(aq) and the oxidation products. In the absence of oxygen, U^{4+}(aq) was found (**Table** 3.1.5-1) and it can be seen that the amount of t-butanol is about 77% of the amount of U^{4+}(aq). If t-butanol is the only oxidation product, these two values should be equal to each other. As discussed in Chapter 1, an alcohol with α-hydrogen can be readily

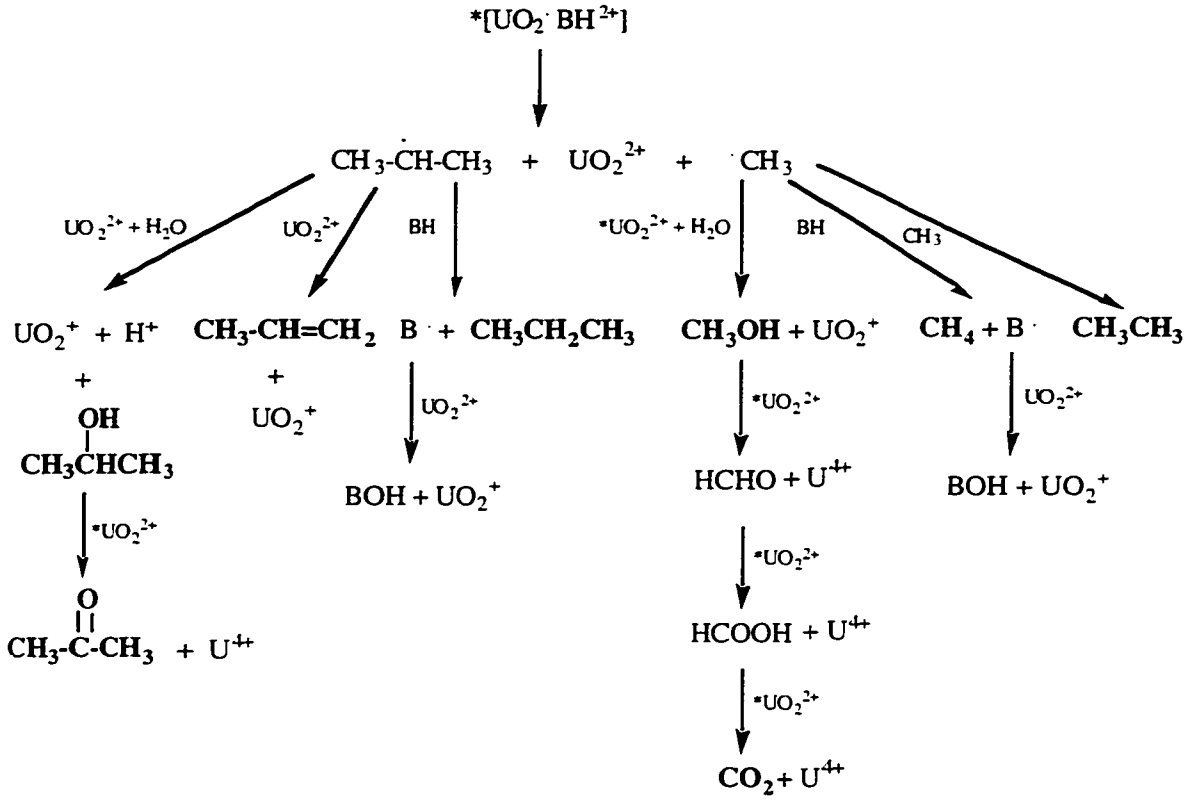

Figure 4.1.1-1. Schematic diagram of the production of minor products.

oxidized to a carboxylic acid. Since isopropanol and methanol are found, carboxylic acids might be produced in our system. Carboxylic acids can not be detected by our GC column. These acid products could account for the missing products. Since oxidation to acid rather than to an alcohol gives more electrons, it is expected that there would be more $U^{4+}(aq)$ found than there is loss of isobutane, as shown in **Table** 3.1.5-1.

In the presence of oxygen and at pH = 3, irradiation of isobutane yields a yellow precipitate. This precipitate has the same color and solubility properties as that found in the cyclopentane system (see Section 4.3). It could be $[UO_2(O_2)]\cdot 2H_2O$, and this will be discussed in Section 4.4.

Addition of oxygen affects the organic products. In the absence of oxygen, t-butanol is the predominant product. However, acetone is produced once oxygen is introduced into the solution (**Figure** 3.1.12-1). This is because oxygen can react with t-butyl radical (B·), and the resulting alkyl peroxide radical can then lead to the formation of acetone:[147]

$$B\cdot + O_2 \longrightarrow BOO\cdot \qquad (4.1.1\text{-}29)^{148}$$

$k = 1 \times 10^9\ M^{-1}s^{-1}$

$$2BOO\cdot \longrightarrow 2BO\cdot + O_2 \qquad (4.1.1\text{-}30)^{149}$$

$k = 4 \times 10^8\ M^{-1}s^{-1}$

$$BO\cdot \longrightarrow (CH_3)_2CO + \cdot CH_3 \qquad (4.1.1\text{-}31)$$ [147,148,150,151,152,153]

$$BO\cdot + BH \longrightarrow BOH + B\cdot \qquad (4.1.1\text{-}32)$$

The effect of the addition of F^- to the solution is noteworthy. The coordination reaction of F^- and $H_2PO_4^-$ to UO_2^{2+} shifts the absorption of UO_2^{2+}. Both F^- and HPO_4^{2-} shift the absorption of UO_2^{2+} to the red by about 7 nm and greatly increase the life-time of $*UO_2^{2+}$ (to ~ 160 μs). However, F^- and $H_2PO_4^-$ have much different effects on the oxidation ability of $*UO_2^{2+}$. The red shift of the absorption spectrum of UO_2^{2+} could be due to the strong coordination role of F^- or $H_2PO_4^-$ in the equatorial plane of UO_2^{2+}, which weakens the bonds of the axial oxygens and slightly diminishes the gap between the filled p-orbital and non-bonding orbital of UO_2^{2+} (see Chapter 1). It is reported that the replacement of the water molecules in the UO_2^{2+} equatorial plane by F^- or $H_2PO_4^-$ and HPO_4^{2-} is the reason for the increased life-time of $*UO_2^{2+}$.[22]

It was also found that the emission spectra in fluoride solution and in ClO_4^- solution are about the same except that a blue shift of 8 nm in F^- system is observed. This means that the electronic structures of $*UO_2^{2+}$ in the above three systems should be similar. The blue shift indicates the difference in the solvation shell structure between $*UO_2^{2+}$ and UO_2^{2+} is diminished in the F^- system. As described in

Chapter 1, electronic excitation of uranyl ion involves an electron transfer from the highest filled p-orbital to a non-bonding orbital on the uranium atom. A high-electron density anion, such as F^-, coordinating in the uranium equatorial plane is expected to increase the electron density of the non-bonding orbital of uranium atome, and thus decrease the oxidation potential of $*UO_2^{2+}$. Consistent with this is the fact that the potential of $*UO_2^{2+}$ is 2.88 V in the ClO_4^- system whereas it is 2.4 V in the F^- system.[23]

There is oxygen exchange between $*UO_2^{2+}$ and water molecule in the $HClO_4$ system but no oxygen exchange occurs in the F^- system, even though the alcohol is oxidized in the F^- system.[55] It is noteworthy that in the F^- system, the quantum yield for isobutane photolysis is zero while that for methanol it is not, as mentioned above, even though the tertiary hydrogen atom has about the same bond strength as that of α-hydrogen bond in methanol. Another interesting fact is that in the systems of $HClO_4$, HNO_3, H_2SO_4, and H_3PO_4, the quantum yields for formation of $U^{4+}(aq)$ are close to each other even though the excited uranyl ion has considerably different lifetimes in these systems. In these systems, the coordinated atoms are oxygen atoms.

From these facts, in the absence of a reducing reagent, the following micro-initial processes are proposed:

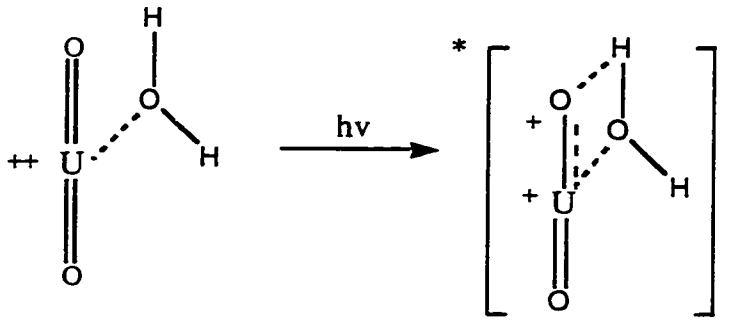

(4.1.1-33)

$^*UO_2^{2+}$ reacts with one of its coordinated water molecule to form a transitional complex $^*[UO_2 \cdots OH_2]^{2+}$ that has been proposed by some researchers.[85,86,154,155] Based on our experimental results and other reported facts, a reversible reaction between excited species is proposed, which is similar to that suggested by Formosinho and co-workers (see Chapter 1).[88]

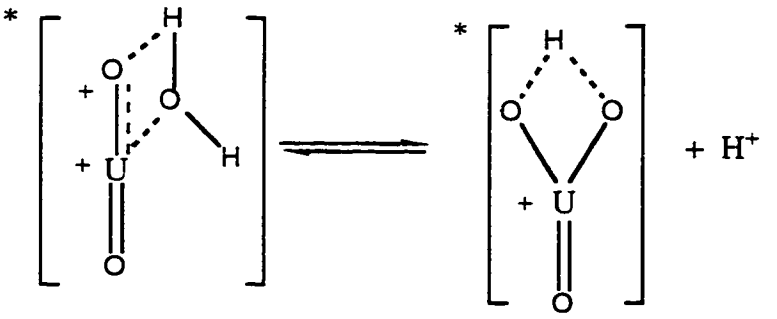

Form (A) Form (B)

(4.1.1-34)

Gaziev and coworkers proposed a similar process to explain the photostimulated oxygen exchange through UO_2^+.[52]

When isobutane is present, form (B) already interacts with a water molecule so the isobutane presumably reacts mainly with form (A) by two pathways:

Pathway (a) (one electron process):

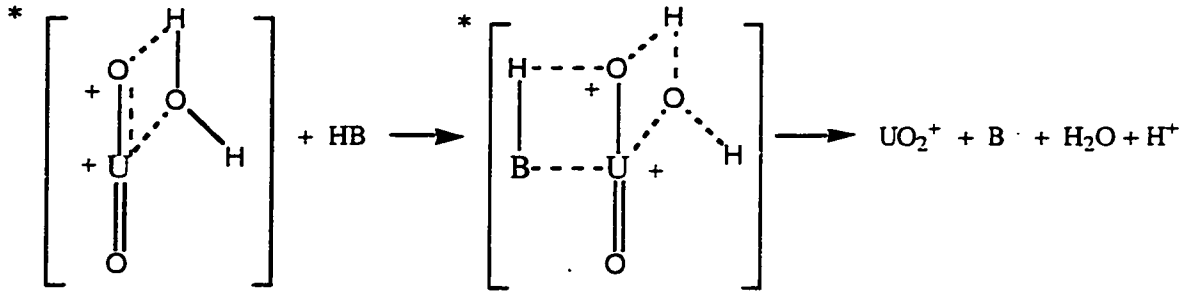

(4.1.1-35)

and pathway (b) (two electron process):

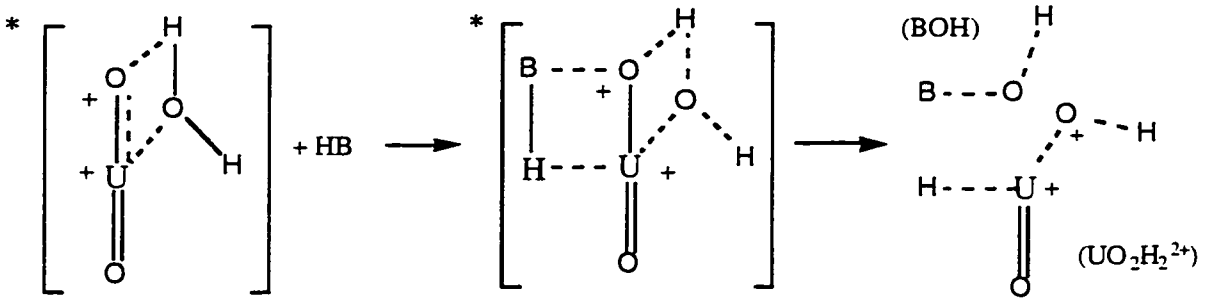

(4.1.1-36)

$UO_2H_2^{2+}$ could reacts further via the following reactions:

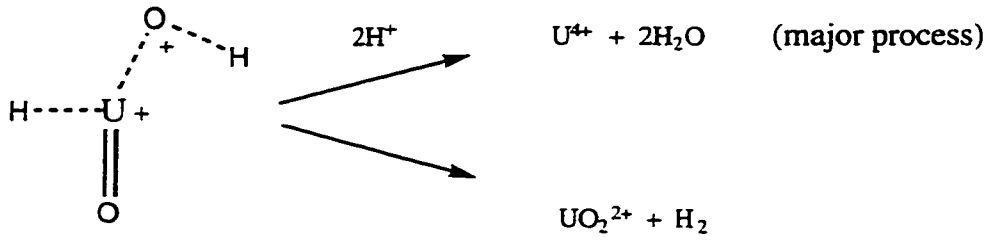

(4.1.1-37)

Pathway (a) is a one-electron process. In the oxidation of hydrocarbon derivatives, this mechanism is generally proposed.[156] The UO_2^{+} that is expected in pathway (a) is found in our system at pH = 3. With oxygen present, acetone is found as a final product of BOO·. This corroborates the presence of B·(see reactions (4.1.1-29) to (4.1.1-32). Pathway (b) is a two-electron process. It is proposed in the oxidation of the alcohol system to explain the fact that, in some cases, the quantum yield is greater than 0.5.[55] In our system, the direct production of $U^{4+}(aq)$, that is expected to occur by pathway (b), is confirmed at pH = 3.1 by the following fact. In **Table** 3.1.5-2, It is found that when the irradiation is stopped, $U^{4+}(aq)$ concentration decreases and that of UO_2^{+} increases. This means that under those conditions, the following reaction tends towards the reactant side:

$$2UO_2^{+} + 4H^{+} \rightleftharpoons UO_2^{2+} + U^{4+} + 2H_2O \qquad (4.1.1\text{-}38)$$

Calculations based on the equilibrium constant (K = 1.7 x 10^6)[157] also support this trend. The $U^{4+}(aq)$ that has been measured in this case must be directly produced rather than arising solely from the disproportionation of UO_2^+.

In the oxidation of alcohol, Rofer-Depoorter and coworker suggested other pathways for production of $U^{4+}(aq)$:[55]

$$UO_2^+ + \cdot CHROH + 3H^+ \longrightarrow U^{4+} + RCHO + 2H_2O \qquad (4.1.1\text{-}39)$$

or:

$$2*(UO_2)^+ + RCH_2OH + 6H^+ \longrightarrow 2U^{4+} + RCHO + 4H_2O \qquad (4.1.1\text{-}40)$$

It is possible to have analogous reactions in the isobutane system:

$$UO_2^+ + B\cdot + 3H^+ \longrightarrow U^{4+} + BOH + H_2O \qquad (4.1.1\text{-}41)$$

or:

$$*UO_2^+ + BH + 3H^+ \longrightarrow U^{4+} + B\cdot + 2H_2O \qquad (4.1.1\text{-}42)$$

However at pH = 3.1, the reduction potential of UO_2^+ is negative, and reaction (4.1.1-41) may be less likely to occur in our case. Sakuraba and co-workers disagreed with Depooters' mechanism for the production of $U^{4+}(aq)$.[158] Even though both reactions (4.1.1-41) and (4.1.1-42) are

possible, they cannot account for hydrogen gas found in our system.

From the proposed mechanism, in addition to UO_2^+ (from pathway (a)) and U^{4+}(aq) (from pathway (b)), hydrogen gas is also expected to be produced. When D_2O is used as the solvent in place of H_2O, trace amounts of HD are found.[159] Production of HD is consistent with the expectation that one of the hydrogen atoms comes from isobutane.

This mechanism is also in good agreement with the fact that the luminescence efficiency increases with increasing acid concentration.[92] If form (B) in reaction (4.1.1-34) has a much greater decay constant than form (A), which is the case (see next Section), then when the acid concentration increases, the concentration of form (A) or the total concentration of form (A) and form (B) increases, and thus the luminescence efficiency increases. From our mechanism, luminescence efficiencies are expected to have the following expression. The symbols are those given in **Appendix 1**.

$$\phi_f = \frac{K2 + (k_{-H})[H^+]}{(K1 + (k_{-H}))K2 + K1(k_{-H})[H^+]} \qquad (4.1.1\text{-}43)$$

This expression has the same form as that reported by Formosinho and coworkers.[90]

Depoorter and Rofer-Depoorter found that in the F^- system, no oxygen exchange occurs. This can be explained by our

proposed mechanism as follows. In the the presence of F^-, the potential of the excitation uranyl ion decreases from 2.88 V to 2.4 V, as previously mentioned, and thus it is not possible for $*UO_2^{2+}$ to oxidize the water molecule as shown below:

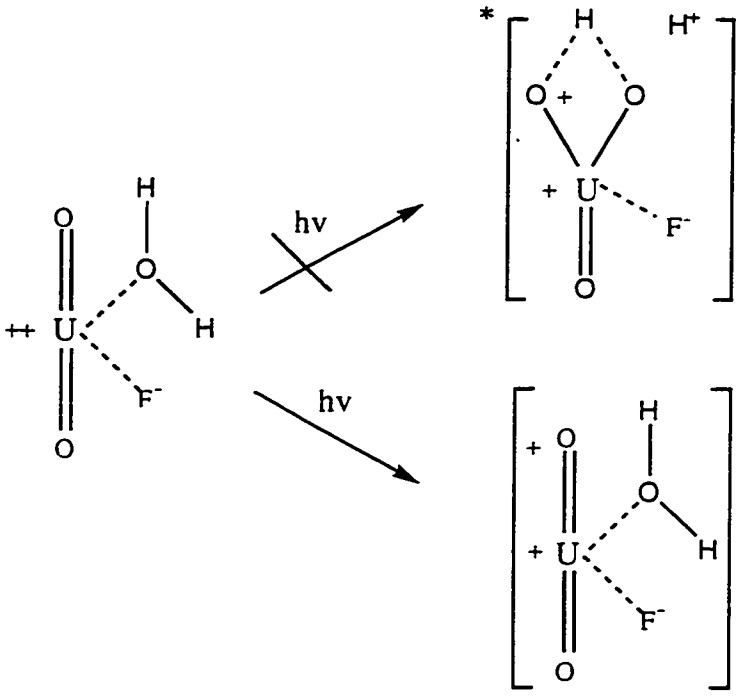

(4.1.1-44)

i.e. form (B) can not be formed and no oxygen exchange is expected. The blue shift of the emission spectrum of the uranyl fluoride system supports the above explanation since it implies that the difference in solvation-shells between the excited and ground uranyl ions is less in the presence of F^-.

The isotopic exchange results can be explained as follows: $UO_2^{+\cdot}$ is generally assumed to be the intermediate for the O^{18} exchange of UO_2^{2+*} with a water molecule.[52] As $UO_2^{+\cdot}$ is also an intermediate in the photochemistry of UO_2^{2+*}, it is expected that irradiation should induce isotopic exchange. Gaziev and co-workers[52] found that irradiation of the uranyl solution caused O^{18} exchange with water, and that with an increase in the concentration of oxidant (that can oxidize $UO_2^{+\cdot}$), the O^{18} exchange quantum yield decreases to a limiting value of 0.08. This can be explained by equation 4.1.1-34, where it can be seen that after excitation, the excited complex (form (A)) has a reversible reaction with form (B). In form (B), the oxygen from the water molecule and the oxygen from the uranyl ion are identical. Thus when form (B) returns to form (A), followed by a decay to UO_2^{2+*}, half of the oxygens have been exchanged.

4.1.2 Proposed kinetic mechanism

The following reactions are proposed as the major processes.

E1, E2 and E3 represent $*[H_2OUO_2^{+\cdot}]$, $*[HOUO_2^{+\cdot}]$ (They are Form (A) and Form (B), respectively. (see equation 4.1.1-34)) and $*[H_2OUO_2{\cdot}BH^{2+\cdot}]$, respectively.

The first step is activation by irradiation:

$[H_2OUO_2^{2+}] \xrightarrow{I_a.\ h\nu} *[H_2OUO_2^{2+}]$ (see 4.1.1-1)

(absorption) I_a = rate of light absorption

The excited $*[H_2OUO_2^{2+}]$ deactives via the following main pathways (reactions with the same starting species are distinguished by a, b, ...):

$*[H_2OUO_2^{2+}] \xrightarrow{k_{fl}} [H_2OUO_2^{2+}] + h\upsilon'$ (4.1.2-1a)

(fluorescence emission) $(\upsilon > \upsilon')$

$*[H_2OUO_2^{2+}] \xrightarrow{k_{nrl}} [H_2OUO_2^{2+}] + \text{heat}$ (4.1.2-1b)

(radiationless deactivation)

$*[H_2OUO_2^{2+}]$ reacts with its coordinated water molecule:

$*[H_2OUO_2^{2+}] \underset{k_{-H}}{\overset{k_{-H}}{\rightleftarrows}} *[HOUO_2^{+}] + H^+$ (4.1.2-1c)

Several groups also proposed similar reversible reactions.[160,161,162]

In the presence of isobutane:

$*[H_2OUO_2^{2+}] + BH \xrightarrow{k_{ql}} *[H_2OUO_2 \cdot BH^{2+}]$ (4.1.2-1d)

The base form $*[HOUO_2^{\cdot}]$ of equation (4.1.2-1c) has the following possible reactions:

$$*[HOUO_2^{\cdot}] \xrightarrow{k_{nr2}} HOUO_2^{\cdot} \qquad (4.1.2\text{-}2a)$$

$$HOUO_2^{\cdot} + H^{+} \longrightarrow UO_2^{2+} + H_2O \qquad (4.1.2\text{-}3)$$

$$*[HOUO_2^{\cdot}] \xrightarrow{k_{nr3}} UO_2^{\cdot} + HO\cdot \qquad (4.1.2\text{-}2b)$$

$$*[HOUO_2^{\cdot}] \xrightarrow{k_{f2}} HOUO_2^{\cdot} + h\upsilon'' \qquad (4.1.2\text{-}2c)$$

$$*[HOUO_2^{\cdot}] + BH \xrightarrow{k_{q2}} HOUO_2^{\cdot} + BH \qquad (4.1.2\text{-}2d)$$

This is also graphically illustrated in **Figure** 4.1.2-1. Most of hydroxyl radicals produced from reaction (4.1.2-2b) could recombine with $UO_2^{\cdot}$, some may form H_2O_2 and further reacts with $UO_2^{\cdot}$, and so no net products can be observed. However, as will be discussed in the next Section, the photoinduced isotopic exchange still occurs.
$*[H_2OUO_2\cdot BH^{2+}]$ formed in reaction (4.1.2-1d) then decomposes according to:

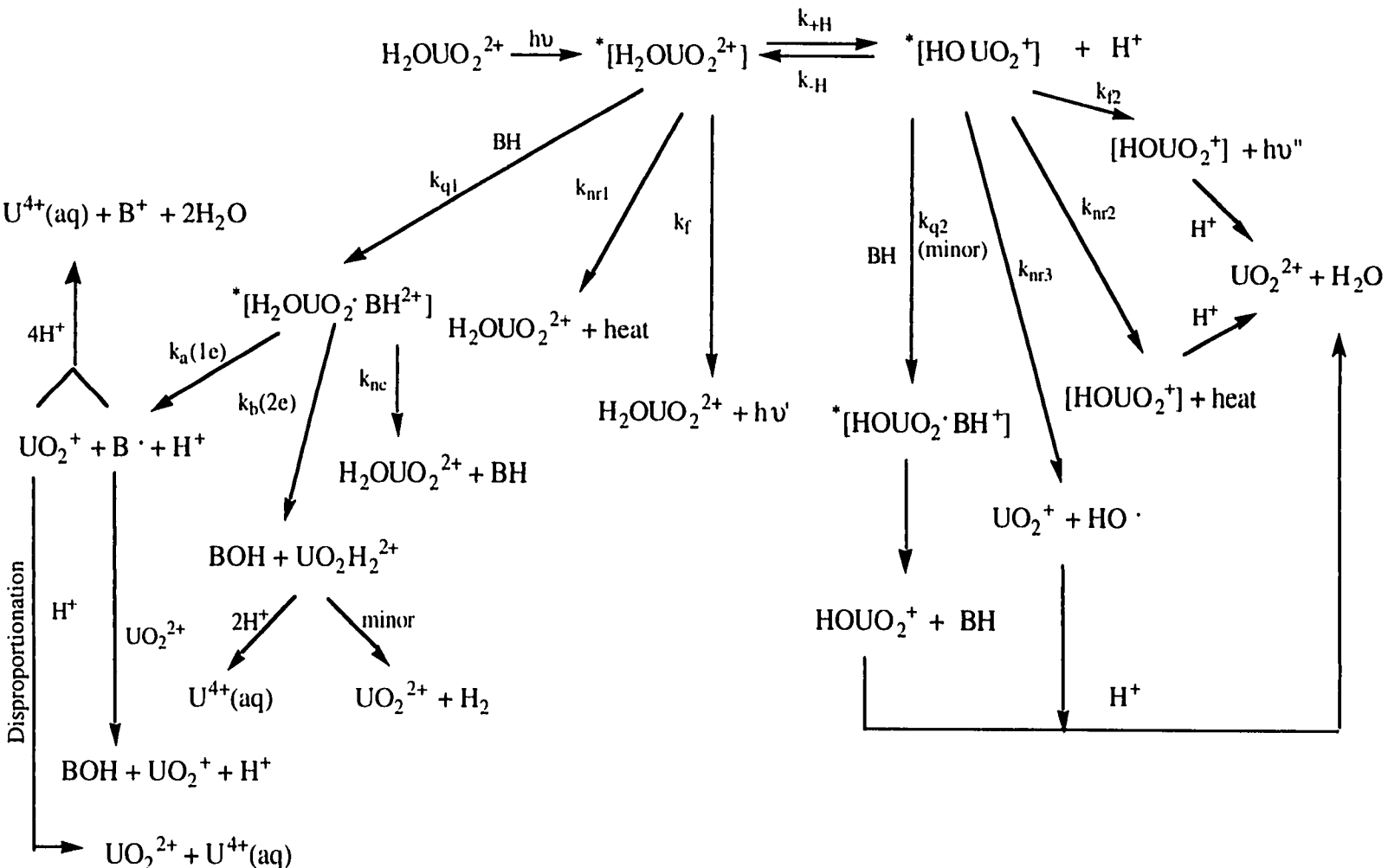

Figure 4.1.2-1. Schematic diagram of reaction mechanism I.

$$*[H_2OUO_2{\cdot}BH^{2+}] \xrightarrow{k_a} UO_2^{+} + B{\cdot} + H_3O^{+} \qquad (4.1.2\text{-}4a)$$

(1 e^- mech.)

$$*[H_2OUO_2{\cdot}BH^{2+}] \xrightarrow{k_b} BOH + UO_2H_2^{2+} \qquad (4.1.2\text{-}4b)$$

(2 e^- mech.)

$$*[H_2OUO_2{\cdot}BH^{2+}] \xrightarrow{k_{nc}} UO_2^{2+} + BH + H_2O \qquad (4.1.2\text{-}4c)$$

$UO_2H_2^{2+}$ decomposes as follows:

$$UO_2H_2^{2+} \longrightarrow U(OH)_2^{2+} \qquad (4.1.2\text{-}5a)$$

$$UO_2H_2^{2+} \longrightarrow UO_2^{2+} + H_2 \qquad (4.1.2\text{-}5b)$$

These two processes are pathway (b) described previously.

The UO_2^{+} produced can also disproportionate to $U^{4+}(aq)$:

$$2UO_2^{+} + 4H^{+} \xrightarrow{k_d} UO_2^{2+} + U^{4+} + 2H_2O \quad k_d = 435\ M^{-2}s^{-1} \qquad (4.1.2\text{-}6)^{34}$$

There are several possibilities for the decay of the free radical B·. It can disproportionate through:

$$B{\cdot} + B{\cdot} \longrightarrow (CH_3)_2CH{=}CH_2 + BH \qquad (4.1.2\text{-}7)$$

or two B· can also combine:

$$B\cdot + B\cdot \longrightarrow (CH_3)_3C\text{-}C(CH_3)_3 \qquad (4.1.2\text{-}8)$$

These reactions are not the major reactions because only trace amounts of B-B (2,2,3,3-tetramethylbutane) and a small amount of isobutene are found. Although the hydrolysis of isobutene is known, this reaction has a small rate constant (k_{B2} =3.8 x 10^{-5} $M^{-1}s^{-1}$) and the halflife of isobutene is calculated to be about 300 minutes under the reaction conditions (**Figure** 3.1.3-2). If it is produced via reaction 4.1.2-7), then it should have been detected in substantial amounts before signifcant hydrolysis occured.

In γ-radiation of isobutane, BOH is found in about the same amount as the B-B product.[163] This means that the B· produced in the γ-radiolysis does not readily form t-butanol in the absence of UO_2^{2+}. In our system, t-butanol is the predominant product. It is proposed that the major reaction for the formation of BOH is:

$$B\cdot + UO_2^{2+} + H_2O \longrightarrow BOH + UO_2^{+} + H^{+} \qquad \text{(major)} \quad (4.1.2\text{-}9a)$$

$$B\cdot + UO_2^{2+} \longrightarrow (CH_3)_2C{=}CH_2 + UO_2^{+} + H^{+} \qquad \text{(minor)} \quad (4.1.2\text{-}9b)$$

α-hydroxyalkyl radicals are well known to be reducing agents of UO_2^{2+}.[95,164] UO_2^{2+} is reported to oxidize $Ph_2(OH)C\cdot$

radical with a rate constant of 1.3 x 10^5 $M^{-1}s^{-1}$.[41] It is reported that the alkyl radical and hydroxyalkyl radical reduce Ni^+ to Ni^0 with about the same rate constant.[165] It thus seems possible that the alkyl radical can be oxidized by UO_2^{2+}.

From these major reactions, the following relationships can be derived for quantum yield of BOH (**Appendix 1**):

$$\phi = \left(\frac{(k_a + k_b)k_{q1}[BH]}{K03}\right)\left(\frac{1}{K1 + \frac{(k_{+H})(k_{-H})[H^+]}{(k_{-H})[H^+] + K2}}\right)$$

$$= \left(\frac{(k_a + k_b)k_{q1}[BH]}{(k_a + k_b + k_{nc})}\right)$$

$$\times \left(\frac{1}{k_{nr1} + k_{f1} + (k_{+H}) + k_{q1}[BH] - \frac{(k_{+H})(k_{-H})[H^+]}{(k_{-H})[H^+] + (k_{f2} + k_{nr2} + k_{nr3} + k_{q2}[BH])}}\right)$$

(4.1.2-10)

or:

$$\phi = \frac{k_{q1}[BH]}{(k_{q1}[BH] + k_T)} \cdot \frac{(k_a + k_b)}{(k_a + k_b + k_{nc})} \qquad (4.1.2\text{-}11)$$

where:

$$k_T = (k_{nr1} + k_{f1} + (k_{+H})) - \frac{(k_{+H})(k_{-H})[H^+]}{(k_{-H})[H^+] + (k_{f2} + k_{nr2} + k_{nr3} + k_{q2}[BH])} \quad (4.1.2\text{-}12)$$

or:

$$k_T = K_{01} - \frac{(k_{+H})(k_{-H})[H^+]}{(k_{-H})[H^+] + K2} \quad (4.1.2\text{-}13)$$

k_T is different from k_0. k_0 is the decay constant of $*UO_2^{2+}$ in the absence of isobutane. It has the following expression (see **Appendix 1**):

$$k_0 = K_{01} - \frac{(k_{+H})(k_{-H})[H^+]}{(k_{-H})[H^+] + K_02} \quad (4.1.2\text{-}14)$$

k_T can be considered approximately as the apparent decay constant of $*UO_2^{2+}$. The value of k_T, as will be discussed later, is close to the value of k_0. As shown in equation (A1-21), k_0 is a function of $[H^+]$. This conclusion is consistent with experimental results. At pH = 1, k_0 is measured to be 4.5×10^5 $M^{-1}s^{-1}$.

From equation (4.1.2-10), it can be seen that the quantum yield is a function of the concentrations of isobutane and proton. Equation (4.1.2-10) is consistent with the results shown in **Figure** 3.1.10-1 and **Table** 3.1.11-1, where, no significant change in the quantum yield occurs with

variations in light intensity or in concentration of uranyl ion.

Equation (4.1.2-10) can also be expressed as apparent functions of [BH] and [H$^+$]:

$$\frac{1}{\phi} = \frac{(k_a + k_b + k_{nc})k_T}{(k_a + k_b)k_{q1}[BH]} + \frac{k_a + k_b + k_{nc}}{k_a + k_b} \qquad (4.1.2\text{-}15)$$

$$\phi = \frac{k_{q1}(k_a+k_b)[BH]}{k_a+k_b+k_{nc}} \cdot \frac{\frac{k_{-H}[H^+]}{K2} + 1}{(K1 - k_{-H})\frac{k_{-H}[H^+]}{K2} + K1} \qquad (4.1.2\text{-}16)$$

From the data of **Figure** 3.1.8-2, the relationship of $1/\phi$ via 1/[BH] is plotted in **Figure** 4.1.2-2. As expected, it is a straight line, with slope = 0.031 and an intercept = 2.1. From this figure and equation (4.1.2-15), the following values are obtained:

$$k_{q1}(\text{calc}) = (\text{intercept/slope})k_T \approx (\text{intercept/slope})k_0$$
$$= 3.1 \times 10^7\ M^{-1}s^{-1} \qquad (4.1.2\text{-}17)$$

$$(k_a + k_b + k_{nc})/(k_a + k_b) = \text{intercept} = 2.1 \qquad (4.1.2\text{-}18)$$

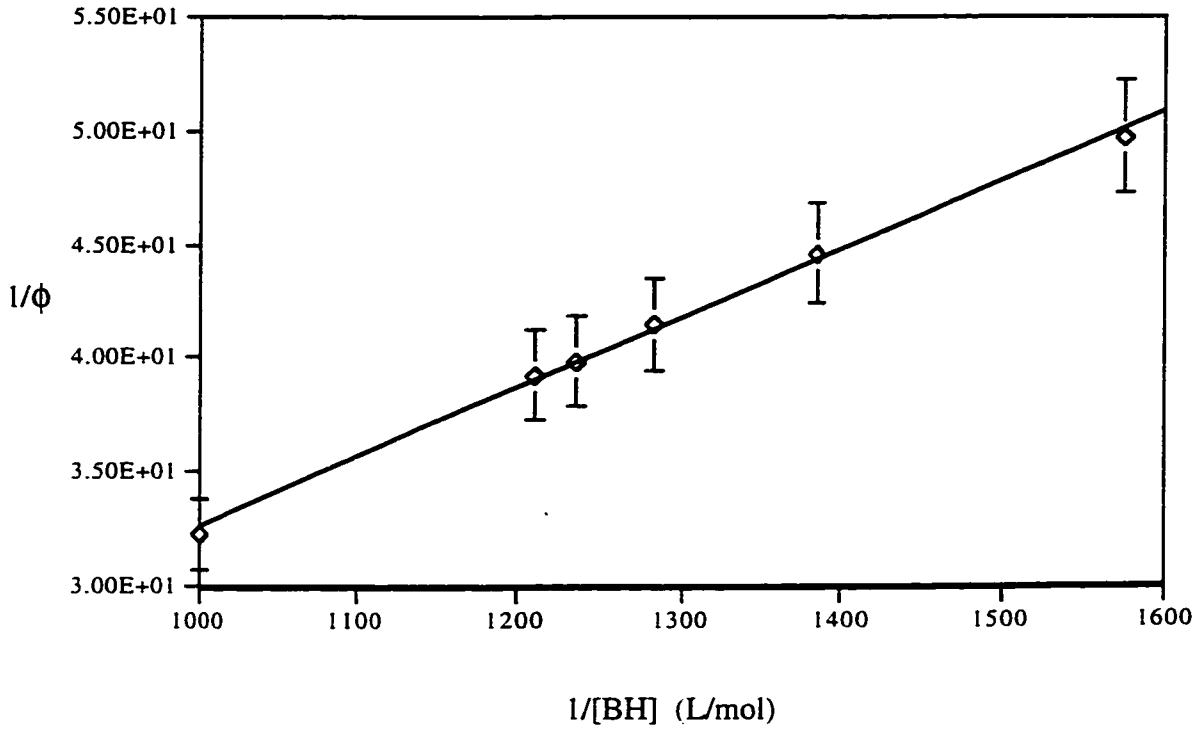

Figure 4.1.2-2. Relationship of $1/\phi$ and 1/[isobutane]. $[UO_2^{2+}]$ = 34.8 mM; pH = 1.1 ($HClO_4$); V_{irrad} = 145 mL; T = 25 °C; I = 9.32 x 10^{-6} Einstein/min; λ_{irr} = 415 nm. Before irradiation nitrogen was bubbled for 20 min then isobutane was bubbled for 5 min. During irradiation, isobutane is continuously bubbled at the rate of 10 mL/min.

Curve fitting equation: $y = 3.05E\text{-}02x + 2.10E+00$ $r^2 = 9.97E\text{-}01$

The k_{q1}(calc) calculated from the data of tertiary butyl alcohol quantum yields is close to the k_{q1} measured from the emission experiments, which is 3.5 x 10^7 $M^{-1}s^{-1}$. At pH = 3.1, UO_2^+ is stable. From the measurement of UO_2^+ and U^{4+}(aq) at pH = 3.1, the ratio of UO_2^+/U^{4+}(aq) is about 10/1. As the extinction coefficient ε of U(IV) at pH = 3.1 is unknown, the value of ε at pH = 1.6 was used to estimate it and this value is a little higherthan that at pH = 3.1. This means that the ratio of k_a/k_b should be about 10/1 at pH = 3.1 (see equations 4.1.2-4a and 4.1.2-4b). This ratio should not be influenced by pH as they are fast irreversible reactions. This conclusion is also supported by our experimental results. Experimentally, we found that the amplification factor of peroxydisulfate was not significantly affected by pH (**Table** 3.2.5-1). In our mechanism, only Path (a) favors the amplification. If k_a/k_b changes with pH, a change in the amplification factor should be observed (this will be discussed in the next Section). Assuming k_a/k_b = 10/1, then from the expression (4.1.2-18) the following relationships are obtained:

$$k_a/k_{nc} = 0.83 \qquad (4.1.2\text{-}19)$$

$$k_b/k_{nc} = 0.083 \qquad (4.1.2\text{-}20)$$

The experimental results for the dependence of quantum yield on acid concentration are shown in **Figures** 3.1.9-1 and 3.1.9-2. From this mechanism, some important reaction constants can be deduced. If [H^+] is very small, equation (4.1.2-16) can be expressed as:

$$\phi = \frac{\frac{k_{q1}(k_a+k_b)}{(k_a+k_b+k_{nc})}[BH]}{K1} = \frac{\frac{k_{q1}(k_a+k_b)}{(k_a+k_b+k_{nc})}[BH]}{K_01+k_{q1}[BH]} \qquad (4.1.2\text{-}21)$$

k_{q1} is measured to be 3.5 x 10^7 $M^{-1}s^{-1}$ (see Chapter 3); when this value, $(k_a + k_b)/(k_a + k_b + k_{nc})$ = 0.476 and [BH] = 0.60 x 10^{-3} M are substituted into equation (4.1.2-21), the following expression is obtained:

$$\phi = \frac{1.0\times10^4}{K_01+2.1\times10^4} \qquad (4.1.2\text{-}22)$$

From the quantum yield (0.0143) at low [H^+] (pH = 3.1), $\mathbf{K_0 1}$ can be calculated from above equation to be 6.8 x 10^5 s^{-1}.

With K1 = ($K_0$1 + k_q[BH]) = 7.0 x 10^5 s^{-1}, equation (4.1.2-16) can be written as:

$$\phi = \frac{\frac{k_{q1}((k_a+k_b)[BH]}{(k_a+k_b+k_{nc})}\frac{k_{-H}}{K2}[H^+]+1.0\times10^4}{(7.0\times10^5-k_{-H})\frac{k_{-H}}{K2}[H^+]+7.0\times10^5} \qquad (4.1.2\text{-}23)$$

or:

$$\phi = \frac{A \times [H^+] + 1.0 \times 10^4}{B \times [H^+] + 7.0 \times 10^5} \qquad (4.1.2\text{-}24)$$

using the data for quantum yield versus acid concentration (discussed in Section 3.1.9), the above equation was fitted using TABLECURVE 2D software(Jandel Co.) to determine the constants A = 4.4 x 10^4 and B = 7.6 x 10^5, respectively. The following equation is thus obtained:

$$\phi = \frac{4.4 \times 10^4 \times [H^+] + 1.0 \times 10^4}{7.6 \times 10^5 \times [H^+] + 7.0 \times 10^5} \qquad (4.1.2\text{-}25)$$

In **Figure** 4.1.2-3, a comparsion of the experimental data and the fitted curve is shown. It is seen that the fitted curve is in good agreement with the data. Comparing equations (4.1.2-23) and (4.1.2-25), the $\mathbf{k_{+H}}$ is calculated to be 5.3 x 10^5 s^{-1} and the ratio of $k_{-H}/K2$ to be 4.4/1. The value of k_{-H} can be estimated using the equilibrium constant equation (4.1.2-2c) reported by Formosinho and coworkers (pK_a = 2 to 2.5).[46] Using pK_a = 2.2 and k_{+H} = 5.3 x 10^5, $\mathbf{k_{-H}}$ is calculated to be 8.4 x 10^7 $M^{-1}s^{-1}$. From the ratio of $k_{-H}/K2$ = 4.4/1, K2 can be obtained as **K2** = 1.9 x 10^7 s^{-1}. K_02 can be estimated to be $\mathbf{K_02}$ = K2 - k_{q2}[BH] ≈ 1.9 x 10^7 s^{-1}. With these constants, k_T can be now calculated by equation (4.1.2-13). At pH = 0.95, $\mathbf{k_T}$ is calculated to be 5.1 x 10^5 s^{-1}. Thus

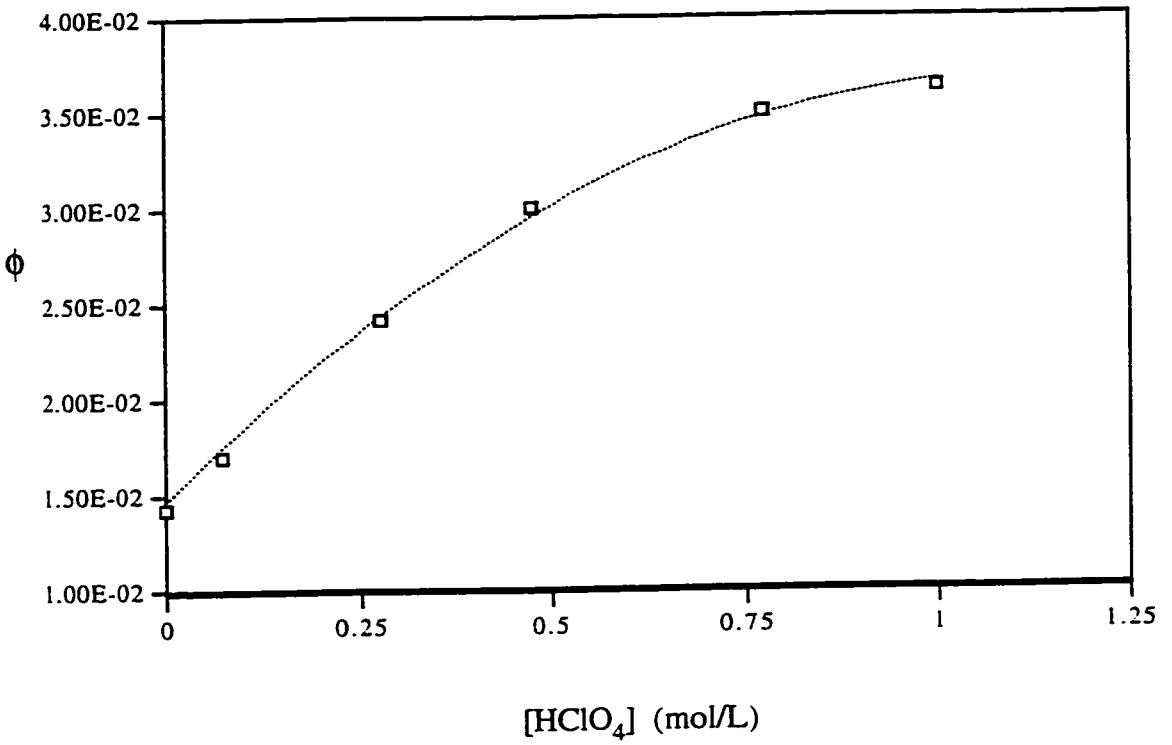

Figure 4.1.2-3. Comparison of experimental and curve fitting results.

Curve fitting equation:

$$\phi = (4.4 \times 10^4 \times [H^+] + 1.0 \times 10^4)/(7.6 \times 10^5 \times [H^+] + 7.0 \times 10^5)$$

k_{q1}(calc) can be recalculated using equation (4.1.2-17), and it is 3.5 x 10^7 $M^{-1}s^{-1}$. This value is the same as the one measured. Based on k_a/k_{nc} = 0.83 and k_b/k_{nc} = 0.083, the percentage of the following three reactions can also be calculated as shown below:

$$*[H_2OUO_2 \cdot BH^{2+}] \xrightarrow{k_a} UO_2^{+} + B\cdot + H_3O^{+} \qquad 43\% \qquad (4.1.2\text{-}4a)$$

$$*[H_2OUO_2 \cdot BH^{2+}] \xrightarrow{k_{nc}} UO_2^{2+} + BH + H_2O \qquad 52\% \qquad (4.1.2\text{-}4b)$$

$$*[H_2OUO_2 \cdot BH^{2+}] + \xrightarrow{k_b} BOH + UO_2H_2^{2+} \qquad 5\% \qquad (4.1.2\text{-}4c)$$

In the absence of isobutane, the changes of species $*[H_2OUO_2]^{2+}$, $*[HOUO_2]^{+}$ and $[H^{+}]$ have the following kinetic equations (ref. **Figure** 4.1.2-1), where Hi is the initial concentration of proton:

$$d[E1]/dt = k_{-H}[E2][Hi] - K_01[E1] \qquad (4.1.2\text{-}26)$$

$$d[E2]/dt = k_{+H}[E1] - k_{-H}[E2][Hi] - K_02[E2] \qquad (4.1.2\text{-}27)$$

$$d[H^{+}]/dt = k_{+H}[E1] - k_{-H}[E2][Hi] - (k_{nr2}+k_{f2})[E2] \qquad (4.1.2\text{-}28)$$

This is a system of linear first-order differential equations. Solving this system using AMPLE software package (Waterloo Maple Inc.), and substituting the rate constants

($K_0 1 = 6.8 \times 10^5$, $k_{+H} = 5.3 \times 10^5$, $k_{-H} = 8.4 \times 10^7$, $K_0 2 = 1.9 \times 10^7$, [Hi] = 4×10^{-3} (pH = 2.4), the following relations were obtained:

$$[E1](t) = 0.9995 \times \exp(-6.706 \times 10^5 t) + 0.0005012 \times \exp(-1.935 \times 10^7 t) - 0.1032 \quad (4.1.2\text{-}29)$$

$$[E2](t) = 0.02785 \times \exp(-6.706 \times 10^5 t) + 0.2785 \times \exp(-1.935 \times 10^7 t) \quad (4.1.2\text{-}30)$$

$$\Delta[H^+](t) = 0.02785 \times \exp(-6.706 \times 10^5 t) + 0.2785 \times \exp(-1.935 \times 10^7 t) + 0.004000 \quad (4.1.2\text{-}31)$$

From the above equations, it can be seen that the magnitude of [E2] is small, and has almost the same decay curve as [E1]. In the time-resolved experiments, E1 can be traced by its emission and H^+ can be detected by its conductivity. From the above equations, the emission and conductivity have the same first-order rate constant of 6.7×10^5 s^{-1}. This expectation is consistent with our time-resolved experimental results.[166]

In this experiment, the ratio of conductivities in the presence to the absence of isobutane was 1.5/1. From the ratio, a quantum yield of HO· can be estimated. From **Figure** 4.1.2-1, in the absence of isobutane, the production rate of proton can be expressed as:

$$\frac{d[H^+]}{dt} \propto E2 \times k_{nr3} = \frac{(k_{+H})E1}{K_02 + (k_{-H})[H^+]} \times k_{nr3} \qquad (4.1.2\text{-}32)$$

When there is isobutane in solution:

$$\frac{d[H^+]'}{dt} \propto E2' \times k_{nr3} + E3' \times k_a = \left(\frac{(k_{+H})[E1]'}{K_02 + (k_{-H})[H] + k_{q2}[BH]} \times k_{nr3} \right) + \left(\frac{k_{q1}[BH][U1]_a}{K_03} \times k_a \right) \qquad (4.1.2\text{-}33)$$

and the ratio:

$$\frac{d[H^+]'}{d[H^+]} = \frac{\dfrac{(k_{+H})[E1]' k_{nr3}}{K_02 + (k_{-H})[H] + k_{q2}[BH]} + \dfrac{k_{q1}[BH][E1]' k_a}{K_03}}{\dfrac{(k_{+H})[E1]k_{nr3}}{K_02 + (k_{-H})[H]}} \qquad (4.1.2\text{-}34)$$

In the presence of isobutane, the equilibrium concentration [E1]' should be close to [E1], as it was found that k_{q1}[BH] is a very small part of the total decay rate of E1. For the same reason, k_{q2}[BH] is also negligible, thus the ratio of [H$^+$]'/[H$^+$] is:

$$\frac{d[H^+]'}{d[H^+]} = 1 + \frac{\dfrac{k_{q1}[BH]k_a}{K_03}}{\dfrac{(k_{+H})k_{nr3}}{K_02 + (k_{-H})[H]}} \qquad (4.1.2\text{-}34)$$

Substituting values of the constants into the above equation, one obtains:

$$\frac{d[H^+]'}{d[H^+]} = 1 + \frac{5.0\times10^5}{k_{nr3}} \qquad (4.1.2\text{-}35)$$

When we compare the stable levels of $[H^+]'$ and $[H^+]$ at the same time t, then we can use the integration form of equation (4.1.2-35):

$$\frac{[H^+]'}{[H^+]} = 1 + \frac{5.0\times10^5}{k_{nr3}} \qquad (4.1.2\text{-}36)$$

From the experimental value of $[H^+]'/[H^+]$ = 1.5, then $\mathbf{k_{nr3}}$ is calculated to be about 1.0 x 10^6 s^{-1}. Thus the quantum yield of HO· can be calculated to be (k_{nr3}/K_02) x $(k_{\cdot H}/k_01)$ = 0.04. It is reported that HO· is found in some uranyl photolysis systems.[110,167,168]

4.2 Isobutane System in the Presence of $K_2S_2O_8$

4.2.1 Discussion of results

The addition of peroxydisulfate significantly increases the quantum yield (**Figure** 3.2.1-1). There are no thermal or post-irradiation reactions. In the absence of uranyl ion, irradiation of isobutane-saturated peroxydisulfate solution with visible light does not lead to any products. This indicates that peroxydisulfate must react with some intermediates produced in the irradiation process.

In the presence of peroxydisulfate, mass balance was achieved after a short period of irradiation (**Tables** 3.2.2-1, 3.2.2-2). The quantum yield of the formation of tertiary butyl alcohol can exceed unity and it varies inversely with the light intensity (**Figure** 3.2.6-5). These features indicate a chain mechanism. When peroxydisulfate is added, the following three reactions with the excited species are possible:

$$*[H_2OUO_2]^{2+} + S_2O_8^{2-} \longrightarrow UO_2^{+} + S_2O_8^{-} \qquad (4.2.1\text{-}1)$$

$$*[HOUO_2]^{+} + S_2O_8^{2-} \longrightarrow HOUO_2^{+} + S_2O_8^{2-} \qquad (4.2.1\text{-}2)$$

$$*[H_2OUO_2 \cdot BH]^{2+} + S_2O_8^{2-} \xrightarrow{k_{SU3}} UO_2^{2+} + B\cdot + SO_4^{-} + HSO_4^{-} \qquad (4.2.1\text{-}3)$$

However, from emission experiments, it is known that peroxydisulfate does not quench the excited uranyl ion. This means that the above reactions are not significant.

Propagation processes are considered to be:

$$\mathbf{UO_2^{+}} + S_2O_8^{2-} \xrightarrow{k_{SU1}} UO_2^{2+} + SO_4^{-} + SO_4^{2-} \qquad (4.2.1\text{-}4)$$

$$SO_4^{-} + BH \xrightarrow{k_{FBH}} B\cdot + HSO_4^{-} \qquad (4.2.1\text{-}5)^{169}$$

$k_{FBH} = 1.05 \times 10^{8}\ M^{-1}s^{-1}$

$$B\cdot + UO_2^{2+} + 2H_2O \xrightarrow{k_{BU2}} \mathbf{BOH} + \mathbf{UO_2^{+}} + H^{+} \qquad \text{(see 4.1.2-9)}$$

$$B\cdot + S_2O_8^{2-} + H_2O \xrightarrow{k_{SB}} \mathbf{BOH} + SO_4^{-} + HSO_4^{-} \qquad (4.2.1\text{-}6)^{170}$$

$k_{SB} = 1 \times 10^5\ M^{-1}s^{-1}$

There are two cycles. The first one consists of reactions (4.2.1-4), (4.2.1-5) and (4.1.2-9); the second consists reactions (4.2.1-5) and (4.2.1-6).

From the concentrations and reaction rates, the following two reaction are the most likely termination processes for SO_4^{-}:

$$SO_4^{-} + UO_2^{+} \xrightarrow{k_{FU1}} UO_2^{2+} + SO_4^{2-} \qquad (4.2.1\text{-}7)$$

$k_{FU1} > 10^8\ M^{-1}s^{-1}$

$$SO_4^{-} + SO_4^{-} \xrightarrow{2k_{FF}} S_2O_8^{2-} \qquad (4.2.1\text{-}8)^{171}$$

$2k_{FF} = 3.7 \times 10^8\ M^{-1}s^{-1}$

No rate constant is available for reaction (4.2.1-7), but it is expected to be very high. NpO_2^{+} has a very high rate constant with SO_4^{-} ($7 \times 10^8\ M^{-1}s^{-1}$). The reduction potential of NpO_2^{2+}/NpO_2^{+} ($E^{\circ} = 1.14$ V) is higher than that of UO_2^{2+}/UO_2^{+} ($E^{\circ} = 0.052$ V) and NpO_2^{+} is also more stable than UO_2^{+} in solution. **Figure** 4.2.1-1 shows graphically the main reactions in the presence of peroxydisulfate.

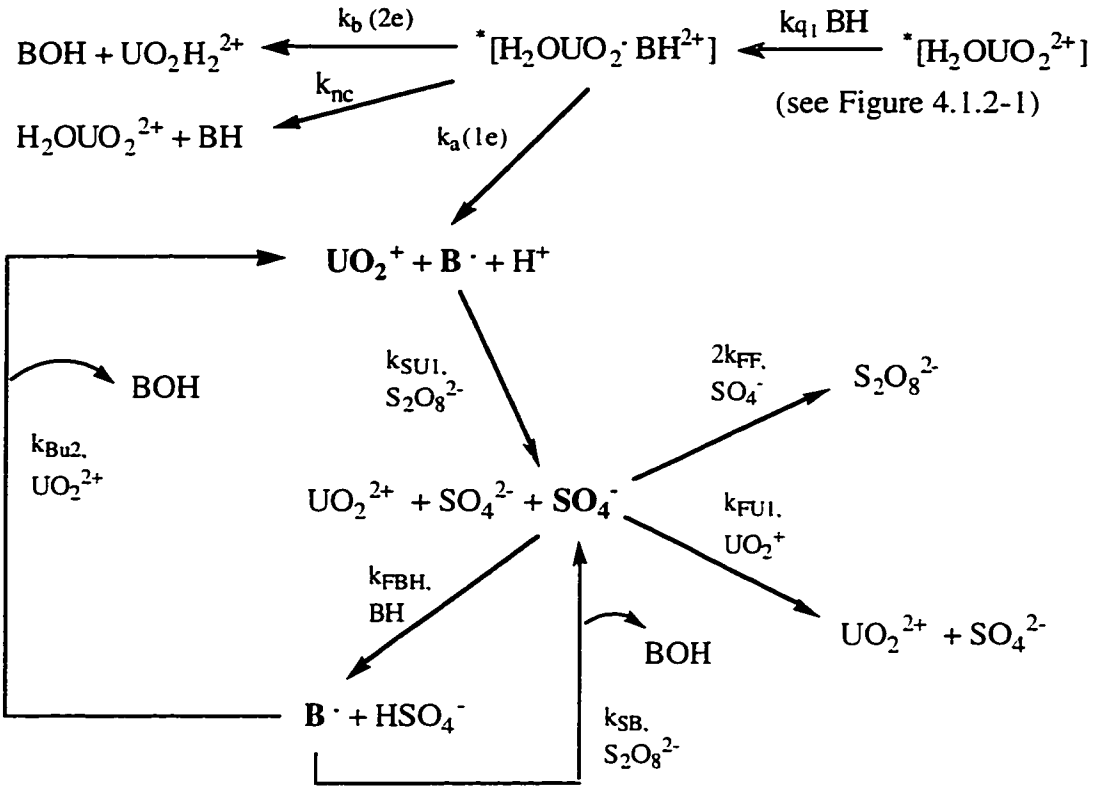

Figure 4.2.1-1. Schematic diagram of reaction mechanism II (in the Presence of Peroxydisulfate. note : in this case, we presume that other species derived from *[$HOUO_2^+$] are not important).

4.2.2 Proposed Kinetic Mechanism

The important reactions discussed above are rewritten below. The initiating process is considered to be:

$$*[H_2OUO_2 \cdot BH^{2+}] \xrightarrow{k_a} UO_2^{+} + B\cdot + H_3O^{+} \qquad \text{(see 4.1.2-4a)}$$

Propagation processes are considered to be:

$$\mathbf{UO_2^{+}} + S_2O_8^{2-} \xrightarrow{k_{SU1}} UO_2^{2+} + SO_4^{-} + SO_4^{2-} \qquad \text{(see 4.2.1-4)}$$

$$SO_4^{-} + BH \xrightarrow{k_{FBH}} B\cdot + HSO_4^{-} \qquad \text{(see 4.2.1-5)}$$

$k_{FBH} = 1.05 \times 10^8\ M^{-1}s^{-1}$

$$B\cdot + UO_2^{2+} \xrightarrow{k_{BU2}} \mathbf{BOH} + \mathbf{UO_2^{+}} + H^{+} \qquad \text{(see 4.1.2-9)}$$

$$B\cdot + S_2O_8^{2-} + H_2O \xrightarrow{k_{SB}} \mathbf{BOH} + SO_4^{-} + HSO_4^{-} \qquad \text{(see 4.2.1-6)}$$

$k_{SB} = 1 \times 10^5\ M^{-1}s^{-1}$

Termination processes for SO_4^{-} are:

$$SO_4^{-} + \mathbf{UO_2^{+}} \xrightarrow{k_{FU1}} UO_2^{2+} + SO_4^{2-} \qquad \text{(see 4.2.1-7)}$$

$k_{FU1} \geq 10^8\ M^{-1}s^{-1}$

$SO_4^{\cdot-} + SO_4^{\cdot-} \xrightarrow{2k_{FF}} S_2O_8^{2-}$ (see 4.2.1-8)

$2k_{FF} = 3.7 \times 10^8\ M^{-1}s^{-1}$

From these proposed major reactions and using some approximations, the following equations were derived: (see **Appendix 2**):

$$\phi = \frac{(k_a + k_b)k_{q1}[BH]}{K_03} F_{(H)} + \left(k_{FBH} \left(\frac{k_{q1}k_a k_{SU1}}{k_{FF}k_{FU1}K_03} \right)^{1/3} [BH]^{4/3}[S_2O_8^{2-}]^{1/3}(F_{(H)})^{1/3} \frac{1}{I^{2/3}} \right) \quad (4.2.2\text{-}1)$$

$$F_{(H)} = \frac{1}{K1 - \frac{(k_{+H})(k_{-H})[H^+]}{(k_{-H})[H^+] + K2}} \quad (4.2.2\text{-}2)$$

or:

$$F_{(H)} = \frac{1}{k_{q1}[BH] + K_01 - \frac{(k_{+H})(k_{-H})[H^+]}{(k_{-H})[H^+] + K2}} = \frac{1}{k_{q1}[BH] + k_T} \quad (4.2.2\text{-}3)$$

where: $K_01 = k_{f1} + k_{nr1} + k_{+H}$; $K_03 = k_a + k_b + k_{nc}$; $K1 = k_{f1} + k_{nr1} + k_{+H} + k_{q1}[BH]$; $K2 = k_{f2} + k_{nr2} + k_{nr3} + k_{q2}[BH]$ (k_T: see (4.1.2-12).

The first term of equation (4.2.2-1) can be expressed as:

$$A = \frac{k_{q1}[BH]}{(k_{q1}[BH] + k_T)} \cdot \frac{(k_a + k_b)}{(k_a + k_b + k_{nc})} \quad (4.2.2\text{-}4)$$

It is identical to equation (4.1.2-11).

From equation (4.2.2-1), it can be seen that the quantum yield should be linear functions of $[BH]^{4/3}$ (the intercept can be ignored compared to the second term). Using data from **Figure** 3.2.4-1, **Figure** 4.2.2-1 is made and it shows consistent with above conclusions. When the concentration of isobutane is high, the curve bends downwards. This may be due to the affects of K1 and K2. There are [BH] terms in K1 and K2 and both K1 and K2 increase with increasing [BH]. An increase of K1 and K2 will diminish the $F_{(H)}$ and thus make the curve concave downwards.

Figure 4.2.2-2 is plotted from data in **Figure** 3.2.6-5, and it shows the dependence of $1/(I)^{2/3}$ on quantum yield. It is in good agreement with our expectations.

The effect of acid concentration is shown in **Figure** 3.2.5-1. In equation (4.2.2-1), the effect of acid concentration should be reflected in the term $F_{(H)}$. As the intercept is small, the quantum yield should be a linear function of $(F_{(H)})^{1/3}$. Substituting for the constants, the following expression was obtained (see Section 4.1):

$$F_{(H)} = \frac{0.23 + [H^+]}{1.6 + 1.7[H^+]} \times 10^{-5} \qquad (4.2.2\text{-}5)$$

The values of $(F_{(H)})^{1/3}$ at different acid concentrations were calculated, and the quantum yields plotted as a function

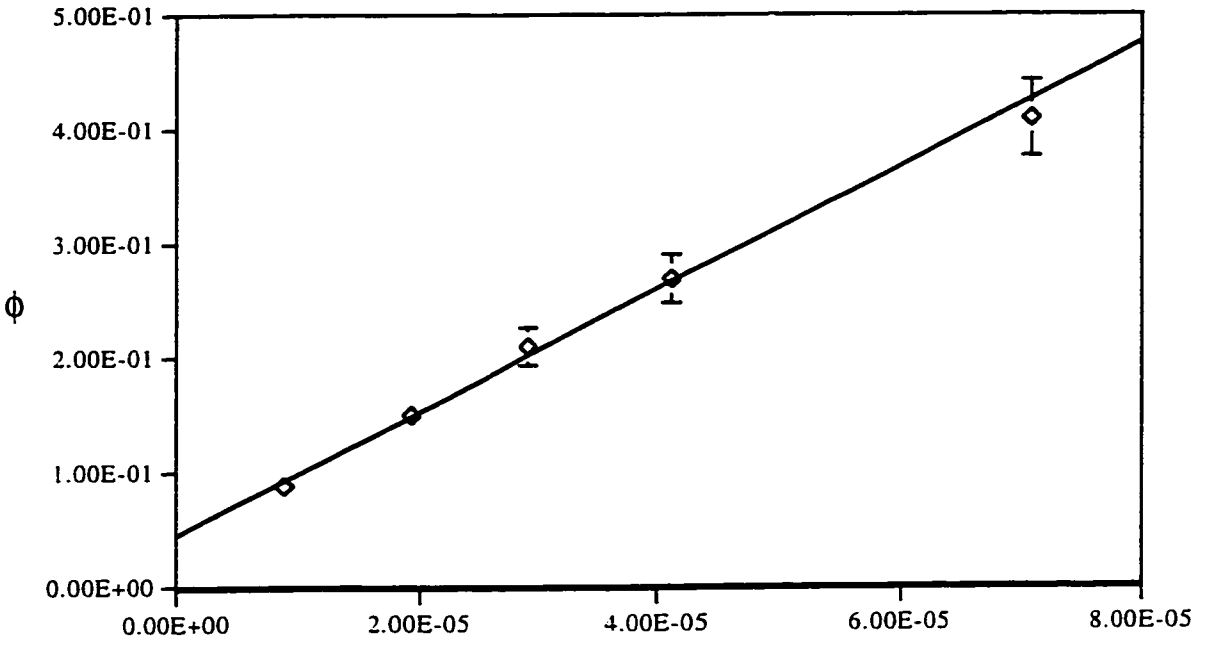

Figure 4.2.2-1. Effect of isobutane concentration on the t-butanol quantum yield in the presence of peroxydisulfate.
$[UO_2^{2+}]$ = 33.8 mM; pH = 0.95 ($HClO_4$); $[K_2S_2O_8]$ = 14.3 mM; V_{irrad} = 95.8 mL; T = 25 °C; I = 1.28 x 10^{-6} Einstein/L·s; λ_{irr} = 415 nm.

Curve fitting equation:

$$y = 5385.871x + 0.045 \quad r^2 = 0.995$$

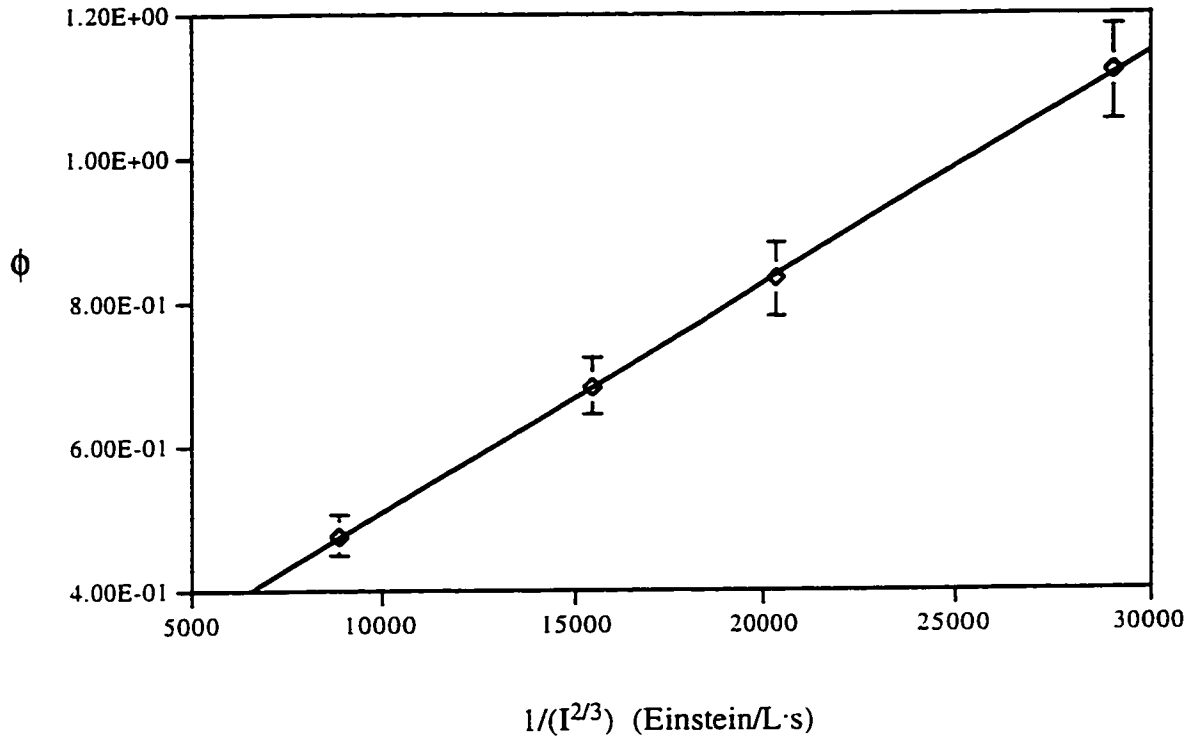

Figure 4.2.2-2. Effect of light intensity on the t-butanol quantum yield in the presence of peroxydisulfate.
$[K_2S_2O_8]$ = 14.3 mM; $[UO_2^{2+}]$ = 36.9 mM; $[BH]_{average}$ = 0.84 mM; pH = 0.95 ($HClO_4$); V_{irrad} = 103.2 mL; T = 25 ± 0.15 °C; λ_{irr} = 415 nm; Millipore water. Isobutane was bubbled for 30 min before irradiation and continuously bubbled during irradiation.

Curve fitting equation:

$$y = 3.19E\text{-}05x + 1.89E\text{-}01 \quad r^2 = 1.00E+00$$

of $(F_{(H)})^{1/3}$ in **Figure** 4.2.2-3. As expected, the quantum yield is a linear function of $(F_{(H)})^{1/3}$.

The relationship of quantum yield with $[S_2O_8^{2-}]^{1/3}$ is also close to a straight line as expected (**Figure** 4.2.2-4).

4.3 Photolysis of Cyclopentane

When an aqueous solution of UO_2^{2+} + CpH_2 system was irradiated, CpHOH and CpO were found to be the main products. In the absence of oxygen, CpHOH was first produced and then CpO appeared (**Figure** 3.3.2-5). The *initial* quantum yields of CpHOH and CpO are 0.086 and zero, respectively. The *initial* quantum yield is the production rate at time approaching zero. In the following, the abbreviations CpH_2, CpHOH, CpO, $CpeH_2$, CpeHOH and CpeO are used to represent cyclopentane, cyclopentanol, cyclopentanone, cyclopentene, 2-cyclopenten-1-ol and 2-cyclopenten-1-one, respectively.

The mechanism of production is proposed to be similar to that for the isobutane system, except that now a ketone as well as an alcohol are being formed:

$$*[H_2OUO_2^{2+}] + CpH_2 \longrightarrow *[H_2OUO_2CpH_2^{2+}] \qquad (4.3\text{-}1)$$

$$*[H_2OUO_2CpH_2^{2+}] \longrightarrow UO_2^{+} + CpH\cdot + H_3O^{+} \qquad (4.3\text{-}1a)$$

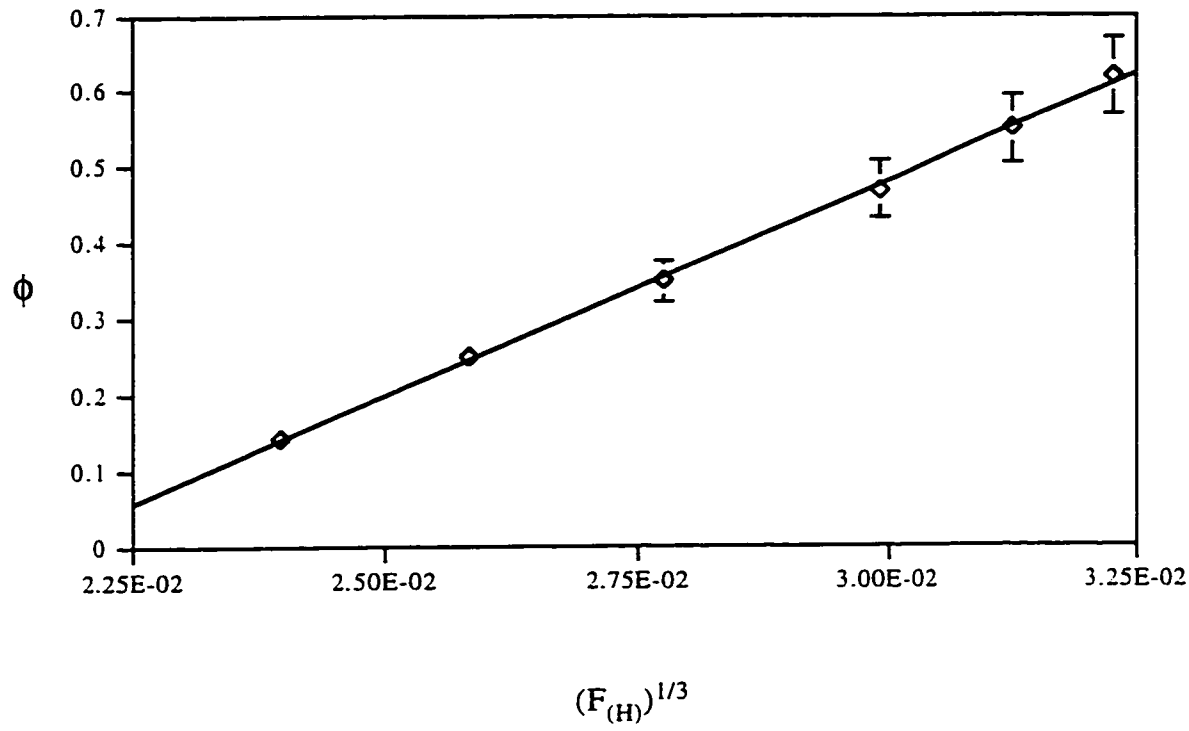

Figure 4.2.2-3. Effect of acid function $F_{(H)}$ on the t-butanol quantum yield in the presence of peroxydisulfate.

$$F_{(H)} = (0.23 + [H^+]) \times 10^{-5} / (1.6 + 1.7 \times [H^+])$$

Curve fitting equation:

$$y = 5.64E+01x - 1.21E+00 \quad r^2 = 9.99E-01$$

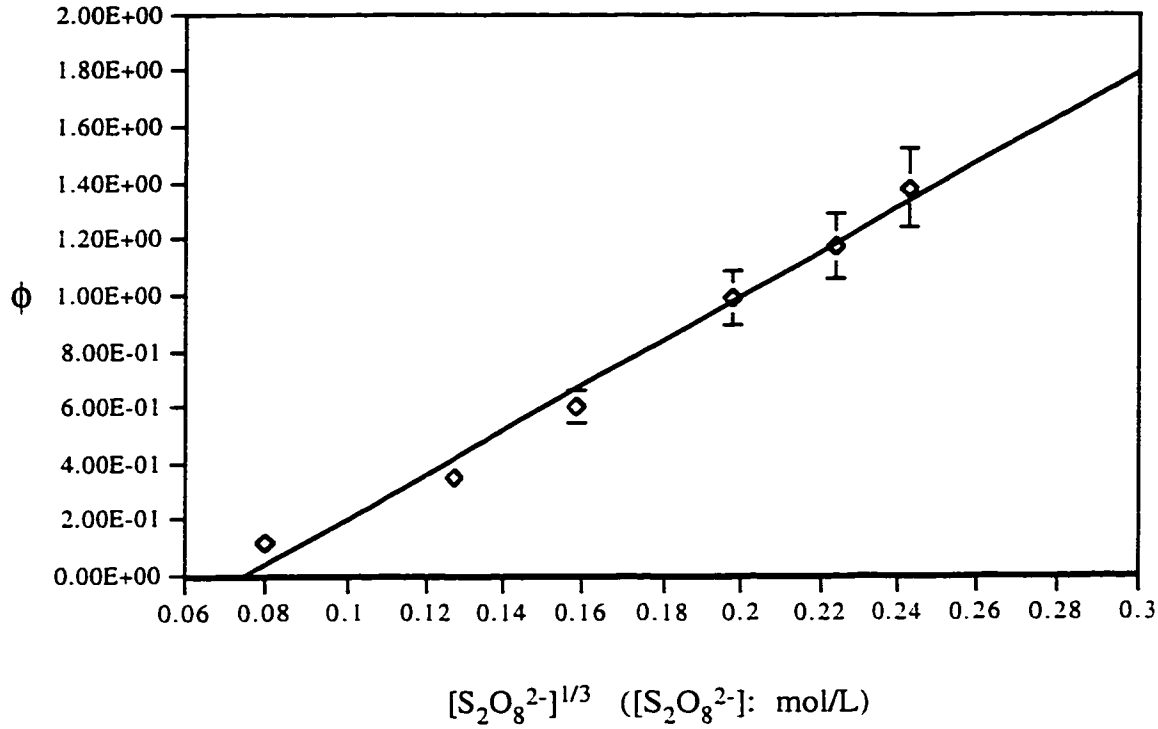

Figure 4.2.2-4. Effect of concentration of peroxydisulfate on the t-butanol quantum yield.
$[UO_2^{2+}]$ = 34.8 mM; pH=0.95 ($HClO_4$); $[BH]_{average}$= 0.80 mM; T = 25 °C; I = 2.11 x 10^{-7} Einstein/L·s; λ_{irr}=415 nm.

Curve fitting equation:

$y = 7.96E+00x - 5.98E-01 \quad r^2 = 9.86E-01$

$$*[H_2OUO_2CpH_2^{2+}] \longrightarrow UO_2^{2+} + CpHOH \qquad (4.3\text{-}1b)$$

$$*[H_2OUO_2CpH_2^{2+}] \longrightarrow UO_2^{2+} + CpH_2 + H_2O + heat \qquad (4.3\text{-}1c)$$

$$UO_2^{2+} + CpH\cdot + H_2O \longrightarrow UO_2^{+} + CpHOH + H^{+} \quad (major) \quad (4.3\text{-}2a)$$

$$UO_2^{2+} + CpH\cdot \longrightarrow UO_2^{+} + CpeH_2 + H^{+} \quad (minor) \quad (4.3\text{-}2b)$$

At higher concentrations of cyclopentanol, abstraction of an α-hydrogen by CpH· to form cyclopentane is also significant.

The production of CpO, as shown in **Figure** 3.3.2-5 suggests the possible oxidation of CpHOH:

$$*UO_2^{2+} + CpHOH + 2H^{+} \longrightarrow U^{4+} + CpO + 2H_2O \qquad (4.3\text{-}3)$$

Figure 3.3.1-5 shows the photoproduction of CpO from CpHOH. CpO can also be further oxidized but the oxidation rate is much lower than that for the oxidation of CpHOH. This point is shown in **Figure** 3.3.1-6, as the rate of loss of CpHOH is slightly higher than the rate of formation of CpO.

In the presence of oxygen, the major product is CpO rather than CpHOH (**Figure** 3.3.1-1), and the *initial* quantum yields of CpHOH and CpO are now about the same (**Figure** 3.3.1-3). This means that CpO is also produced very early in

the reaction. These results indicate a different CpO production mechanism from that in the absence of oxygen.

The mechanism proposed is as follows: oxygen is reported not to quench the $*UO_2^{2+}$ and it reacts very fast with the free radical CpH·:[149,172,173]

$$CpH\cdot + O_2 \longrightarrow CpHOO\cdot \qquad (4.3\text{-}4)$$

$k = 4.9 \times 10^{10}\ M^{-1}s^{-1}$

$$2CpHOO\cdot \longrightarrow CpHOOOOHCp \qquad (4.3\text{-}5)$$

$2k = 1.5 \times 10^{7}\ M^{-1}s^{-1}$

CpHOOOOHCp is not stable and decomposes to form the ketone:[174]

$$CpHOOOOHCp \longrightarrow CpO + CpHOH + O_2 \qquad (4.3\text{-}6)$$

$$CpHOOOOHCp \longrightarrow 2CpO + H_2O_2 \qquad (4.3\text{-}7)$$

$$CpHOOOOHCp \longrightarrow \text{Ring-opened products} \qquad (4.3\text{-}8)$$

Cyclopentanol is oxidized to ketone by the following mechanism:[175,176,177,178]

$$*UO_2^{2+} + CpHOH \longrightarrow UO_2^{+} + \cdot CpOH + H^{+} \qquad (4.3\text{-}9)$$

$$\cdot CpOH + O_2 \longrightarrow CpO + HO_2 \qquad (4.3\text{-}10)^{179}$$

Here, HO_2 is formed and is the main source for the production of $UO_2(O_2)$, which will be discussed in the next Section. In the isobutane system, the precipitate is more difficult to form than in the alcohol system. This could be due to the absence of a reaction similar to (4.3-10), as t-butanol has no α-hydrogen and therefore formation of a free radical is difficult.

HO_2 can partake in the following reactions:[180,181]

$$2HO_2 \longrightarrow H_2O_2 + O_2 \qquad (4.3\text{-}11)$$
$$k = 1.0 \times 10^7\ M^{-1}s^{-1}$$

$$HO_2 + UO_2^{2+} \longrightarrow [U(VI)\cdot HO_2]^{2+} \qquad (4.3\text{-}12)$$

$$[U(VI)\cdot HO_2]^{2+} \longrightarrow H_2O_2 + O_2 + UO_2^{2+} \qquad (4.3\text{-}13)$$
$$k = 1.5 \times 10^5\ M^{-1}s^{-1}$$

Cyclopentane has a higher quenching constant than isobutane. The quenching constant for cyclopentane k_{qCp} is measured to be $7.5 \times 10^7\ M^{-1}s^{-1}$, and if $k_0 = 4.5 \times 10^5\ M^{-1}s^{-1}$ is used, then F_{qCp} can be estimated at [Cp] = 1.1 mM as follow:

$$F_{qCpH_2} = \frac{k_{qcp}[CpH_2]}{k_0 + k_{qcp}[CpH_2]} = 0.15 \qquad (4.3\text{-}14)$$

If we assume that the mechanism in the cyclopentane system is similar to that in isobutane system and still use k_0 for k_T, as in equation (4.1.2-11), then the obtained quantum yield is 0.086 at $[CpH_2]$ = 1.1 mM and the quenching percentage of CpH_2 to $*UO_2^{2+}$ is 15%, the percentage of $*[H_2OUO_2 \cdot CpH_2^{2+}]$ (CpHOH%) reacting by reactions (4.3-1a) and (4.3-1b) can be estimated as below (CpH· will leads to BOH):

$$\phi = 15\% \times CpHOH\% \quad \text{or} \quad CpHOH\% = 0.086/0.15 = 57\%$$

For isobutane, this value is 48%. It seems that this ratio for different hydrocarbons is not much different. This indicates that the ratio of $k_a/(k_a + k_h + k_{nc})$ is about the same for different systems (see equations (4.1.2-4a) and (4.1.2-4c)). When the light intensity increases, irradiation produces a precipitate, which will be discussed in Section 4.4.

UO_2^{+} and superoxide O_2^{-} are proposed to be the species responsible for the formation of the precipitate. In order to prevent the formation of the precipitate, Ag^{+}, Fe^{3+} and Cu^{2+} were investigated. All the ions can oxidize UO_2^{+}. Fe^{3+} and Cu^{2+} can also catalyze the decomposition of superoxide. In addition, Cu^{2+} has a remarkable feature that it can react rapidly with alkyl radicals. Ag^{+} and Fe^{3+} were found to be

ineffective in preventing the formation of the precipitate, while Cu^{2+} is effective.

As well, the presence of copper ion leads to a new substance, and this has been identified as "2-cyclopenten-1-one" (CpeO). Small amounts of $CpeH_2$ and CpeHOH were also detected. In this case, a much lower concentration of CpO is obtained than that in the absence of copper ion (**Figures** 3.3.2-1 and 3.3.2-2). From these two figures, it can be seen that the rates of production of CpeO and CpHOH at different copper ion concentrations, are about the same, but different for CpO. It seems that an induction period accompanies the production of CpeO. When CpO is used as the starting substance, CpeO is also obtained and the rate of production is almost equal to the loss of CpO (**Figure** 3.3.2-4). As CpO can be oxidized to other substances even in the absence of copper ion, the similar magnitudes of the rates means that, in the presence of the copper ion, other reaction processes are strongly inhibited. From **Figure** 3.3.1-3, it can be seen that higher concentration of CpHOH, hinders the production of CpeO. This is expected from following discussion.

Cu^{2+} can form a complex with a free alkyl radical which can then undergo either β-proton elimination or electron transfer.[182] The β-proton elimination results in an alkene and electron transfer gives a positive alkyl group which in aqueous media yields an alcohol. In our system, the following reactions are proposed when copper was added,:

$$CpH\cdot + Cu^{2+} \longrightarrow CpHCu^{II} \qquad (4.3\text{-}15)$$

$$CpHCu^{II} \longrightarrow CpeH_2 + Cu^{+} + H^{+} \quad \text{(minor)} \qquad (4.3\text{-}16)$$

$$CpHCu^{II} \longrightarrow CpH^{+} + Cu^{+} \quad \text{(major)} \qquad (4.3\text{-}17)$$

$$CpH^{+} + H_2O \longrightarrow CpHOH + H^{+} \qquad (4.3\text{-}18)$$

Just as in the case of other alcohols, the reaction of CpHOH with $*UO_2^{2+}$ could occur by α-hydrogen abstraction followed by reaction with copper ion:

$$\cdot CpOH + Cu^{2+} \longrightarrow CpOHCu^{II} \qquad (4.3\text{-}19)$$

$$CpOHCu^{II} \longrightarrow CpeOH + Cu^{+} + H^{+} \quad \text{(minor)} \qquad (4.3\text{-}20)$$

$$CpOHCu^{II} \longrightarrow CpO + Cu^{+} + H^{+} \quad \text{(major)} \qquad (4.3\text{-}21)$$

An α-hydrogen can also be abstracted from CpO (C_5H_8O) which can then undergo the following reactions:

$$\cdot C_5H_7O + CpHOH \longrightarrow CpO + \cdot CpOH \qquad (4.3\text{-}22)$$

$$\cdot C_5H_7O + Cu^{2+} \longrightarrow C_5H_7OCu^{II} \qquad (4.3\text{-}23)$$

$C_5H_7OCu^{II} \longrightarrow CpeO + Cu^{+} + H^{+}$ (4.3-24)

The Cu^{+} produced is reoxidized to Cu^{2+} by oxygen.[183] If there is ROO· present, then reoxidation of Cu^{+} can also occur rapidly by the reaction with the alkyl peroxide free radical:

$Cu^{+} + ROO\cdot \longrightarrow Cu^{2+} + ROO^{-}$ (4.3-25)[46]

$k = 1 \times 10^{9}\ M^{-1}s^{-1}$

Cyclopentanol reacts more effectively with $*UO_2^{2+}$ than cyclopentanone, and the ·CpOH radical produced reacts with Cu^{2+}. If tertiary butyl alcohol is added to the solution, it predominates over CpO in the reactions with $*UO_2^{2+}$. The CpO produced has less of a chance to react with $*UO_2^{2+}$ and to undergoe further reactions (4.3-23). **Figure** 3.3.2-3 supports this conclusion and it can be seen that formation of cyclopentenone is inhibited when cyclopentanol is present.

The level of cyclopentanone is higher with lower copper ion concentration (**Figures** 3.3.2-1 and 3.3.2-2) and this should result from competition of reaction (4.3-22) with reaction (4.3-23).

The forgoing reactions account at least qualitatively for the occurrence of the observed products and the effects of oxygen. Because the products themselves are photoreactive, a

detailed quantitative interpretation is not feasible. A further complication is the occurrence of a yellow precipitate at higher pHs. In the next Section, we consider the nature of the yellow precipitate.

4.4 Peroxide Products

4.4.1 $[UO_2(O_2)]\cdot 2H_2O$

When the pH is higher, for example pH = 3 and there is oxygen in the solution, the irradiation of CpH_2, CpHOH or CpO produces a yellow precipitate. The analyses for uranium (**Table** 3.3.4-1), hydrogen (**Table** 3.3.4-2) and peroxide (**Table** 3.3.4-3) show that the precipitate has the formula $[UO_2(O_2)]\cdot 2H_2O$. Comparison of the IR spectra of synthesized samples and photoproduced precipitates further support this identification (**Figure** 3.3.4-1). It can be seen from this figure that the spectrum of the yellow precipitate is identical to that of the synthesized sample. They are also consistent with the results reported by Deane[184] for $[UO_2(O_2)]\cdot 2H_2O$. Although Deane did not find peaks at 810 cm^{-1} and 544 cm^{-1}, this could be due to the lower resolution of his measurement. He did not resolve as separate peaks those at 930 cm^{-1} and peak 907 cm^{-1}, but rather noticed there was a peak at 914 cm^{-1} with a shoulder. In the spectrum, peaks above 3000 cm^{-1} can be associated with the vibration of water

molecules. The peak at 1622 cm^{-1} is due to the presence of water of hydration.[185,186,187] Peaks at 930 and 863 cm^{-1} are the asymmetric and symmetric vibrations of the uranyl group, respectively.[4,187,188] These two bands are characteristic of the absorption of O=U=O, and are very sensitive to the coordination groups. Usually, the difference between these two peaks is about 75 cm^{-1}. The shoulder at 907 cm^{-1} was considered to be the asymmetric vibration of a uranyl group, one oxygen of which is hydrogen bonded to a water molecule.[184,187,186] The peak at 810 cm^{-1} is the symmetric stretching vibration of peroxide O-O and that at 667 cm^{-1} is the asymmetric vibration of U-peroxide (peroxide as a rigid group).[26,189] Bands at 2413 and 2221 cm^{-1} may have some association with the peroxide group because they are not found in the spectra of UO_3.[184]

When the precipitate forms in irradiated solution, hydrogen peroxide is always detected in the solution at a concentration of about 1×10^{-5} M. However, in the presence of copper ion in solution, no precipitate was found. When a high light intensity was used, the precipitate appeared again even in the presence of copper ion. This indicates that there are competition reactions for a species that is responsible for the formation of the precipitate. To study the mechanism of precipitate formation, an understanding of the role(s) of copper ion is important.

Copper plays an essential role in some biological and chemical processes. It is an effective catalyst for

converting O_2^- to O_2^{2-} and O_2, but the mechanism of this catalytic process is still open to question.[184,190,191,192]

Copper is a good catalyst for the decomposition of O_2^-. There are several mechanisms proposed. The copper enzyme superoxide dismutase catalyzes the disproportionation of O_2^- was proposed as follows where E refers to an enzyme:[193]

$$E\text{-}Cu^{2+} + O_2^- \longrightarrow E\text{-}Cu^{+} + O_2 \qquad (4.4.1\text{-}1)$$

$$E\text{-}Cu^{+} + O_2^- + 2H^+ \longrightarrow E\text{-}Cu^{2+} + H_2O_2 \qquad (4.4.1\text{-}2)$$

Catalytic processes involving Cu(III) or Cu(0) are also proposed:[190,194]

$$Cu(II) + O_2^- + 2H^+ \longrightarrow Cu(III) + H_2O_2 \qquad (4.4.1\text{-}3)$$

$$Cu(III) + O_2^- \longrightarrow Cu(II) + O_2 \qquad (4.4.1\text{-}4)$$

or:

$$Cu(I) + O_2^- \longrightarrow Cu(0) + O_2 \qquad (4.4.1\text{-}5)$$

$$Cu(0) + O_2^- + 2H^+ \longrightarrow Cu(I) + H_2O_2 \qquad (4.4.1\text{-}6)$$

Cu(I) was considered to be a good agent for complexing O_2 to form CuO_2^{+}.[190,195,196] This species can abstract a hydrogen atom:

$$CuO_2^{+} + RH \longrightarrow (CuO_2H)^{+} + R\cdot \longrightarrow Cu^{2+} + HO_2^{-} + R\cdot \quad (4.4.1\text{-}7)$$

In our experiments, copper ion is able to prevent the formation of $UO_2(O_2)$, but when the precipitate has already been formed, addition of copper ion does not effectively diminish it. Thus copper ion appears to react with some intermediate(s) which is associated with the formation of the precipitate. The following reaction, which is well known is one of the pathways for precipitate formation:[197]

$$UO_2^{2+} + H_2O_2 \rightleftharpoons UO_2(O_2)(s) + 2H^{+} \quad (4.4.1\text{-}9)$$

$K = 1 \times 10^2$

As described previously, both UO_2^{2+} and H_2O_2 have equilibria reactions with UO_2^{+} and O_2^{-}, respectively. The initial step for the above reaction could be:

$$UO_2^{+} + O_2^{-} \longrightarrow UO_2(O_2) \quad (4.4.1\text{-}10)$$

Superoxide anion O_2^{-} may come from reaction (4.3-10) and from H_2O_2 that can be formed from reaction (4.3-7). It can also come from:[4c,198]

$$UO_2^{+} + O_2 \longrightarrow UO_2^{2+} + O_2^{-} \qquad (4.4.1\text{-}11)$$

Furthermore, H_2O_2 and O_2^{-} are interrelated by disproportionation. On the other hand, both UO_2^{+} and O_2^{-} have the acid-favored disproportionations:[199,200]

$$2O_2^{-} + H^{+} \rightleftharpoons O_2 + HO_2^{-} \qquad (4.4.1\text{-}12)$$

$K = 2.5 \times 10^{8}$

or:

$$O_2^{-} + H^{+} \rightleftharpoons HO_2 \qquad (4.4.1\text{-}13)$$

$K = 6.3 \times 10^{8}$

$$2HO_2 \longrightarrow O_2 + H_2O_2 \qquad (4.4.1\text{-}14)^{201}$$

$K = 8.6 \times 10^{5}$

$$2UO_2^{+} + 4H^{+} \rightleftharpoons UO_2^{2+} + U^{4+} + 2H_2O \qquad (4.4.1\text{-}15)$$

$K = 1.7 \times 10^{6}$

When the pH is low, both O_2^{-} and UO_2^{+} concentrations are greatly decreased and no precipitate appears. At higher pH, the precipitate appears. In the presence of copper ion, UO_2^{+} can be oxidized to UO_2^{2+}:[40,46]

$UO_2^{\bullet}$ + Cu^{2+} ⟶ UO_2^{2+} + Cu^{+} (4.4.1-16)

$k = 915\ M^{-1}s^{-1}$

As previously described, Cu^{2+} is also a very effective catalyst for decomposing superoxide:[25]

Cu^{2+} + O_2^{-} ⟶ Cu^{+} + O_2 (4.4.1-17) [202]

$k = 1.7 \times 10^9\ M^{-1}s^{-1}$

Cu^{2+} + HO_2 ⟶ Cu^{+} + O_2 + H^{+} (4.4.1-18) [192]

$k = 1 \times 10^8\ M^{-1}s^{-1}$

At the same time, copper ion also retards the production of $UO_2^{\bullet}$. The reaction of Cu^{2+} with an alkyl radical is very fast ($k > 10^9\ M^{-1}s^{-1}$)[203] and likely dominates over the reaction of UO_2^{2+} with the alkyl radical. It can also hinder the production of O_2^{-} and H_2O_2 by competing with O_2 in reacting with alkyl radical ((4.3-5) and (4.3-11)). It was reported that Cu^{2+} is 200 times faster than O_2 in reactions with alkyl radicals.[204]

Cu^{+} formed by the above processes can be reoxidized to Cu^{2+} by alkyl radicals (or by molecular oxygen):[204]

Cu^{+} + R· ⟷ CuR^{+} (4.4.1-19)

$$CuR^{\cdot} + H^{+} \longrightarrow Cu^{2+} + \text{products} \qquad (4.4.1\text{-}20)$$

It can also be oxidized by O_2^- or HO_2:[202]

$$Cu^{+} + O_2^- \longrightarrow Cu^{2+} + H_2O_2 + 2OH^- \qquad (4.4.1\text{-}21)$$

$k > 10^9\ M^{-1}s^{-1}$

$$Cu^{+} + HO_2 \xrightarrow{H^+} Cu^{2+} + H_2O_2 \qquad (4.4.1\text{-}22)$$

$k = 10^{10}\ M^{-1}s^{-1}$

Hydrogen peroxide can also be decomposed catalytically to by Cu(II).[205]

The above discussion shows that the formation of the precipitate is due to molecular oxygen. The oxygen oxidizes organic free radical to produce superoxide O_2^-, which reacts with the photoproduced UO_2^+ and they form the precipitate $UO_2(O_2)$. In the presence of copper ion, the formation of the precipitate is hindred because 1) Cu^{2+} competes with oxygen to react with organic free radicals to prevent the production of superoxide; 2) Cu^{2+} catalyzes the disproportionation of superoxide to oxygen and hydrogen peroxide; 3) Cu^{2+} oxidizes UO_2^+ to UO_2^{2+}. Fe^{3+} is an effective oxidant for UO_2^+ and it is also a good catalyst for the decompositon of the superoxide,[206] but the precipitate still appears with the Fe^{3+}. This means that reason 1) is the most important one.

4.4.2 $[UO_2(O_2)_n]^{m-}$ and Polymer

As mentioned in the last Chapter, long irradiation times of the cyclopentane system with high light intensity turns the color of the solution to a deep yellow. From the nature of the yellow substance and comparison with synthesized samples, it is identified $[UO_2(O_2)_n]^{m-}$. The main component is likely to be $[UO_2(O_2)_3]^{4-}$.

Figure 3.3.6-1 and **Figure** 3.3.6-2 are the IR spectra of synthesized $K_4[UO_2(O_2)_3]$ and $Na_4[UO_2(O_2)_3]$. The absorption bands are consistent with those reported by Alcock.[26] In **Figure** 3.3.6-1, absorption bands of 756 and 696 cm^{-1} are associated with the asymmetric and symmetric vibrations of O=U=O, respectively. The band of 804 cm^{-1} is the absorption of the U-peroxide bond. The absorption of O-O group is at about 880 cm^{-1} for asymmetric vibration and 831 cm^{-1} for symmetric vibrations.

Figure 3.3.6-3 is the IR spectrum of the deep yellow substance of the photoproduced sample. The main interference in our yellow sample is $KClO_4$. Taking into account the spectrum of $KClO_4$ (Figure 3.3.6-4), we can see that these two spectra for the synthesized sample and the photoproduced sample are very close. All peaks associated with the peroxide are also found in the spectrum of the photoproduced

sample. The bands from about 1350 cm^{-1} to 1600 cm^{-1} in both samples can be associated with hydration.[197]

The soluble yellow substance may involve the following reaction:[207]

$$UO_2^{2+} + H_2O_2 \rightleftharpoons UO_2(O_2)(s) + 2H^+ \qquad (4.4.1\text{-}9)$$

$K = 1 \times 10^2$

It seems that the produced precipitate further reacts with H_2O_2 to form $UO_2(O_2)_2^{2-}$. Another possibility is the reaction:

$$UO_2(O_2) + O_2^- \longrightarrow UO_2(O_2)_2^- \qquad (4.4.2\text{-}1)$$

$$UO_2(O_2)_2^- + O_2^- \longrightarrow UO_2(O_2)_3^{3-} \qquad (4.4.2\text{-}2)$$

A sticky mixture is found when the solution is further irradiated (more than 8 hours). This mixture contains no uranium and it can be dissolved in organic solvents. This suggests an organic polymer. It is probably one of the following types of structures:

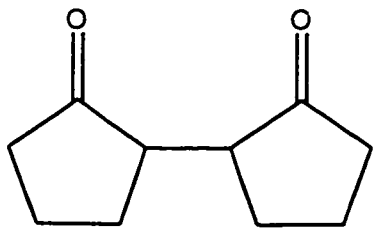

and

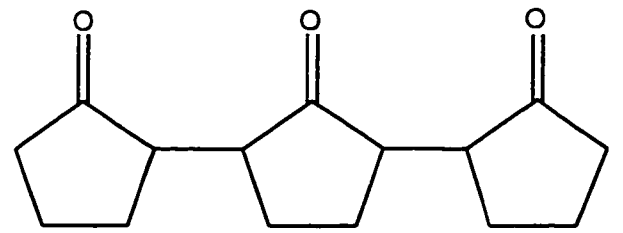

For the two and three unit polymers, the mass ratio of H/C are 0.117 and 0.111, respectively. These values are very close to our measured value of 0.111. The CpO is the main product in the irradiation and its β-hydrogen atom can be abstracted by $^{*}UO_2^{2+}$, so the above proposed structures seem reasonable.

4.5 Cyclohexane and n-Pentane

Cyclohexane and pentane can be also photooxygenated. In the presence of oxygen, the initial quantum yields for cyclohexanol and cyclohexanone are 0.028 ± 0.003 and 0.027 ± 0.003, respectively. These values are about half of those found for CpO and CpHOH. The lower values for the cyclohexane case could be mainly due to the differences of solubility and to the different C-H bond strength. The solubility of cyclohexane under our conditions (0.61 mM) is about 1/3 that for cyclopentane (1.74 mM). However, it is found that in the cyclohexane system, different sources of the cyclohexane give different quantum yields. Older sources previously exposed to oxygen tend to have larger quantum yields. Thus some reactive impurity(ies) is present, and maybe traces of peroxides formed by exposure to air.

n-Pentane has primary and secondary hydrogen atoms in a 1:1 ratio. Its solubility is 0.58 mM and the quantum yield

is about 0.008. The main products are alcohols and ketones arising from attack on the secondary hydrogen. This selectivity presumeably reflects the stronger primary C-H bond as opposed to the weaker secondary C-H bond. Peroxydisulfate can increase the quantum yield of the pentane to 0.03. The mechanism may be similar to that of the isobutane system.

[140] Bell, J. T.; Billings, M. R. *J. Inorg. Nucl. Chem.* **1975**, *39*, 631.

[141] Patai, S.; Rappoport, Z. *The Chemistry of Alkanes and Cycloalkanes* ; Wiley: New York, 1992.

[142] Duan, Y.; Xu, H.; Zhang. X.; Hu, J.; Zhou, Z.; Zhang, R. *He Huaxue Yu Fangshe Huaxue* **1984**, *6(3)*, 125.

[143] Butter, K. R.; Kemp, T. K. *J. Chem. Soc., Dalton Trans.* **1984**, 923.

[144] Greatorex, D.; Hill, R. J.; Kemp, T. J.; Stone, T. J. *J. Chem. Soc., Faraday 1* **1974**, *70*, 216.

[145] Burrows, H. D.; Greatorex, D.; Kemp, T. J.; Stone, T. J. *J. Am. Chem. Soc.* **1971**, *93*, 2539.

[146] Kraus, J. W.; Calvert, J. G. *J. Am. Chem. Soc.* **1957**, *79*, 5921.

[147] Cvelanovic, R. J.; Paraskevopoulos, G. J. *J. Phys. Chem.* **1977**, *81*, 2598.

[148] Maillard, B.; Ingold, U.; Scaiano, J. C. *J. Am. Chem. Soc.* **1983**, *105*, 5095.

[149] Piechowsk, M. V.; Thelen, M. J.; Hoigne, J.; Bühler, R. E. *Ber Bunsenges Phys. Chem.* **1992**, *96*, 1448.

[150] Thomas, J. R. *J. Am. Chem. Soc.* **1965**, *87*, 3935.

[151] Williams, A. L. Oberright, E. A.; Brooks, T. W. *J. Am. Chem. Soc.* **1956**, *8*, 1190.

[152] Walling, C.; Padwa, A. *J. Am. Chem. Soc.* **1963**, *83*, 1593.

[153] Schuchmann, M. N.; Sonntag, C. V. *J. Phys. Chem.* **1979**, *83*, 780.

[154] Formosinho, S. J.; Miguel, M. G. M; Burrows, H. D. *J. Chem. Soc., Faraday Trans.1* **1984**, *80*, 1717.

[155] Benson, P.; Cox, A.; Kemp, T. J.; Saltana, Q. *Chem. Phys. Lett.* **1975**, *35*, 195.

[156] Balzani,V; Carassiti, F. *Uranyl Compounds*; Academic: New York, 1970; Chapter 15.

[157] Selbin, J.; Ortego, J. D. *Chem. Rev.* **1969**, 657.

[158] Sakuraba, S; Matsushima, R. *Bull. Chem. Soc. Jpn.* **1970**, *43*, 2359.

[159] Personal communication from P. sedlák.

[160] Azenha, M. E. D. G.; Burrows, H. D.; Formosinho, S. J.; Miguel, M. G. M.; Daramanyan, A. P.; Khudyakov. *J. Luminescence* **1991**, *48&49*, 522.

[161] Park, Y. Y.; Sakai. Y. *J. Chem. Soc., Faraday Trans. 1*, **1990**, *86*, 55.

[162] Wang, Z. L.; Zheng, D.; Hue, J. C. *J. Phys. Chem.* **1990**, *6(2)*, 139.

[163] Personal communication from T Bergfeldt.

[164] Elliot, A. J.; Padamshi, S.; Pika, T. *Can. J. Chem.* **1986**, *64*, 314.

[165] Kelm, M.; Lilie, J.; Henglein, A.; Janata, E. *J. Phys. Chem.* **1974**, *78*, 882.

[166] Waltz, W. L; Lilie, J.; Xu, X.; Sedlák, P.; Möckel, H. (submitted).

[167] Yamase, T.; Kurozumi, T. *J. Chem. Soc., Dalton Trans.* **1983**, 2205.

[168] Ward, M. D.; Brazdil, J. F.; Greselli, R. K. *J. Phys. Chem.* **1984**, *88*, 4210.

[169] Huie, R.E.; Clifton, C.L. *Int. J. Chem. Kinet.* **1989**, *21*, 611.

[170] Ross, A. B.; Neta, P. *Natl. Stand. Ref. Data Ser. (U. S., Natl. Bur. Stand)* **1982**, NSRDS-NBS70.

[171] Dogliotti, L.; Hayon, E. *Phys. Chem.* **1967**, *8*, 2511.

[172] Kropp, J. L. *J. Chem. Phys.* **1967**, *46*, 843.

[173] Wilshire, J; Sawyer, D. T. *J. Am. Chem. Soc.* **1979**, 105.

[174] Zegota, H.; Schuchmann, M. N.; Sonntag, C.. *J. Am. Chem. Soc.* **1984**, *88*, 5589.

[175] Suib, S. L.; Janguay, J. F.; Occelli, M. L. *J. Am. Chem. Soc.* **1986**, *108*, 6972.

[176] Carter, W. P. L. *J. Phys. Chem.* **1979**, *83*, 2305.

[177] *The Chemistry of Peroxides;* Patai, S., Ed.; Hebrew University: Jerusalem, 1983; pp 429-456.

[178] Meisel, D.; Llan, Y. A.; Czapski, G. *J. Am. Chem. Soc.* **1973**, *95*, 4148.

[179] Matthews, R. W. *Pure & Appl. Chem.* **1992**, *64(9)*, 1285.

[180] Meisel, D.; Llan, Y. A.; Czapski, G. *J. Phys. Chem.* **1974**, *78*, 779.

[181] Meisel, D.; Llan, Y. A.; Czapski, G. *J. Phys. Chem.* **1974**, *78*, 2330.

[182] Kochi, J. K. *Free Radical*; Wiley: New York, 1974; Chapter 11.

[183] Mi, L.; Zuberbuhler, A. D. *Helv. Chim. Acta.* **1991**, *74*, 1679.

[184] Deane, A. M., *J. Inorg. Nucl. Chem.* **1961**, *21*, 238.

[185] Colentz, W. W. *Phys. Rev.*, **1905**, *20*, 252.

[186] Colentz, W. W. *Phys. Rev.*, **1906**, *23*, 125.

[187] Demarco, R.E. *J. Am. Chem. Soc.* **1959**, *81*, 4167.

[188] McGlynn, S. P. *J. Chem. Physics,* **1961**, *35*, 105.

[189] Westland, A. D. *Inorg. Chem.* **1981**, *20*, 3992.

[190] Davies, J. A.; Watson, P. L.; Greenberg, A.; Liebman, J. F. *Selective Hydrocarbon Activation;* VCH: New York, 1990; pp 337-366.

[191] Jolly, W. L. *Modern Inorganic Chemistry;* McGraw Hill: New York, 1991; p 569.

[192] Rabani, J.; Klug-Roth, D.; Lilie, J. *J. Phys. Chem.* **1973**, *77*, 1169.

[193] Klug-Roth, D. Rabani, J. *J. Am. Chem. Soc.* **1973**, *95*, 2786.

[194] Sawyer, D. T. *Inorg. Chem.* **1986**, *25*, 2089.

[195] Balla, J. Kiss, T.; Jameson, R. F. *Inorg. Chem.* **1992**, *31*, 58.

[196] Karlin, K. D. *Prog. Inorg. Chem.* **1987**, *35*, 219.

[197] Jones, L. H. *Spectrochimica Acta* **1959**, 409.

[198] Bielski, B. H. J.; Cabelli, D. E. *Int. J. Radiat. Biol.* **1991**, *59*, 291.

[199] Bielski, B. H. J.; Cabelli, D. E.; Arudi, R. L.; Ross, A. B. *J. Phys. Chem. Ref. Data 14*, **1985**, 1041-1100.

[200] Czapski, G., Bieski, B. H. J. *J. Phys. Chem.* **1963**, *67*, 2180.

[201] Bull, C,; Mcdune, G. J.; Fee, J. A. *Am. Chem. Soc.* **1983**, 5290.

[202] Khudyakov, I. V.; Kuzmin, V. A. *Russian Chem. Rev.* **1978**, *47(1)*, 22.

[203] Maclachlan, A. *J. Phys. Chem.* **1967**, *71*, 4132.

[204] Buxton, G. V.; Sellers, R. M. *Coord. Chem. Rev.* **1977**, *22(3)*, 195.

[205] Lunák, S.; Sedlák, P. *J. Photochem. Photobiol. A: Chem.* **1992**, *67*, 1.

[206] Brown, S. B.; Jones, P.; Suggett, A. *Prog. Inorg. Chem.* **1970**, *13*, 159.

[207] Sillén, L.G.; Martell, A. E. In *Stability Constants Supplement No.1.* The Chemical Socciety: London, 1971; Part 1, p 126.

5. CONCLUSIONS AND FUTURE DIRECTION

Results presented in this work show that at room temperature and atomspheric pressure, and using visible light, the resulting excited uranyl ion $^{*}UO_2^{2+}$ is an effective species for oxygenation of all three alkane subcategories (cyclic, branched and straight chain hydrocarbons). Observed quantum yields of 0.022, 0.087 and 0.01 are found for the isobutane, cyclopentane and pentane systems, respectively.

Peroxydisulfate has been shown to be an effective amplification agent for all these processes. In the presence of 1 mM peroxydisulfate, the quantum yields increase 4 to 50 times for the different systems.

The quantum yield increases with increases in the alkane and the proton concentrations. In the absence of peroxidisulfate, uranyl ion concentration and light intensity have no significant influences on the quantum yield. In the presence of peroxydisulfate, decreasing light intensity increases the quantum yield, i.e., the efficiency of the process is higher at lower light intensities. Higher concentrations of peroxydisulfate favor higher quantum yields.

In the isobutane system, quantum yields higher than unity can be achieved even though only 6% of excited uranyl ions are quenched by isobutane. Quantum yields as high 1.1 have been found. After correcting for the quenching efficiency, the quantum yield at 100% quenching is expected to be 17. Since the quantum yield exceeds unity, this means that there must be thermal processes that follow the photochemical step to achieve such large amplification.

In these uranyl ion sensitized photooxidation processes, where oxygen is present and/or with peroxydisulfate (pH $\leq$ 1), no net consumption of UO_2^{2+} is detected. This means that UO_2^{2+} is being recycled and it effectively serves as a light antenna or a catalyst.

When the pH is higher, a precipitate of $UO_2O_2 \cdot 2H_2O$ can be formed. Extensive irradiation can lead to formation of other peroxo-uranium species and some substances that are likely to be organic polymers. Copper ion is an effective agent to prevent the formation of the precipitate and these peroxo-species.

Uranyl-ion sensitized photooxidation is potentially a very useful method for the oxygenation of many organic substances. Even with the low solubilities of alkanes in aqueous solution, it is a highly effective approach. Moreover, there are still other ways to increase the efficiencies of this system as described below.

Isobutane is a gas at room temperature and thus its solubility can be readily increased by a moderate increase

in pressure. With liquid alkanes, solubility presents a more significant limitation. Thus, in order to achieve a higher quenching efficiency, one might consider using a solubilizing agent or the use of two or more phases (aqueous-nonaqueous).

The strength of the C-H bond significantly affects the quantum yield. A small change in the strength of the C-H bond will result in a great change in the quantum yield. It is known that some metal ions, such as Pd(II),[134] Co(II),[208] Rh, Ir and Pt[209] can activate the C-H bond and have been employed in some thermal oxidation processes of hydrocarbons to decrease the otherwise high temperatures required. Thus, some metal ions or other compounds could be investigated to see if they can be used in these photochemical processes.

Coordination of ligands in the equatorial plane of the uranyl ion has a major effect on the reduction potential of excited uranyl ion. For example, $^{*}UO_2^{2+}$ coordinating with O atom has a higher potential (2.88 V) than that coordinated with F^- (2.4 V). The excited uranyl ion coordinated with F can oxidize alcohols but not alkanes, while that coordinated with O atom can oxidize both. It seems that using less electronegative atoms as coordination ligands favors the oxidation ability of $^{*}UO_2^{2+}$. Thus the studies of other solvent systems, other ligand complexes of uranyl ion or some solid phases of uranyl compounds could be another useful direction to explore. Some of these efforts have been started. For example, aerogel doped uranyl ion,[210] polymolybdate with

uranyl ion,[111] uranyl-exchanged zeolites[211] and $UO_2(O_2)$[212] systems have been reported for this purposes.

Even though peroxydisulfate can not oxidize alkanes at room temperature, or under the irradiation of visible light in the absence of uranyl ion, it can do so in the presence of uranyl ion and irradiation. Moreover, it has a significant amplification role. This role is proposed to come from the formation of the highly active species SO_4^- by oxidation of organic free radicals or other reducing agents that are produced during the irradiation. Further study of other amplification agents could also be useful, notably H_2O_2 has been studied recently. Even though H_2O_2 can oxidize an alkane with visible irradiation, its absorption coefficient in the visible range is very small. The system containing both H_2O_2 and UO_2^{2+} could supply some new information for the mechanism.

To fully explore the potential applications of these photooxygenation processes, a more complete and comprehensive understanding of the mechanism is needed. In view of this, the following directions should be further investigated:

1. The production of UO_2^+ and $U^{4+}(aq)$ in the oxidation processes should be further studied. These two species correspond to $1e^-$ and $2e^-$ mechanisms, respectively. We find the amplification effect of peroxydisulfate to be different with different alkanes. In our proposed mechanism, only the $1e^-$ process favors the amplification because of its free

radical nature. Different ratios of these two processes may signal different amplification effects.

2. The intermediate(s) and the associated micro-processes should be further investigated. The structure and the state of the intermediate(s) is still unknown. We propose two pathways, one being the interaction of the uranium atom with a carbon atom of alkanes(U-R) and the other being the interaction of an uranium atom with the hydrogen atom of alkanes (U-H).

3. In the photooxidation of alkanes at higher pHs, H_2O_2 is found. H_2O_2 can precipitate UO_2^{2+} and can also photo-oxidize alkanes. Copper ion is found to be effective in preventing the formation of a precipitate and in leading to formation of an alkene. The studies of these processes are useful for understanding the mechanism and for application purposes.

4. H_3PO_4 is an interesting system because it is found that in this system the lifetime of $*UO_2^{2+}$ increases greatly. In this system, the coordinating atom is still "O" as in HNO_3 or $HClO_4$ systems, therefore the quantum yield is expected to increase with the increased lifetime of $*UO_2^{2+}$. However, the quantum yield remains almost unchanged. Investigation of H_3PO_4 system may supply useful information about the mechanism.

[208] Goldstein, A.S.; Drago, R. S. *Inorg. Chem.* **1991**, *30*, 4506.

[209] William, R. M.; Donald, W. S. *Homgeneous Transtion Metal Catalyzed Reactions;* ACS: Washinton, DC, 1992.

[210] Carlos, C. U.S. patent 5 0330 607, 1986.

[211] Suib, S. L.; Kotapapas, A.; Psaras, D. *J. Am. Chem. Soc.* **1984**, *106*, 1614.

[212] Welch, J. T.; Seper, K. W. *Synthetic Commun.* **1984**, *14*, 933.

Appendix 1

1) Mechanism for Isobutane System in the Absence of $S_2O_8^{2-}$.

In the following equations:

$K_01 = k_{f1} + k_{nr1} + k_{+H}$;

$K_02 = k_{f2} + k_{nr2} + k_{nr3}$;

$K_03 = k_a + k_b + k_{nc}$;

$K1 = k_{f1} + k_{nr1} + k_{+H} + k_{q1}[BH]$;

$K2 = k_{f2} + k_{nr2} + k_{nr3} + k_{q2}[BH]$;

E1, E2 and E3 represent $*[H_2OUO_2^{2+}]$, $*[HOUO_2^{+}]$ and $*[H_2OUO_2 \cdot BH^{2+}]$ respectively.

The major reactions for the isobutane system are rewritten below:

$$[H_2OUO_2^{2+}] \xrightarrow{I_a.\, h\nu} *[H_2OUO_2^{2+}] \qquad (4.1.1\text{-}1)$$

(absorption) I_a = rate of light absorption

$$*[H_2OUO_2^{2+}] \xrightarrow{k_{f1}} [H_2OUO_2^{2+}] + h\upsilon' \qquad (4.1.2\text{-}1a)$$

(fluorescence emission) $(\upsilon > \upsilon')$

$$*[H_2OUO_2^{2+}] \xrightarrow{k_{nr1}} [H_2OUO_2^{2+}] + \text{heat} \qquad (4.1.2\text{-}1b)$$

(radiationless deactivation)

$$*[H_2OUO_2^{2+}] \underset{k_{-H}}{\overset{k_{+H}}{\rightleftharpoons}} *[HOUO_2^{+}] + H^{+} \qquad (4.1.2\text{-}1c)$$

(reversible)

$$*[H_2OUO_2^{2+}] + BH \xrightarrow{k_{q1}} *[H_2OUO_2{\cdot}BH^{2+}] \qquad (4.1.2\text{-}1d)$$

$$*[HOUO_2^{+}] \xrightarrow{k_{nr2}} [HOUO_2^{+}] \qquad (4.1.2\text{-}2a)$$

$$*[HOUO_2^{+}] \xrightarrow{k_{nr3}} UO_2^{+} + HO\cdot \qquad (4.1.2\text{-}2b)$$

$$*[HOUO_2^{+}] \xrightarrow{k_{f2}} HOUO_2^{+} + h\upsilon \qquad (4.1.2\text{-}2c)$$

$$*[HOUO_2^{+}] + BH \xrightarrow{k_{q2}} HOUO_2^{+} + BH \qquad (4.1.2\text{-}2d)$$

$$*[H_2OUO_2{\cdot}BH^{2+}] \xrightarrow{k_a} UO_2^{+} + B\cdot + H_3O^{+} \qquad (4.1.2\text{-}4a)$$

(1 e^- Mech.)

$$*[H_2OUO_2{\cdot}BH^{2+}] \xrightarrow{k_b} BOH + UO_2H_2^{2+} \qquad (4.1.2\text{-}4b)$$

(2 e^- Mech.)

$$*[H_2OUO_2{\cdot}BH^{2+}] \xrightarrow{k_{nc}} UO_2^{2+} + BH + H_2O \qquad (4.1.2\text{-}4c)$$

$$B\cdot + UO_2^{2+} + H_2O \xrightarrow{k_{BU2}} BOH + UO_2^{+} + H^{+} \qquad (4.1.2\text{-}9)$$

From the above reactions, the following differential equations can be obtained :

$$\frac{d[BOH]}{dt} = k_{BU2}[B\cdot][UO_2^{2+}] + k_b[E3] \qquad \text{(A1-1)}$$

$$\frac{d[B\cdot]}{dt} = k_a[E3] - k_{BU2}[B\cdot][UO_2^{2+}] \qquad \text{(A1-2)}$$

$$\frac{d[E3]}{dt} = k_{q1}[E1][BH] - K_03[E3] \qquad \text{(A1-3)}$$

$$\frac{d[E2]}{dt} = (k_{+H})[E1] - (k_{-H})[E2][H^+] - K2[E2] \qquad \text{(A1-4)}$$

$$\frac{d[E1]}{dt} = I_a + (k_{-H})[E2][H^+] - K1[E1] \qquad \text{(A1-5)}$$

Assuming that the steady-state approximation applies, and so, all of the left sides of equations (A1-2) to (A1-5) equal zero:

$$k_a[E3] - k_{BU2}[B\cdot][UO_2^{2+}] = 0 \qquad \text{(A1-6)}$$

$$k_{q1}[E1][BH] - K_03[E3] = 0 \qquad \text{(A1-7)}$$

$$(k_{+H})[E1] - (k_{-H})[E2][H^+] - K2[E2] = 0 \qquad \text{(A1-8)}$$

$$I_a + (k_{-H})[E2][H^+] - K1[E1] = 0 \qquad \text{(A1-9)}$$

From equations (A1-8) and (A1-9), we have:

$$[E1] = \frac{I_a}{K1 - \dfrac{(k_{+H})(k_{-H})[H^+]}{(k_{-H})[H^+] + K2}} \qquad \text{(A1-10)}$$

From equations (A1-8), we have:

$$[E2] = \frac{(k_{+H})E1}{(k_{-H})[H^+] + K2} \qquad \text{(A1-11)}$$

From equations (A1-7) and (A1-10), we have:

$$[E3] = \frac{k_{q1}[BH]}{K_03} \frac{I_a}{K1 - \dfrac{(k_{+H})(k_{-H})[H^+]}{(k_{-H})[H^+] + K2}} \qquad \text{(A1-12)}$$

From equations (A1-1) and (A1-6), we have:

$$\frac{d[BOH]}{dt} = (k_a + k_b)[E3] \qquad \text{(A1-13)}$$

The quantum yield is defined as

$$\phi = \frac{(\frac{d[BOH]}{dt})}{I_a} \qquad \text{(A1-14)}$$

Combining equation (A1-12), (A1-13) and (A1-14), we obtain:

$$\phi = \left(\frac{(k_a + k_b)k_{q1}[BH]}{K03}\right)\left(\frac{1}{K1 + \frac{(k_{+H})(k_{-H})[H^+]}{(k_{-H})[H^+] + K2}}\right)$$

$$= \left(\frac{(k_a + k_b)k_{q1}[BH]}{(k_a + k_b + k_{nc})}\right)$$

$$\times\left(\frac{1}{k_{nr1} + k_{f1} + (k_{+H}) + k_{q1}[BH] - \frac{(k_{+H})(k_{-H})[H^+]}{(k_{-H})[H^+] + (k_{f2} + k_{nr2} + k_{nr3} + k_{q2}[BH])}}\right) \qquad \text{(A1-15)}$$

2) Luminesence

As the luminescence efficiency (ϕ_{f1}) of E1 is directly proportional to the concentration of E1, then from (A1-10) and (A1-12), ϕ_{f1} and ϕ_{f2} can be expressed as:

$$\phi_{f1} = \frac{I_a k_{f1}(K2 + (k_{-H})[H^+])}{K1K2 + K1(k_{-H})[H^+]} \qquad \text{(A1-16)}$$

and:

$$\phi_{f2} = \left(\frac{k_{f2}(k_{+H})}{(K2 + k_{-H})[H^+]}\right)\left(\frac{I_a(K2 + (k_{-H})[H^+])}{K1K2 + K1(k_{-H})[H^+]}\right) \qquad \text{(A1-17)}$$

3) Decay Constant k_0

From equation (A1-5), it can be seen that the decay of E1 has the following expression:

$$-\frac{d[E1]}{dt} = ((k_{+H}) + k_{f1} + k_{nr1})[E1] - (k_{-H})[H^+][E2]' \qquad \text{(A1-18)}$$

E2' is the concentration of $*[HOUO_2]^*$ in the absence of isobutane. It can be derived the same way as that for E2 except using K_02 instead of K2:

$$[E2]' = \frac{(k_{+H})E1}{(k_{-H})[H^+] + K_02} \qquad \text{(A1-19)}$$

Substituting E2' into equation (A1-18), we obtain:

$$-\frac{d[E1]}{dt} = \left(K_01 - \frac{(k_{+H})(k_{-H})[H^+]}{K2 + (k_{-H})[H^+]}\right)[E1] \qquad \text{(A1-20)}$$

So, the decay constant k_0 is:

$$k_0 = K_01 - \frac{(k_{+H})(k_{-H})[H^+]}{(k_{-H})[H^+] + K_02} \qquad \text{(A1-21)}$$

Appendix 2

Mechanism for Isobutane System in the Presence of $S_2O_8^{2-}$.

In the following equations:

$K_0 1 = k_{f1} + k_{nr1} + k_{+H}$;

$K_0 2 = k_{f2} + k_{nr2} + k_{nr3}$;

$K_0 3 = k_a + k_b + k_{nc}$;

$K1 = k_{f1} + k_{nr1} + k_{+H} + k_{q1}[BH]$;

$K2 = k_{f2} + k_{nr2} + k_{nr3} + k_{q2}[BH]$;

E1, E2 and E3 represent $*[H_2OUO_2^{2+}]$, $*[HOUO_2^{+}]$ and $*[H_2OUO_2 \cdot BH^{2+}]$, respectively.

The basic reactions discussed in Appendix 1 are listed as below:

$$[H_2OUO_2^{2+}] \xrightarrow{I_a.\, h\nu} *[H_2OUO_2^{2+}] \qquad (4.1.2\text{-}1)$$

(absorption) I_a = rate of light absorption

$$*[H_2OUO_2^{2+}] \xrightarrow{k_{f1}} [H_2OUO_2^{2+}] + h\upsilon' \qquad (4.1.2\text{-}2a)$$

(fluorescence emission) $(\upsilon > \upsilon')$

$$*[H_2OUO_2^{2+}] \xrightarrow{k_{nr1}} [H_2OUO_2^{2+}] + \text{heat} \qquad (4.1.2\text{-}2b)$$

(radiationless deactivation)

$$*[H_2OUO_2^{2+}] \underset{k_{-H}}{\overset{k_{+H}}{\rightleftharpoons}} *[HOUO_2^{+}] + H^{+} \qquad (4.1.2\text{-}2c)$$

(reversible)

$$*[H_2OUO_2^{2+}] + BH \xrightarrow{k_{q1}} *[H_2OUO_2{\cdot}BH^{2+}] \qquad (4.1.2\text{-}2d)$$

$$*[H_2OUO_2{\cdot}BH^{2+}] \xrightarrow{k_a} UO_2^{+} + B{\cdot} + H_3O^{+} \qquad (4.1.2\text{-}4a)$$

(1 e^- Mech.)

$$*[H_2OUO_2{\cdot}BH^{2+}] \xrightarrow{k_b} BOH + UO_2H_2^{2+} \qquad (4.1.2\text{-}4b)$$

(2 e^- Mech.)

$$*[H_2OUO_2{\cdot}BH^{2+}] \xrightarrow{k_{nc}} UO_2^{2+} + BH + H_2O \qquad (4.1.2\text{-}4c)$$

$$B{\cdot} + UO_2^{2+} + H_2O \xrightarrow{k_{BU2}} BOH + UO_2^{+} + H^{+} \qquad (4.1.2\text{-}9a)$$

In the presence of $S_2O_8^{2-}$, the major reactions are rewritten below:

Propagation processes are considered to be:

$$\mathbf{UO_2^{+}} + S_2O_8^{2-} \xrightarrow{k_{SU1}} UO_2^{2+} + \mathbf{SO_4^{-}} + SO_4^{2-} \qquad (4.2.1\text{-}4)$$

$$\mathbf{SO_4^{-}} + BH \xrightarrow{k_{FBH}} \mathbf{B\cdot} + HSO_4^{-} \qquad (4.2.1\text{-}5)$$

$k_{FBH} = 1.05 \times 10^8\ M^{-1}s^{-1}$

$$B\cdot + UO_2^{2+} + H_2O \xrightarrow{k_{BU2}} BOH + UO_2^{+} + H^{+} \qquad \text{(see 4.1.2-9a)}$$

$$B\cdot + S_2O_8^{2-} + H_2O \xrightarrow{k_{SB}} BOH + SO_4^{-} + HSO_4^{-} \qquad (4.2.1\text{-}6)$$

$k_{SB} = 1 \times 10^5\ M^{-1}s^{-1}$

There are two cycles. The first one consists of reactions (4.2.1-4), (4.2.1-5) and (4.1.2-9); the second one consists of reactions (4.2.1-5) and (4.2.1-6), which should be the main cycle. The termination processes for SO_4^- is:

$$SO_4^{-} + UO_2^{+} \xrightarrow{k_{FU1}} UO_2^{2+} + SO_4^{2-} \qquad (4.2.1\text{-}7)$$

$k_{FU1} \geq 10^8\ M^{-1}s^{-1}$

$$SO_4^{-} + SO_4^{-} \xrightarrow{2k_{FF}} S_2O_8^{2-} \qquad (4.2.1\text{-}8)$$

$2k_{FF} = 3.7 \times 10^8\ M^{-1}s^{-1}$

From the above reactions, the following differential equations are obtained:

$$\frac{d[BOH]}{dt} = k_{SB}[S_2O_8^{2-}][B\cdot] + k_b[E3] + k_{BU2}[B\cdot][UO_2^{2+}] \qquad (A2\text{-}1)$$

$$\frac{d[B\cdot]}{dt} = k_a[E3] + k_{FBH}[SO_4^{-}][BH] - k_{SB}[S_2O_8^{2-}][B\cdot] - k_{BU2}[B\cdot][UO_2^{2+}] \qquad (A2\text{-}2)$$

$$\frac{d[SO_4^-]}{dt} = k_{SB}[S_2O_8^{2-}][B\cdot] + k_{SU1}[S_2O_8^{2-}][UO_2^+] - k_{FBH}[SO_4^-][BH] - 2k_{FF}[SO_4^-]^2 - k_{FU1}[SO_4^-][UO_2^+]$$

(A2-3)

$$\frac{d[UO_2^+]}{dt} = k_a[E3] - k_{FU1}[SO_4^-][UO_2^+] - k_{SU1}[UO_2^+][S_2O_8^{2-}] + k_{BU2}[B\cdot][UO_2^{2+}]$$

(A2-4)

Assuming that in the presence of $S_2O_8^{2-}$, B· mainly reacts with $S_2O_8^{2-}$, thus the term $k_{BU2}[B\cdot][UO_2^{2+}]$ in equations (A2-2) and (A2-4) is not important; and also assuming that the steady-state approximation applies, so the following equations are obtained:

$$k_a[E3] + k_{FBH}[SO_4^-][BH] - k_{SB}[S_2O_8^{2-}][B\cdot] = 0 \qquad \text{(A2-5)}$$

$$k_{SB}[S_2O_8^{2-}][B\cdot] + k_{SU1}[S_2O_8^{2-}][UO_2^+] - k_{FBH}[SO_4^-][BH] - 2k_{FF}[SO_4^-]^2 - k_{FU1}[SO_4^-][UO_2^+] = 0 \qquad \text{(A2-6)}$$

$$k_a[E3] - k_{FU1}[SO_4^-][UO_2^+] - k_{SU1}[S_2O_8^{2-}][UO_2^+] = 0 \qquad \text{(A2-7)}$$

or:

$$[B\cdot] = \frac{k_a[E3] + k_{FBH}[SO_4^{\cdot-}][BH]}{k_{SB}[S_2O_8^{2-}]} \qquad \text{(A2-8)}$$

$$[SO_4^{\cdot-}]^2 = \frac{k_{SB}[S_2O_8^{2-}][B\cdot] + k_{SU1}[UO_2^{+}][S_2O_8^{2-}] - k_{FBH}[SO_4^{\cdot-}][BH] - k_{FU1}[UO_2^{+}][SO_4^{\cdot-}]}{2k_{FF}} \qquad \text{(A2-9)}$$

$$k_a[E3] = k_{FU1}[SO_4^{\cdot-}][UO_2^{+}] + k_{SU1}[UO_2^{+}][S_2O_8^{2-}] \qquad \text{(A2-10)}$$

Substituting $k_{SB}[S_2O_8^{2-}][B\cdot]$ in equation (A2-8) into equation (A2-9), we obtain:

$$[SO_4^{\cdot-}]^2 = \frac{k_a[E3] + k_{SU1}[S_2O_8^{2-}][UO_2^{+}] - k_{FU1}[SO_4^{\cdot-}][UO_2^{+}]}{2k_{FF}} \qquad \text{(A2-11)}$$

Substituting $k_a[E3]$ in equation (A2-10) into equation (A2-11), we obtain:

$$[SO_4^{\cdot-}]^2 = \frac{2k_{SU1}[S_2O_8^{2-}][UO_2^{+}]}{2k_{FF}} \qquad \text{(A2-12)}$$

or:

$$[SO_4^{\cdot-}] = \sqrt{\frac{k_{SU1}[S_2O_8^{2-}][UO_2^{+}]}{k_{FF}}} \qquad \text{(A2-13)}$$

Substituting the expression of UO_2^{+} in equation (A2-10) into the above equation, we have:

$$[SO_4^-] = \sqrt{\frac{k_a k_{SU1}[E3][S_2O_8^{2-}]}{\frac{k_{FU1}[SO_4^-] + k_{SU1}[S_2O_8^{2-}]}{k_{FF}}}} \qquad \text{(A2-14)}$$

If we use the approximation $k_{FU1}[S_2O_8^{2-}] >> k_{SU1}[S_2O_8^{2-}]$, the above equation becomes:

$$[SO_4^-] = \sqrt{\frac{k_a k_{SU1}[E3][S_2O_8^{2-}]}{k_{FF} k_{FU1}[SO_4^-]}} \qquad \text{(A2-15)}$$

or:

$$[SO_4^-] = \left(\frac{k_a k_{SU1}[E3][S_2O_8^{2-}]}{k_{FF} k_{FU1}}\right)^{1/3} \qquad \text{(A2-16)}$$

From equation (A2-1) and equation (A2-8), we have:

$$\frac{d[BOH]}{dt} = k_b[E3] + k_a[E3] + k_{FBH}[SO_4^-][BH] \qquad \text{(A2-17)}$$

Substituting (A2-16) into the above equation leads to:

$$\frac{d[BOH]}{dt} = (k_a + k_b)[E3] + k_{FBH}[BH]\left(\frac{k_a k_{SU1}[E3][S_2O_8^{2-}]}{k_{FF} k_{FU1}}\right)^{1/3} \qquad \text{(A2-18)}$$

As discussed in Appendix 1, E3 has the expression:

$$[E3] = \frac{k_{q1}[BH]}{K_03} \frac{I_a}{K1 - \frac{(k_{+H})(k_{-H})[H^+]}{(k_{-H})[H^+] + K2}} \qquad \text{(see A1-11)}$$

Substituting the above equation into equation (A2-18) and then substituting the result into $\phi = (d[BOH]/dt)/I_a$, and after rearrangement, we obtain:

$$\phi = (k_a + k_b)\left(\frac{k_{q1}[BH]}{K_03} \frac{1}{K1 - \frac{(k_{+H})(k_{-H})[H^+]}{(k_{-H})[H^+] + K2}} \right)$$

$$+k_{FBH}[BH]\left(\frac{k_a k_{SU1}[S_2O_8^{2-}]}{k_{FF}k_{FU1}} \right)^{1/3} \left(\frac{k_{q1}[BH]}{K_03} \frac{1}{K1 - \frac{(k_{+H})(k_{-H})[H^+]}{(k_{-H})[H^+] + K2}} \right)^{1/3} \frac{1}{I^{2/3}} \qquad \text{(A2-19)}$$

or:

$$\phi = \frac{(k_a + k_b)k_{q1}[BH]}{K_03} F_{(H)} + \left(k_{FBH}\left(\frac{k_{q1}k_a k_{SU1}}{k_{FF}k_{FU1}K_03} \right)^{1/3} [BH]^{4/3}[S_2O_8^{2-}]^{1/3}(F_{(H)})^{1/3} \frac{1}{I^{2/3}} \right) \qquad \text{(A2-20)}$$

where:

$$F_{(H)} = \frac{1}{K1 - \dfrac{(k_{+H})(k_{-H})[H^+]}{(k_{-H})[H^+] + K2}} \qquad \text{(A2-21)}$$

TABLE OF ABBREVIATION

BH	Isobutane
BOH	Tertiary butyl alcohol
CpH_2	Cyclopentane
CpHOH	Cyclopentanol
CpO	Cyclopentanone
$CpeH_2$	Cyclopentene
CpeHOH	2-cyclopen-1-ol
CpeO	2-cyclopen-1-one
DCTA	1,2-cyclohexadiaminetraacetate
EDTA	Ethylenediaminetetraacetate
THF	Tetrahydrofuran

IMAGE EVALUATION
TEST TARGET (QA-3)

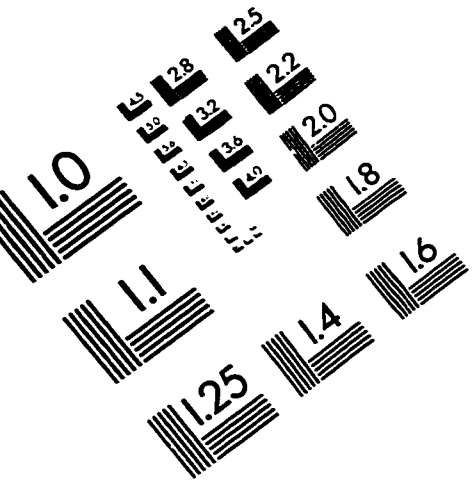

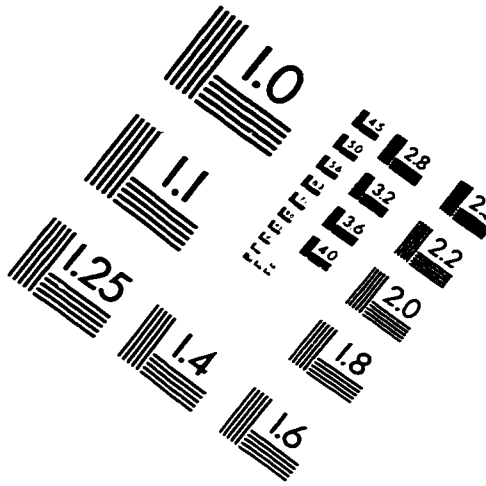

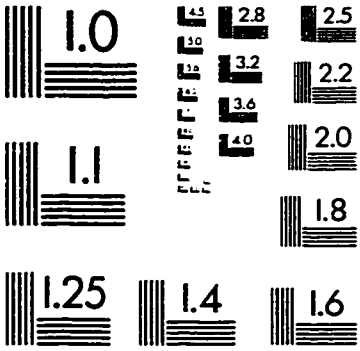

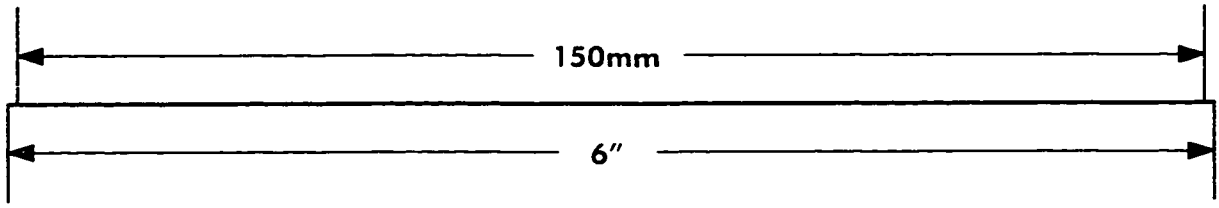

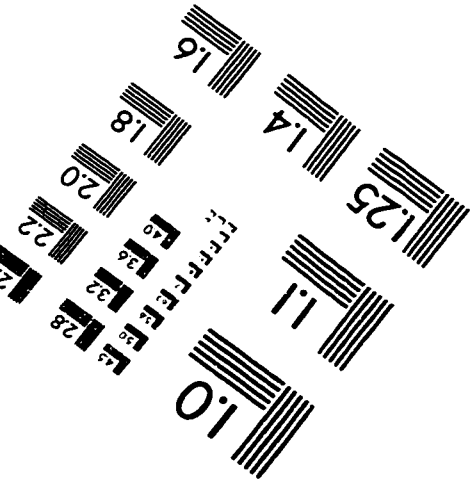

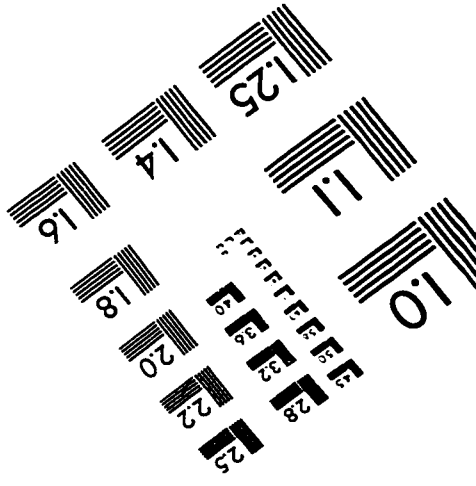

APPLIED IMAGE, Inc
1653 East Main Street
Rochester, NY 14609 USA
Phone: 716/482-0300
Fax: 716/288-5989